universität
wien

# MASTERARBEIT / MASTER'S THESIS

Titel der Masterarbeit / Title of the Master's Thesis

## „Group 5 Metal Complexes with Stilbene-Type Ligands – Synthesis, Characterization and Application in Hydroaminoalkylation and Hydroamination of Alkenes"

verfasst von / submitted by

### Quentin Magnus Riedl, BSc

angestrebter akademischer Grad / in partial fulfilment of the requirements for the degree of

### Master of Science (MSc)

Wien, 2023 / Vienna 2023

| | |
|---|---|
| Studienkennzahl lt. Studienblatt / degree programme code as it appears on the student record sheet: | UA 066 862 |
| Studienrichtung lt. Studienblatt / degree programme as it appears on the student record sheet: | Masterstudium Chemie |
| Betreut von / Supervisor: | Univ.-Prof. Dr. Kai Carsten Hultzsch |
| Mitbetreut von / Co-Supervisor: | Mag. Dr. Mariusz Jozef Wolff |

# Acknowledgements

# Abstract

Organic molecules containing nitrogen, such as amines and amides display an important molecular scaffold and have been found to be essential for many applications, not only in the realm of chemistry, but also in medicine, biology, and material sciences. The hydroaminoalkylation and hydroamination are powerful catalytic methodologies to facilitate the reaction of amines with unsaturated hydrocarbon frameworks, such as alkenes or alkynes, to form new, valuable amines in a virtually 100 % atom-economic fashion.

3,3'-bis(arylalkylsilyl)- and 3,3'-bis(alkylsilyl)-substituted 2,2'-dihydroxystilbene ligands and their niobium(V) and tantalum(V) complexes were prepared and spectroscopically and structurally characterized. All monoligated metal complexes were investigated in regard to their catalytic activity in hydroaminoalkylation and hydroamination of alkenes and 1-phenyl-1-propyne. The reaction progress was monitored using $^1$H and $^{13}$C NMR spectroscopy, as well as GC-MS.

No product formation was observed in the hydroaminoalkylation reaction of various simple alkenes with *N*-methylaniline and its derivatives. Reactions utilizing various additives showed no conversion, however, low product formation was observed if trimethylsilyl chloride is added. The intramolecular hydroamination reaction of 2,2-diphenylamino-4-pentene gave low yields of the desired pyrrolidine product. No activity was observed in the intermolecular hydroamination of unactivated alkenes.

# Zusammenfassung

Stickstoffhaltige organische Moleküle wie Amine und Amide stellen ein wichtiges molekulares Grundgerüst dar und haben sich für viele Anwendungen nicht nur in der Chemie, sondern auch in der Medizin, Biologie und den Materialwissenschaften als unverzichtbar erwiesen. Die Hydroaminoalkylierung und Hydroaminierung sind leistungsstarke katalytische Methoden, um die Reaktion von Aminen mit ungesättigten Kohlenwasserstoffgerüsten, wie Alkenen oder Alkinen, praktisch zu 100 % atomökonomisch zu neuen, wertvollen Aminen zu ermöglichen.

Es wurden 3,3'-Bis(arylalkylsilyl)- und 3,3'-Bis(alkylsilyl)-substituierte 2,2'-Dihydroxystilben-Liganden und ihre Niob(V)- und Tantal(V)-Komplexe hergestellt. Alle monoligierten Metall-Komplexe wurden hinsichtlich ihrer katalytischen Aktivität in der Hydroaminoalkylierung und Hydroaminierung von Alkenen und 1-Phenyl-1-propin untersucht. Der Reaktionsfortschritt wurde mittels $^1$H und $^{13}$C NMR-Spektroskopie sowie GC-MS überwacht.

Bei der Hydroaminoalkylierungsreaktion verschiedener einfacher Alkene mit *N*-Methylanilin und seinen Derivaten wurde keine Produktbildung beobachtet. Reaktionen unter Verwendung verschiedener Additive zeigten keine Umsetzung, jedoch wurde eine geringe Produktbildung beobachtet, wenn Trimethylsilylchlorid zugegeben wurde. Die intramolekulare Hydroaminierungsreaktion von 2,2-Diphenylamino-4-penten ergab geringe Ausbeuten des gewünschten Pyrrolidinprodukts. Bei der intermolekularen Hydroaminierung wurde keine Aktivität beobachtet.

# Abbreviations

| | | | | |
|---|---|---|---|---|
| Å | Angstrom | | Mes | Mesityl |
| Bn | Benzyl | | min | Minutes |
| Boc | *tert*-butoxycarbonyl | | MOF | Metal-organic framework |
| cod | Cycloocta-1,5-diene | | NaSCN | Sodium thiocyanate |
| COF | Covalent organic framework | | NMR | Nuclear magnetic resonance |
| d | Days | | NOESY | Nuclear Overhauser |
| dba | Dibenzylideneacetone | | | Enhancement Spectroscopy |
| DCM | Dichloromethane | | *n*Pr | *n*-propyl |
| DEAD | Diethyl diazenedicarboxylate | | OLED | Organic light-emitting diode |
| DFT | Density-functional theory | | Ph | Phenyl |
| Dipp | 2,6-di*iso*propylphenyl | | PhCN | Benzonitrile |
| DNP-SENS | Dynamic nuclear polarization surface | | PMP | *para*-methoxyphenyl |
| | enhanced NMR spectroscopy | | ppm | Parts per million |
| *ee* | Enantiomeric excess | | R | Rest |
| eq. | Equation | | rt | Room temperature |
| equiv | Equivalents | | SPS | solvent purification system |
| ESI | Electrospray ionization | | *t*Bu | *tert*-butyl |
| Et | Ethyl | | *t*BuNC | *tert*-butylisocyanide |
| Et$_2$O | Diethylether | | *t*BuLi | *tert*-butyl lithium |
| EXSY | Exchange Spectroscopy | | temp | Temperature |
| GC-MS | Gas chromatography-mass | | TFA | Trifluoroacetic acid |
| | spectrometry | | THF | Tetrahydrofuran |
| GP | General procedure | | TLC | thin layer chromatography |
| h | Hours | | TMS | Trimethylsilyl |
| HMBC | Heteronuclear Multiple Bond | | TOF | Time of flight |
| | Correlation | | UV | Ultraviolet |
| HMTA | Hexamethylenetetramine | | Xantphos | (9,9-Dimethyl-9H-xanthene- |
| HSQC | Heteronuclear Single Quantum | | | 4,5-diyl)bis(diphenyl- |
| | Coherence | | | phosphane) |
| Hz | Hertz | | | |
| *i*Pr | *iso*-propyl | | | |
| KH | Potassium hydride | | | |
| Me | Methyl | | | |

# Table of contents

10

# 1. Introduction

## 1.1. Importance of Nitrogen-Containing Molecules

Organic molecules containing nitrogen, such as amines and amides, are of major interest as they are often found in nature e.g., in form of peptides or alkaloids and known to be promotive towards biological activity, hence exhibiting great value for pharmaceutical and agrochemical compounds.[1–6] C–N bonds are also an important chemical moiety in functional materials and have a wide range of applications such as in organic light-emitting diodes (OLEDs), in highly porous materials like metal-organic frameworks (MOFs) and covalent-organic frameworks (COF) as well as in various responsive and self-healing materials.[7–12] Performing reactions of simple unsaturated hydrocarbons with simple primary and secondary amines or even ammonia has presented a challenge, especially on an industrial level, as poor chemoselectivity in form of undesired side products and non-negligible waste are unavoidable with conventional organic methods.[13] On the other hand, the chemospecific synthesis of nitrogen-containing target molecules generally requires multiple synthetic steps in order to obtain the desired product, which is, again, linked to undesired waste, expenditure of time and as a result of that, lowering economic interests. In order to overcome the aforementioned disadvantages, it is highly desirable, not only for the industry, but also for the synthetic chemist, to investigate catalytic methods to facilitate the synthesis of precious amines and other nitrogen-containing molecules.

Traditionally, amines are prepared from well-established synthesis protocols and can be obtained from reductive amination,[14] Gabriel synthesis,[15] Buchwald-Hartwig amination[16] of arylhalides, the Mannich reaction,[17] reduction of cyanides[18,19] or azides[20,21] or the Mitsunobu[22,23] reaction (Scheme 1).

(1) $R^1$ ... $R^2$ ... O $\quad$ + $\quad$ HNR$^3$R$^4$ or H$_2$NR$^3$ $\quad$ imine or enamine formation $\quad$ $-$ H$_2$O $\quad \longrightarrow \quad$ $R^1$...$R^2$...NR$^3$R$^4$ or $R^1$...$R^2$...NR$^3$ $\quad$ reduction $\quad \longrightarrow \quad$ $R^1$...$R^2$...NR$^3$R$^4$ or $R^1$...$R^2$...NHR$^3$

(2) (phthalimide, NH) $\quad$ 1. base (e.g. KOH, KH, ...) $\quad$ 2. $\quad$ X$\frown$R $\quad$ $-$ KX $\quad \longrightarrow \quad$ (phthalimide, N–R) $\quad$ N$_2$H$_4$ $\quad \longrightarrow \quad$ H$_2$N$\frown$R $\quad$ (phthalhydrazide, NH NH)

(3) $R^1$...O...N...R$^3$, R$^2$ $\quad$ LiAlH$_4$ $\quad \longrightarrow \quad$ $R^1\frown$N...R$^3$, R$^2$

(4) $R$...(benzene ring)...X $\quad$ + $\quad$ HNR$^2$R$^3$ or H$_2$NR$^2$ $\quad$ Pd$_2$(dba)$_3$, ligand, NaO$t$Bu $\quad$ toluene or DME rt to 100 °C $\quad \longrightarrow \quad$ $R_1$...(benzene ring)...NR$^2$R$^3$ or $R_1$...(benzene ring)...NHR$^2$

(5) $R^1$...O...R$^3$, R$^2$ $\quad$ + $\quad$ R$^5$...R$^4$...O $\quad$ + $\quad$ HN...R$^7$, R$^6$ $\quad$ acid (cat.) or base (cat.) $\quad$ $-$ H$_2$O $\quad \longrightarrow \quad$ $R^1$...O... R$^4$ R$^5$ ...N...R$^7$, R$^2$ R$^3$ R$^6$

(6) $R\frown$CN $\quad$ or $\quad$ $R\frown$N$_3$ $\quad$ reduction $\quad \longrightarrow \quad$ $R\frown$NH$_2$

(7) $R\frown$OH $\quad$ + $\quad$ H$_2$NTs $\quad$ PPh$_3$, DEAD $\quad \longrightarrow \quad$ $R\frown$NHTs

*Scheme 1:* Traditional and well-established strategies to prepare amines.[14–23]

Most reactions require a prefunctionalization of the hydrocarbon which is later transformed into the amine. This predominantly leads to elongated reaction sequences and the formation of side products as well as waste. Virtually, every amine synthesis is connected to the formation of a by-product which is further separated from the desired product and finally discarded. The synthesis of amines therefore may result in poor atom economy.[24] Poor atom economy can be illustrated by the Gabriel synthesis of methylamine from methyl iodide and phthalimide (Scheme 1, eq. 2; R = H, X = I), a reaction which is rarely performed in the laboratory but serves

as a perfect thought experiment. After the *N*-methylphthalimide is obtained, hydrazine is added in order to release the desired methylamine and form phthalhydrazide as the by-product. Theoretically, if 1 g phthalimide was used as starting material and if 100 % yield was obtained, 0.21 g of methylamine and 1.10 g of phthalhydrazide are formed. Hence only 16 % of the resulting total mass is the desired product and merely 22 % of all used atoms, including all starting materials, such as sodium hydride and methyl iodide, can be found in the product. Despite the low atom economy, it is challenging to prepare methylamine as the mono-alkylated species using a different synthetic procedure and consequently the Gabriel synthesis is a robust methodology to synthesize primary amines chemoselectively. In contrast, the stoichiometric reaction of ammonia with alkyl halides, such as methyl iodide, does not stop at the mono-alkylated species and a wild mixture of unreacted starting material, primary, secondary and tertiary amines, as well as quaternary ammonium salts are generated.[25]

The catalytic hydroamination and hydroaminoalkylation reactions however are virtually 100 % atom economic and display a promising concept for a green, waste-free, and co-reagent-free process to prepare various amines (Scheme 2).[26–29]

**Hydroamination**



**Hydroaminoalkylation**
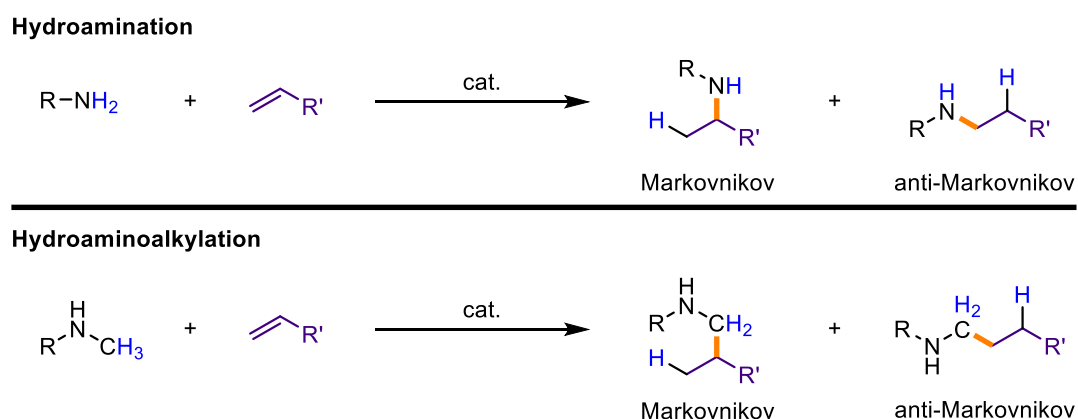


*Scheme 2:* Metal-catalyzed intermolecular hydroamination and hydroaminoalkylation reactions of alkenes with amines.

Additionally, no prefunctionalization of the olefin is required, which is highly desirable from an industrial point of view, since the olefinic hydrocarbon feedstock could be directly transformed into various precious amines. The production of *tert*-butylamine from isobutene and ammonia, catalysed by a heterogeneous zeolite catalyst is one hydroamination reaction, which is performed industrially.[30]

Alkaloids, such as (±)-Clavicipitic Acid[1,31] **1**, (+)-Xenovenine[32,33] **2**, (−)-Dihydroisocodeine[34] **3**, and other nitrogen containing molecules like for example the conjugated π-systems[35] **5** and **6**

have been synthesized applying the catalytic hydroamination, whereas 1,5-benzodiazepine[36] **4** has been synthesized by the hydroaminoalkylation reaction (Figure 1).
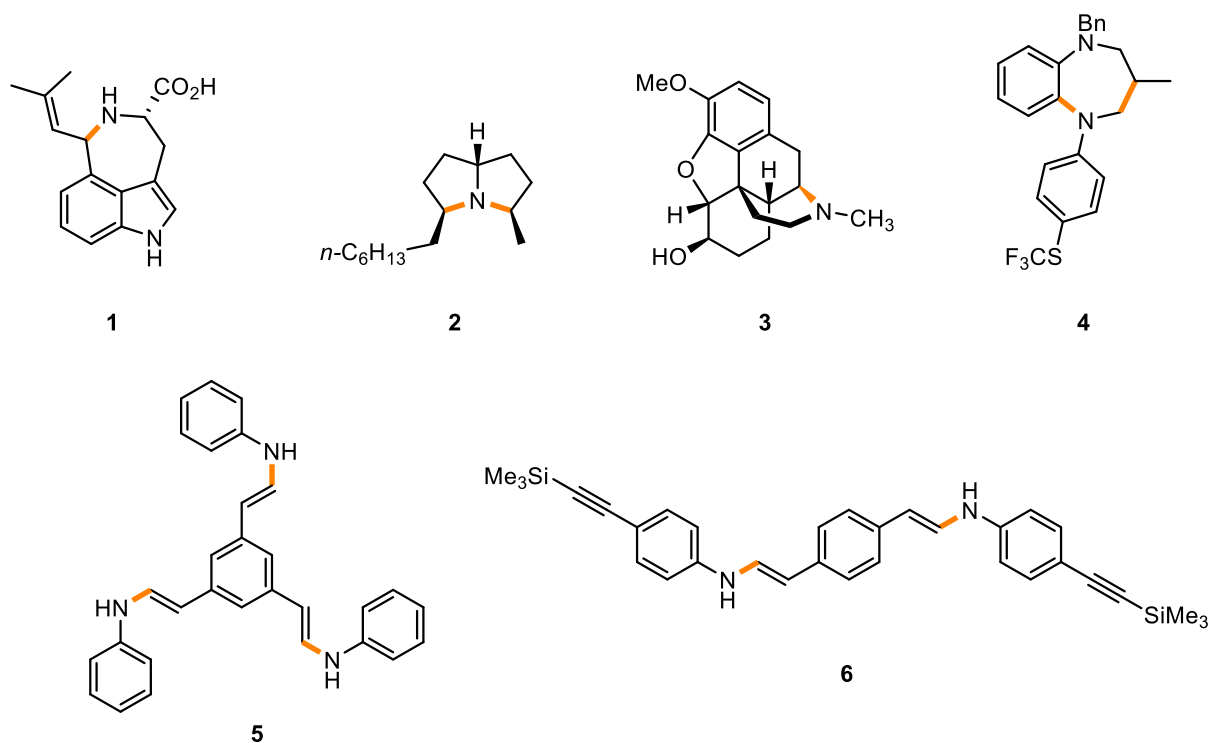


*Figure 1:* Nitrogen containing molecules which were synthesized utilizing the hydroamination or hydroaminoalkylation catalysis approach.[1,31–36]

The shown molecules demonstrate the importance of novel, powerful strategies to create new C–N and C–C bonds in a way that no over-alkylation is possible and the use of protecting groups becomes dispensable.

## 1.2. Hydroaminoalkylation

In the hydroaminoalkylation reaction, an α-C(sp$^3$)–H bond of an amine is added across the double bond of an alkene, diene or allene or the triple bond of an alkyne (Scheme 3).
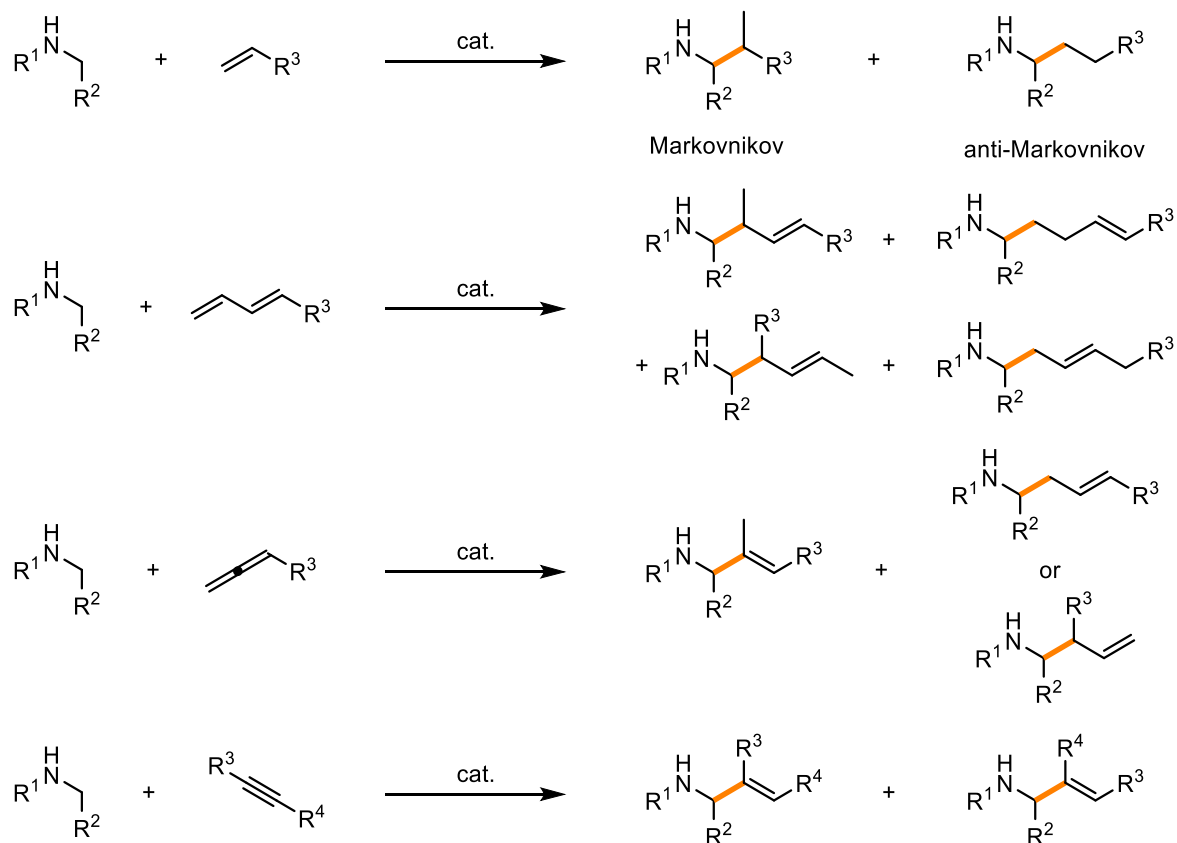


*Scheme 3:* Different unsaturated hydrocarbon substrates in hydroaminoalkylation and their products.

This can be accomplished by using early-transition-metal, late-transition-metal and photoredox catalysis.[6,27–29,37] Depending on the catalytic system and conditions used, different products can be obtained in extraordinary selectivity. For example, Group 5 transition-metals, niobium(V) and tantalum(V) usually yield the branched product (Markovnikov product) exclusively and even though most Group 4 transition-metal catalysts preferentially give the same product, some systems have been developed to access the linear product (anti-Markovnikov product) in good to excellent regioselectivity.[38–45] On the other hand, late-transition-metals typically exclusively yield the anti-Markovnikov product.[28,37] However, there are examples of late-transition-metal-based catalysts, that facilitate the formation of the branched product.[37,46,47] One big disadvantage of late-transition-metal hydroaminoalkylation over early-transition-metal hydroaminoalkylation is the fact that suitable directing groups, which could be challenging to be removed as well as protecting groups have to be implemented in order to achieve the desired reactivity.[47–54] Traditionally, linear amines, which are prepared from alkenes are accessed *via*

the hydroaminomethylation method.[46,55,56] This process typically utilizes transition metal complexes containing rare and expensive metals like rhodium as the catalysts and consists formally of a hydroformylation combined with a reductive amination.[57] The linear product can be obtained in excellent yields, e.g. if the cationic rhodium(I) precursor [Rh(cod)$_2$]BF$_4$ and ligand Xantphos are used.[57] Even internal alkenes yield the linear product due to isomerization facilitated by rhodium, which is of major importance to the chemical industry since no costly separation of simple alkenes is needed. However, the hydroaminoalkylation has some advantages over the hydroaminomethylation, and no hazardous and pressurized CO, H$_2$ gas mixture is needed. Furthermore, the Markovnikov or the anti-Markovnikov product is obtained regioselectivley if the right catalyst is used.[43,58]

The intermolecular hydroaminoalkylation of simple, unactivated alkenes is the most investigated type of reaction, and only a few reports about the hydroaminoalkylation of 1,3-butadiens in the presence of a titanium(IV) catalyst,[58–60] styrenes in the presence of a titanium(IV) or tantalum(V) catalyst[42,58,60–62] are published and only one article addressing the hydroaminoalkylation of allenes in the presence of a titanium(IV) catalyst to obtain allylic amines, using propadiene,[63] is reported. The hydroaminoalkylation of secondary amines with internal alkynes in the presence of a titanium(IV) or zirconium(IV) catalyst exclusively yield the corresponding (Z)-alkene.[64,65]

## 1.2.1.  Early-Transition-Metal based Hydroaminoalkylation

The first hydroamioalkylation utilizing dimethylamine and unactivated alkenes, such es ethylene, propylene or 1-hexene was reported by Clerici and Maspero in 1980.[66] They used the dimethylamido complexes of the Group 4 or 5 metals zirconium(IV), niobium(V) and tantalum(V) as catalysts to facilitate the monoalkylation of dimethylamine (Scheme 4).



| [M(NMe$_2$)$_x$] | temperature | time | yield |
|---|---|---|---|
| [Zr(NMe$_2$)$_4$] | 160 °C | 24 h | 18 % |
| [Nb(NMe$_2$)$_5$] | 160 °C | 24 h | 12 % |
| [Ta(NMe$_2$)$_5$] | 200 °C | 150 h | 38 % |
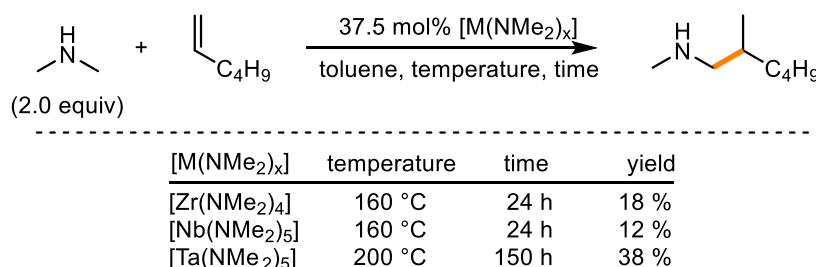
Scheme 4: Hydroaminoalkylation reaction of dimethylamine and 1-hexene in the presence of [Zr(NMe$_2$)$_4$], [Nb(NMe$_2$)$_5$] and [Ta(NMe$_2$)$_5$].[66]

Despite high catalyst loadings of 37.5 mol% and harsh reaction conditions, only low yields of the mono-alkylated product were obtained. However, this reaction was highly selective towards the formation of the mono-alkylated Markovnikov product and did not form any bis-alkylated or anti-Markovnikov products. No reaction occurred if primary or tertiary amines were used instead of dimethylamine. Other amido complexes, such as [Ti(NMe$_2$)$_4$], [V(NMe$_2$)$_4$], [Mo(NMe$_2$)$_4$], or [Sn(NMe$_2$)$_4$] were inactive or afforded only trace amounts of the desired product.

In 1982, Nugent *et al.* investigated the mechanism of the hydroaminoalkylation reaction by employing isotope labelled studies of *N-d*-dimethylamine in the presence of homoleptic dimethylamido complexes of catalytically active zirconium(IV), niobium(V), tantalum(V), and tungsten(VI).[67] They observed deuterium scrambling, hence the incorporation of deuterium into the methyl group and postulated the mechanism of the hydroaminoalkylation reaction, which is valid until today (Scheme 5).
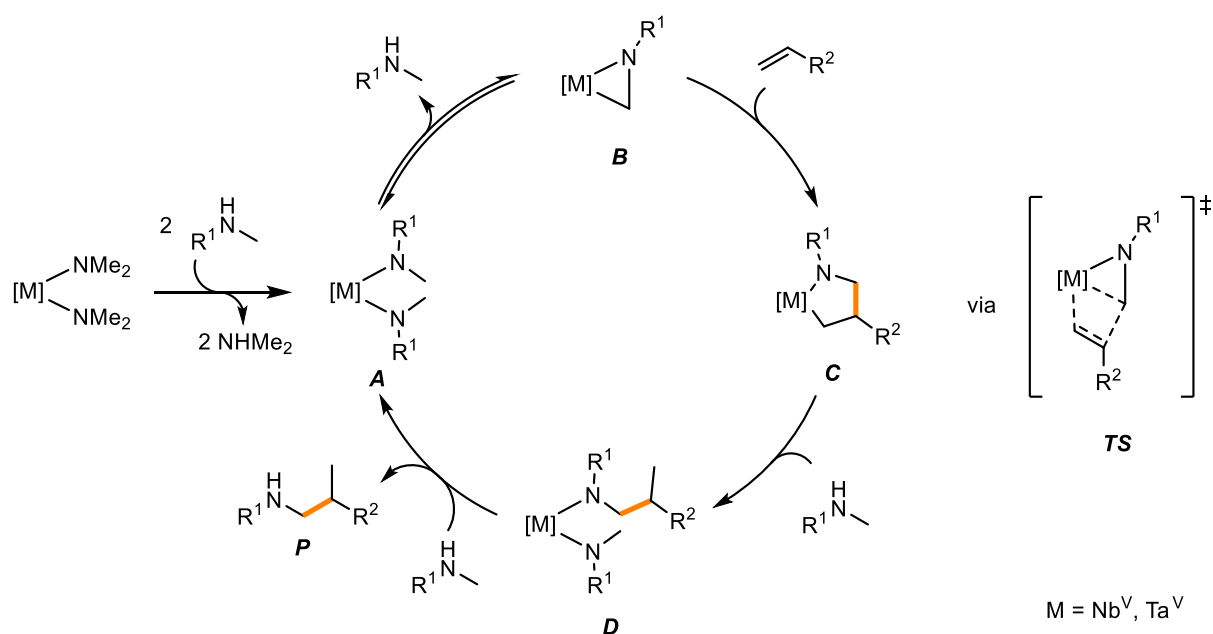


*Scheme 5:* Mechanism of intermolecular hydroaminoalkylation.[67]

In a first step, two dimethylamido ligands are exchanged with two molecules of the amine substrate to give *A*, then a C–H activation of the bisamide leads to metallaaziridine *B*. This step is reversible, however, it was shown that virtually no protonolysis of the M–C bond and therefore no reaction back to *A* is possible.[39] Subsequent alkene insertion yields intermediate *C*, and after protonolysis and coordination of the amine substrate intermediate *D* is obtained. Product *P* is released upon an amine exchange and intermediate *A* is formed to close the catalytic cycle.

In 2007, Herzon and Hartwig published their first catalytic hydroaminoalkylation study using a variety of *N*-alkylanilines and different olefins.[38] Based on previous reports which showed that the formation of zirconocene-$\eta^2$-imine complexes was faster from *N*-alkylanilines than from dialkylamines,[68] they envisioned that *N*-methylaniline and its derivatives would undergo hydroaminoalkylation more efficiently than their alkyl counterparts. Additionally, early-transition-metal amides are typically exceedingly reactive towards any proton source and since arylamines are less basic than alkylamines, an irreversible exchange is to be expected.[69–71] Fortunately, their hypothesis turned out to be true and high yields were obtained for the reaction of *N*-methylaniline with different alkenes using only a slight excess of 1.5 equiv of the olefin in the presence of 4 to 8 mol% of [Ta(NMe₂)₅] (Scheme 6).
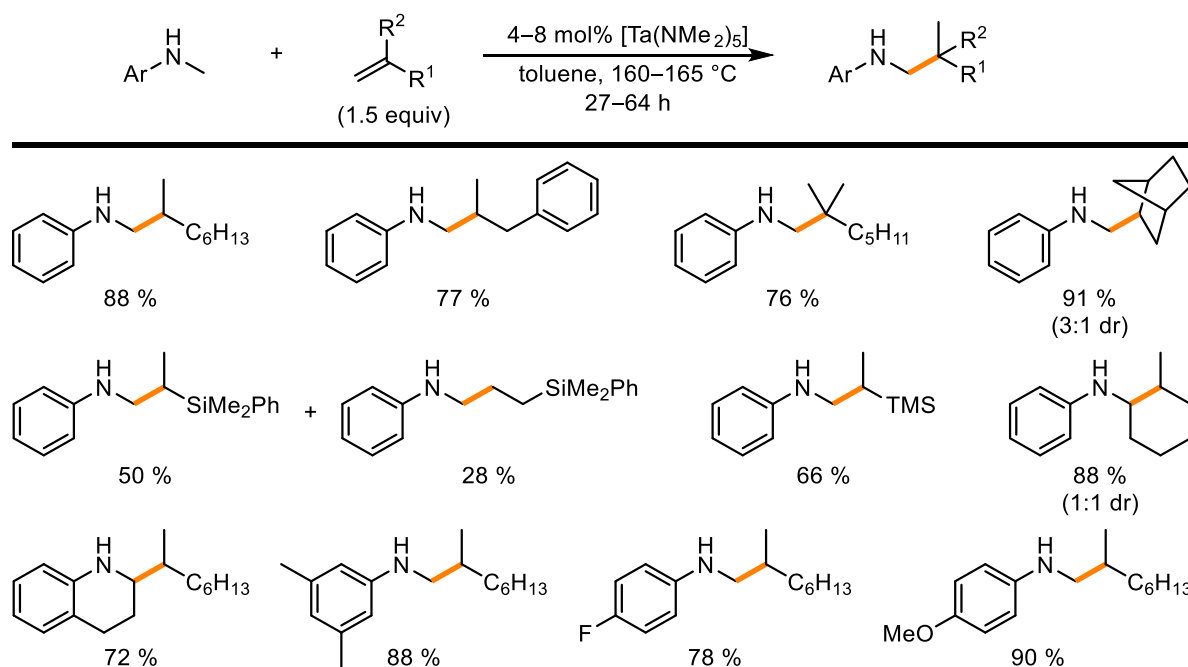


*Scheme 6:* Hydroaminoalkylation of different alkenes with *N*-methylamines in the presence of [Ta(NMe₂)₅].[38]

A variety of alkenes were tested, and the best results were obtained for mono- or 2,2-disubstituted alkenes giving the Markovnikov product exclusively. Vinylsilanes also gave high yields, however, in the case of dimethylphenylvinylsilane a mixture of the Markovnikov and the anti-Markovnikov product were obtained in a ratio of approximately 2:1, respectively. The reason for the formation of the anti-Markovnikov product is most likely due to electronic effects of the vinylsilanes.[72] Internal alkenes remain unreacted and only the highly reactive and ring-stained norbornene participated in the hydroaminoalkylation reaction. Interestingly, 10 – 20 % of the unreacted starting material isomerized to the internal alkenes. They also tested the reaction of different substituted *N*-methylanilines, as well as 1,2,3,4-tetrahydroquinoline with

1-octene under the above-mentioned conditions and isolated the desired products in high yields ranging from 72 to 93 %. The intramolecular cyclization of *N*-(7-heptenyl)aniline yielded the product in 88 % as a mixture of diastereoisomers. These results were quite extraordinary compared to the previously published works and support the authors hypothesis that *N*-alkylanilines react more efficiently than their alkyl-analogues.[38] Furthermore, the hydroaminoalkylation catalysis turned out to be highly selective for the addition of one alkene and no second insertion of another olefin would occur.

Despite experimental evidence for *ortho*-metalation of the aromatic moiety, no insertion of the olefin into the aryl C–H bond is observed. In 2008, it was demonstrated that in contrast to electron-donating alkylalcoholato and alkylamido ligands, which displayed no activity, and biphenolate-type ligands, which showed little reactivity, the electron-withdrawing chlorido ligands enhance the reactivity of the complex.[39] This resulted in catalyst-loadings of only 2 mol% and efficient hydroaminoalkylation of dialkylamines, such as *N*-methylcyclohexylamine, *N*-methyl*iso*propylamine, linear *N*-methylpropylamine and even diethylamine were possible, giving yields ranging from 78 to 96 %. It was also shown that the reaction of *N*-methylaniline and 1-octene in the presence of 4 mol% of [Ta(NMePh)$_2$Cl$_3$]$_2$ only required 90 °C to give 72 % of the desired product.

Several catalytically active early-transition-metal complexes have been published since the breakthrough of Herzon and Hartwig and some catalysts have been developed to facilitate enantioselective hydroaminoalkylation (Figure 2).
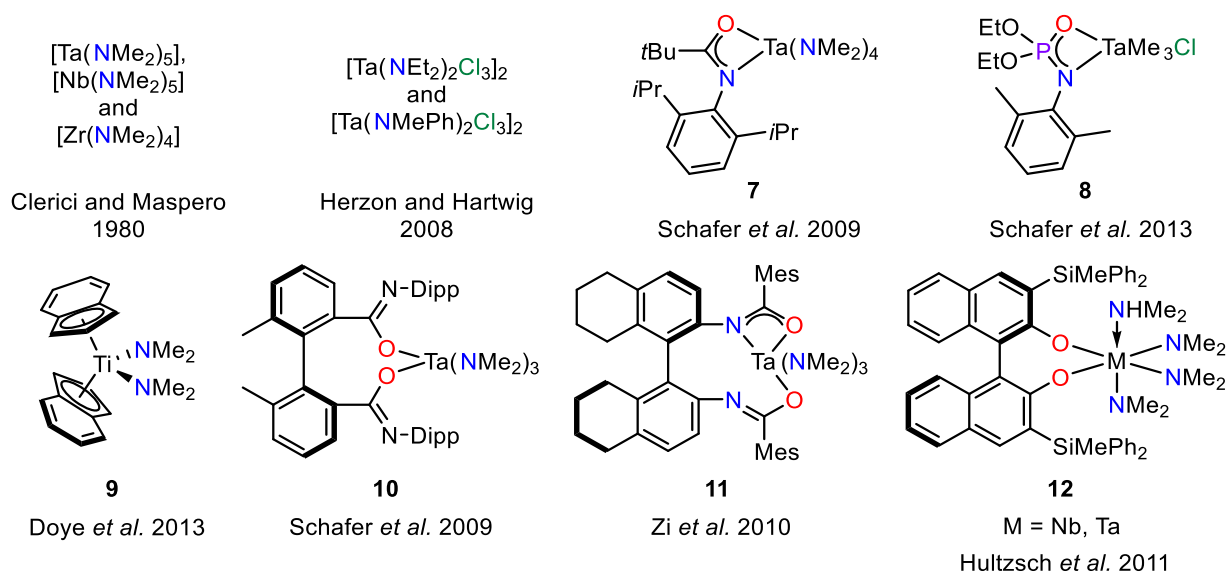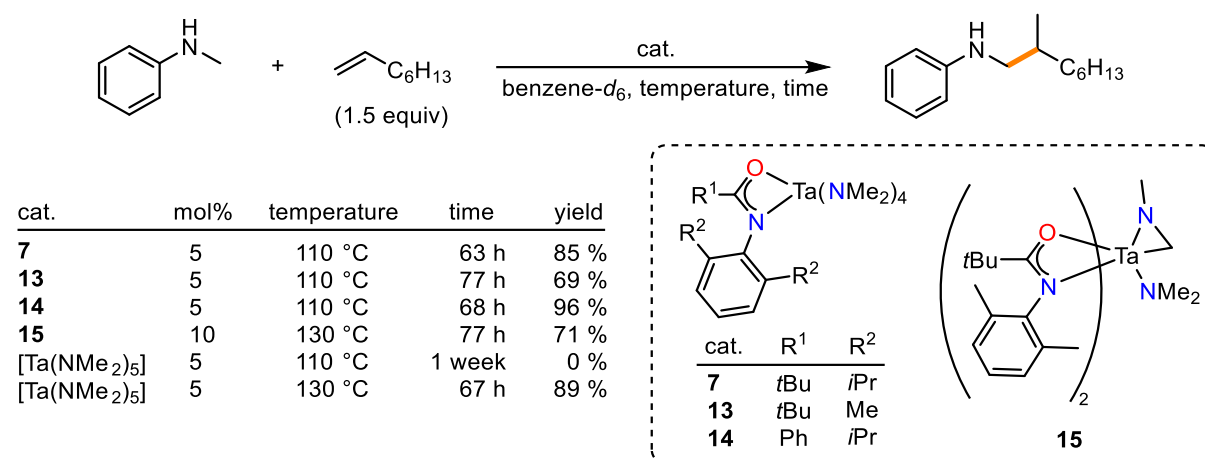


*Figure 2:* Early-transition-metal hydroaminoalkylation catalysts.[39–41,61,66,73–75]

In 2009, it was demonstrated that tuneable mono- and bis(amidate)-based tantalum(V) complexes readily catalyze the hydroaminoalkylation reaction.[74] In this study, the authors varied the substituents at the amidate ligand and investigated the influence of the resulting steric bulk towards the catalytic activity (Scheme 7).
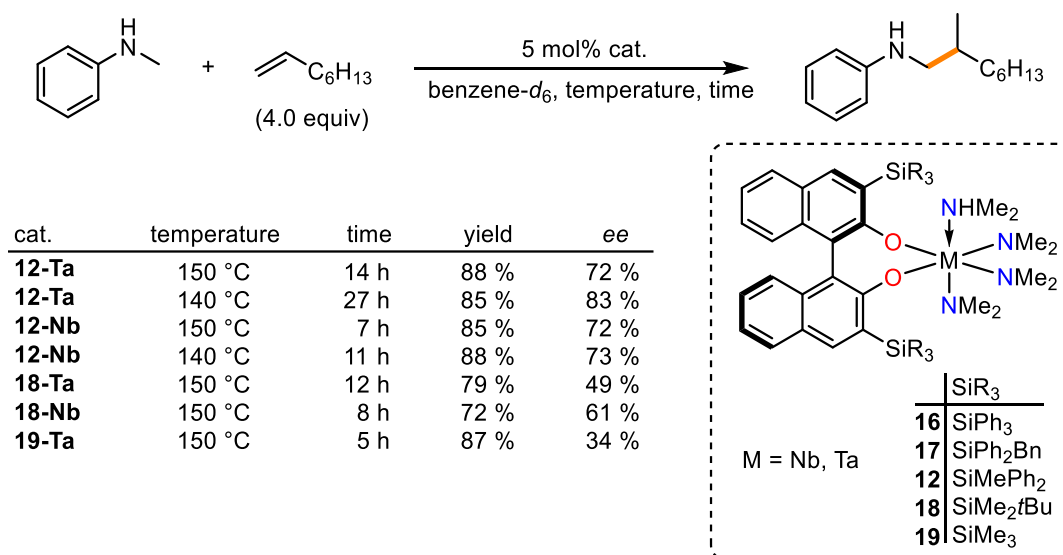


| cat. | mol% | temperature | time | yield |
|---|---|---|---|---|
| **7** | 5 | 110 °C | 63 h | 85 % |
| **13** | 5 | 110 °C | 77 h | 69 % |
| **14** | 5 | 110 °C | 68 h | 96 % |
| **15** | 10 | 130 °C | 77 h | 71 % |
| [Ta(NMe$_2$)$_5$] | 5 | 110 °C | 1 week | 0 % |
| [Ta(NMe$_2$)$_5$] | 5 | 130 °C | 67 h | 89 % |

| cat. | R$^1$ | R$^2$ |
|---|---|---|
| **7** | *t*Bu | *i*Pr |
| **13** | *t*Bu | Me |
| **14** | Ph | *i*Pr |

*Scheme 7:* Hydroaminoalkylation of *N*-methylaniline and 1-octene catalyzed by tantalum(V) complexes bearing mono- and bis(amidate)-based ligands.[74]

The catalysts became more active as more bulky substituents were introduced and thus **7** has shown the highest reactivity compared to **13** and **14**. The electronic features of the amidate ligands are required for catalytic activity and no conversion was observed if pentakis(dimethylamido)tantalum(V) is used under the same conditions. Interestingly, they observed the spontaneous formation of tantallaaziridine **15** upon the addition of two equiv of *N*-(2,6-dimethylphenyl)pivalamide to pentakis(dimethylamido)tantalum(V). The bis(amidate)-tantalum(V) complex **15** has also shown to be active, however, harsher conditions, like elongated reaction times to several days, higher temperatures and higher catalyst loading, were necessary to obtain good yields. In contrast, only 67 h and 5 mol% catalyst loading of the pentakis(dimethylamido)tantalum(V) precursor were sufficient to give 89 % of the desired product. These results suggest that bulky substituents are necessary to increase the reactivity of the catalyst. However, a severely crowded coordination sphere with bulky ligands could prevent alkene insertion and thus inhibit the catalytical activity. This has also been proven and stochiometric reactions of **15** with various alkenes, internal alkynes and conjugated ketones at elevated temperatures of 90 °C were unsuccessful.[71] It is anticipated that steric bulk is required to facilitate the C–H activation. Hence, bisligated complex **15** is already spontaneously formed at room temperature.

Phosphoramidate tantalum(V) complex **8** is an highly active catalyst which operates already at room temperature.[41] Complex **8**, gave the desired hydroaminoalkylation product in yields ranging from 41 to 93 % in mostly under 20 h. Additionally, the authors demonstrated that even the challenging secondary aliphatic amines, such as *N*-methylcyclohexylamine and dibutylamine, can be suitable substrates. However, the precatalyst has shown to be highly sensitive to steric bulk and because of that, *tert*-butylmethylamine did not participate in the hydroaminoalkylation reaction. Since the catalyst operates at room temperature, it was possible to investigate the hydroaminoalkylation of temperature sensitive vinylarenes. Both, electron-rich and electron-deficient vinylarenes, gave good yields of up to 93 % if the reaction time was elongated to 168 h. The desired products were obtained in 58 to 91 % yield if the reaction mixture was heated at 50 °C for 20 h.

### 1.2.2. Enantioselective Hydroaminoalkylation

Only a few catalytically active Group 5 complexes, which facilitate the hydroaminoalkylation in an enantioenriching fashion, have been developed to date.[40,74,76] One group of these Nb(V) and Ta(V) complexes are based on the 3,3'-silylated binaphtholate ligand scaffold.[40,77] They were found to exhibit good reactivity with yields up to 91 % and enantioselectivities as high as 98% *ee* were obtained (Scheme 8).



| cat. | temperature | time | yield | ee |
|------|-------------|------|-------|-----|
| **12-Ta** | 150 °C | 14 h | 88 % | 72 % |
| **12-Ta** | 140 °C | 27 h | 85 % | 83 % |
| **12-Nb** | 150 °C | 7 h | 85 % | 72 % |
| **12-Nb** | 140 °C | 11 h | 88 % | 73 % |
| **18-Ta** | 150 °C | 12 h | 79 % | 49 % |
| **18-Nb** | 150 °C | 8 h | 72 % | 61 % |
| **19-Ta** | 150 °C | 5 h | 87 % | 34 % |

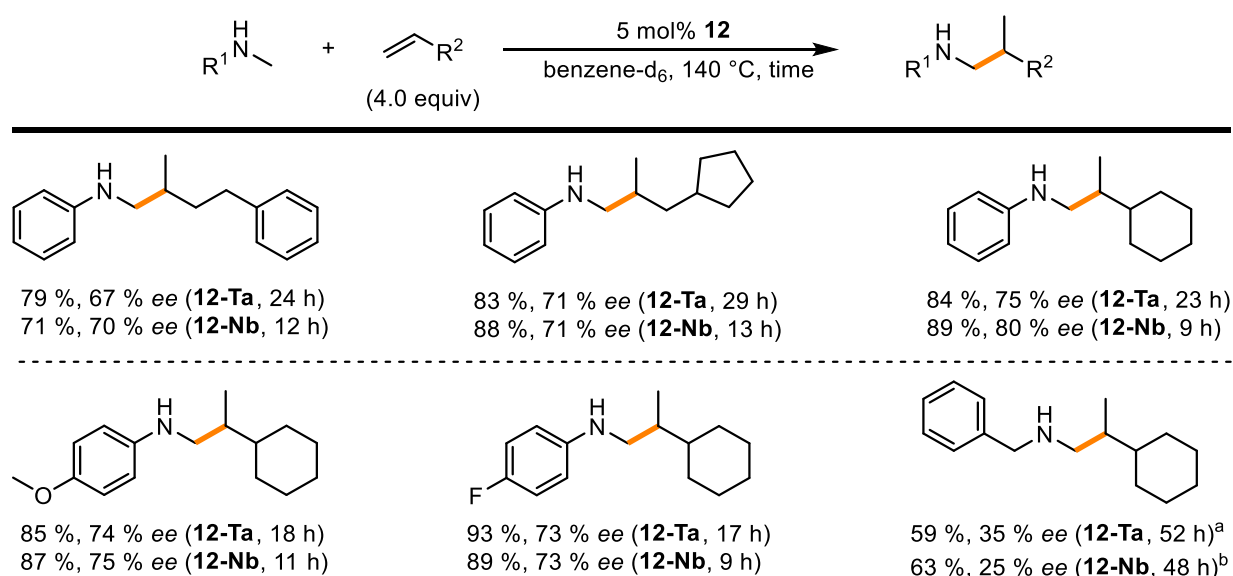| | SiR$_3$ |
|---|---------|
| **16** | SiPh$_3$ |
| **17** | SiPh$_2$Bn |
| **12** | SiMePh$_2$ |
| **18** | SiMe$_2$*t*Bu |
| **19** | SiMe$_3$ |

*Scheme 8:* Asymmetric hydroaminoalkylation of *N*-methylaniline with 1-octene in the presence of different Nb(V) and Ta(V) catalysts.[40]

The substituents on the Si atoms crucially determined the activity and enantioselectivity of the catalysts. Complexes **12-Ta** and **12-Nb**, which bear a SiMePh$_2$ groups display reasonably high

activity and yields as high as 88 % were obtained after less than 28 h. The bulk of the SiMePh$_2$ groups was necessary to obtain high enantioselectivities of up to 83 %. Interestingly, complexes **16-M** and **17-M**, which bear much bulkier phenyl and benzyl groups on the Si atoms, are almost inactive and only yield traces of the desired product. This is another empirical hint for the overly sensitive correlation of sterically demanding ligands and the catalytic activity of Group 5 complexes. The complexes **18-Ta**, **18-Nb** and **19-Ta**, which bear smaller silyl groups than **12-Ta** and **12-Nb**, were catalytically more active, however, lower enantioselectivities were obtained.

Catalysts **12-Nb** and **12-Ta** facilitated the hydroaminoalkylation reaction of *N*-methylanilines with unactivated alkenes in high yields of the Markovnikov product with good *ee*-values. The individual catalyst showed similar results for the same reaction and are therefore quite comparable; except for the fact that lower reaction times are needed for **12-Nb** than for **12-Ta**. The dialkylamine *N*-methylbenzylamine has shown to be much less reactive than its aniline counterparts and harsher reaction conditions were required to facilitate the hydroaminoalkylation reaction. The reaction of *N*-methylbenzylamine with vinylcyclohexane required 150 °C, 48 h and 7 mol% of **12-Nb** to yield 63 % of the product with 25 % *ee*. Much harsher conditions were necessary in the presence of **12-Ta**, and after 52 h at 180 °C with 10 mol% catalyst loading 59 % of the desired product with an *ee* of 35 % were formed. In both instances a minor percentage of the benzylic C–H activated regioisomer formed.



79 %, 67 % *ee* (**12-Ta**, 24 h)
71 %, 70 % *ee* (**12-Nb**, 12 h)

83 %, 71 % *ee* (**12-Ta**, 29 h)
88 %, 71 % *ee* (**12-Nb**, 13 h)

84 %, 75 % *ee* (**12-Ta**, 23 h)
89 %, 80 % *ee* (**12-Nb**, 9 h)

85 %, 74 % *ee* (**12-Ta**, 18 h)
87 %, 75 % *ee* (**12-Nb**, 11 h)

93 %, 73 % *ee* (**12-Ta**, 17 h)
89 %, 73 % *ee* (**12-Nb**, 9 h)

59 %, 35 % *ee* (**12-Ta**, 52 h)[a]
63 %, 25 % *ee* (**12-Nb**, 48 h)[b]

*Scheme 9:* Asymmetric intermolecular hydroaminoalkylation reaction of unactivated alkene and amine substrates in the presence of Nb(V) and Ta(V) catalysts **12-Nb** and **12-Ta**. a) reaction conditions: 10 mol% **12-Ta**, 180 °C. b) reaction conditions: 7 mol% **12-Nb**, 150 °C.[40]

### 1.2.3. Examples for Valuable Synthetic Strategies involving Hydroaminoalkylation

An excellent demonstration regarding the huge potential of the hydroaminoalkylation reaction is displayed in the synthesis of 1,5-benzodiazepines starting from simple *N*-allyl-2-bromoanilines and *N*-methylanilines (Scheme 10).[36] The target molecules were conveniently accessed *via* a one-pot strategy, performing a hydroaminoalkylation using catalyst **20**, which exclusively yields the Markovnikov product followed by the addition of a palladium catalyst to enable the intramolecular Buchwald-Hartwig amination.[60] The authors reported good overall yields ranging from 51 to 73 %.
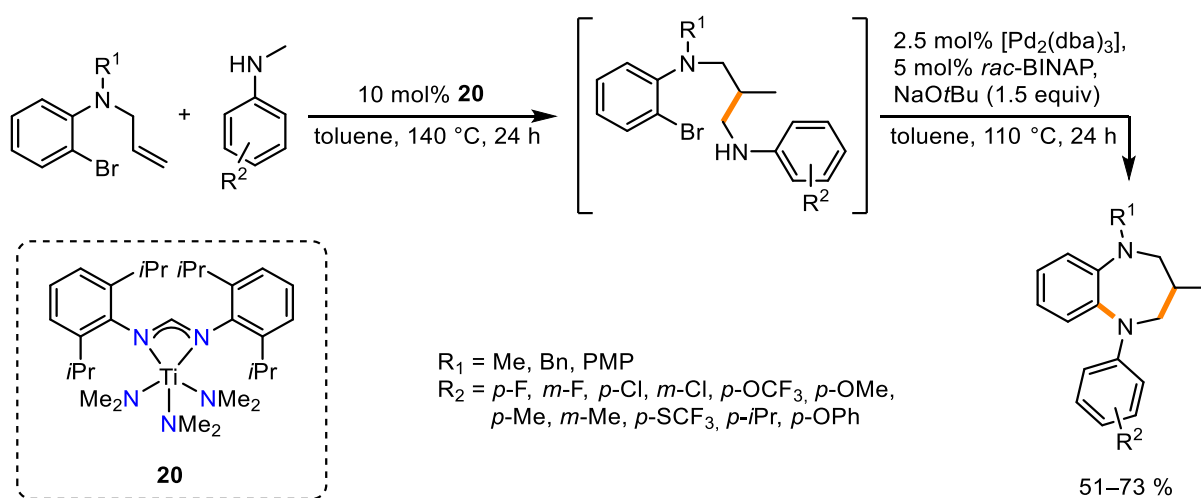


*Scheme 10:* One-pot-synthesis of 1,5-Benzodiazepines starting from different *N*-allyl-2-bromoanilines and various *N*-methylanilines.[36]

The hydroaminoalkylation reaction does not only give access to complex biologically relevant molecules but is also a highly interesting method for the synthesis of amine-containing polymers. The stereospecific functionalization of vinyl containing polyolefins might be of great interest for the development of novel materials.[11,12]

### 1.3. Hydroamination

The hydroamination reaction is a highly attractive method, where the N–H bond is inserted into C–C multiple bonds. However, despite tremendous efforts studying the hydroamination process in the last 60 years, the anti-Markovnikov addition is still one of the most persistent problems in catalysis and first reports were only published recently.[78–80] The Markovnikov addition on the other hand is a well explored and suitable synthesis strategy.

One of the earlier reports on transition metal-catalyzed additions of secondary amines to ethylene was published by Coulson in 1971.[81] Even though the first reported hydroamination reactions catalyzed by transition metals included alkenes as substrates, it was proven that simple nonactivated alkenes are a rather challenging substrate class and quite unreactive compared to other unsaturated C–C functionalities, such as dienes, vinylarenes, allenes and alkynes (Scheme 11).
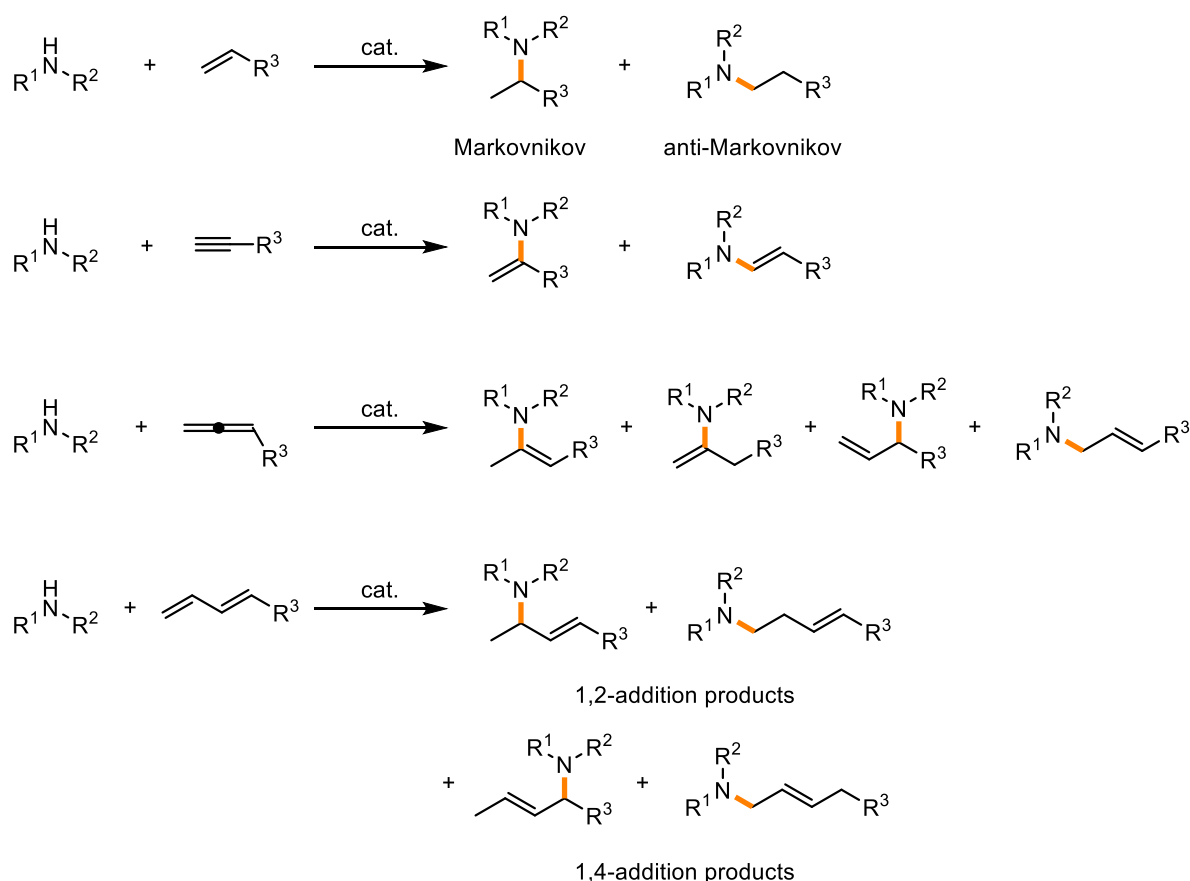


Scheme 11: Different unsaturated substrates in hydroamination and their products.

The main reasons for this, to briefly elaborate, are different C–C π-bonds which participate in the various proposed reaction mechanisms. Dienes can form an $\eta^3$-organometallic complex in the presence of an acidic proton or by migratory insertion with an metal hydride, leading to a more feasible nucleophilic attack from amines.[26,82–84] Vinylarenes can react in a quite similar fashion and the arene moiety can function as an additional coordinative side.[85,86] Allenes and alkynes have a higher electron density, thus coordinate more easily to a transition metal.[83,87,88]

The intermolecular hydroamination of simple, nonactivated olefins is a far less feasible process than the corresponding intramolecular reaction and thus only a few systems have been published.[86,89–92] This can be generally explained by the electrostatic repulsion between the

lone pair electrons of the nitrogen and the electron-rich π-bond of the akene, which not only leads to a high activation barrier, but also to a kinetically and thermodynamically disfavour compared to an intramolecular hydroamination.[86] A conventional [2+2]-cycloaddition of N–H bonds with C=C double bonds is orbital-forbidden under thermal conditions, but can be achieved by light irradiation.[93] Additionally, the weakly binding alkenes have to compete with strongly coordinating amines for vacant coordination sites at the metal centre if early-transition-metal catalysts are used. Therefore, a better catalyst performance in intermolecular reactions may be achieved if an excess of alkene is used.

Alkali metals, as well as metal hydrides, historically played a major role in intermolecular hydroaminations and similar systems are still under investigation.[94–97] Traditionally, these reactions come alongside harsh reaction conditions, such as high temperatures, as well as high pressures and are known to show less tolerance towards polar functional groups compared to late-transition metals.[94–96,98] Early-transition-metals from Group 4,[99–102] late transition metals,[90,92,103] as well as complexes from rare-earth elements, like scandium, yttrium and the f-block elements[91,104–112] have been used to study the addition of a N–H bond across unsaturated C–C bonds. Rare-earth metal complexes have shown to be highly efficient in the catalysis of intramolecular hydroaminations of unsaturated C–C compounds, such as olefins, dienes, vinylarenes, allenes and alkynes featuring remarkably high turnover frequencies and excellent stereoselectivities. However, a catalytic system which efficiently facilitates the cyclization of an aminoalkene may operate with significantly reduced to no conversion rates in intermolecular hydroamination reactions.[86,110] To give an example, the intermolecular hydroamination of 1-pentene and $n$-propylamine in the presence of a neodymium(III) catalyst, bearing a dimethylsilyl-bridged biscyclopentadienyl ligand, leads to the formation of $N$-propyl-1-methylbutylamine (Scheme 12; equation 8).
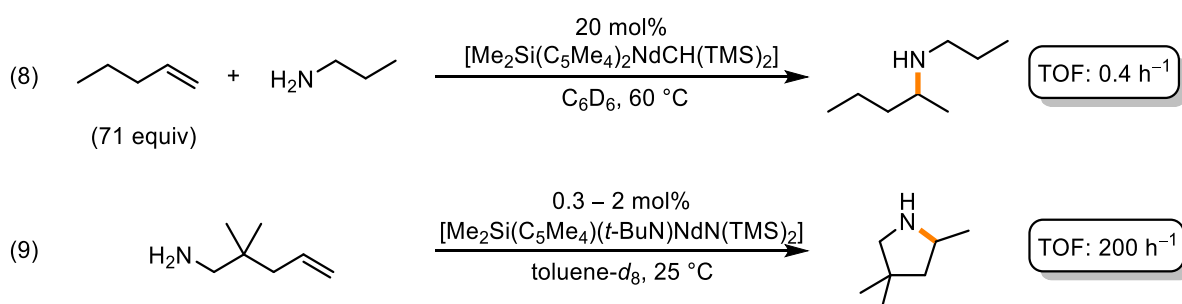


Scheme 12: Intermolecular (8) and intramolecular (9) hydroamination catalyzed by neodymium(III) complexes.[89,113]

The reaction requires an unflattering 71 equiv of the nonactivated alkene, 60 °C and a catalyst loading of 20 mol%, while only showing a turn-over frequency (TOF) of 0.4 h$^{-1}$.[89] Recent reports in early-transition-metal-based intermolecular hydroaminations show that the excess of the unactivated alkene can be scaled down to 1 to 5 equiv,[92] but 10 to 15 equiv[91,114,115] represent an acceptable range to give satisfying yields. The intramolecular hydroamination of 2,2-dimethyl-4-pentenylamine to 2,4,4-trimethylpyrrolidine catalyzed by a similar neodymium silyl-bridged amido cyclopentadienyl system does not only show a higher TOF of 200 h$^{-1}$, but also requires only 0.3 to 2 mol% catalyst loading at 25 °C (Scheme 12; equation 9).[113] In this particular comparison, the intramolecular hydroamination is approximately 500 times more rapid than the intermolecular hydroamination and requires only a fraction of the catalyst loading and lower reaction temperatures.

The first mechanism for the Group 4 and Group 5 metal-catalyzed hydroamination was proposed by Bergman *et al.* in 1992 (Scheme 13).[116,117]
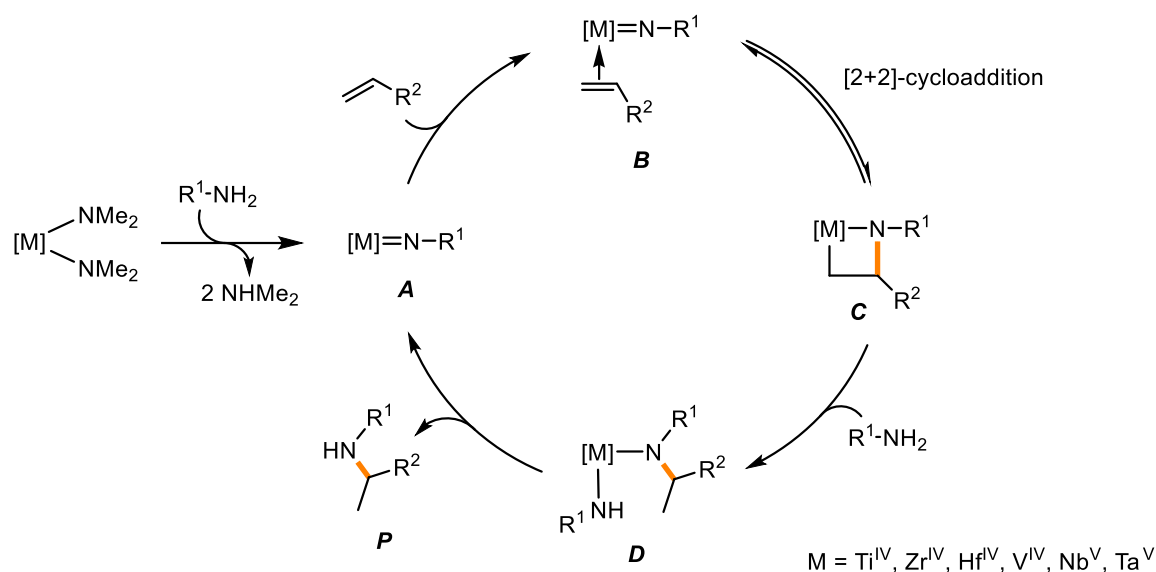


*Scheme 13:* Proposed catalytic cycle for the Group 4- and Group 5-based hydroamination of alkenes with primary amines.[116,117]

Originally, the authors addressed the hydroamination using alkynes, but the mechanism for unactivated alkenes is thought to be the same. In a first step, if starting from a bis(amido)complex, both amido ligands are replaced by one primary amine, yielding imido complex **A**. After the coordination of an alkene to form intermediate **B**, a reversible [2+2]-cycloaddition can take place to form metallaazetidine **C**. An additional amine substrate opens the four-membered ring by protonolysis and coordinates to form the bis(amido)complex **D**. A second protonolysis of the secondary amido-metal bond regenerates the catalytically active

species **A** and forms the desired hydroamination product **P**. This mechanism for the hydroamination of alkynes has recently been validated experimentally for a tantalum-based heterogeneous catalyst.[118] A spectroscopic state-of-the-art technique, named dynamic nuclear polarization surface enhanced NMR spectroscopy (DNP-SENS) was employed to characterize the individual intermediates of the catalytic cycle and density functional theory (DFT) calculations were performed to validate the results for the proposed mechanism.

Intramolecular hydroamination reactions are usually performed with 2,2-dialkyl- or 2,2-diaryl-aminoalkenes to profit from the Thorpe-Ingold effect.[119] An 2,2-unsubstituted aminoalkene, such as 4-pentenylamine, which is coordinated to a lanthanide or an early-transition-metal complex, would presumably have a staggered, *anti-periplanar* conformation of the propylene moiety in respect to the complex (Scheme 14).



favoured for
R = Me, Ph,
$CH_2(CH_2)_2CH_2$

favoured for
R = H
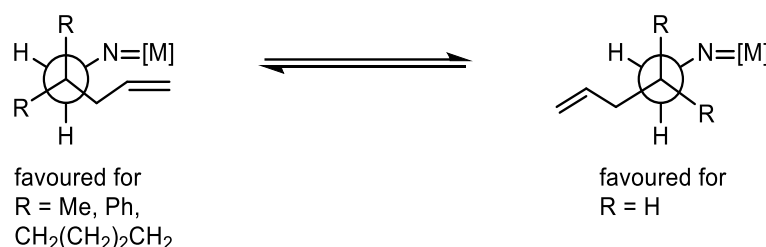
*Scheme 14:* The steric influence of the substituent R on the conformation of an aminoalkene coordinated to a Group 4 or Group 5 complex.

A *gauche* conformation, which is needed to get the olefin into proximity to the metal centre, can be obtained by implementing substituents in position 2. The size of the substituent has a significant influence on the cyclization rates, leading to higher rates for more sterically demanding substituents.[114]

## 1.3.1. Early-Transition-Metal catalyzed Hydroamination

Early-transition-metals play a key role in the hydroamination catalysis. Especially, Group 3 metals have shown to be highly active and regioselective in the hydroamination of unactivated alkenes.[91,114,115,120–122] Group 4 metals are usually significantly less reactive than Group 3 metals or lanthanides; however, since they are well explored due to their applicability in polymerization and are also inexpensive, earth abundant metals, it is of great interest to investigate their activity in the hydroamination reaction.[123] Group 4 metals-based catalysts are typically employed in the intra- or intermolecular hydroamination of alkynes or allenes and only

a few reports of intramolecular, and no reports addressing the intermolecular hydroamination of unactivated alkenes, have been published so far.[35,99–102,124]

The Group 5 metals have not been employed very frequently in hydroamination catalysis.[40,76,125–127] The underlying reason is the generally poor activity or inactivity in hydroamination and in the preference of the Group 5 elements to catalyze the hydroaminoalkylation, especially if secondary amines are used as substrates. Surprisingly, many reports on Group 5 metal complexes address the asymmetric hydroamination, and three enantioenriching catalyst systems, **16**, **24** and **25**, which were published in the same year are displayed in Figure 3.[40,76,125]



**21**
Bergman *et al.* 2004

**22**
Vendier *et al.* 2004

**23**
Vendier *et al.* 2004

**24**
Johnson *et al.* 2011

**25**
Zi *et al.* 2011

**16**
M = Nb, Ta
Hultzsch *et al.* 2011
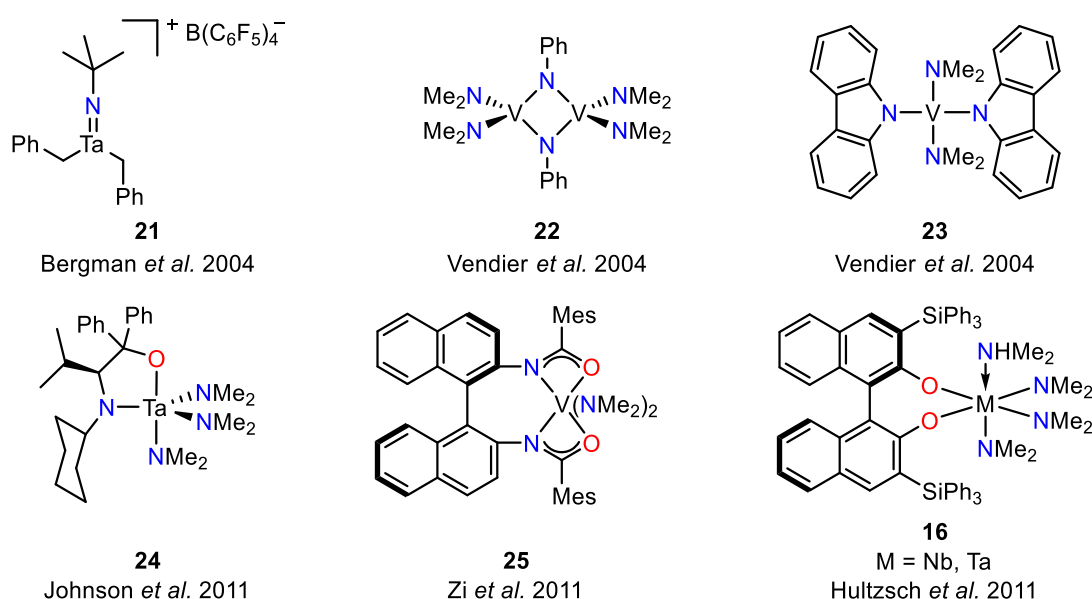
*Figure 3:* Selected Group 5-based compounds which catalyze the hydroamination reaction.[40,76,125–127]

In 2004, the first neutral and cationic tantalum(V) complexes were prepared, which were found to be catalytically active in the hydroamination of alkynes, norbornene, allene and 1,2-cyclononadiene with primary anilines.[127,128] This was the first example of the intermolecular hydroamination of an alkene, namely norbornene with aniline (Scheme 15).



(2.0 equiv)

10 %

22 %
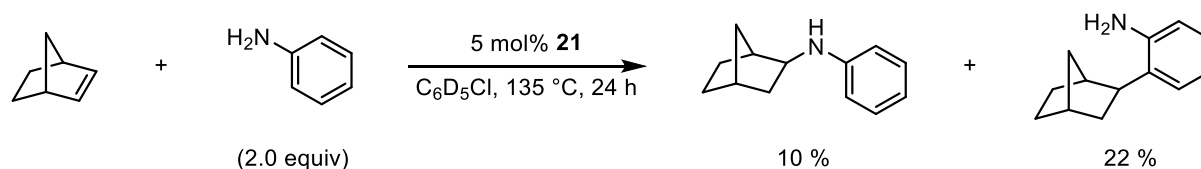
*Scheme 15:* Intermolecular hydroamination of norbornene and aniline in the presence of the cationic tantalum(V) catalyst **21**.[127]

The reaction yielded 10 % of the desired hydroamination product in the presence of catalyst **21**; however, 22 % of a hydroarylated side-product was obtained as well. The authors also reported the formation of a significant amount of polymer and other byproducts, which were not identified further. No reports of Group 5 metal catalyzed intermolecular hydroamination of simple alkenes have been published in the literature.

In the same year, it was shown that tetrakis(dimethylamido)vanadium(IV), **22** and **23** are suitable catalysts to perform the intermolecular hydroamination of internal and terminal alkynes with primary anilines in a regioselective fashion.[126] Pentakis(dimethylamido)tantalum(V) has also shown to be moderately active in this reaction.[126]

To date, only two reports, which address the hydroamination of unactivated alkenes, have been published. Group 5 metal complexes are indeed catalyzing the intramolecular hydroamination of *gem*-2,2-disubstituted aminoalkenes.[40,76] Since both publications address chiral catalysts for asymmetric hydroaminoalkylation and hydroamination, enantioenriched products have been obtained with enantiomeric excesses of up to 80 % (Scheme 16).

| cat. | mol% | temperature | time | product | conversion | *ee* |
|------|------|-------------|------|---------|------------|------|
| **16-Ta** | 5 | 100 °C | 16 h | | >95 % | 64 % |
| **16-Nb** | 5 | 140 °C | 18 h | | >95 % | 50 % |
| **12-Ta** | 5 | 100 °C | 12 h | | >95 % | 10 % |
| | | | | | | |
| [V(NMe$_2$)$_4$] | 10 | 120 °C | 24 h | | 100 % | - |
| [Nb(NMe$_2$)$_5$] | 10 | 120 °C | 24 h | | 100 % | - |
| [Ta(NMe$_2$)$_5$] | 10 | 120 °C | 24 h | | 100 % | - |
| **16-Ta** | 5 | 140 °C | 34 h | | >95 % | 41 % |
| **25** | 10 | 140 °C | 24 h | | 89 % | 76 % |
| **25** | 10 | 130 °C | 28 h | | 20 % | 80 % |

*Scheme 16:* Intramolecular Group 5-based hydroamination of various aminoalkenes bearing different substituents in position 2 and consisting of a linear 5 to 7 membered carbon chain.[40,76]

The 3,3'-disilylated binaphtholate based tantalum(V) and niobium(V) complexes readily yield 2-methyl-4,4-diphenylpyrrolidine from 2,2-diphenylamino-4-pentene. The different substituents on the silyl groups influenced the activity of the complexes ranging from 11 h for the smallest silyl group to 16 h for the triphenyl-substituted silyl group to achieve >95 % conversion. However, the impact of the silyl groups was not as pronounced as in the hydroaminoalkylation. Contrarily, the enantioselectivities were much more pronounced by the substituents on the silyl groups and the highest selectivity was obtained for **16-Ta**. Complex **12-Ta**, which achieved very

good enantioselectivities in the hydroaminoalkylation reaction showed poor enantioselectivity for the intramolecular hydroamination. The dimethylamido complexes of vanadium(IV), niobium(V) and tantalum(V) readily catalyzed the cyclization of 2,2-dimethylamino-4-pentene, a more challenging substrate than its 2,2-diphenylamino-4-pentene analogue and full conversion was achieved after 24 h at 120 °C. Catalyst **16-Ta** required harsher conditions for the same reaction to realize similar results with a moderate enantiomeric excess of 41 %. 10 mol% of V(IV)-based complex **25** yielded up to 89 % of the desired cyclized product with up to 80 % *ee*.

Despite the development of enantioselective Group 5 and Group 4 hydroamination catalysts displaying moderate to good activity and selectivity, such catalysts cannot compete with many catalytic systems based on rare-earth-metals or main group elements.[115,122,129–131] The enantioselective rare-earth-metal-catalyzed intramolecular hydroamination of 2,2-diphenylamino-4-pentene can be accomplished within 15 minutes at room temperature to give excellent yields of up to 98 % and excellent enantiomeric excesses of up to 95 %.[115]


## 1.4.  Previous Work Done in the Hultzsch–Group

After the successful application of the 3,3'-disilylated binaphtholate-based Group 3 and Group 5 metal complexes as catalysts in hydroamination and hydroaminoalkylation, the Hultzsch group decided to further expand the library of possible ligands possessing similar scaffolds. New bisphenolate-type ligands with different spacers between the phenolate units were designed and prepared in order to investigate how the effect of the bite angle of the ligands in the corresponding metal complexes will influence the catalytic activity (Figure 4).
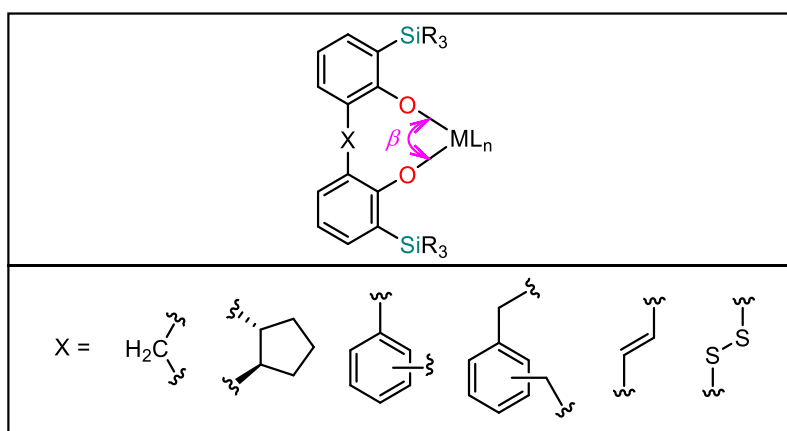


*Figure 4:* Bisphenolate-type ligands with different spacers (X), prepared in the Hultzsch group to influence the bite angle *β* of various early-transition-metal-based complexes.

A correlation between the catalytic activity of a metal complex and the bite angle $\beta$, which is the bond angle between the donor atom, the metal center and a second donor atom in a metal complex, has been the subject of many research papers throughout the last decades.[132,133] The bite angle $\beta$ can have a great impact on the activity and chemoselectivity of metal catalyst.[134,135] Therefore, it was presumed by the Hultzsch group that an increased bite angle $\beta$ might influence the catalytic activity in a beneficial manner.

One of the ligand systems of interest were the stilbene-based bisphenolates. They were synthesized and used for complexation with early-transition-metal salts for the first time by John Soltys in 2013 and 2014 (Scheme 17).[136,137]
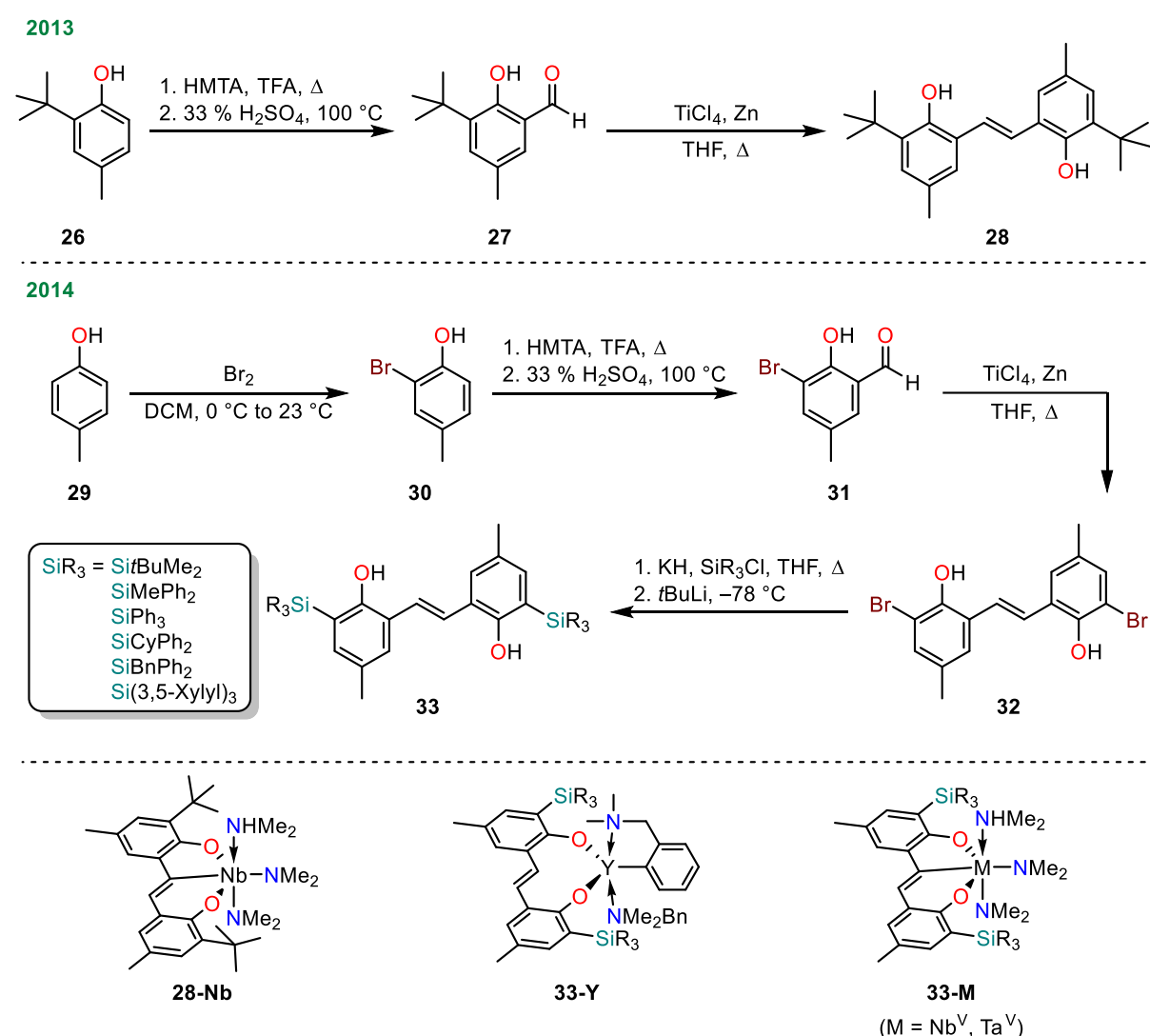


Scheme 17: Developed synthetic routes to prepare ligands **28** and **33**. Prepared early-transition-metal-complexes **28-Nb**, **33-Y** and **33-M** (M = Nb, Ta) are displayed.

The yttrium(III)-complexes **33-Y**, which are based on the ethylene-linked bisphenolate **33** were highly active catalysts in the intramolecular hydroamination of aminoalkenes and intermolecular

hydroamination of alkenes.[138] Preliminary experiments indicated, that the stilbene-based niobium(V)- and tantalum(V)-complexes **28-Nb**, **33-Nb** and **33-Ta** were not active in the intermolecular hydroaminoalkylation reaction of unactivated alkenes with anilines.[138,139] Prior to this thesis, compexes **33-Nb** and **33-Ta** had only been prepared in situ and had been structually characterized by $^1$H and $^{13}$C NMR spectroscopy and single crystal X-ray diffraction analysis.[136–138]

## 2. Aim of Work

The aim of this master thesis project was to investigate the catalytic activity of novel Group 5-based transition-metal complexes in hydroaminoalkylation and hydroamination. Therefore, it was the intention to synthesize 3,3'-bis(arylalkylsilyl)- and 3,3'-bis(alkylsilyl)-substituted 2,2'-dihydroxystilbene ligands, as a part of a greater study concerning the effect of the bite angle on the activity of early-transition-metal catalysts in hydroamination and hydroaminoalkylation, and their niobium(V) and tantalum(V) amido complexes. Different analytical techniques were used to characterize the target compounds, including nuclear magnetic resonance spectroscopy (^{1}H, ^{13}C NMR), single crystal X-ray crystallography and elemental analysis. The prepared metal complexes were investigated in regard to their complexation, behaviour and activity in hydroaminoalkylation and hydroamination catalysis.

# 3. Results and Discussion

## 3.1. Synthesis of O,O-donor Ligands – 3,3'-Bis(arylalkylsilyl)- and 3,3'-Bis(alkylsilyl)-Substituted 2,2'-Dihydroxystilbenes

*para*-Cresol **29** serves as an inexpensive and readily available starting material for the multistep synthesis of ligands **33a-c**. The monobromination of **29** with molecular bromine yields 2-bromo-4-methylphenol **30** in 95 % yield (Equation 1).[136–138,140]
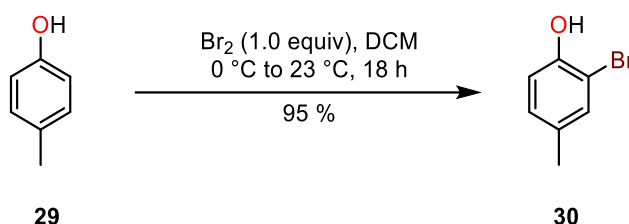


*Equation 1:* Bromination of *para*-cresol **29**.

An aldehyde functionality was implemented into the *ortho* position in respect to the hydroxy group of 2-bromo-4-methylphenol **30** to yield 77 % of the desired 3-bromo-5-methylsalicylaldehyde **31** (Equation 2). This was done *via* the Duff reaction by employing hexamethylenetetramine (HMTA) and trifluoroacetic acid (TFA). The resulting imine was then hydrolysed to give aldehyde **31**.[136–138,141]
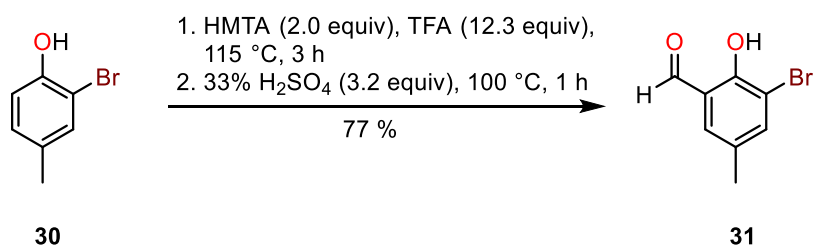


*Equation 2:* Synthesis of 3-bromo-5-methylsalicylaldehyde **31** from 2-bromo-4-methylphenol **30**.

3-bromo-2-hydroxy-5-methylbenzaldehyde **31** was converted into the corresponding 2,2'-dihydroxy-(*E*)-stilbene **32** by performing a McMurry coupling. In this reaction, $TiCl_4$ and zinc powder form a low valent titanium species, which enables the formation of the new C–C bond of the carbonyl carbon atoms and the deoxygenation. After partial removal of the solvent, ethyl acetate, **32** started crystallizing and was obtained in 70 % yield as a pale-yellow solid (Equation 3).[136–138,142]
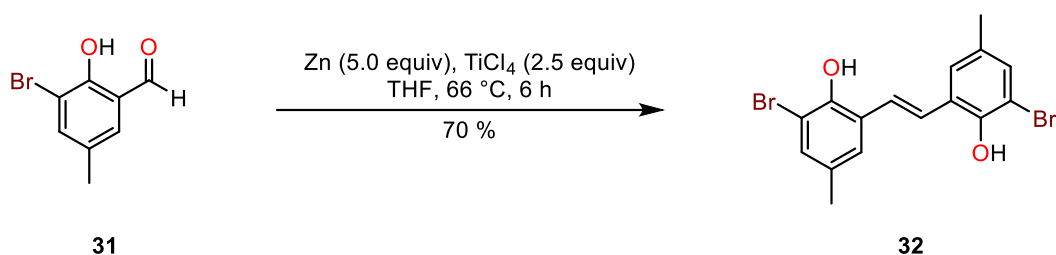
*Equation 3:* Synthesis of 3,3'-dibromo-2,2'-dihydroxy-5,5'-dimethyl-(*E*)-stilbene **32** starting from **31**.

A one-pot silylation-retro-Brook rearrangement was performed to transform 3,3'-dibromo-2,2'-dihydroxy-5,5'-dimethyl-(*E*)-stilbene **32** and the corresponding silyl chloride into the desired 3,3'-bis(arylalkylsilyl)-substituted bisphenolic-(*E*)-stilbenes **33a-c** (Equation 4). A well-established procedure from Yamamoto *et al.*[143] was adopted and slightly modified.[136–138] In the first step, dihydroxy-stilbene **32** was deprotonated using KH, followed by the addition of the silyl chloride to form the silyl ether. Two equiv of *tert*-butyl lithium per bromide yielded the carbanion, which readily attacks the silyl ether in a nucleophilic fashion at the silicone atom to give the anionic pentavalent 1,2-oxasiletanide intermediate. Upon the cleavage of the Si–C bond, the 4-membered-ring is opened and the desired product is formed as the anionic phenolate.[144,145] Depending on the introduced silyl group, **33** was obtained in yields of 38–46 %. Single crystals of compound **33a** and **33b**, suitable for single crystal X-ray diffraction analysis, were obtained by slow evaporation from ethyl acetate and their ORTEP diagrams are displayed in Figure 5.



**33a**  SiR$_3$ = SiMePh$_2$, 38 %
**33b**  SiR$_3$ = SiMe$_2$Ph, 38 %
**33c**  SiR$_3$ = SiMe$_3$, 46 %
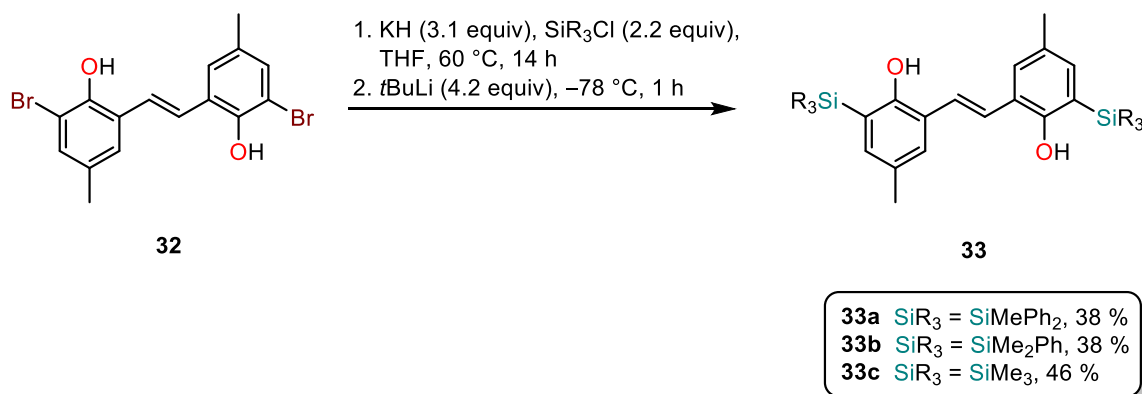
*Equation 4:* Synthesis of 3,3'-bis(arylalkylsilyl)-2,2'-dihydroxy-(*E*)-stilbenes **33a**, **33b** and 3,3'-bis(trialkylsilyl)-2,2'-dihydroxy-(*E*)-stilbene **33c**.
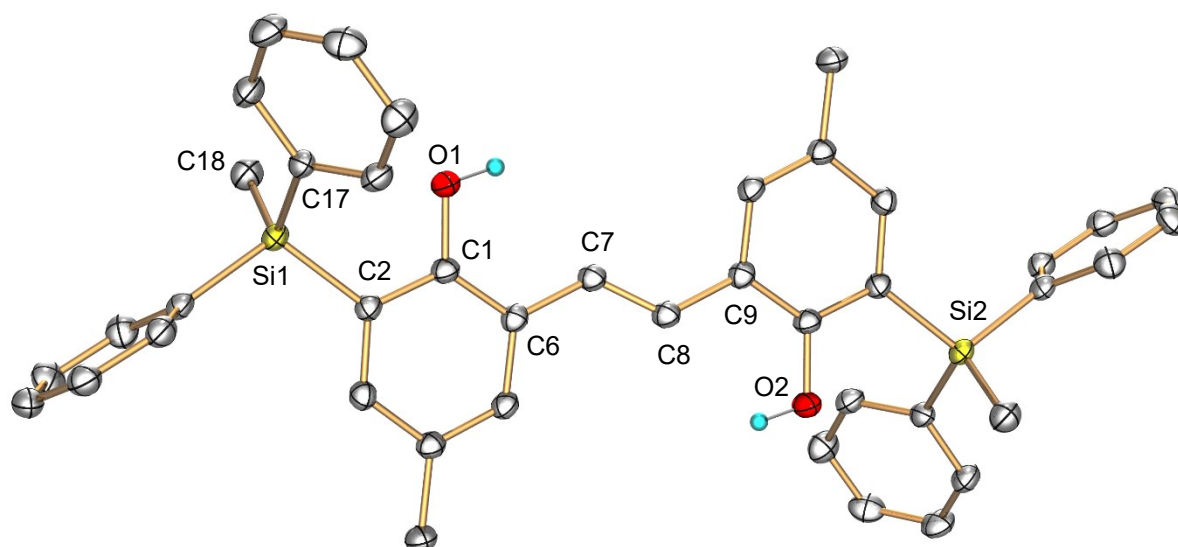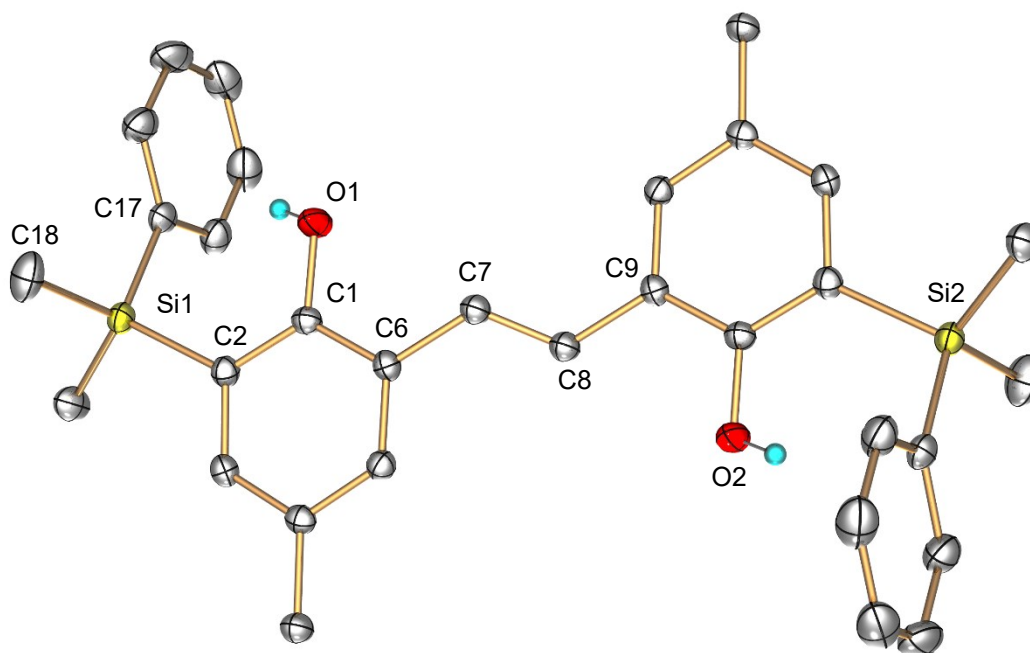
*Figure 5:* ORTEP diagrams of compounds a) **33a** and b) **33b**. Hydrogen atoms, except for the phenolic O*H*, are omitted for clarity and thermal ellipsoids are set at 50% probability.
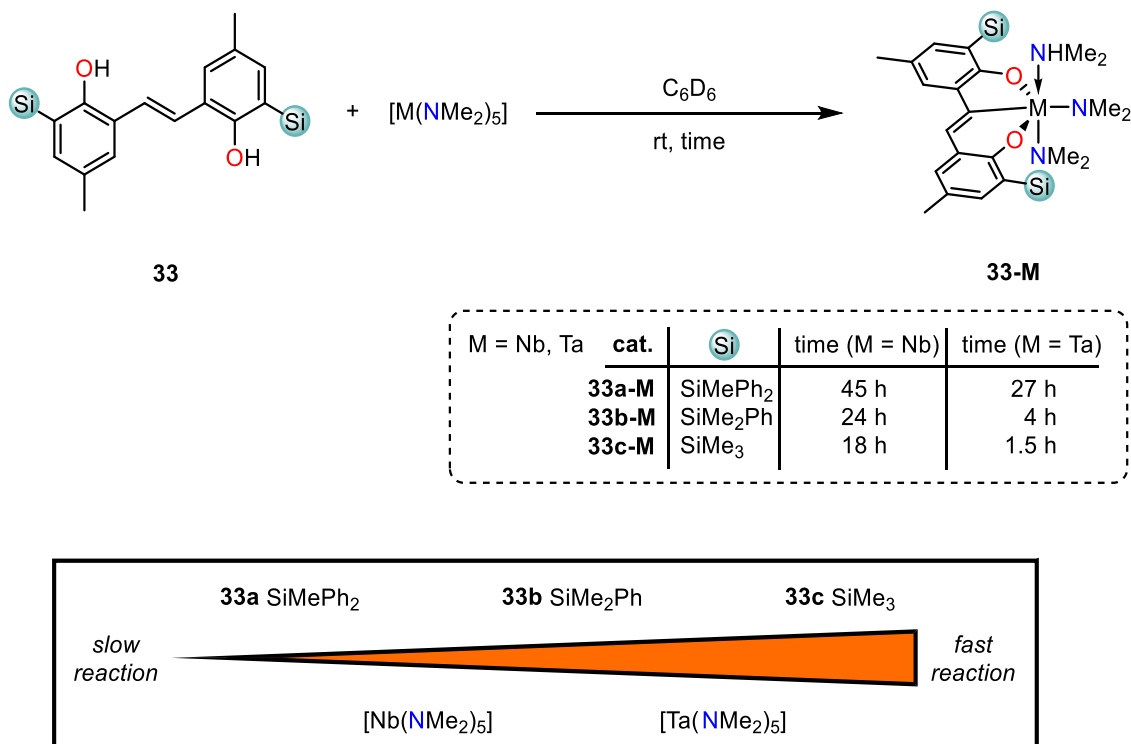
*Table 1:* Selected crystallographic parameters, as well as bond lengths (Å) and torsion angles (°) of compounds **33a** and **33b**.

|  | 33a | 33b |
|---|---|---|
| **Crystal system** | P 1 | P $2_1$/c |
| **Space group** | triclinic | monoclinic |
| **Volume** | 1127.81 Å$^3$ | 1431.34 Å$^3$ |
| **Z** | 1 | 21 |
| **C1–O1** | 1.3723(17) | 1.3859(17) |
| **C6–C7** | 1.465(2) | 1.468(2) |
| **C7–C8** | 1.341(3) | 1.330(3) |
| **Si1–C2** | 1.8781(15) | 1.8776(15) |
| **Si1–C17** | 1.8780(16) | 1.8900(17) |
| **Si1–C18** | 1.8713(17) | 1.8560(19) |
| **C6–C7–C8–C9** | 180.0(1) | 180.0(1) |
| **C1–C6–C7–C8** | 161.1(2) | 155.0(2) |

## 3.2. Synthesis of Nb(V) and Ta(V) Complexes

All complexation reactions were performed under inert conditions. The complexation reactions were conducted on a 0.05 mmol scale, with a ratio of 1:1 of metal precursor to ligand and the reaction was followed by ^{1}H NMR spectroscopy at room temperature.

### 3.2.1. Monoligated Nb(V) and Ta(V) Complexes



| M = Nb, Ta | cat. | Si | time (M = Nb) | time (M = Ta) |
|---|---|---|---|---|
| | 33a-M | SiMePh$_2$ | 45 h | 27 h |
| | 33b-M | SiMe$_2$Ph | 24 h | 4 h |
| | 33c-M | SiMe$_3$ | 18 h | 1.5 h |



*Scheme 18:* Complexation of ligand **33** with pentakis(dimethylamido)niobium(V) or its tantalum(V) analogue at room temperature in C$_6$D$_6$ to yield **33-M**.

The complexation reaction was examined and full complexation to the C–H activated complex **33-M** at room temperature was found to range from 1.5 h to 45 h. All reactions formed **33-M** quantitatively. The reaction times required to obtain the fully C–H activated complexes depended on the metal precursor used, as well as on the size of the silyl substituent of the ligand. Generally, [Ta(NMe$_2$)$_5$] reacted more rapidly with the O,O-donor ligands **33** to **33-M** than [Nb(NMe$_2$)$_5$]. The reaction time was increased with the steric bulk of the silyl groups, meaning ligand **33c** bearing SiMe$_3$ as silyl substituents reacted faster than its SiMe$_2$Ph analogue **33b**, whereas the ligand bearing the SiMePh$_2$ substituents **33a** reacted the slowest (Scheme 18). As an example for the observations made using ^{1}H NMR spectroscopy over time, the reaction of [Nb(NMe$_2$)$_5$] and **33a** at room temperature to form **33a-Nb** is displayed in Figure 6.
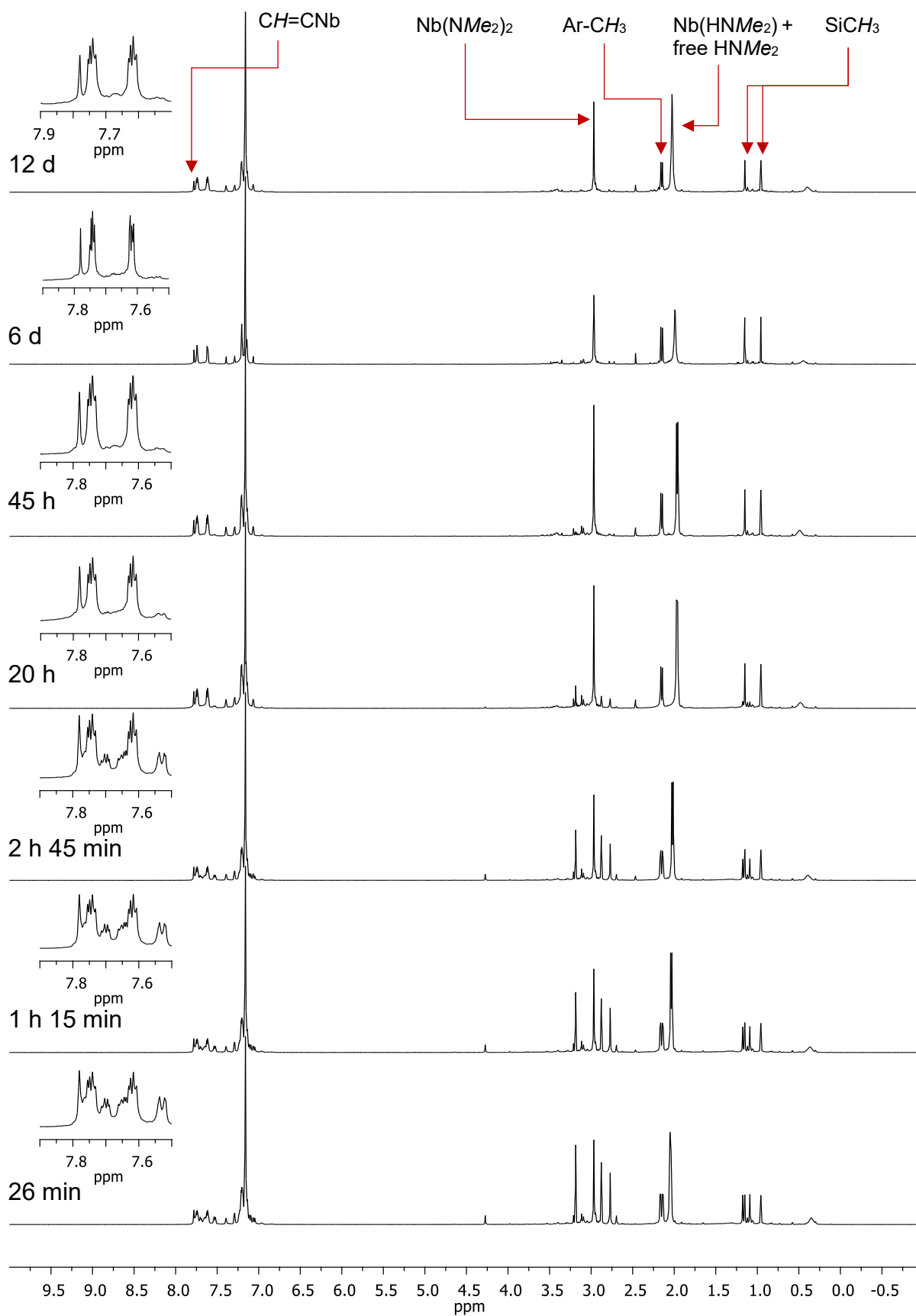
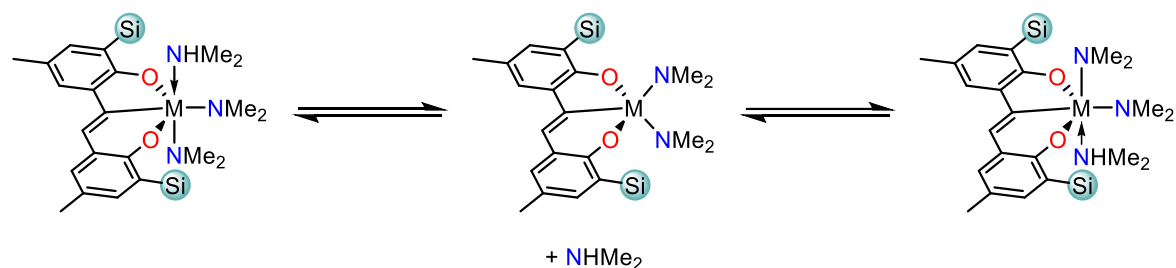*Figure 6*: Monitoring the complexation progress between [Nb(NMe₂)₅] and ligand **33a** at room temperature as a function of time by ¹H NMR spectroscopy. Diagnostic peaks of **33a** are indicated by red arrows.

Regarding the possible mechanism of complexation, it is postulated that upon the coordination of ligand **33**, two molecules of dimethylamine are formed (Scheme 19). One of the two dimethylamine molecules dissociates from the niobium(V) metal centre and the other molecule of dimethylamine presumably remains in the coordination sphere of the metal centre to give **33-M'**. Next, the ethylene-bridge of the ligands coordinates in an $\eta^2$ fashion to form **33-M''**. Evidence for **33-M''** was observed in the $^1$H, as well as in the $^{13}$C NMR spectra of each complex in the early stage of the reaction (Figure 7). The protons of the coordinated ethylene bridge experience a strong upfield shift in the $^1$H and $^{13}$C NMR spectra. Complexes **33-M** are quantitatively formed and intermediates **33-M''** are not detectable after 45 h in any of the complexation reactions at room temperature. The abstraction of one proton of the ethylene bridge by one of the dimethylamido ligands leads to the formation of the C–M bond and yields **33-M**. According to the $^1$H and $^{13}$C NMR spectroscopic experiments, **33-M** is formed quantitatively in all cases.
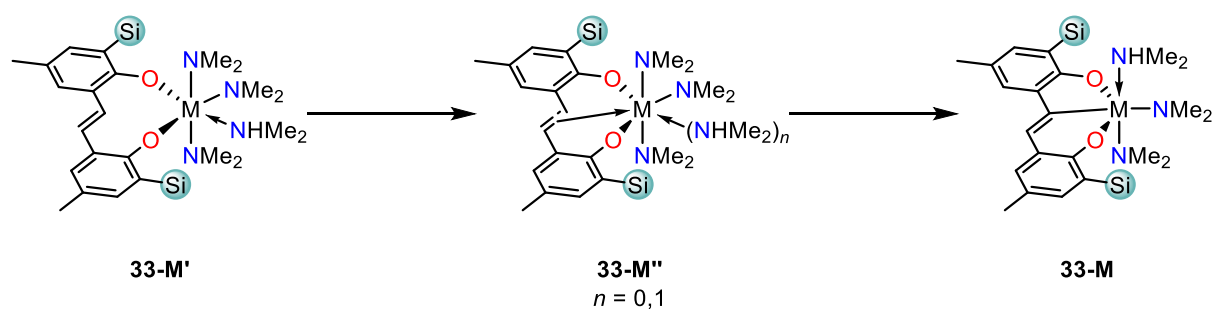


Scheme 19: Hypothesized formation of **33-M** *via* the intermediate **33-M''**.

Once full C–H activation is achieved, complexes **33-M** undergo a fast exchange process with the coordinated dimethylamine and free dimethylamine (Scheme 20).



Scheme 20: Proposed mechanism of amine exchange.
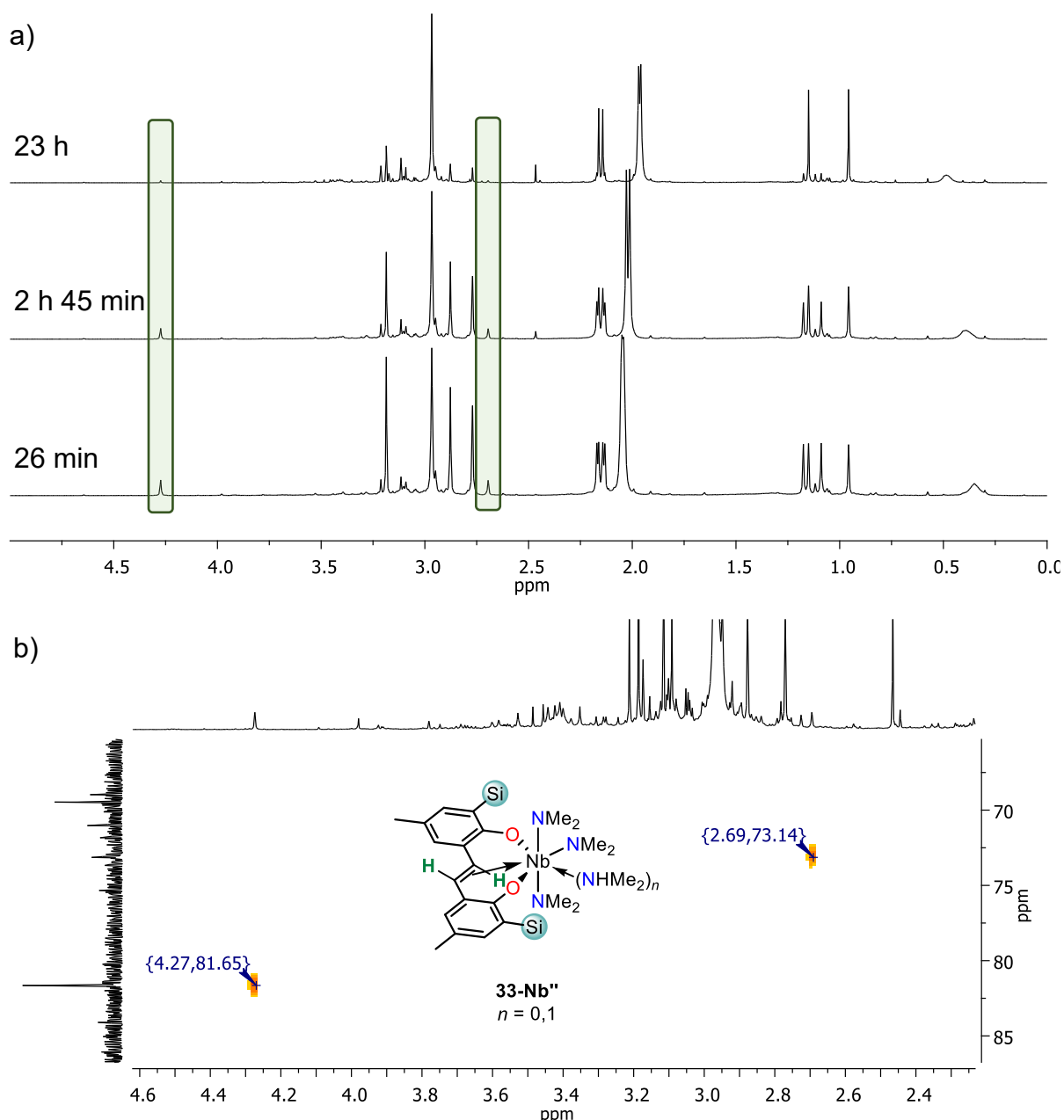
*Figure 7*: a) Section of the monitoring of the complexation progress between [Nb(NMe$_2$)$_5$] and ligand **33a** at room temperature as a function of time by $^1$H NMR spectroscopy from Figure 5. The peaks highlighted in green correspond to the protons of the η$^2$-coordinating ethylene bridge of species **33-M"**. b) $^1$H,$^{13}$C HSQC spectrum of the same reaction after 23 h. Cross peaks correspond to the protons of the η$^2$-coordinating ethylene bridge of **33-M"**.

This is suggested by the NMR spectroscopic data, since only one signal is detected at 25 °C for the coordinated and the free dimethylamine (Figure 8). Additionally, both peaks in the $^1$H and $^{13}$C NMR spectra are relatively sharp, indicating a rapid exchange.[146] After removal of the free dimethylamine, both, the $^1$H NMR spectroscopic signal of the dimethylamido ligands at 3.30 ppm and the signal obtained for the coordinated, as well as the free dimethylamine at 2.11 ppm shift upfield to 3.26 ppm and 1.83 ppm, respectively. The signal of the dimethylamino ligand is
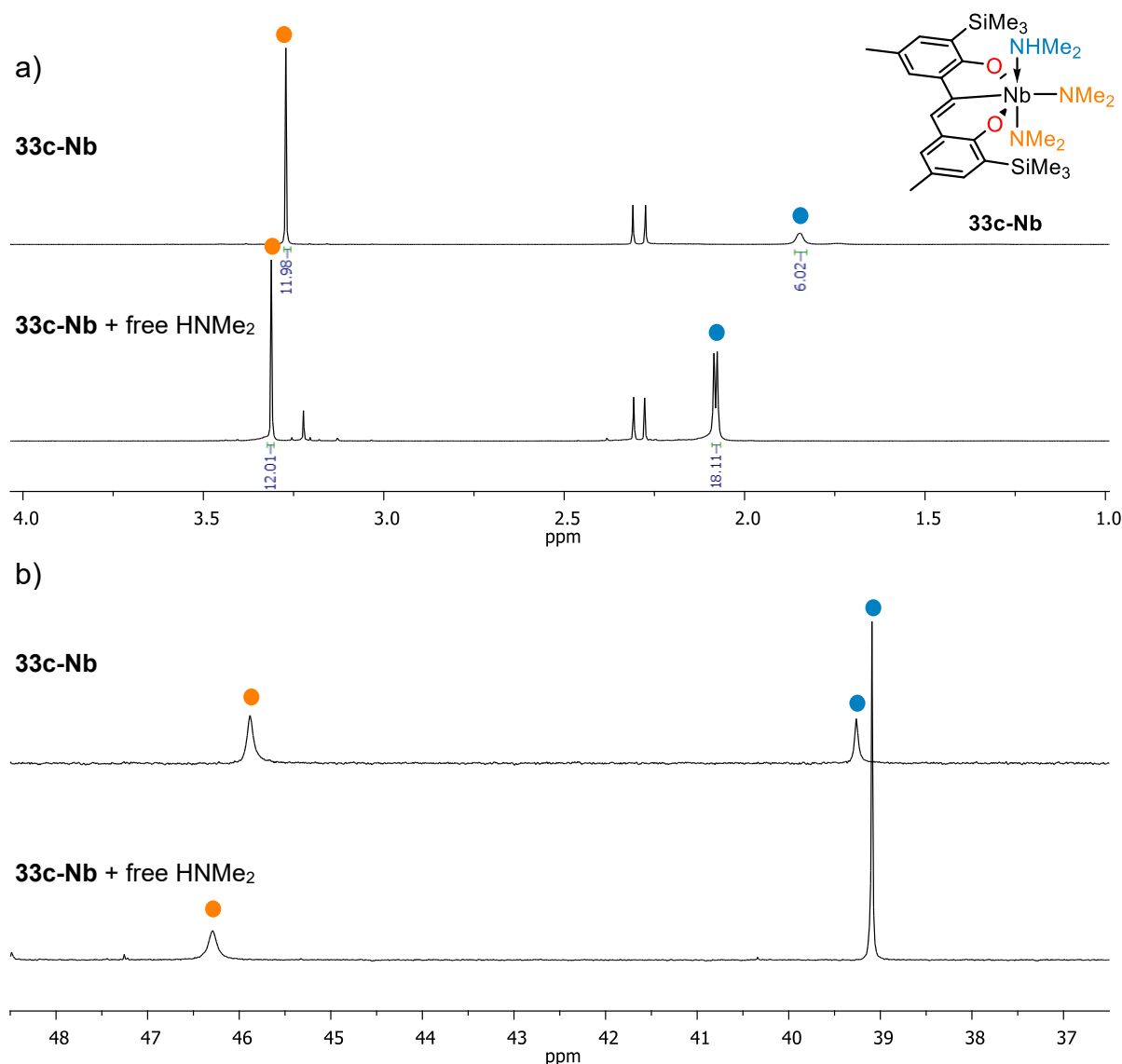
*Figure 8:* a) Selected section of $^1$H NMR spectra of **33c-Nb** after full complexation in the presence of free, uncoordinated dimethylamine (bottom) and **33c-Nb** in absence of free, uncoordinated dimethylamine (top). b) Selected section of $^{13}$C NMR spectra of **33c-Nb** after full complexation in the presence of free, uncoordinated dimethylamine (bottom) and **33c-Nb** in absence of dimethylamine (top). Orange dots indicate the dimethyamido ligands and blue dots indicate coordinated dimethylamine (top spectra) and coordinated as well as free dimethylamine (bottom spectra).

now a broad singulet at 25 °C and both signals of the dimethylamido and amino ligand in the $^{13}$C NMR spectrum are still broad. The reason for the broadening of the mentioned peaks is not yet verified, but it is hypothesized that the rotation around the N–M σ-bond of the dimethylamido ligands and the metal is hindered by the π-donation of the nitrogen into the empty d-orbitals of the metal. The rotational barrier could be reasonably low, making it feasible at room temperature to disrupt the π-donation and enable a rotation around the N–M σ-bond, leading to a reasonably fast exchange and hence peak broadening (Scheme 21).
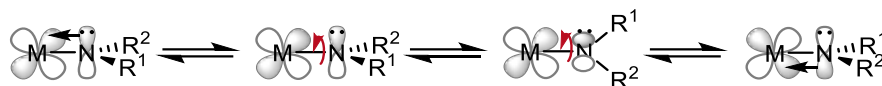
*Scheme 21:* Schematic representation of rotation around the M–N bond.

This phenomenon has already been reported for tantalum(V) and niobium(V) amides bearing cyclopentadienyl ligands.[147–149] Rotational barriers around the M–N σ-bond were sufficiently high and broad signals were obtained at room temperature for $^1$H and $^{13}$C NMR spectra. Alternatively, the broadening of the peaks could be the result of a slower equilibrium reaction (Scheme 20), caused by the absence of an excess of free dimethylamines.

Crystals suitable for single crystal X-ray diffraction analysis were obtained for **33a-Nb**, **33a-Ta**, **33b-Ta**, **33c-Nb** and **33c-Ta** (Figure 9 and Figure 10). Interestingly, all complexes bearing a phenyl moiety on the silyl group show an H–π interaction of the coordinated dimethylamine with the aromatic ring. In the case of **33b-Ta**, an intermolecular instead of an intramolecular H–π interaction of the N*H* and phenylsilyl group is observed. The bond lengths and angles of the complexes are comparable and do not differ significantly, especially within the same ligand system (Table 2). The dimethylamino ligand in complexes **33c-Nb** and **33c-Ta** display a bond length **M–N1** of 2.432(11) and 2.424(2) Å, respectively. Contrarily, complexes **33a-Nb**, **33a-Ta** and **33b-Ta** show a smaller bond length of 2.397(11), 2.394(12) and 2.350(3) Å, respectively. Additionally, **33c-Nb** and **33c-Ta** have the shortest **M–O2** bond with 1.926(9) and 1.920(1) Å, respectively. The shortest **M–C13** bond is observed for **33a-Ta** with 2.175(16) Å, followed by **33c-Ta** and **33b-Ta** with bond lengths of 2.219(2) Å and 2.220(3) Å, respectively. The niobium(V) analogues **33c-Nb** and **33a-Nb** demonstrate faintly longer **M–C13** bonds of 2.228(13) Å and 2.248(16) Å, respectively. The dimethylamido ligand in trans position to the metalated carbon C13 in complexes **33a-Nb**, **33c-Nb**, **33b-Ta** and **33c-Ta** show a distorted geometry and the **M–N2–C3** angle is significantly smaller than the expected 120°. Angular values ranging from 117° down to 111° were observed, indicating an β-agostic interaction of the metal with one of the protons on the methyl group C3. Typical M–N–C angles for transition metal amides, which interact with β-C–H bonds in an agostic manner, range from approximately 95° to 117°, and in some instances angles as low as 80° are observed.[150] This is particularly well displayed in the molecular structures of **33c-Nb** and **33c-Ta** (Figure 9b and Figure 10c). Interestingly, the sterically more demanding methyldiphenylsilyl-based complexes **33a-Nb** and **33a-Ta** bear a flat stilbene backbone, whereas the trimethylsilyl-based compounds **33c-Nb** and **33c-Ta** exhibit a slightly tilted stilbene π-system. This is manifested in the torsion angle **C7–C12–C13–C14** of **33c-Nb** and **33c-Ta**, which is approximately 165° for both complexes. This

value is significantly lower than the same torsion angle of **33a-Nb**, **33a-Ta** and **33b-Ta**, which range from 175° to 178°.
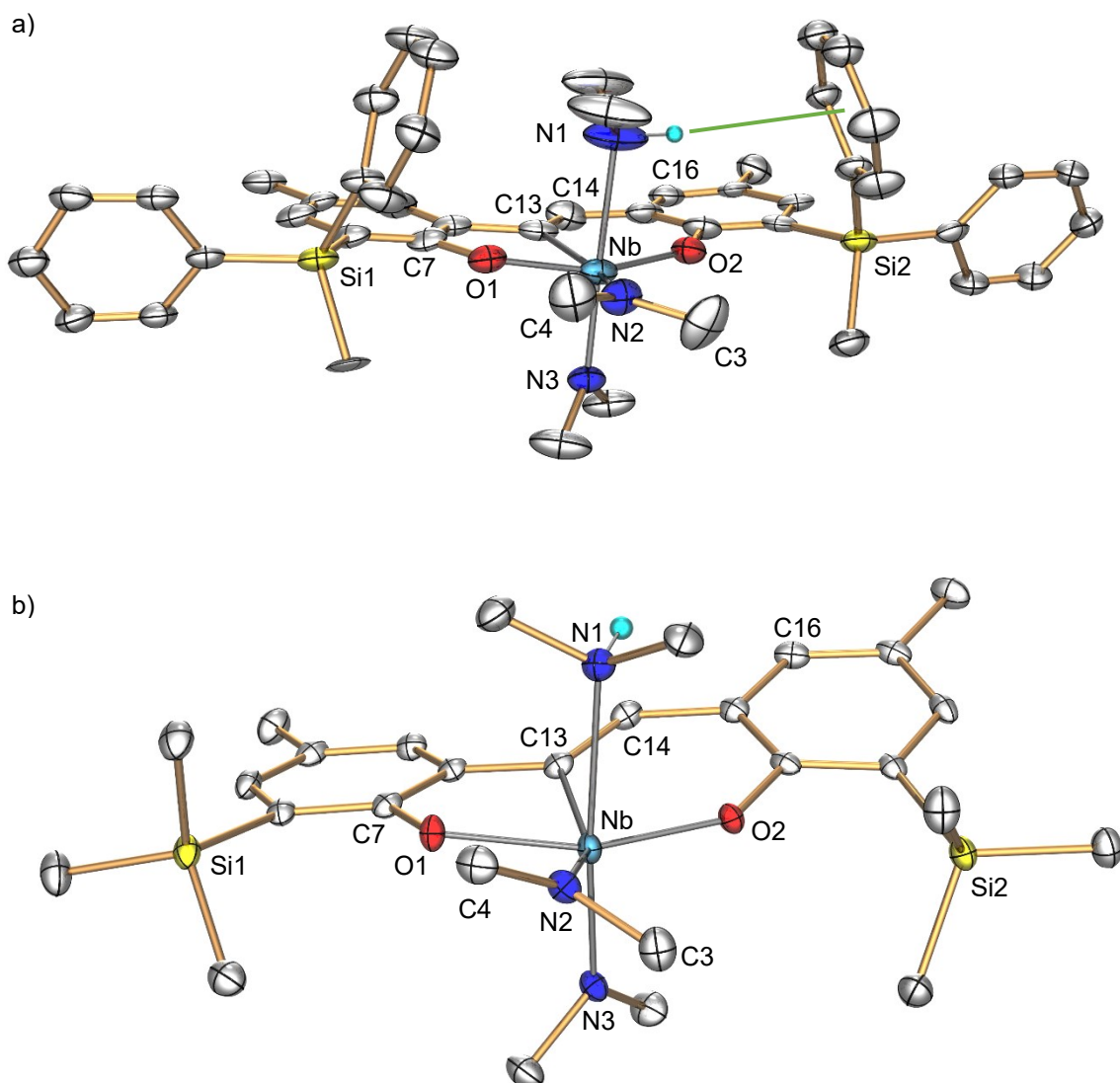
a)



b)



*Figure 9:* ORTEP diagram of complex a) **33a-Nb** and b) **33c-Nb**. The hydrogen on the dimethylamino ligand is shown and thermal ellipsoids are set to 30% probability for **33a-Nb** and to 50% probability for **33c-Nb**. Intermolecular H–π interaction is indicated by green bar.
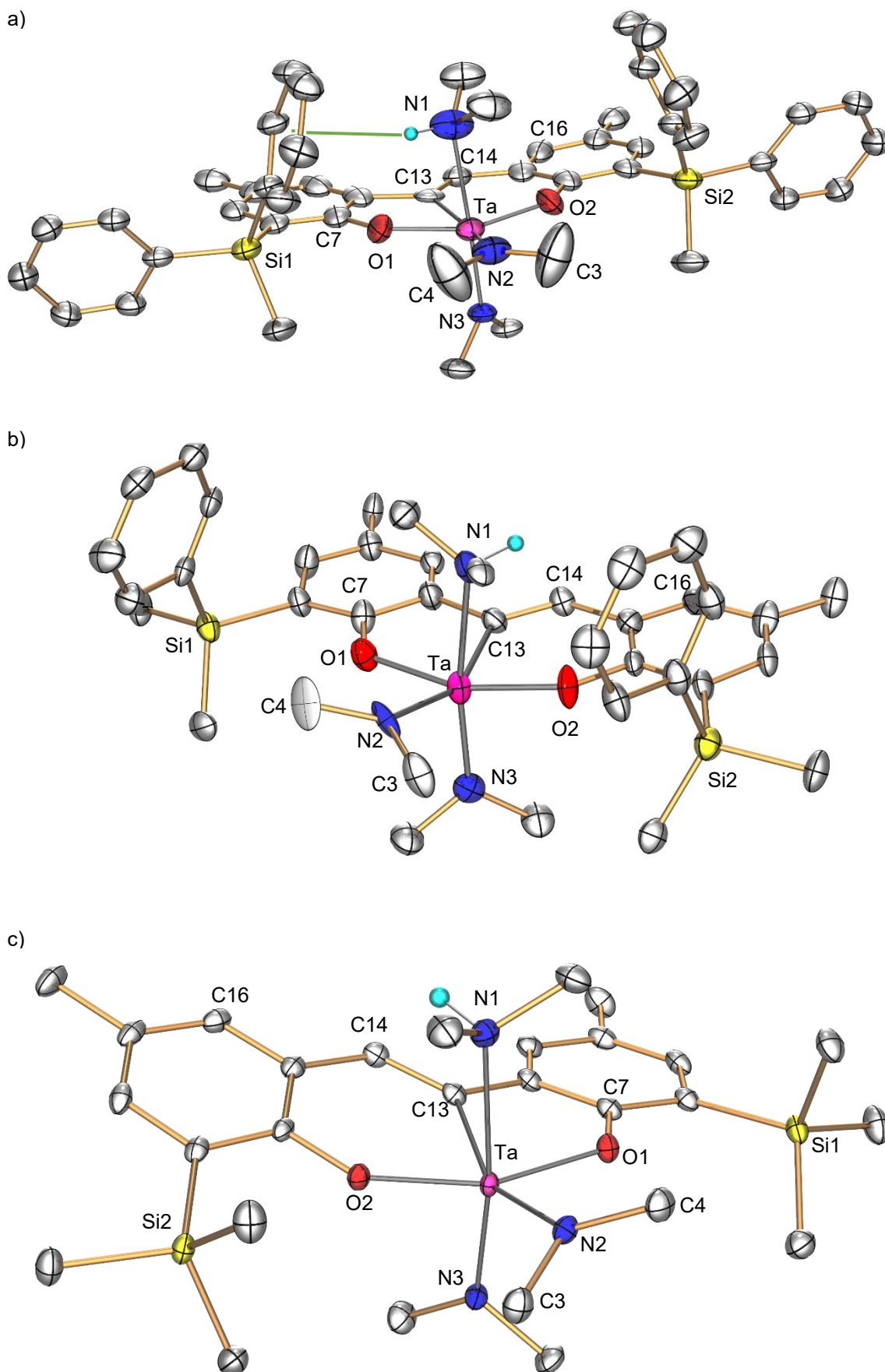
*Figure 10:* ORTEP diagrams of complexes a) **33a-Ta**, b) **33b-Ta** and c) **33c-Ta**. The hydrogen on the dimethylamino ligand is shown and thermal ellipsoids are set to 30% probability for **33a-Ta** and **33b-Ta** and to 50% probability for **33c-Ta**. Intermolecular H–π interaction is indicated by green bar.

*Table 2:* Selected crystallographic parameters, as well as bond lengths (Å), angles and torsion angles (°) of complexes **33a-Nb**, **33c-Nb**, **33a-Ta**, **33b-Ta** and **33c-Ta**.

| | 33a-Nb | 33c-Nb | 33a-Ta | 33b-Ta | 33c-Ta |
|---|---|---|---|---|---|
| **Crystal system** | monoclinic | monoclinic | monoclinic | orthorhombic | monoclinic |
| **Space group** | $P 2_1$ | $P 2_1/n$ | $P 2_1/m$ | $P 2_1 2_1 2_1$ | $P 2_1/n$ |
| **Volume** | 2221.25 Å$^3$ | 3165.88 Å$^3$ | 2228.27 Å$^3$ | 3842.22 Å$^3$ | 3160.56 Å$^3$ |
| **Z** | 2 | 4 | 2 | 4 | 4 |
| **M–N1** | 2.397(11) | 2.432(11) | 2.394(12) | 2.35(3) | 2.424(2) |
| **M–N2** | 1.954(11) | 1.991(11) | 1.959(10) | 2.03(2) | 1.997(2) |
| **M–N3** | 1.974(10) | 1.984(11) | 1.976(9) | 2.02(3) | 1.981(2) |
| **M–O1** | 1.973(13) | 2.0128(9) | 1.945(5) | 2.01(2) | 1.996(1) |
| **M–O2** | 1.985(13) | 1.9260(9) | 1.945(5) | 1.963(19) | 1.920(1) |
| **M–C13** | 2.248(16) | 2.228(13) | 2.175(16) | 2.22(3) | 2.219(2) |
| **C13–C14** | 1.23(2)[a] | 1.3508(18) | 1.347(17) | 1.33(4) | 1.352(3) |
| **M–N2–C3** | 117(1) | 111.77(8) | 129.0(5) | 114(2) | 114.2(1) |
| **M–N2–C4** | 134.8(15) | 135.92(9) | 129.0(5) | 133(2) | 134.34(15) |
| **C3–N2–C4** | 107.5(13) | 112.21(11) | 101.9(11) | 113(2) | 111.50(18) |
| **N1–M–N2** | 86.6(5) | 86.28(4) | 86.1(4) | 87.7(11) | 86.10(7) |
| **N2–M–N3** | 96.1(4) | 101.24(4) | 95.6(4) | 97.3(12) | 100.70(8) |
| **N1–M–N3** | 176.8(7) | 171.84(4) | 171.8(18) | 171.1(11) | 172.07(7) |
| **C13–M–O1** | 76.1(5) | 75.23(4) | 68.1(4) | 74.8(11) | 75.75(7) |
| **C13–M–O2** | 80.7(6) | 82.14(4) | 89.4(4) | 84.3(11) | 82.46(7) |
| **N2–M–O1** | 85.7(7) | 83.96(4) | 100.30(19) | 83.0(10) | 85.50(7) |
| **N2–M–O2** | 116.1(7) | 115.70(4) | 100.30(19) | 115.4(9) | 113.31(7) |
| **N1–M–C13–C14** | 89(2) | 72.5(1) | 88 | 81(3) | 72.7(2) |
| **C3–N2–M–C13** | 170(2) | 165.0(1) | 143 | 168.2(5) | 163.6(2) |
| **C3–N2–M–O2** | 18(2) | 34.4(1) | 10 | 30(2) | 36.3(2) |
| **C7–C12–C13–C14** | 175(2) | 164.9(1) | 178(1) | 175(3) | 165.0(2) |
| **C16–C15–C14–C13** | 179(2) | 179.3(1) | 179(1) | 174(3) | 179.1(2) |
| **C12–C13–C14–C15** | 177(2) | 177.5(1) | 178(1) | 179(3) | 178.0(2) |

[a]Bond length is not correct and might be caused by disorder effects of overlapping structures.

### 3.2.2. Bisligated Ta(V) Complex

All reactions between the ligands **33a-c** and pentakis(dimethylamido)niobium(V) and the ligands **33a** and **33b** with pentakis(dimethylamido)tantalum(V) exclusively yielded the monoligated complexes **33-M**. However, in some cases of the stoichiometric reaction of ligand **33c** with [Ta(NMe$_2$)$_5$] a minor, but not negligible side product was formed (Figure 11, top $^1$H NMR spectra). This arose from the $^1$H NMR spectra, which were collected upon the first synthesis of **33c-Ta** and three peaks in the region of 0.5 to 0.0 ppm were observed, which did not belong to the desired compound. Additionally, unreacted pentakis(dimethyl-amido)tantalum(V) has been detected. In previous experiments, which were carried out in the Hultzsch group, it was found that [Nb(NMe$_2$)$_5$] and 3,3'-di-*tert*-butyl-2,2'-dihydroxy-5,5'-dimethy(*E*)-stilbene **34** react to form the mixture of the monoligated bisphenolate amido complex **34-Nb** and the bisligated complex **(34)$_2$-Nb** as a side product (Scheme 22). Therefore, it was postulated that 2.0 or 2.1 equiv of ligand **33c** and 1.0 equiv of [Ta(NMe$_2$)$_5$] also yield the bisligated Ta(V)-complex (Scheme 23).
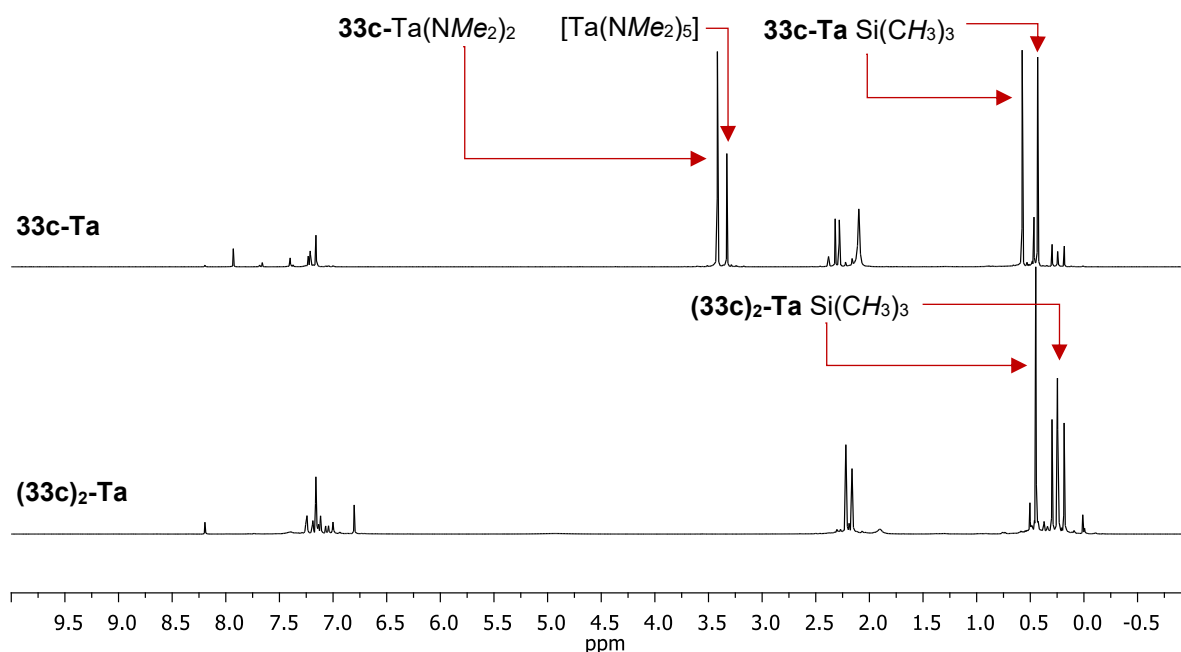


*Figure 11:* $^1$H NMR spectra of the monoligated complex **33c-Ta** (top) and the bisligated complex **(33c)$_2$-Ta** (bottom).
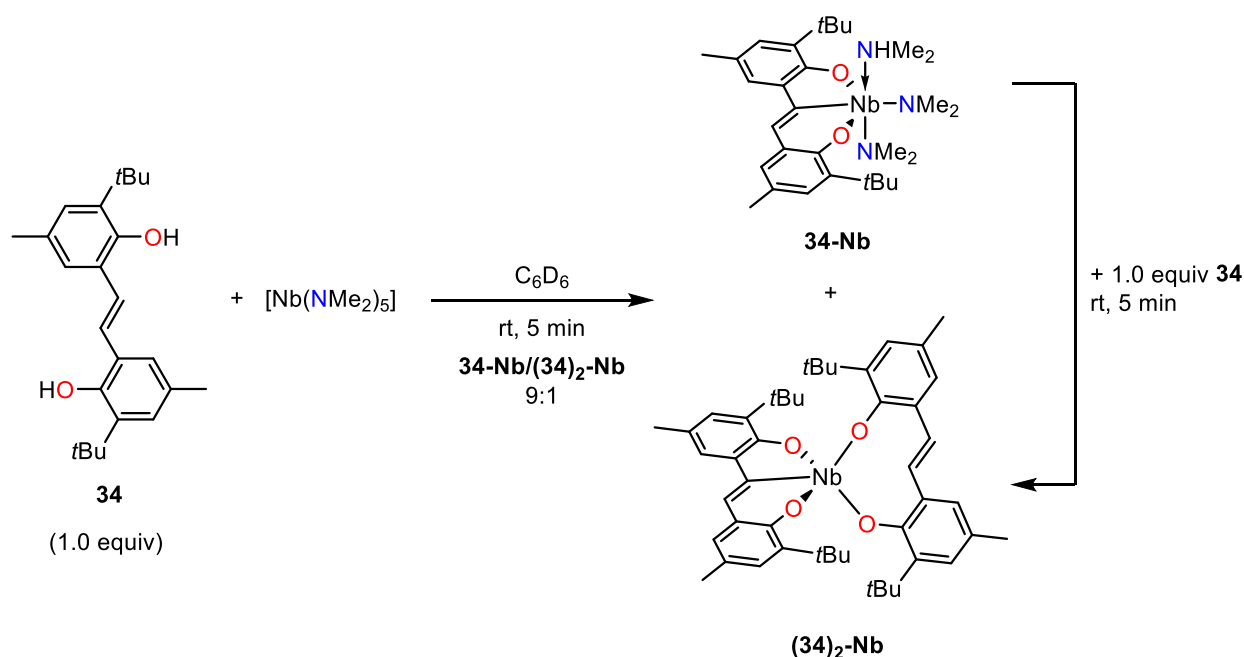
Scheme 22: Equimolar reaction of ligand **34** with [Nb(NMe₂)₅].

The reaction of two equiv of ligand **33c** with one equiv of [Ta(NMe₂)₅] was monitored *via* $^1$H NMR spectroscopy and significant differences within the individual $^1$H NMR spectra were observed, even after nearly two weeks of reaction time. However, the resulting spectra of the complexation showed the same three peaks in the region from 0.5 to 0.0 ppm, which were observed in the stoichiometric reaction of one equiv of ligand **33c** and [Ta(NMe₂)₅]. Attempts to purify the obtained complex by freeze drying or recrystallization from benzene were unsuccessful. Suitable crystals for single crystal X-ray diffraction analysis were obtained from benzene and the crystal structure revealed the bisligated complex (Figure 12).
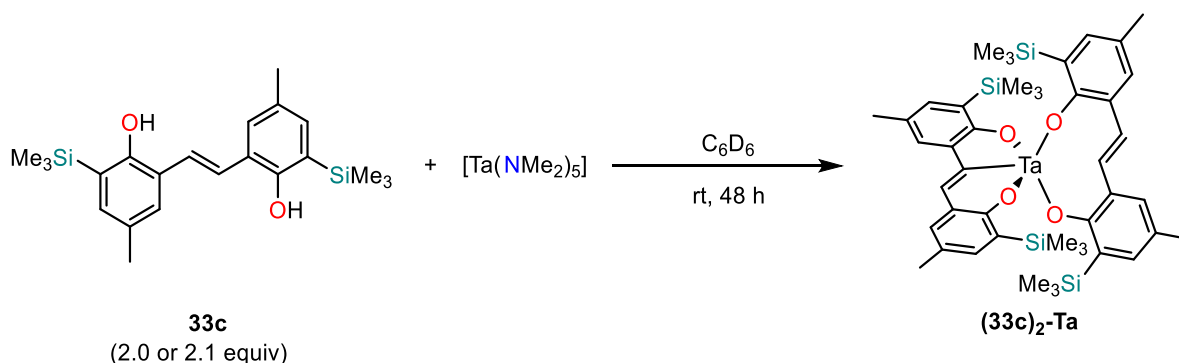


*Scheme 23:* Reaction between two equiv of ligand **33c** with one equiv of pentakis(dimethylamido)tantalum(V).
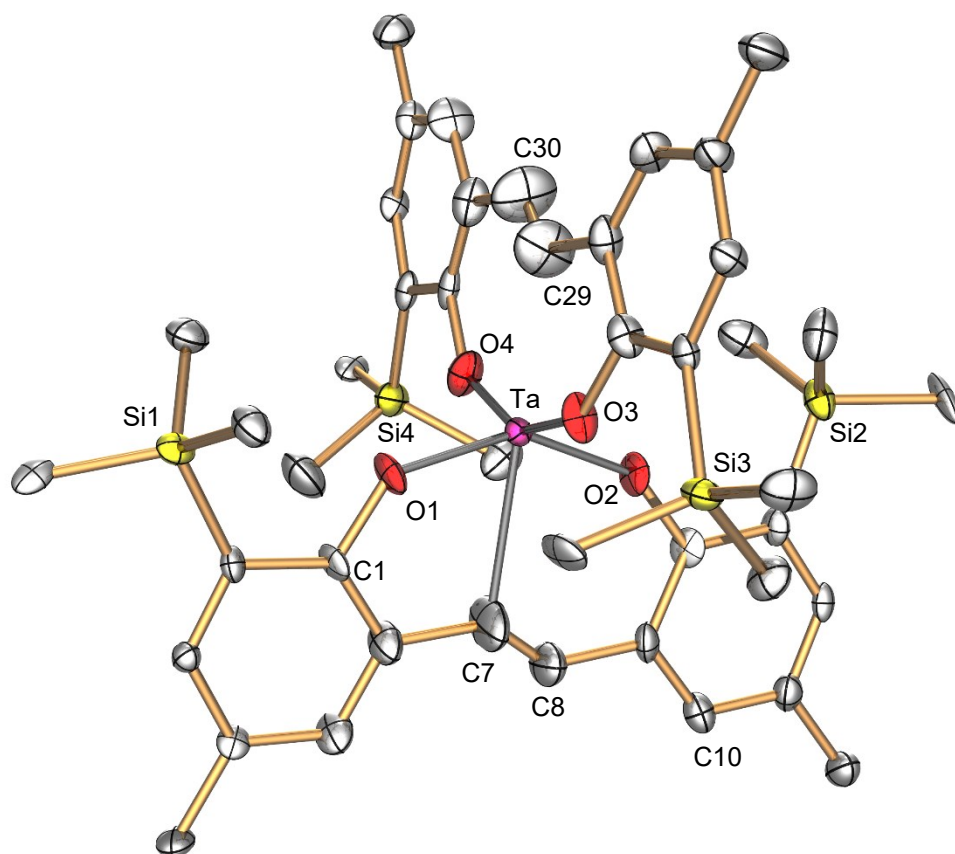
*Figure 12:* ORTEP diagram of complex **(33c)$_2$-Ta**. Hydrogen atoms are omitted for clarity and thermal ellipsoids are set at 30% probability. No crystallographic information is displayed due to the poor data resolution and effects caused by disorder.

Selected crystallographic parameters, as well as bond lengths, angles and torsion angles are not displayed due to the poor quality of the data resolution and due to effects caused by the disorder of overlapping structures.

## 3.3. Catalytic Reactions

The Group 5 metals, especially niobium(V) and tantalum(V), are known to catalyze the intermolecular hydroaminoalkylation reaction,[11,27,28,40–42,67,71,75–77,151–153] as well as the intramolecular hydroamination.[40,76] The catalytic activities of complexes **33-M** in hydroaminoalkylation and hydroamination of alkenes and 1-phenyl-1-propyne were validated by applying reaction conditions, which were suitable for Group 5 metal binaphtholate complexes reported by Hultzsch *et al.*[40,77]

### 3.3.1. Hydroaminoalkylation

All potential catalysts were investigated towards their reactivity in the hydroaminoalkylation of alkenes or alkynes with anilines and amines (Scheme 24). Therefore, two equiv of alkene or 1.2 equiv of alkyne alongside the aniline or amine were used. The resulting mixture was heated to 150 °C for 24 h in the presence of 5 mol% of complex **33-M**.
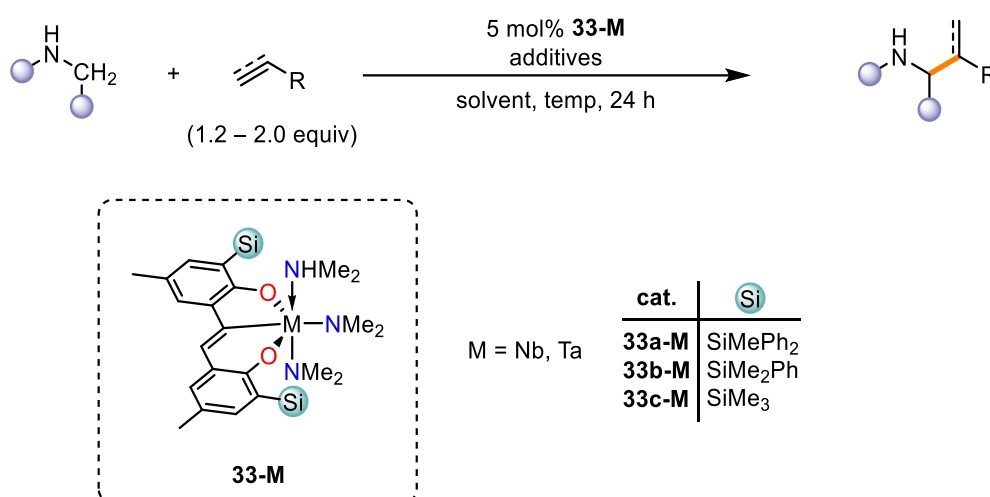


Scheme 24: Intermolecular hydroaminoalkylation of a secondary amine with an alkene or alkyne catalyzed by **33-M**.

The reactions of 1-octene with *N*-methylaniline, and 4-phenyl-1-butene with *N*-methylaniline in the presence of **33a-Nb** were the first two reactions screened. The reaction progress was monitored periodically *via* ^{1}H NMR spectroscopy (Figure 13 for the reaction of 1-octene with *N*-methylaniline as an example). New signals in the olefinic region at ca. 5.5 ppm and aliphatic region at ca. 1.6 ppm formed within the first 1.5 h at 150 °C and after 24 h the peaks of the terminal alkene at ca. 5.0 ppm and at ca. 5.8 ppm disappeared. However, the expected peaks of the product were missing and after careful analysis of the ^{1}H NMR spectra and GC-MS traces it was clear that the terminal olefinic starting material isomerized into a mixture of internal alkenes. This phenomenon was observed for all reactions using isomerizable starting materials
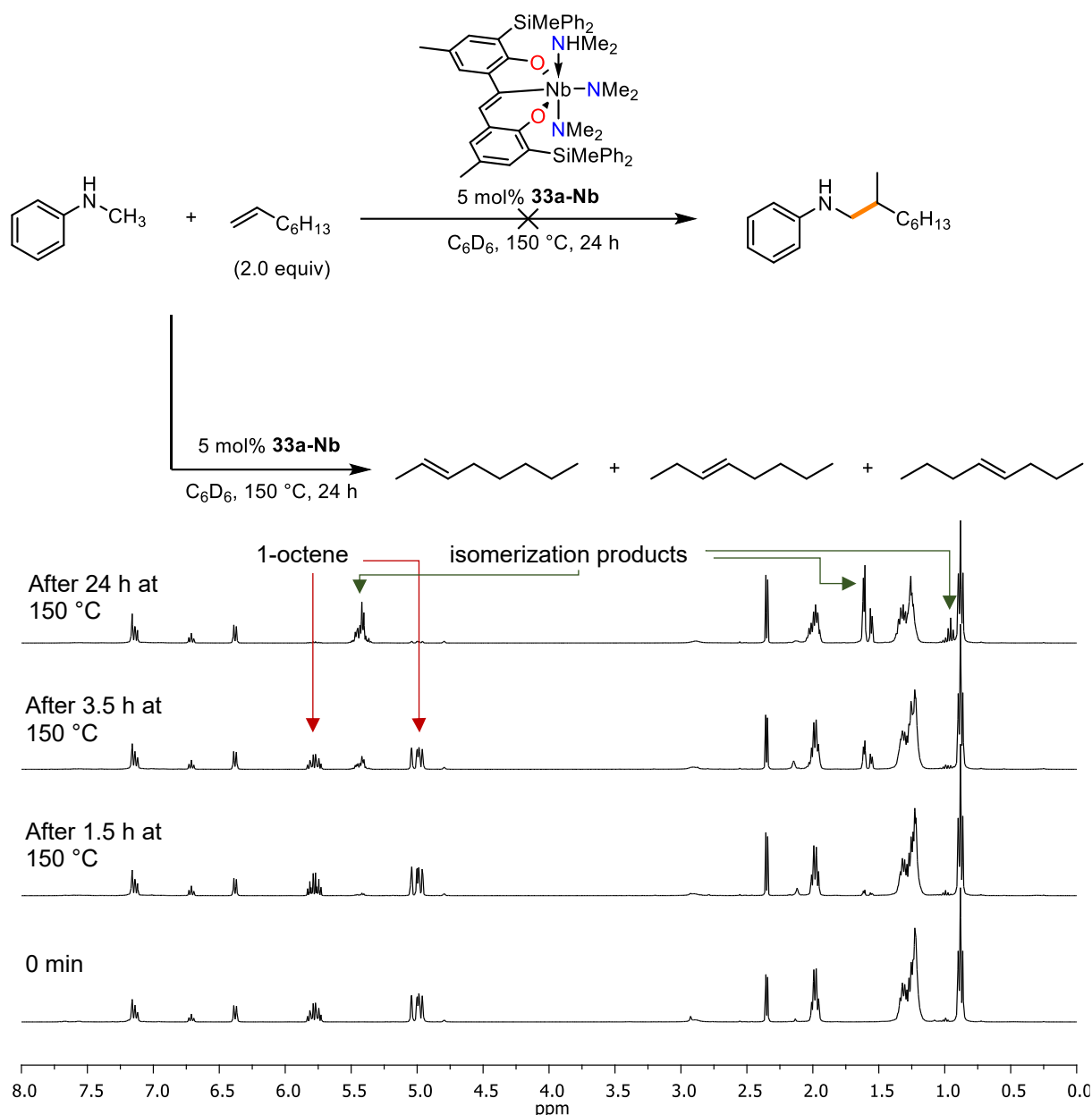
*Figure 13:* Reaction between 1-octene and *N*-methylaniline in the presence of **33a-Nb** at room temperature after combining all reagents and at 150 °C as a function of time, monitored by ^{1}H NMR spectroscopy.

if **33a-Nb**, **33b-Nb** or **33c-Nb** was used. The isomerization catalyzed by **33-M** has not been further explored.

It was anticipated that vinylcyclohexane, a geminal disubstituted alkene, would be sufficiently bulky to avoid isomerization. This assumption turned out to be false and the thermodynamically more stable trisubstituted internal alkene was formed. In order to prevent any isomerization, 3,3-dimethyl-1-butene was chosen as a substrate and in the reaction trial with *N*-methylaniline and **33a-Nb** no reaction occurred. It was assumed that the steric bulk of the *tert*-butyl group might have prevented the alkene from getting into proximity to the metal centre. Therefore,

trimethyl(vinyl)silane was used as a final substrate to validate if **33a-Nb** is active. The longer C–Si bond might be sufficiently long to overcome the potential steric repulsion. Additionally, the anti-Markovnikov product might form alongside the Markovnikov-product, due to the β-silicon effect.[41,72,151] The ^{1}H NMR spectra did not change throughout the reaction progress, and hence no reaction occured.

All the before mentioned reactions were also performed with **33a-Ta**, however no change in any ^{1}H NMR spectra was observed for any reaction No isomerization was observed.

Complexes **33b-Nb** and **33b-Ta** were investigated as potential catalysts in the reaction of 1-octene, 4-phenyl-1-butene, vinylcyclohexane, 3,3-dimethyl-1-butene and trimethyl(vinyl)silane with *N*-methylaniline. Unfortunately, no hydroaminoalkylation products were formed. The isomerization to internal alkenes was observed for 1-octene, 4-phenyl-1-butene and vinylcyclohexane in the presence of **33b-Nb**.

The reason for the inactivity of complexes **33a-Nb**, **33a-Ta**, **33b-Nb** and **33b-Ta** was believed to stem from the sterically demanding substituents at the silyl groups. Therefore, it was proposed to prepare the ligand bearing sterically non-demanding trimethylsilyl groups. The corresponding niobium(V) and tantalum(V) complexes of ligand **33c**, **33c-Nb** and **33c-Ta** were then tested in the hydroaminoalkylation model reactions and 1-octene, 4-phenyl-1-butene, vinylcyclohexane, 3,3-dimethyl-1-butene and trimethyl(vinyl)silane were heated together with *N*-methylaniline and the potential catalyst at 150 °C for 24 h. Despite the small steric bulk of the trimethylsilyl groups, no formation of any hydroaminoalkylation product was observed by ^{1}H NMR spectroscopy. Therefore, all prepared niobium(V) and tantalum(V) complexes **33-M** were inactive in the hydroaminoalkylation reaction of the used substrates (Scheme 25).
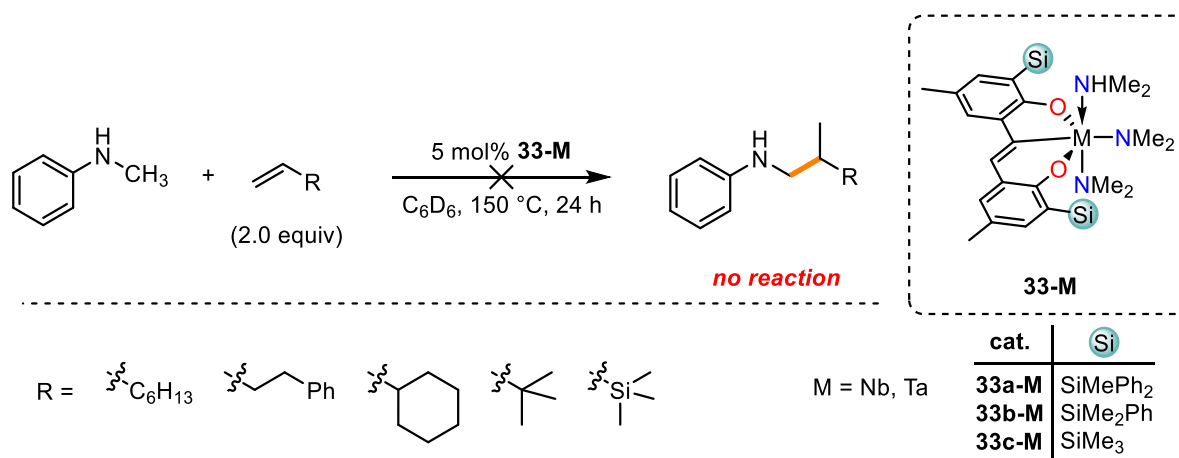


*Scheme 25:* Catalytic hydroaminoalkylation reactions of *N*-methylaniline with various alkenes in the presence of complexes **33-M**.

Different reaction conditions, substrates and various additives were screened on a 0.05 mmol scale. The results were analyzed by GC-MS. Most reactions were conducted utilizing **33c-M** as catalyst in order to prevent or minimize any negative effects, such as steric repulsion of the sterically more demanding silyl groups. The reaction between 4-phenyl-1-butene and *N*-methylaniline was performed at 120 °C and 170 °C to validate if any change in temperature would initiate the reaction. All experiments conducted at different temperatures were unsuccessful. Furthermore, different amines were employed in the reaction with 4-phenyl-1-butene. The applied amines were aliphatic and benzylic amines, such as pyrrolidine, *N*-methylbenzylamine and *N,N*-dimethylbenzylamine, as well as arylamines, such as *N,N*-dimethylaniline and 1,2,3,4-tetrahydroquinoline. The aliphatic and benzylic amines have been chosen because it was demonstrated that aliphatic amines might be preferred over arylamines for some catalyst systems.[151] The hydroaminoalkylation reactions did not yield the expected product and the reaction of 1-phenyl-1-propyne with *N*-methylaniline in the presence of 5 mol% **33c-Nb** or **33c-Ta** was also unsuccessful. However, reduction of the alkyne to the alkene was observed for the reaction with **33c-Nb**. In order to activate the complexes, additives, such as the anilinium salt [PhNHMe$_2$][B(C$_6$F$_5$)$_4$], *t*BuNC, MeCN, PhCN, NaSCN, *t*BuOK, KH, TMS-Cl, were added to the reaction mixture of 4-phenyl-1-butene and *N*-methylaniline in the presence of **33c-Nb** or **33c-Ta** (Scheme 26). It was anticipated that the addition of the ammonium salt [PhNHMe$_2$][B(C$_6$F$_5$)$_4$] would lead to the protonation of one of the amido ligands or the metalated ethylene bridge and therefore enable decoordination to create a vacant coordination side. The solutions of complexes **33c-Nb** and **33c-Ta** in bromobenzene changed instantaneously the color to a dark red for **33c-Nb** and dark orange for **33c-Ta** upon the addition of [PhNHMe$_2$][B(C$_6$F$_5$)$_4$]. *tert*-Butyl isocyanide was expected to coordinate to the metal centre and upon the nucleophilic attack of the amido ligand an activated and potentially catalytically active metallaaziridine would have been formed.[154] A similar reaction was hoped to occur for the addition of sodium thiocyanate. Nitriles have shown to undergo insertion into the M–C bond of metallaaziridines.[71,155] Additionally bases, such as potassium *tert*-butoxide and potassium hydride were used as additives to facilitate the deprotonation of the *N*-methylamido C–H bond.
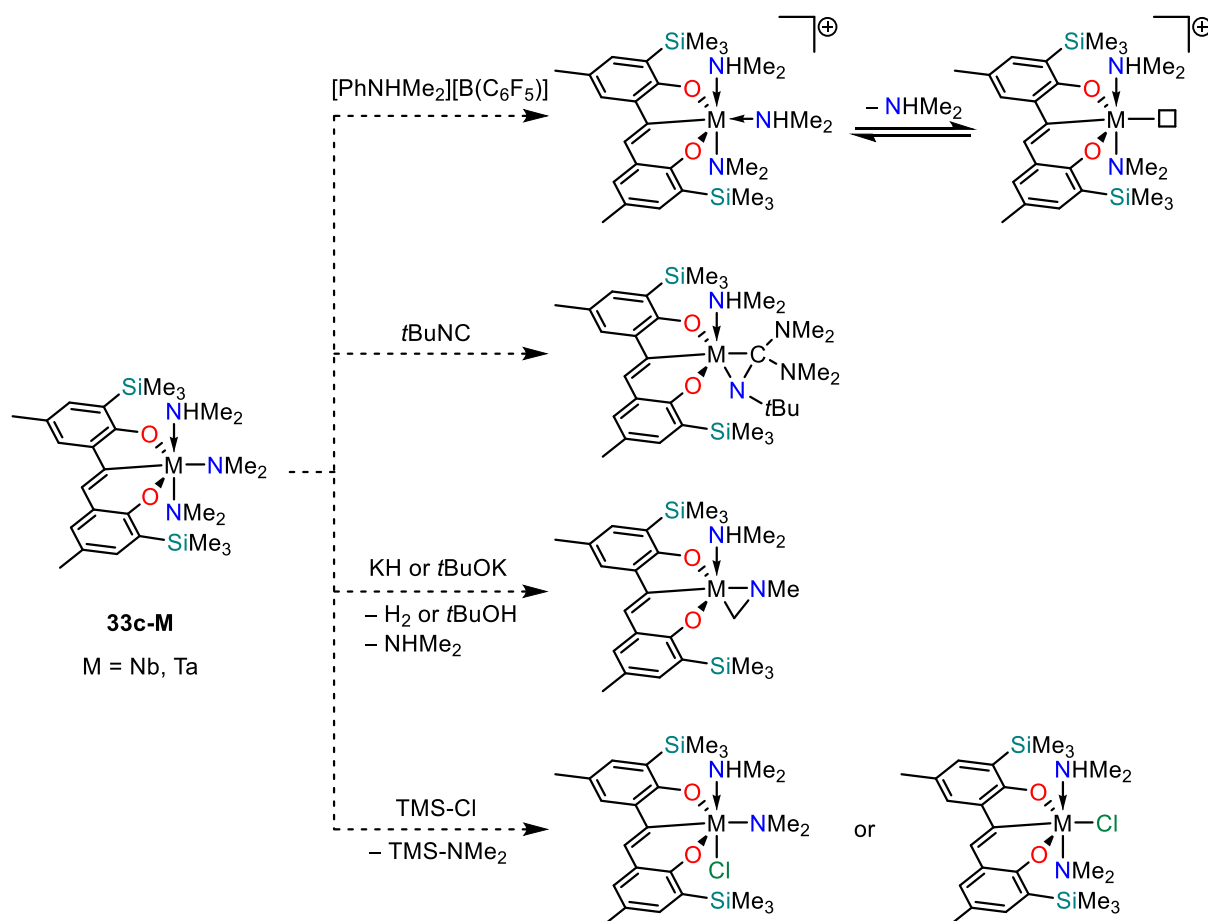
*Scheme 26:* Reaction of **33c-M** with different additives and their anticipated products.

Electron withdrawing ligands, such as chlorido ligands have shown to enhance the catalytic activity of some complex systems, such as $[Ta(NMePh)_2Cl_3]_2$, and hence trimethylsilyl chloride was used as an additive to facilitate the decoordination of the dimethylamido ligands and the coordination of a chloride anion.[156–159]

All reactions employing the ammonium salt $[PhNHMe_2][B(C_6F_5)_4]$, *tert*-butyl isocyanide, acetonitrile, benzonitrile, sodium thiocyanate or potassium *tert*-butoxide did not yield the desired hydroaminoalkylation product. When potassium hydride is added, traces of the desired product were formed for the reaction containing **33c-Nb** as catalyst. No product formation was observed for the same reaction utilizing **33c-Ta**. The product was indicated by GC-MS, as well as $^1$H NMR spectroscopy and was confirmed by HRMS. The reaction of 4-phenyl-1-butene with *N*-methylaniline using 5 mol% **33c-Ta** in the presence of 7.5 mol% trimethylsilyl chloride yielded the desired product and 9 % conversion were achieved. The conversion could be increased to

31 % by applying 10 mol% **33c-Ta** and 15 mol% TMS-Cl. No product formation was observed for the reactions using **33c-Nb** and TMS-Cl (Scheme 27).



0 % (-/150 °C)
for **33b-Nb**, **33b-Ta**, **33c-Nb**, **33c-Ta**

0 % (-/150 °C) for **33c-Nb**, **33c-Ta**

0 % (-/150 °C) for **33b-Nb**, **33b-Ta**

0 % (-/150 °C)
for **33b-Nb**, **33b-Ta**, **33c-Nb**, **33c-Ta**

0 % (-/120 °C) for **33c-Nb**, **33c-Ta**
0 % (-/170 °C) for **33c-Nb**, **33c-Ta**
0 % ([PhNHMe₂][B(C₆F₅)₄]/150 °C)
    for **33c-Nb**, **33c-Ta**
0 % (*t*BuNC/150 °C) for **33c-Nb**, **33c-Ta**
0 % (NaSCN/150 °C) for **33c-Nb**, **33c-Ta**
0 % (PhCN/150 °C) for **33c-Nb**, **33c-Ta**
0 % (MeCN/150 °C) for **33c-Nb**, **33c-Ta**
0 % (KO*t*Bu/150 °C) for **33c-Nb**, **33c-Ta**
traces (KH/150 °C) for **33c-Nb**
0 % (KH/150 °C) for **33c-Ta**
0 % (TMS-Cl/150 °C) for **33c-Nb**
9 % (TMS-Cl/150 °C) for **33c-Ta**
0 % (TMS-Cl/150 °C) for 10 mol% **33c-Nb**
31 % (TMS-Cl/150 °C) for 10 mol% **33c-Ta**

0 % (-/150 °C) for **33c-Nb**, **33c-Ta**

0 % (-/150 °C) for **33c-Nb**, **33c-Ta**

| M = Nb, Ta | cat. | Si |
|---|---|---|
| | **33b-M** | SiMe₂Ph |
| | **33c-M** | SiMe₃ |

*Scheme 27:* Catalytic hydroaminoalkylation reactions in the presence of **33b-Nb**, **33b-Ta**, **33c-Nb** or **33c-Ta**. Products, conversion, and conditions are displayed.

### 3.3.2. Hydroamination

All potential catalysts **33-M** were investigated towards their reactivity in intra- and intermolecular hydroamination.

The intramolecular hydroamination of 2,2-diphenylamino-4-pentene to the corresponding pyrrolidine in the presence of **33-M** was monitored periodically *via* ¹H NMR spectroscopy (Figure 14; example for cyclization reaction using **33b-Nb**). Complexes **33-M** catalysed the cyclization reaction (Scheme 28). The highest conversion which was achieved after 24 h at 150 °C was obtained by **33b-Nb** and 40 % if the cyclized product was formed. The conversion could be increased to 59 % when the reaction mixture was heated for a total of 65 h. When **33a-Ta** was used, 25 % conversion was obtained after 24 h at 150 °C, and when the reaction

time was increased to 42 h, a conversion of 35 % was observed. In general, no clear trend was observed for the activity of the different complexes **33-M**. **33a-Nb** and **33c-Nb** were less active than their tantalum(V) counterparts and achieved only 13 % and 17 % conversion after 24 h at 150 °C, respectively. As mentioned above, **33b-Nb** was the most active catalyst, and it is indicated that a certain degree of steric bulk on the silyl group, which is not too sterically demanding, is beneficial towards the catalytic activity.



| cat. | Si | conversion (M = Nb) | conversion (M = Ta) |
|---|---|---|---|
| **33a-M** | SiMePh$_2$ | 13 % | 25 % (35 % after 42 h) |
| **33b-M** | SiMe$_2$Ph | 40 % (59 % after 65 h) | 27 % |
| **33c-M** | SiMe$_3$ | 17 % | 28 % |
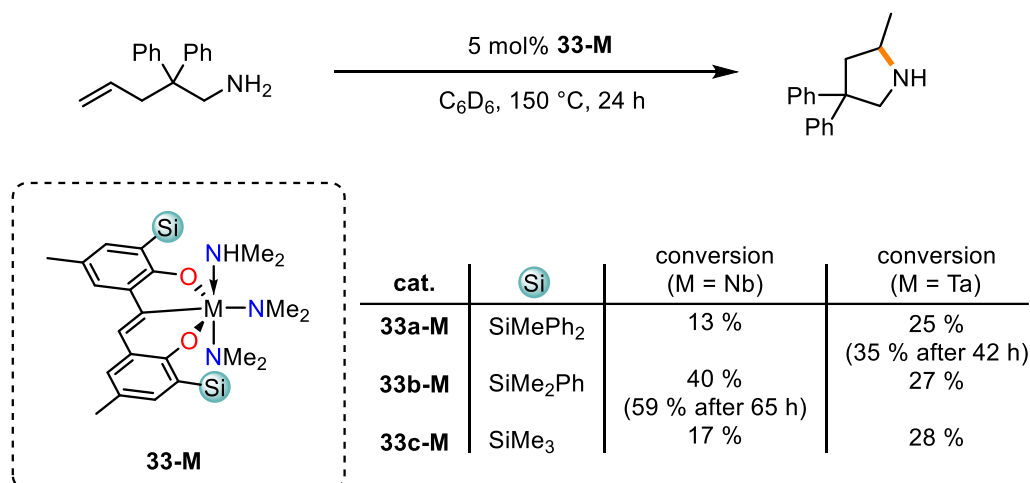
*Scheme 28:* Intramolecular hydroamination of 2,2-diphenylamino-4-pentene catalyzed by **33-M**. Conversions are provided for the reaction in presence of the corresponding catalyst after 24 h at 150 °C.

All complexes **33-M** were catalytically active in the intramolecular hydroamination of 2,2-diphenylamino-4-pentene, yet only low to moderate yields, ranging from 13 % to 40 %, were obtained after 24 h at 150 °C. However, **33-M** cannot compete with their precursors and it was shown that [Nb(NMe$_2$)$_5$] and [Ta(NMe$_2$)$_5$] readily transformed the more challenging substrate 2,2-dimethylamino-4-pentene quantitatively into 2,4,4-trimethylpyrrolidine at 120 °C within 24 h when 10 mol% of the catalyst was used.[76]

There are only two reports on the Group 5 catalysed intramolecular hydroamination reaction of unactivated alkenes,[40,76] however, these systems cannot compete with main group element,[160–163] Group 4[43,164,165] or rare earth metal[115,129,166,167] catalysts.
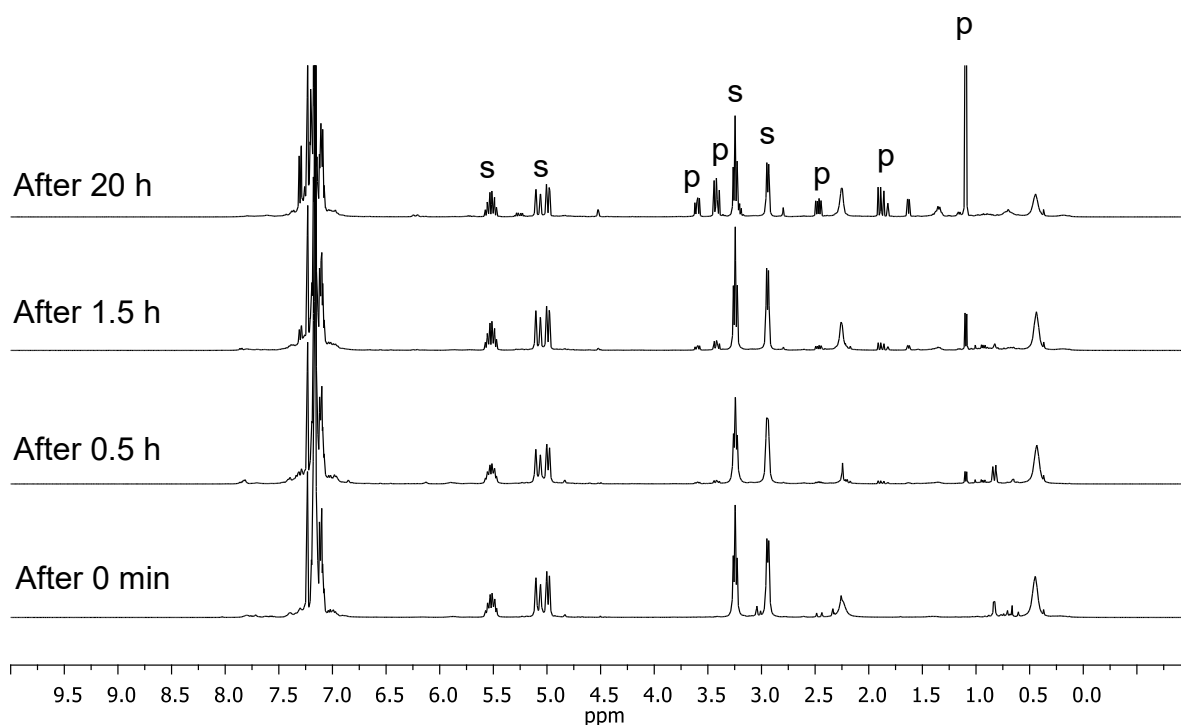
*Figure 14:* $^1$H NMR spectra of the reaction progress of the intramolecular hydroamination of 2,2-diphenylamino-4-pentene catalyzed by **33b-Nb** before heating the reaction mixture at 150 °C, after heating it for 0.5 h, 1.5 h and 20 h. s = 2,2 diphenylamino-4-pentene (starting material); p = 2-methyl-4,4-diphenylpyrrolidine (product).

In order to investigate the activity of **33c-Nb** and **33c-Ta** in the intermolecular hydroamination reaction, 4-phenyl-1-butene and benzylamine were heated to 150 °C for 24 h in the presence of the potential catalyst. Unfortunately, no desired product was formed. However, a GC-MS analysis revealed the products of a condensation reaction; dibenzylamine and *N*-benzylbenzaldimine. When **33c-Nb** was used as a catalyst, 50 % conversion of both condensation products in an equal amount is observed. Unfortunately, any attempts to reproduce the results failed. Traces of the condensation products dibenzylamine and *N*-benzylbenzaldimine were also detected in the reaction using **33c-Ta**. Neither increasing the olefin quantity from 15 equiv to 30 equiv, nor decreasing it to 10 equiv, had an impact on the reaction. The reaction was also unsuccessful when the temperature was increased to 170 °C or decreased to 120 °C. The addition of TMS-Cl did not lead to any product formation, however, in the case of **33c-Nb** mainly isomerization, as well as trace amounts of the reduction product of the alkene, the alkane and the condensation products of the amine, were observed (Scheme 29). Interestingly, isomerization of the alkene occurred when **33c-Ta** is used in the presence of TMS-Cl.

Furthermore, the intermolecular hydroamination reaction of 4-phenyl-1-butene with *N*-methylbenzylamine was performed in the presence of **33c-Nb** and **33c-Ta**. Both reactions were not successful.
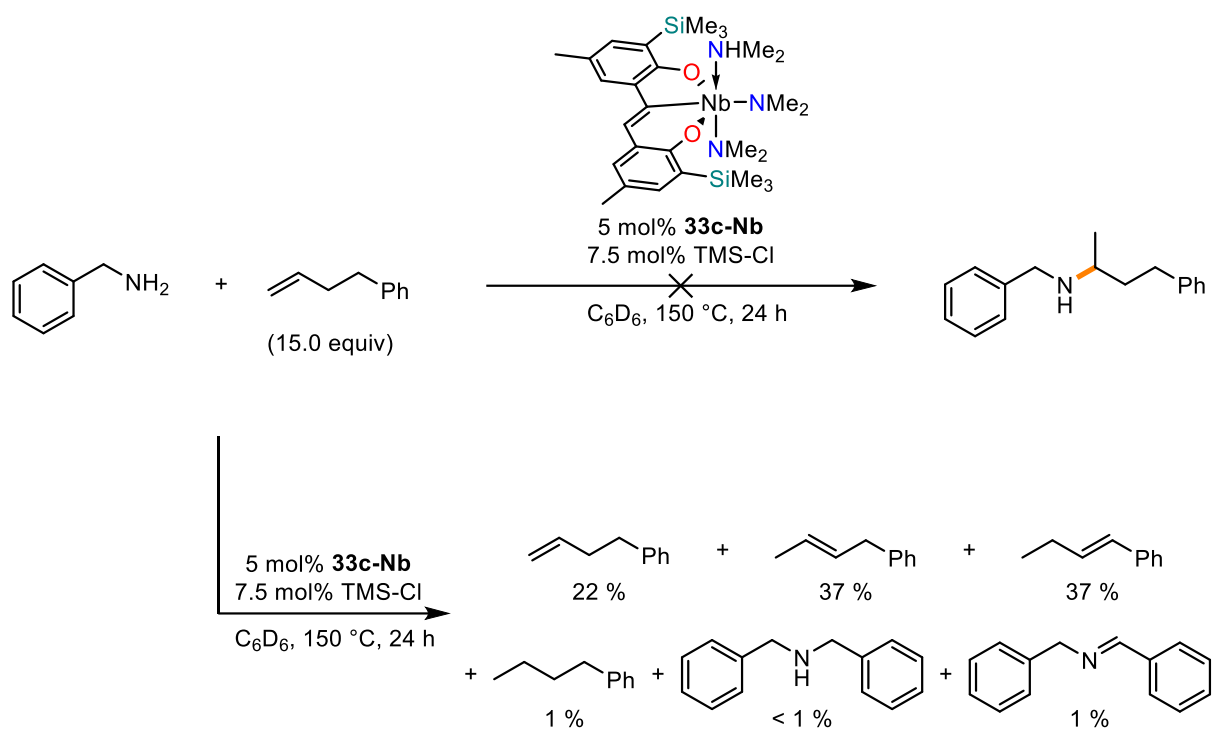
**Scheme 29:** Attempted hydroamination of benzylamine and 4-phenyl-1-butene in the presence of **33c-Nb** and TMS-Cl.

## 3.4. Reactivity of Complexes towards *N*-Methylaniline

Since none of the monitored catalytic hydroaminoalkylation reactions worked, the question arose if and how *N*-methylaniline interacts with the complexes. Most importantly, it was necessary to validate if *N*-methylaniline replaces the dimethylamido and dimethylamine ligands. **33b-Nb** was chosen as the representative of all complexes for several reasons: (i) the sterically less hindering SiMe₂Ph-substituent provides more free space for the phenyl group of the substrate, which leads to less repulsion and therefore a more feasible coordination; (ii) it was anticipated that the diagnostic $^1$H NMR spectroscopy signals of the methyl groups on the silyl substituent could split up due to an rotational inhibition around the C–SiMe₂Ph bond, caused by the bulk of the phenyl groups of the substrate; (iii) previous studies in the Hultzsch group on the reactivity of binaphtholate Group 5 complexes in hydroaminoalkylation, but also studies from the Nugent group, suggested that niobium compounds might be more reactive than their tantalum analogues.[40,67,77]

Therefore **33b-Nb** was dissolved in C₆D₆ and 5.0 equiv of *N*-methylaniline were added. It was envisioned that complex **33b-Nb** would react immediately with the added *N*-methylaniline substrate, since early-transition-metal amides are generally known to be exceedingly reactive towards any protonic source, which is less basic than the corresponding metal amide.[69–71] Surprisingly, no reaction and therefore no change in the $^1$H NMR spectra occurred within the first 90 minutes at room temperature (Figure 15). Since complexes **33-M** were already known to exchange the coordinated dimethylamine with dimethylamines in solution, it was hypothesized that complex **33b-Nb** is also constantly exchanging its amino or amido ligands with the *N*-methylaniline and freeze drying of the mixture would already be enough to release dimethylamine and obtain the desired complex. This method partially worked, however at least two different species were present at this point and both, the dimethylamino and the dimethylamido ligands, were still present. The mixture was further heated to 60 °C for 1 h under a continuous flow of argon but, no noticeable difference was observed in the $^1$H NMR spectra. Heating the mixture to 80 °C for 1 h led to a significant change in the $^1$H NMR spectra. The reaction mixture was further heated to 100 °C for 2 h, which led to the loss of the signals of the dimethylamino and the dimethylamido ligands. The original signals of the phenyl groups on the silyl substituents at 7.71 ppm and 7.56 ppm vanished as well and new signals of the formed complex were found ca. 0.1 ppm upfield at 7.63 ppm and 7.50 ppm. The most diagnostic peaks for the completion of the reaction were the $^1$H NMR signals of the methyl groups on the silyl substituent. Both singlets at 0.79 and 0.63 ppm shifted upfield and split into a total of four peaks at 0.63, 0.61, 0.53 and
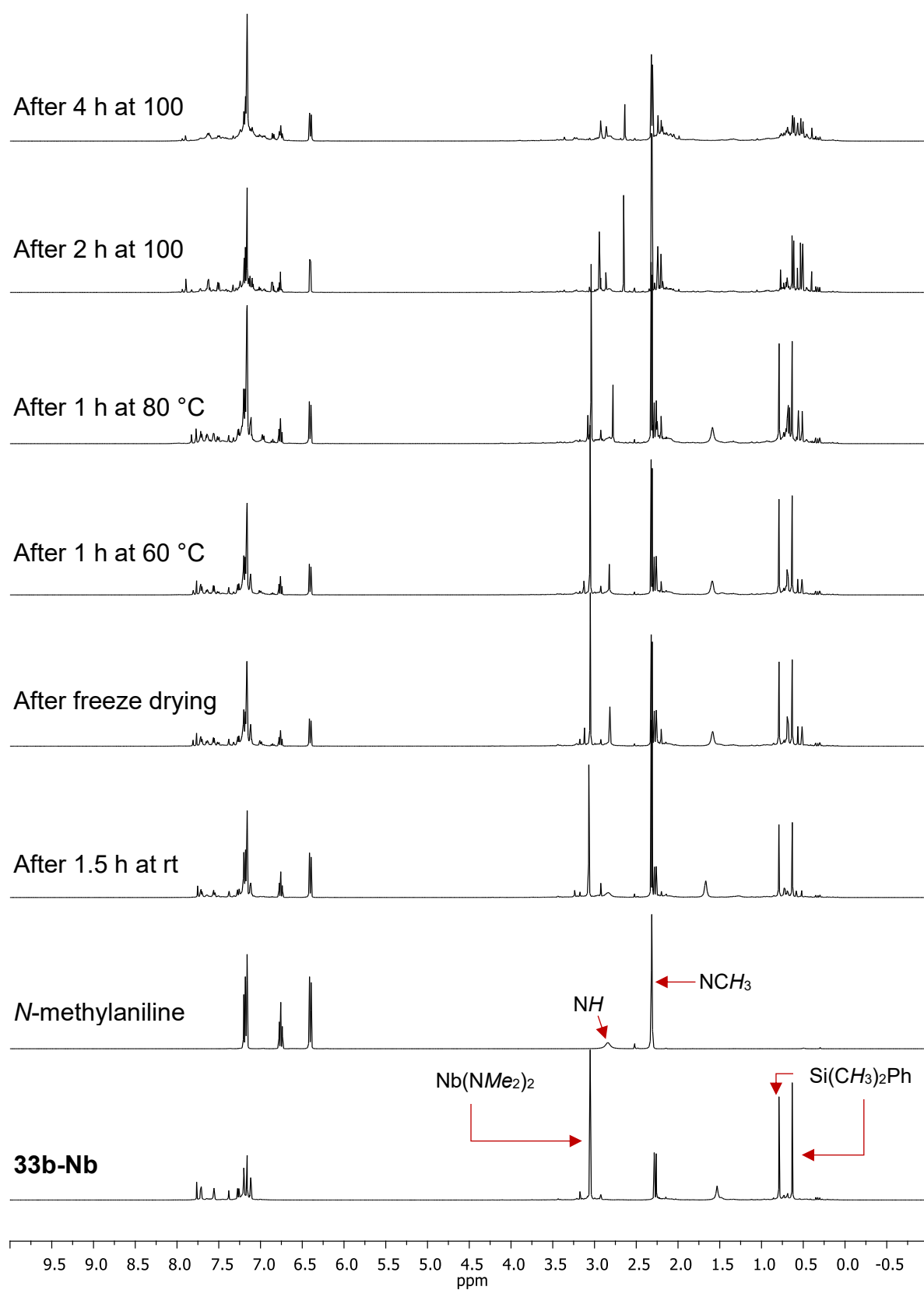
*Figure 15:* Reaction of **33b-Nb** with 5.0 equiv of *N*-methylaniline. The notes indicated on the left side of the individual spectra display the corresponding starting material, the reaction time since the solutions containing the starting material were combined and the reaction times at the corresponding reaction temperature.

0.51 ppm. The reaction was complete at this point and heating the mixture additionally for 2 h led to decomposition and transformation into undefined species.

The signals of the dimethylamino and the dimethylamido ligands in the $^1$H NMR spectra at approximately 1.5 ppm and ca. 3.0 ppm, respectively, shift within the different spectra (Figure 16). Therefore, it is anticipated that the previously described exchange behaviour of complex **33b-Nb** is indeed influenced by the presence of *N*-methylaniline and the reaction progress.
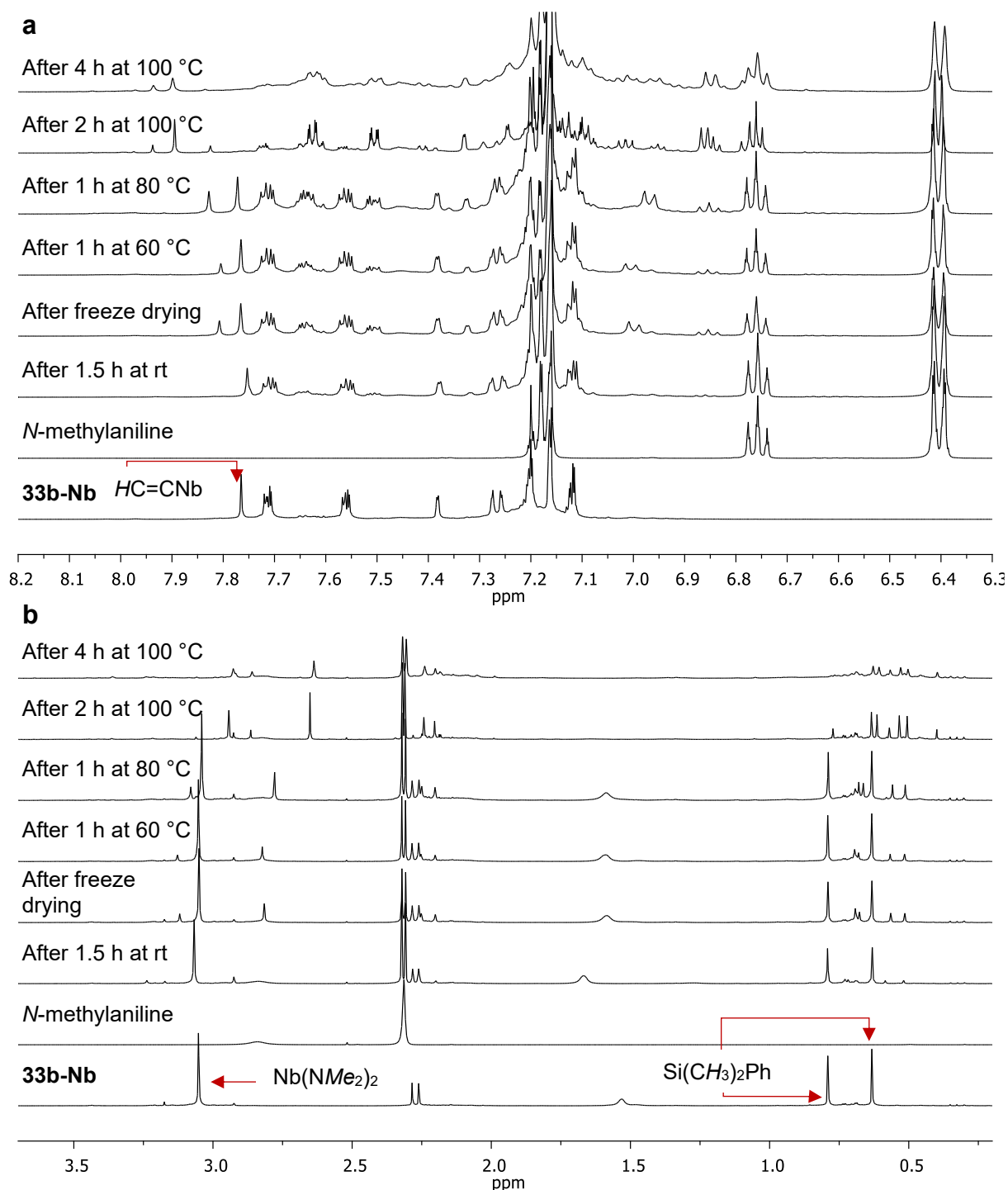


*Figure 16:* Selected sections of the above shown $^1$H NMR of the reaction between **33b-Nb** with 5.0 equiv of *N*-methylaniline in Figure 15. Sections are ranging from 8.2 to 6.3 ppm (**a**) and from 3.7 to 0.2 ppm (**b**).
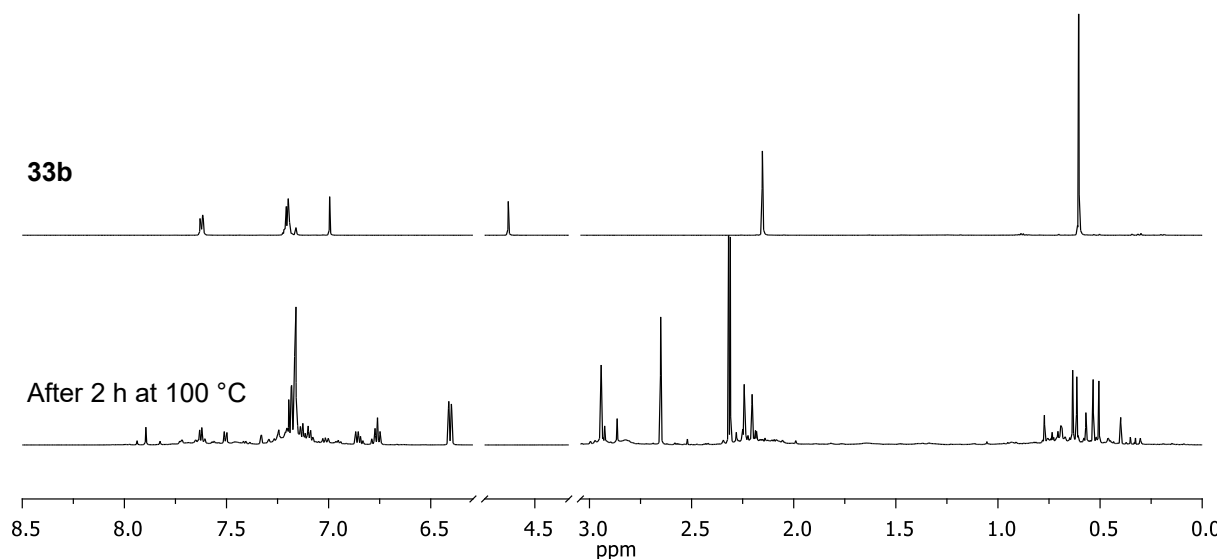
*Figure 17:* $^1$H NMR spectra of free ligand **33b** (top) and the reaction mixture after 2 h at 100 °C (bottom). Sections ranging from 6.3 – 4.7 ppm and 4.3 – 3.0 ppm have been omitted for visualization purposes.

The mixture obtained after 2 h at 100 °C was further investigated and 1D and 2D NMR experiments were interpreted in order to propose a structure. In a first step, it was validated if the ligand **33b** is still in the coordination sphere, since there have been reports of the dissociation of the ligand and substrate coordination.[152] Fortunately, free **33b** was not observed (Figure 17). Additionally, any reaction at the ethylene bridge could be ruled out, as the signal for the proton at 7.9 ppm is still present in the spectra and matches with the integration values of other peaks associated to **33b-Nb**. Additionally, it was necessary to identify if and how *N*-methylaniline coordinated and if any stable metallaaziridine had formed. In order to do so, all peaks of the
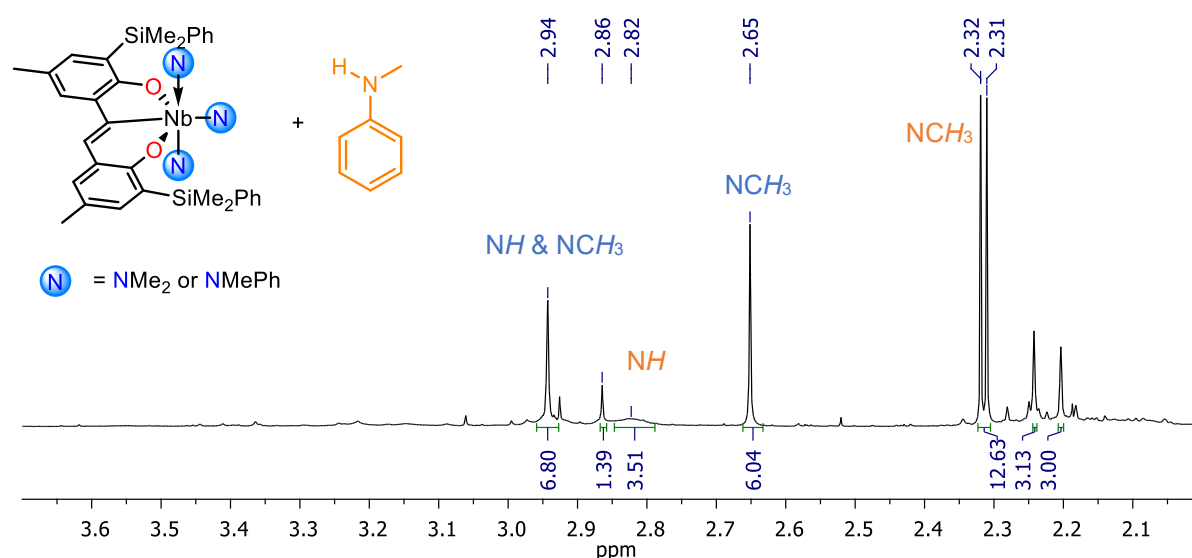


*Figure 18:* Selected range of $^1$H NMR spectrum of the reaction mixture after 2 h at 100 °C. Signals at 2.94 and 2.65 ppm were assigned to the methyl groups of the coordination amino/amido ligands. Doublet at 2.32 ppm corresponds to the methyl group of *N*-methylaniline and the broad signal at 2.82 ppm is the N*H* signal of *N*-methylaniline.

62
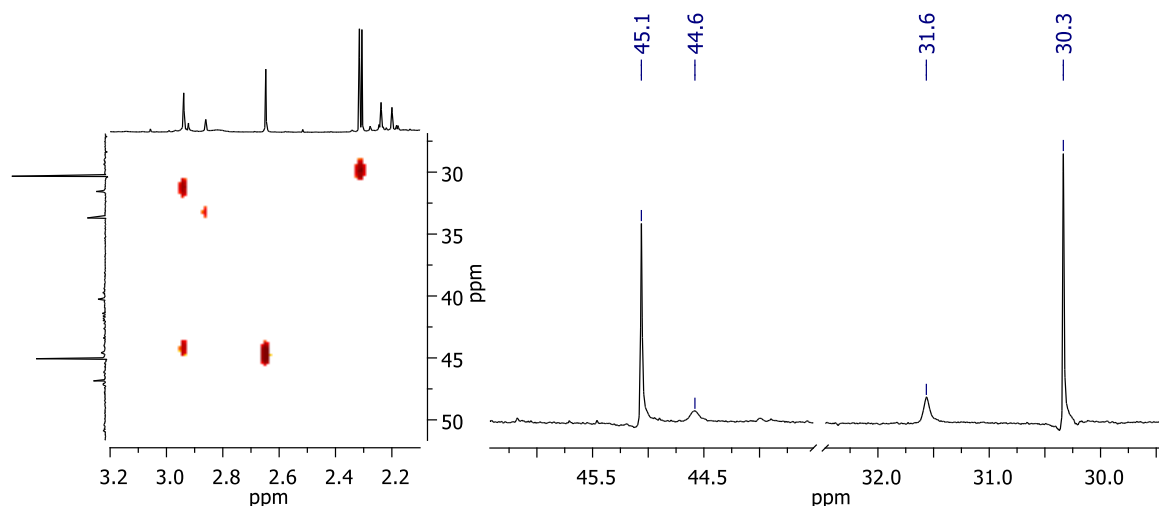
*Figure 19:* Selected sections of $^1$H,$^{13}$C HSQC and $^{13}$C NMR spectra of the reaction mixture after 2 h at 100 °C.

methyl groups which correspond to the amino or amido ligands were assigned (Figure 18). No signals for a possible metallaaziridine have been found in the spectra, since they typically display diagnostic shifts between 60 and 85 ppm for early-transition-metals.[74,154,168,169] The $^1$H,$^{13}$C HMBC experiment revealed and the $^1$H,$^1$H NOESY experiment verified that the peak at 2.94 ppm is indeed the methyl group of the coordinated *N*-methylaniline and the signal at 2.65 ppm showed a cross peak with its own $^{13}$C signal, indicating the dimethylamido ligand. Since only one peak is found and an integration value of 6 is obtained, it is valid to suggest a trans relation between the two *N*-methylanilido ligands. However, this might also result from a fluctuation of the structure. Any isomerization to the bis(*N*-methylanilido)dimethylamino complex can be ruled out, since no exchange peaks are detected in the $^1$H,$^1$H NOESY experiment. However, the $^1$H,$^{13}$C HSQC spectra shows two cross peaks of the *N*-methylanilido methyl groups with two different carbons at 44.6 ppm and 31.6 ppm, respectively (Figure 19). It is known that coalescence can occur at lower temperatures in the $^1$H NMR spectrum while two distinguishable peaks are found in the $^{13}$C NMR spectrum.[170] This was only observed with the signal of the methyl groups and only one signal is detected for the *ipso* carbon of the phenyl ring. This is another strong indication for a trans relationship between the two *N*-methylanilido ligands. The difference between both broad carbon signals of the anilido ligand at 44.6 ppm and the anilino ligand at 31.6 ppm is rather large (30.3 ppm for free PhNH*CH*₃), especially when it is taken into consideration that both methyl groups experience similar environments. While most trans amino-, amido-based early-transition-metal complexes bearing a pseudo-mirror plane show a difference not greater than 6 ppm, some titanium-based pentadentate pincer amido-bis(amidate) complexes have shown to have differences up to 10.2 ppm between the amido- and amino-CH₃.[171] Additionally, it is unlikely that the signal at 44.6 ppm belongs to an metallaaziridine, since it not only has two protons, which would result in a negative signal in the

APT $^{13}C$ NMR spectrum, but diagnostic shifts for an metallaaziridine are expected to be between 60 and 85 ppm for early-transition-metals.[74,154,168,169] Upon a closer look at the $^1H,^1H$ COSY experiment, no cross peak of the identified dimethylamido was found and only one weak cross peak appeared for the *N*-methylanilido methyl group. Therefore, it is anticipated that one *N*-methylanilido and one *N*-methylanilino ligand are coordinating. The signal of the dimethylamido ligand shows a cross peak with the *ortho*-protons of the *N*-methylanilido phenyl ring in the $^1H,^1H$ NOESY experiment, but no cross peak with the methyl groups. Hence, both phenyl rings of the anilido and anilino ligand are facing away from the stilbene scaffold of ligand **33b**, suggesting structure **35b-Nb** (Scheme 30). Structure **35b-Nb** would also explain the splitting of the methyl groups on the silyl substituent. The bulky phenyl groups of the anilino and anilido ligands prevent the rotation along the C–Si bond which results in four signals instead of two.
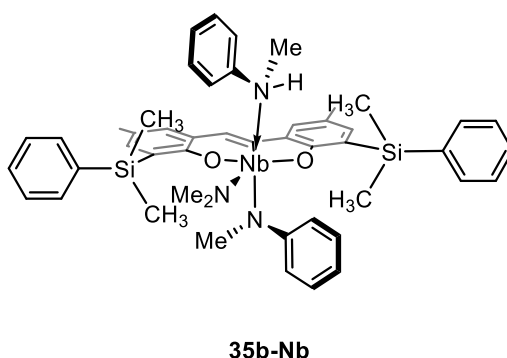


**35b-Nb**

*Scheme 30:* Proposed structure of **35b-Nb**, which is the resulting product of the reaction between **33b-Nb** and *N*-methylaniline.

All attempts to recrystalize and isolate the desired product failed and only decomposition of the compound was observed. Any isolated single crystals, which were harvested, were identified as ligand **33b**. Crystals suitable for single crystal X-ray diffraction analysis were obtained from experiments with **33b-Ta** and deuterium labelled *N*-methylaniline. Unfortunately, the crystals revealed a decomposition product, probably a simple inorganic tantalum salt.


## 3.5. Deuterium Scrambling Experiments

Since none of the monitored catalytic hydroaminoalkylation reactions worked and the experiments of **33b-Nb** with *N*-methylaniline suggested that the substrate is able to coordinate to the metal centre, the question arose if the *N*-methyl group undergoes C–H activation. In order to verify if C–H activation is feasible, **33c-M** was treated with deuterium labelled *N*-(methyl-$d_3$)aniline and *N*-*d*-*N*-methylaniline in a stoichiometric, as well as in a catalytic,

manner and the reactions were monitored *via* $^{1}H$ NMR spectroscopy. It was expected to observe deuterium scrambling if C–H activation occurs (Scheme 31).[67,77,172]
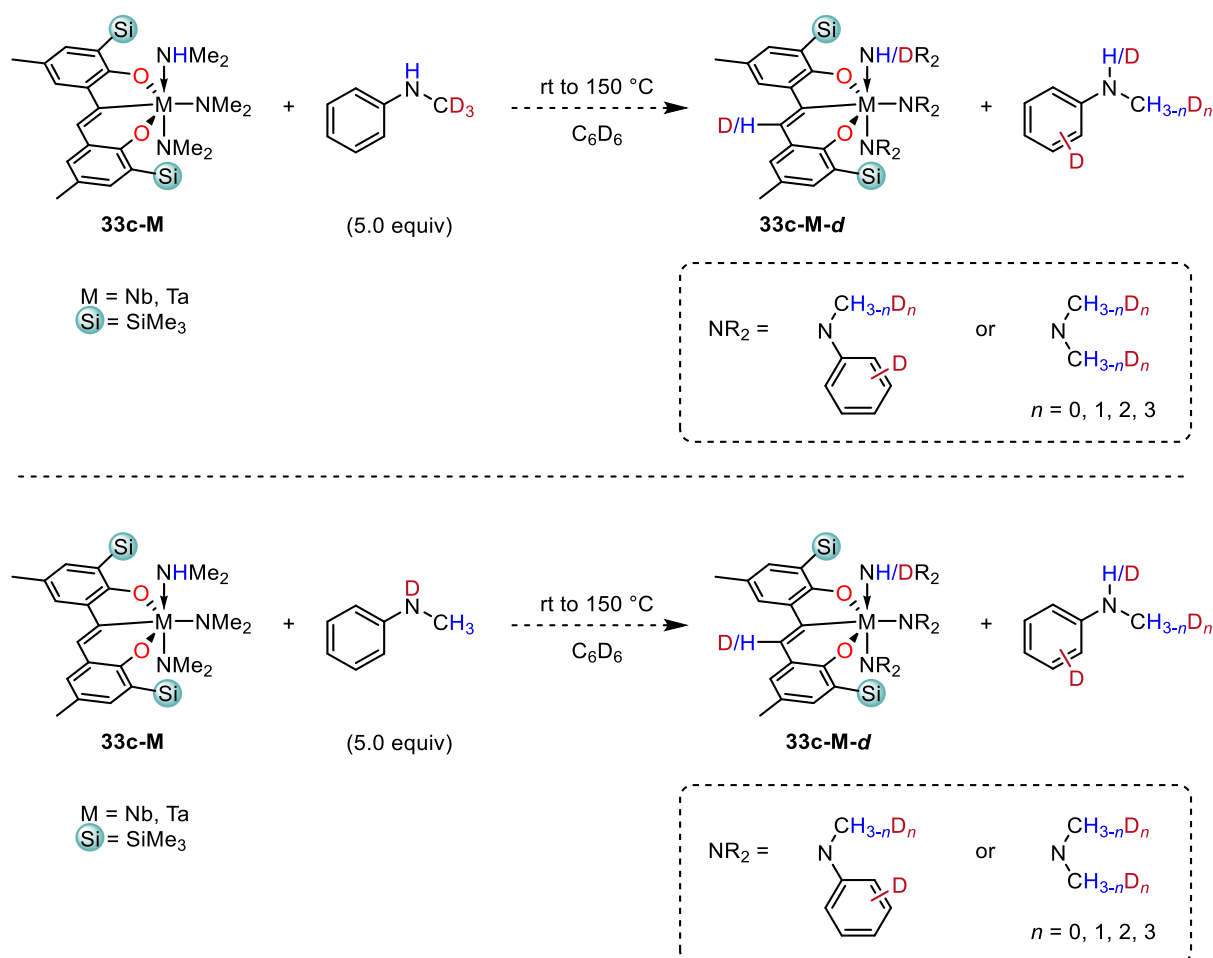


*Scheme 31:* Stochiometric reaction of **33c-M** with 5 equiv of deuterated *N*-methylanilines. The possible results after a successful deuterium scrambling reaction are displayed.

As shown in the mechanism for the hydroaminoalkylation reaction in chapter 1.2., it is expected that the dimethylamido and dimethylamino ligands undergo an amine exchange with the substrate, *N*-(methyl-$d_3$)aniline. The metal centre activates the C–D bond and, upon deuterium transfer to an anilido ligand, a metallaaziridine is formed. If *N*-(methyl-$d_3$)aniline, which bears an N–H bond, is coordinated to the metal centre, it can act as a hydrogen donor and protonate the $CD_2$ group of the metallaaziridine. This leads to the formation of a $CD_2H$ functionality, as well as a new anilido ligand. If the complex is indeed facilitating the C–H activation, it is expected to yield a mixture of differently deuterated methyl groups with the general formula $CH_{3-n}D_n$ ($n = 0$, 1, 2, 3) (Scheme 32). C–H activation might also occur at the *ortho*-carbon of the phenyl moiety, leading to deuterium incorporation into the phenyl ring. Additionally, the formation of *N*-deuterated anilines is expected, which can be easily monitored. This is particularly true for

the reaction between **33c-M** and *N*-(methyl-$d_3$)aniline and a diagnostic signal of the N–H bond is observed.
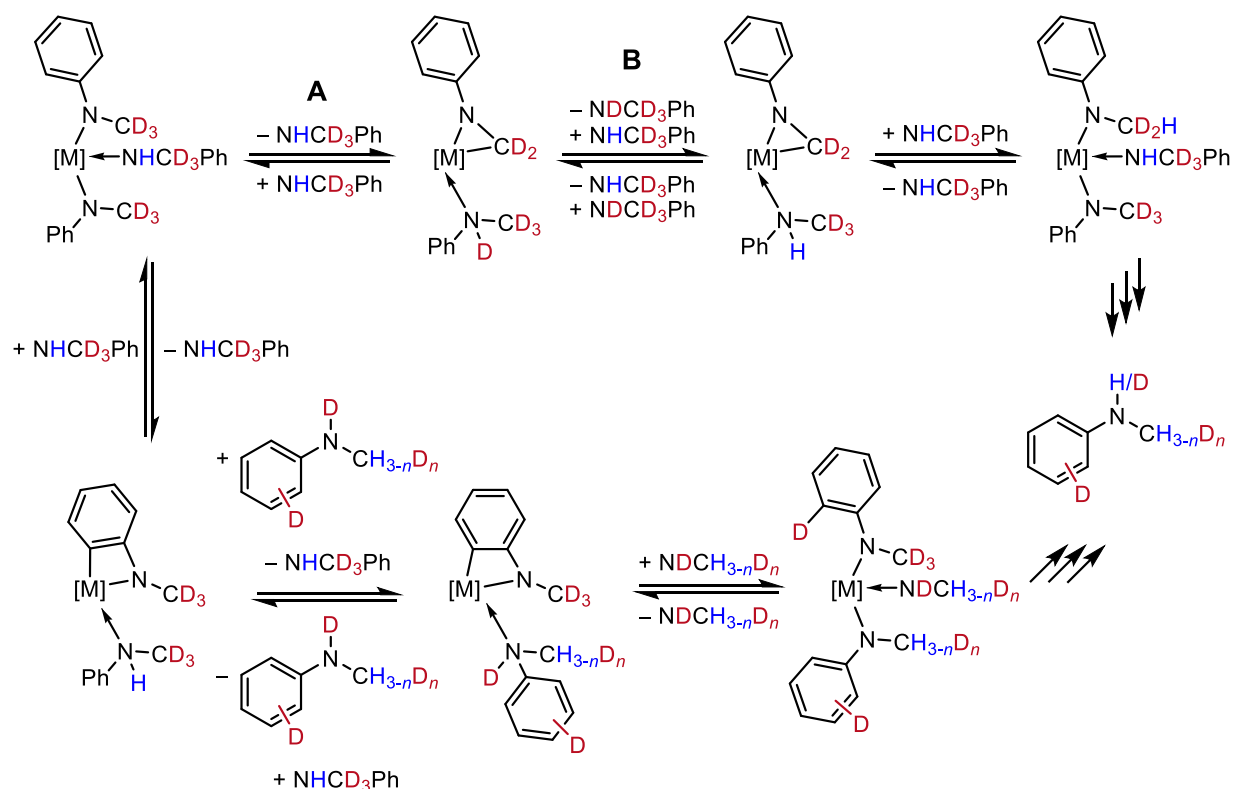


*Scheme 32:* Proposed mechanism for deuterium scrambling of complexes **33c-M** with *N*-(methyl-$d_3$)aniline.

The reaction between 1.0 equiv of **33c-Nb** and 5.0 equiv of *N*-(methyl-$d_3$)aniline was monitored periodically at different temperatures, ranging from room temperature to 150 °C in order to validate if deuterium scrambling is occurring. Within the first 18 h at room temperature no proton deuterium exchange was observed. The mixture was heated at 80 °C for 1.5 h, followed by 1 h at 100 °C. No signal of the *N*-methyl group was detected in the $^1$H NMR spectrum. The reaction mixture was additionally heated for 1 h at 130 °C and a final $^1$H NMR spectrum was measured after heating the reaction at 150 °C for 1 h (Figure 20). No signal for any *N*-CH$_{3-n}$D$_n$ group ($n$ = 0, 1, 2) was observed at 2.31 ppm. Additionally, no deuterium incorporation into the N–H bond of the *N*-(methyl-$d_3$)aniline is detected since the integration value remained unchanged at 2.83 ppm. This isotope labelling experiment indicates that the formation of a metallaaziridine species is highly unlikely or a reversible process (Scheme 32, **A**), in which the abstracted proton or deuterium is transferred back to its original location at the *N*-methyl group and no exchange between the coordininated NDCD$_3$Ph and the free NHCD$_3$Ph occurs (Scheme 32, **B**).
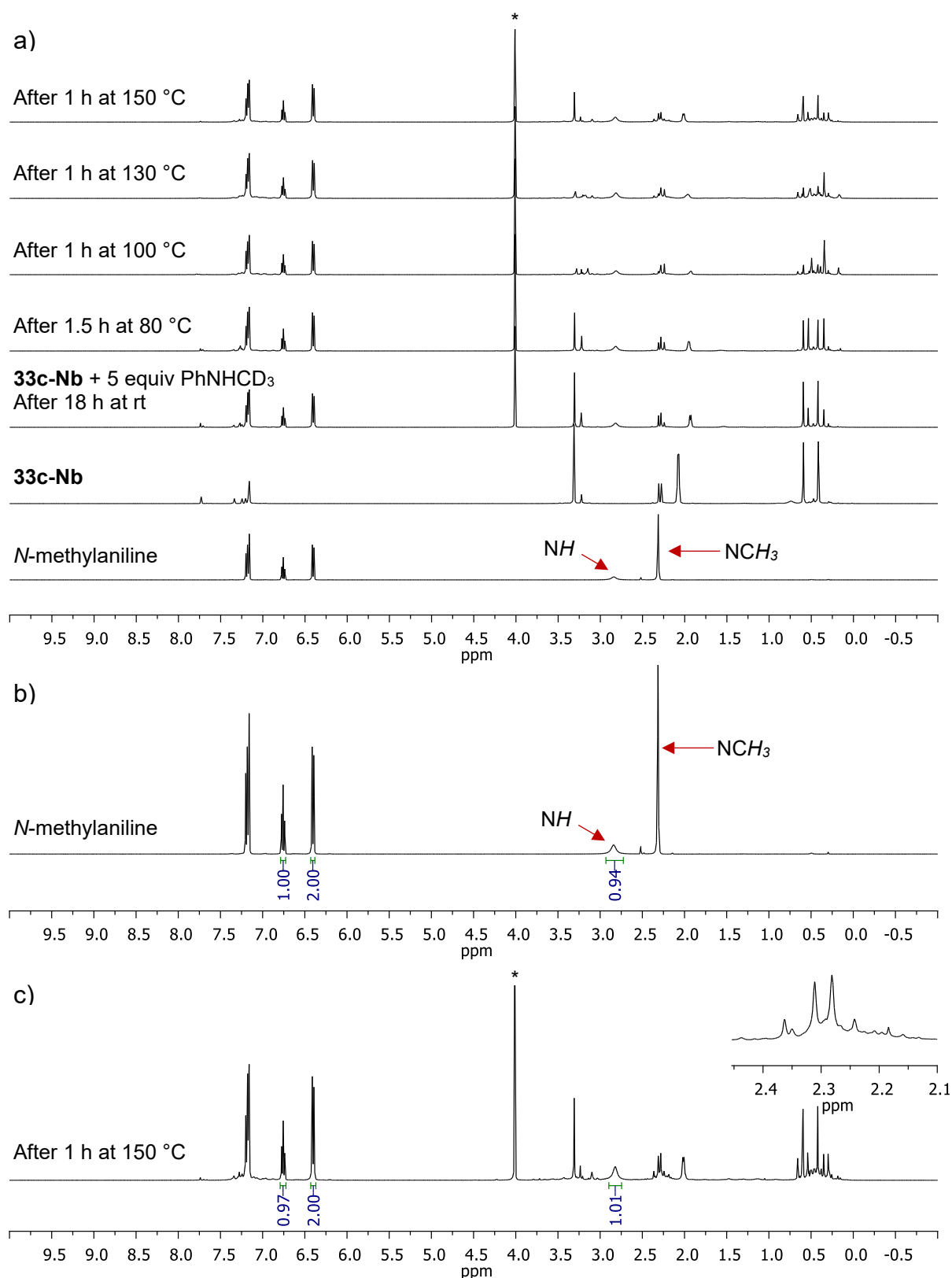
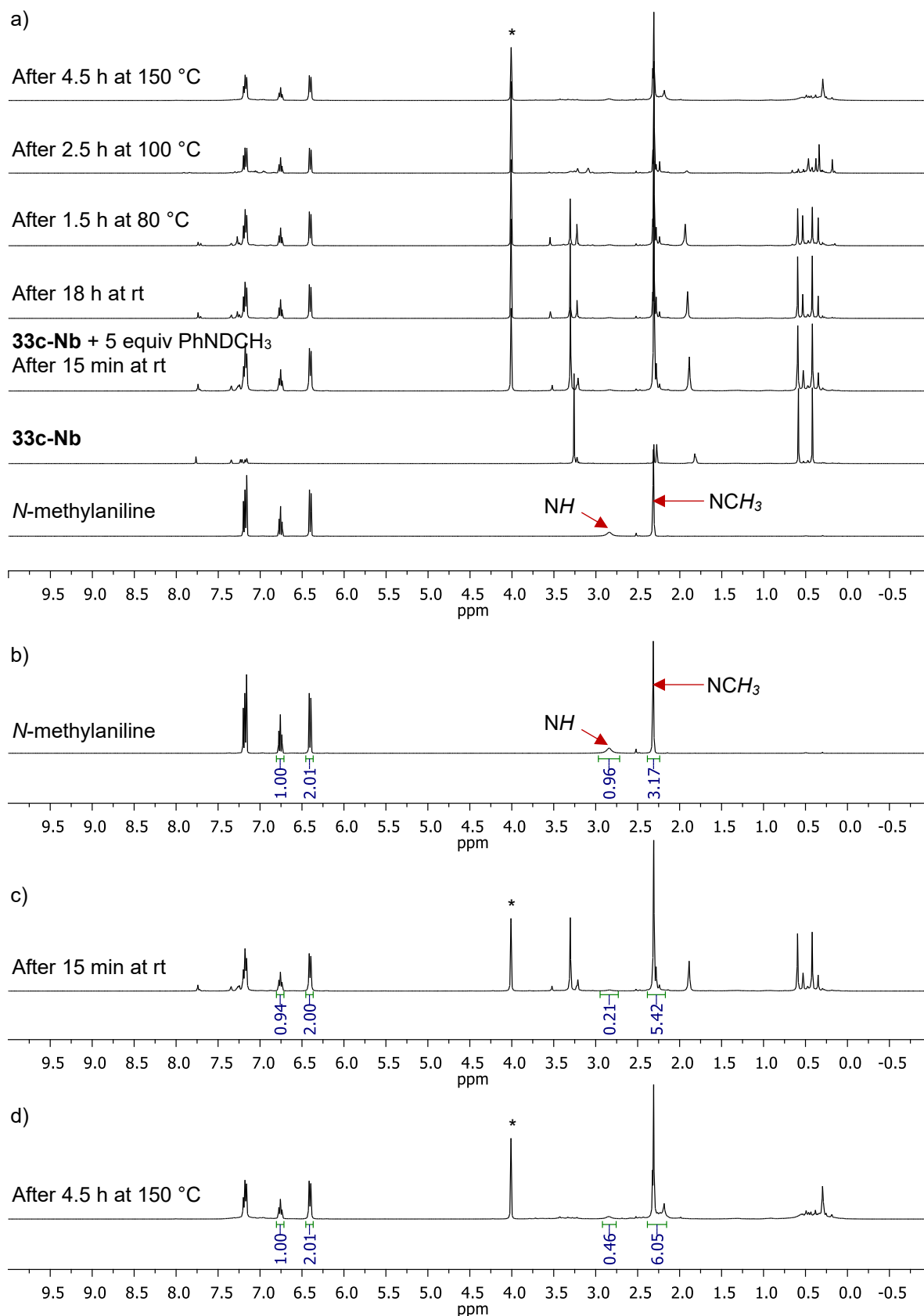*Figure 20:* a) Reaction between **33c-Nb** and 5 equiv *N*-(methyl-*d*$_3$)aniline at different temperatures for a different period of time. b) $^1$H NMR spectrum of *N*-methylaniline. c) $^1$H NMR spectrum of reaction mixture after heating to 150 °C for 15 h. All NMR spectra were recorded in C$_6$D$_6$. Asterisk (*) indicates ferrocene.
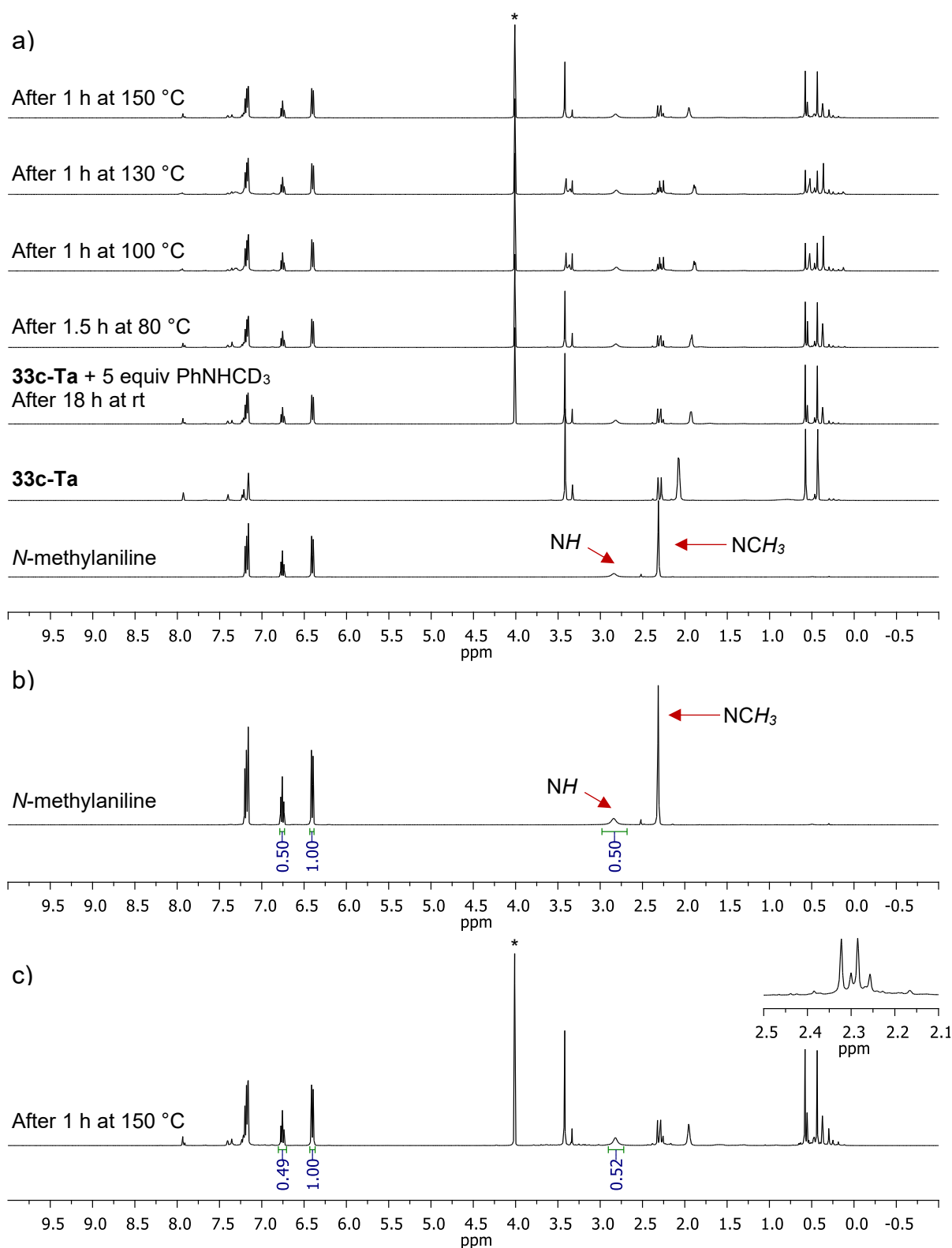
*Figure 21:* a) Reaction between **33c-Ta** and 5 equiv *N*-(methyl-*d₃*)aniline at different temperatures for a different period of time. b) ¹H NMR spectrum of *N*-methylaniline. c) ¹H NMR spectrum of reaction mixture after heating to 150 °C for 15 h. All NMR spectra were recorded in C₆D₆. Asterisk (*) indicates ferrocene.

The same reaction was performed with **33c-Ta** instead of **33c-Nb** and monitored *via* $^1$H NMR spectroscopy. Unfortunately, the results of this experiment show no deuterium scrambling and therefore suggests that a C–H activation is not detectable (Figure 21). Neither a signal for any *N*-CH$_{3-n}$D$_n$group (*n* = 0, 1, 2) was observed at 2.31 ppm, nor was a decreased integration value of the N–H signal of the *N*-(methyl-*d*$_3$)aniline observed.

Furthermore, the reactions of 5 equiv *N-d-N*-methylaniline with 1 equiv **33c-Nb** or 1 equiv **33c-Ta** was performed. This reaction was particularly interesting since not only amido ligands are known to readily abstract protons from less basic substrates, but also η$^1$-vinylic C–M bonds, which display a greater basic character (vinylic C–H bonds display pKa-values of approximately 44) than amido ligands do (N–H bonds of non-protonated dialkylamines display pKa-values of approximately 35 and N–H bonds of non-protonated anilines display pKa-values of approximately 28), hence they should be more prone towards protonation.[173–176] Therefore, it was anticipated that the $^1$H NMR signal of the vinylic proton would disappear upon the addition of the *N-d-N*-methylaniline at room temperature (Scheme 33). Surprisingly, the signal did not vanish at all, and the integration values were the same as before (Figure 22). Even after 2.5 h at 100 °C no deuterium incorporation was observed. This might be devoted to the chelate effect and highlights the stability of the η$^1$-vinylic C–M bond of **33c-Nb** towards comparatively acidic anilines.
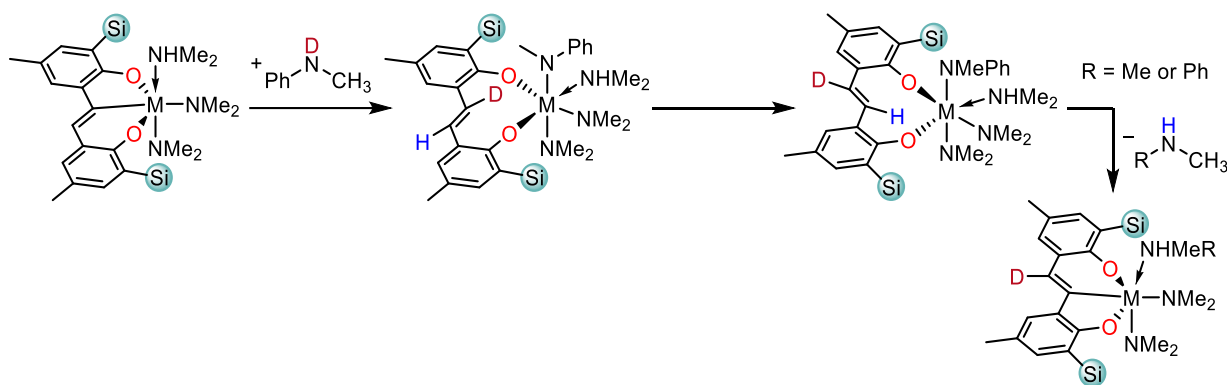


*Scheme 33:* Proposed mechanism of deuterium incorporation into the η$^1$-vinylic ethylene bridge.

The N–H signal of *N*-methylaniline is observed upon the addition of *N-d-N*-methylaniline indicating hydrogen – deuterium exchange. Only one proton in regard to the stoichiometry of complex **33c-Nb** is found, which originated from the dimethylamino ligand, and the signal did not change within 18 h at room temperature. Heating the reaction mixture at 80 °C for 1.5 h and further at 100 °C for 2.5 h did not result in any change of the N–H signal of the coordinated amino ligand. Only when the mixture is heated to 150 °C for 4.5 h, a slight increase in the integral

is observed, but this could be a result of the decomposition or side reactions of the complex or signal overlapping. No $N$-CH$_{3-n}$D$_n$ groups ($n$ = 0, 1, 2) were detected.

The reaction of $N$-$d$-$N$-methylaniline with **33c-Ta** was performed under the same conditions. Similar to the reaction with **33c-Nb**, no deuterium incorporation into the $\eta^1$-vinylic ethylene bridge was observed (Figure 23). After mixing the catalyst solution with $N$-$d$-$N$-methylaniline an instant proton – deuterium exchange of the amino ligand and the aniline substrate was observed, which didn't change after 18 h at room temperature and neither after 2.5 h at 100 °C. Only after heating the mixture for 4.5 h to 150 °C, a higher integrational value for the N–H signal was observed. However, this is most likely a result of complex decomposition and side reactions. No $N$-CH$_{3-n}$D$_n$ groups ($n$ = 0, 1, 2) were detected.

The experimental data from the four experiments utilizing both, $N$-(methyl-$d_3$)aniline and $N$-$d$-$N$-methylaniline as substrates suggest that $N$-methylaniline does not undergo C–H activation, since no deuterium scrambling was observed. Therefore, a metallaaziridine intermediate was supposably not formed.

*Figure 22:* a) Reaction between **33c-Nb** and 5 equiv *N-d-N*-methylaniline at different temperatures for a different period of time. b) $^1$H NMR spectrum of *N*-methylaniline. c) $^1$H NMR spectrum of reaction mixture after the addition of *N-d-N*-methylaniline. d) $^1$H NMR spectrum of reaction mixture after heating to 150 °C for 4.5 h. All NMR spectra were recorded in $C_6D_6$. Asterisk (*) indicates ferrocene.
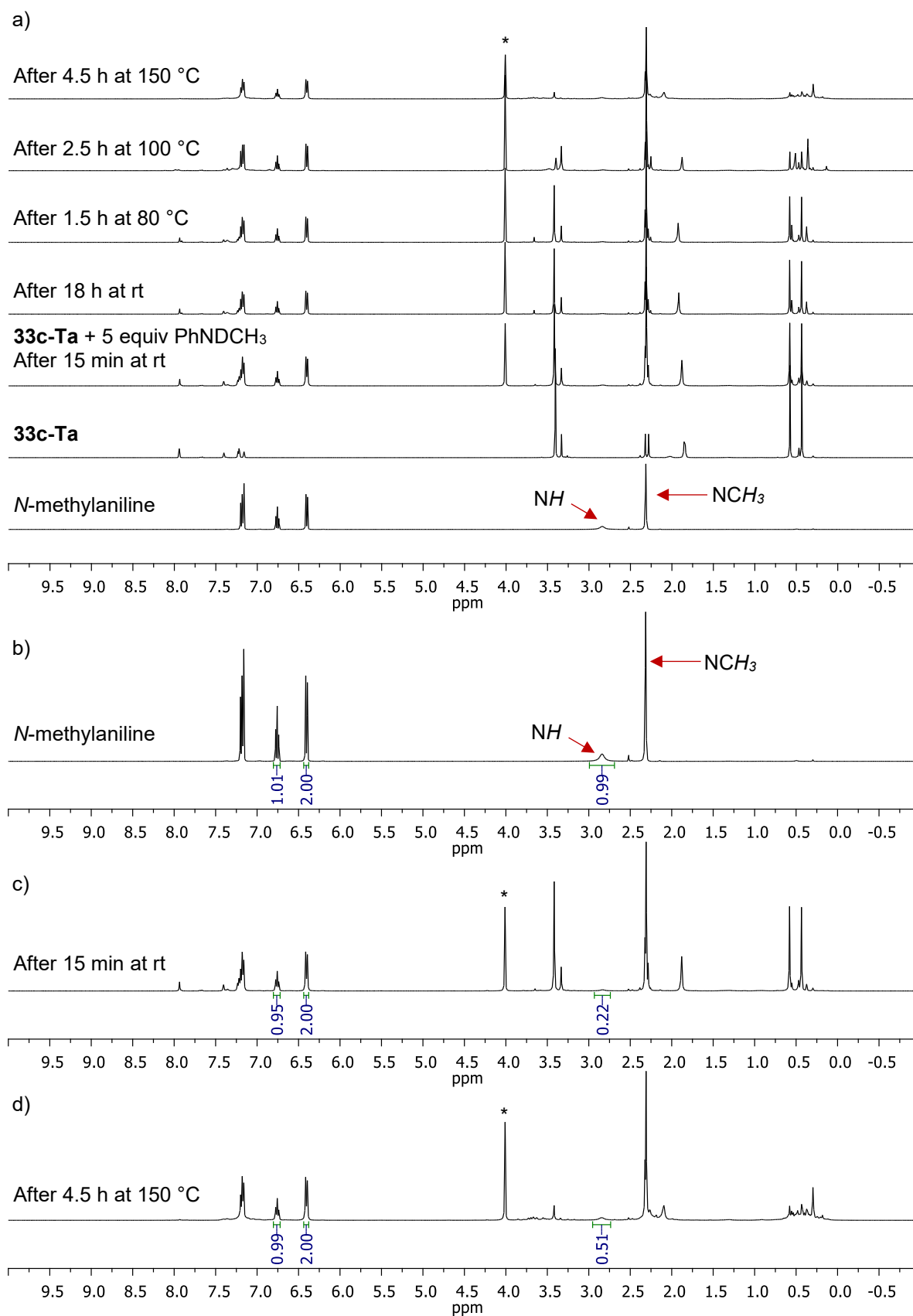
*Figure 23:* a) Reaction between **33c-Ta** and 5 equiv *N-d-N*-methylaniline at different temperatures for a different period of time. b) $^1$H NMR spectrum of *N*-methylaniline. c) $^1$H NMR spectrum of reaction mixture after the addition of *N-d-N*-methylaniline. d) $^1$H NMR spectrum of reaction mixture after heating to 150 °C for 4.5 h. All NMR spectra were recorded in $C_6D_6$. Asterisk (*) indicates ferrocene.

The catalytic hydroaminoalkylation reactions of vinylcyclohexane or trimethyl(vinyl)silane with *N*-(methyl-*d*₃)aniline or *N*-*d*-*N*-methylaniline were performed in order to validate if **33c-Nb** and **33c-Ta** were actively facilitating the C–H activation on a catalytic scale (Scheme 34).
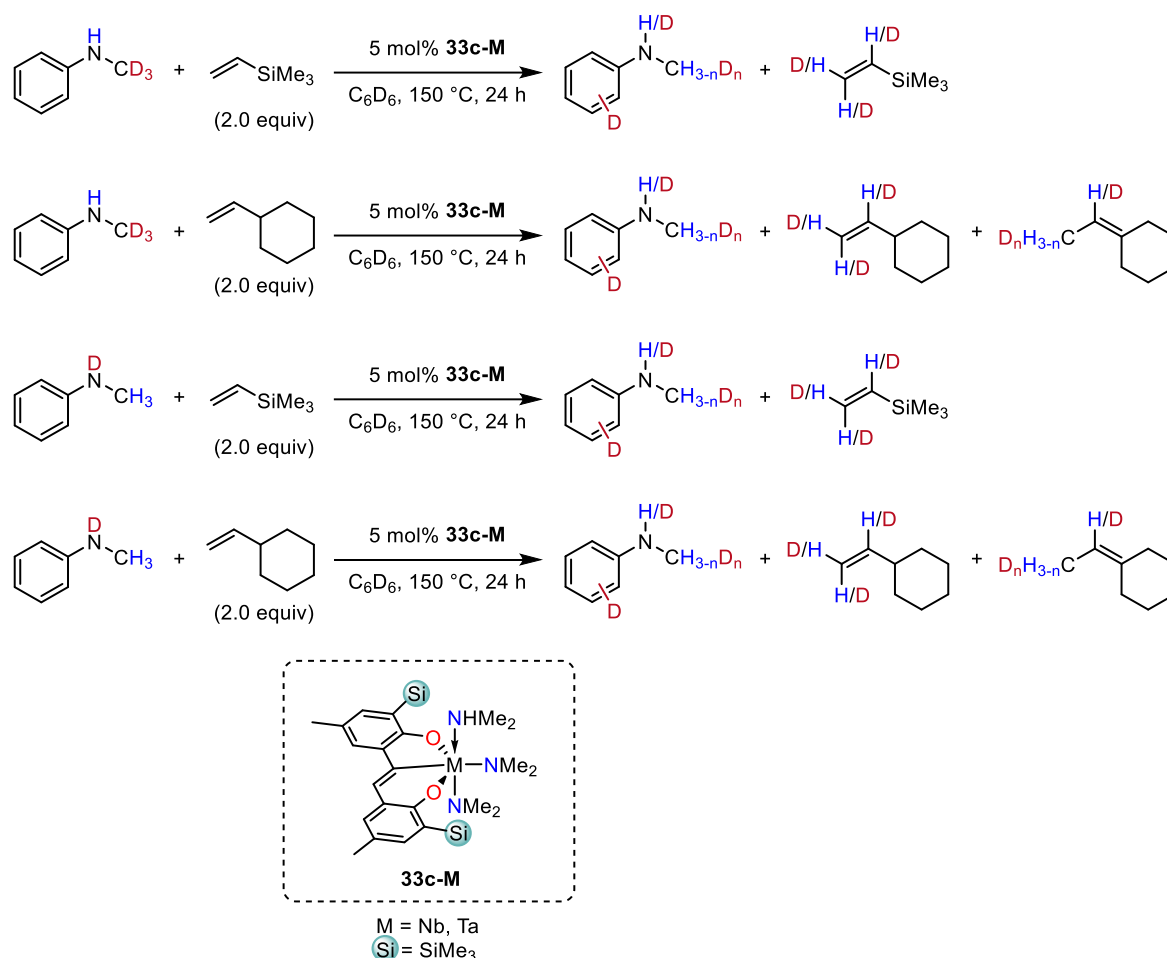


*Scheme 34:* Reactions between 2 equiv trimethyl(vinyl)silane or 2 equiv vinylcyclohexane and *N*-(methyl-*d*₃)aniline or *N*-*d*-*N*-methylaniline in the presence of 5 mol% **33c-Nb** or 5 mol% **33c-Ta** utilizing standard hydroaminoalkylation reactions conditions (GP2).

It was anticipated that deuterium scrambling is observed if the metallaaziridine intermediate is formed. Additionally, deuterium transfer onto the olefinic substrate might occur if the alkene coordinates to the complexes and interacts with **33c-M**.

The catalytic reactions were heated to 150 °C and monitored periodically *via* $^1$H NMR spectroscopy. The reaction of trimethyl(vinyl)silane with *N*-(methyl-*d*₃)aniline in the presence of **33c-Nb** was unsuccessful and the $^1$H NMR spectra remained unchanged throughout the progress of the reaction (Figure 24a). Neither was a different pattern of the olefinic protons observed, nor did the integral of the N–H signal change. Additionally, no *N*-CH$_{3-n}$D$_n$ groups ($n$ = 0, 1, 2) were detected. As expected, the reaction of vinylcyclohexane with *N*-(methyl-*d*₃)aniline in the presence of **33c-Nb** led to an isomerization of the alkene. However, no deuterium

incorporation into the vinylcyclohexane substrate, as well as the formation of a $CH_2D$ group, was observed. The integral of the N–H signal did not change and no $N\text{-}CH_{3-n}D_n$ groups ($n = 0$, 1, 2) were detected (Figure 24b). A similar result is obtained if **33c-Ta** is used. No reaction occurred between trimethyl(vinyl)silane and $N$-(methyl-$d_3$)aniline (Figure 25a). Additionally, no deuterium incorporation into the alkene or aniline was observed. There was no change in the pattern of the olefinic protons, the integrational value of the N–H signal remained unchanged and no peak around 2.31 ppm for the corresponding $N\text{-}CH_{3-n}D_n$ groups ($n = 0$, 1, 2) were detected after heating the mixture to 150 °C for 24 h. The reaction of vinylcyclohexane with $N$-(methyl-$d_3$)aniline in the presence of **33c-Ta** led to no change in the $^1$H NMR spectra (Figure 25b). Hence, it can be concluded that neither **33c-Nb**, nor **33c-Ta** are facilitating C–H activation on a catalytical scale.

The reaction of trimethyl(vinyl)silane with $N$-$d$-$N$-methylaniline in the presence of **33c-Nb** was unsuccessful (Figure 26a). The integral of the N–H signal increased after heating the reaction mixture for 24 h from 0.19 to 0.30. However, there was no indication of deuterium incorporation into the $N$-methyl group, nor into the double bond of the substrate. The integral of the $N$-methyl group, which is overlapping with some signals of the complex, also did not change significantly. The reaction of vinylcyclohexane with $N$-$d$-$N$-methylaniline in the presence of **33c-Nb** led to the isomerization of the alkene (Figure 26b). However, no deuterium incorporation into the substrate and no formation of a $CH_2D$ group was observed. This is a noteworthy result, since it is expected that the most acidic proton, which in this case is the N–D deuterium, protonates the formed C–H activated alkene intermediate to yield a $CH_2D$ group. Similar to the reaction with **33c-Nb**, no reaction of trimethyl(vinyl)silane with $N$-$d$-$N$-methylaniline occurred in the presence of **33c-Ta** (Figure 27a). No deuterium incorporation into the alkene was observed and despite a slight increase in the integration value of the N–H signal, the $N$-methyl group remained unchanged. The reaction of vinylcyclohexane with $N$-$d$-$N$-methylaniline in the presence of **33c-Ta** led to no change in the $^1$H NMR spectra (Figure 27b). Therefore, it is valid to state that neither **33c-Nb**, nor **33c-Ta** participate in C–H activation and the isomerization of the olefin is not affected by the fairly acidic $N$-$d$-$N$-methylaniline.

a)

After 24 h at 150 °C

1.02  2.00                    0.98

After 15 h at 150 °C

1.05  2.00                    1.03

Before heating

0.97  2.00                    1.05

9.5  9.0  8.5  8.0  7.5  7.0  6.5  6.0  5.5  5.0  4.5  4.0  3.5  3.0  2.5  2.0  1.5  1.0  0.5  0.0  -0.5
ppm

b)

5.3   5.2   5.1
ppm

After 24 h at 150 °C

*   NH

1.02  2.00                    0.99

After 15 h at 150 °C

1.00  2.00                    1.02

Before heating

0.96  2.00                    1.00

9.5  9.0  8.5  8.0  7.5  7.0  6.5  6.0  5.5  5.0  4.5  4.0  3.5  3.0  2.5  2.0  1.5  1.0  0.5  0.0  -0.5
ppm

*Figure 24:* a) Reaction between 2 equiv trimethyl(vinyl)silane and *N*-(methyl-*d*₃)aniline in the presence of 5 mol% **33c-Nb**. b) Reaction between 2 equiv vinylcyclohexane and *N*-(methyl-*d*₃)aniline in the presence of 5 mol% **33c-Nb**. All NMR spectra were recorded in $C_6D_6$. Asterisk (*) indicates ferrocene.

*Figure 25:* a) Reaction between 2 equiv trimethyl(vinyl)silane and *N*-(methyl-*d₃*)aniline in the presence of 5 mol% **33c-Ta**. b) Reaction between 2 equiv vinylcyclohexane and *N*-(methyl-*d₃*)aniline in the presence of 5 mol% **33c-Ta**. All NMR spectra were recorded in $C_6D_6$. Asterisk (*) indicates ferrocene.
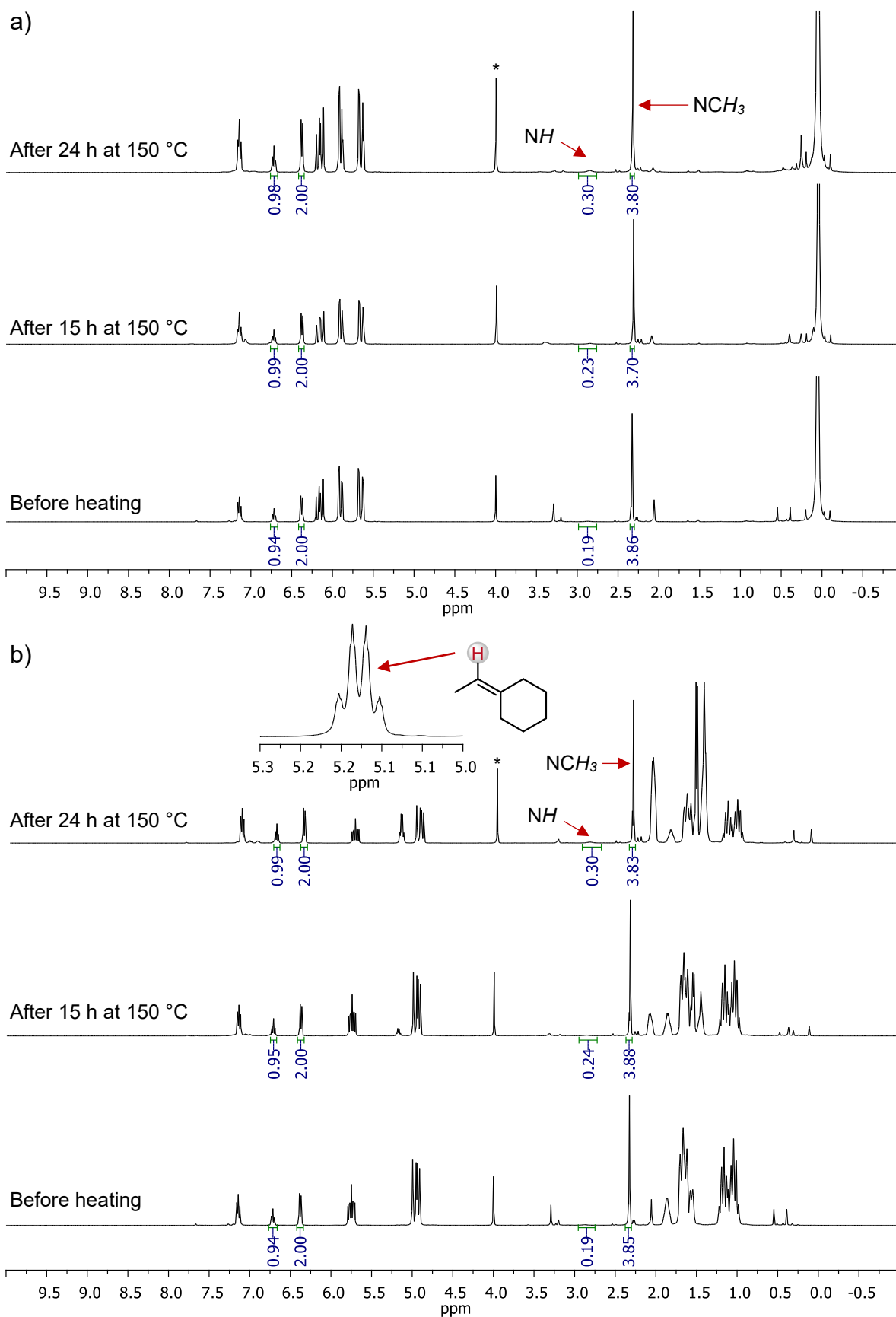
*Figure 26:* a) Reaction between 2 equiv trimethyl(vinyl)silane and *N-d-N*-methylaniline in the presence of 5 mol% **33c-Nb**. b) Reaction between 2 equiv vinylcyclohexane and *N-d-N*-methylaniline in the presence of 5 mol% **33c-Nb**. All NMR spectra were recorded in C6D6. Asterisk (*) indicates ferrocene.
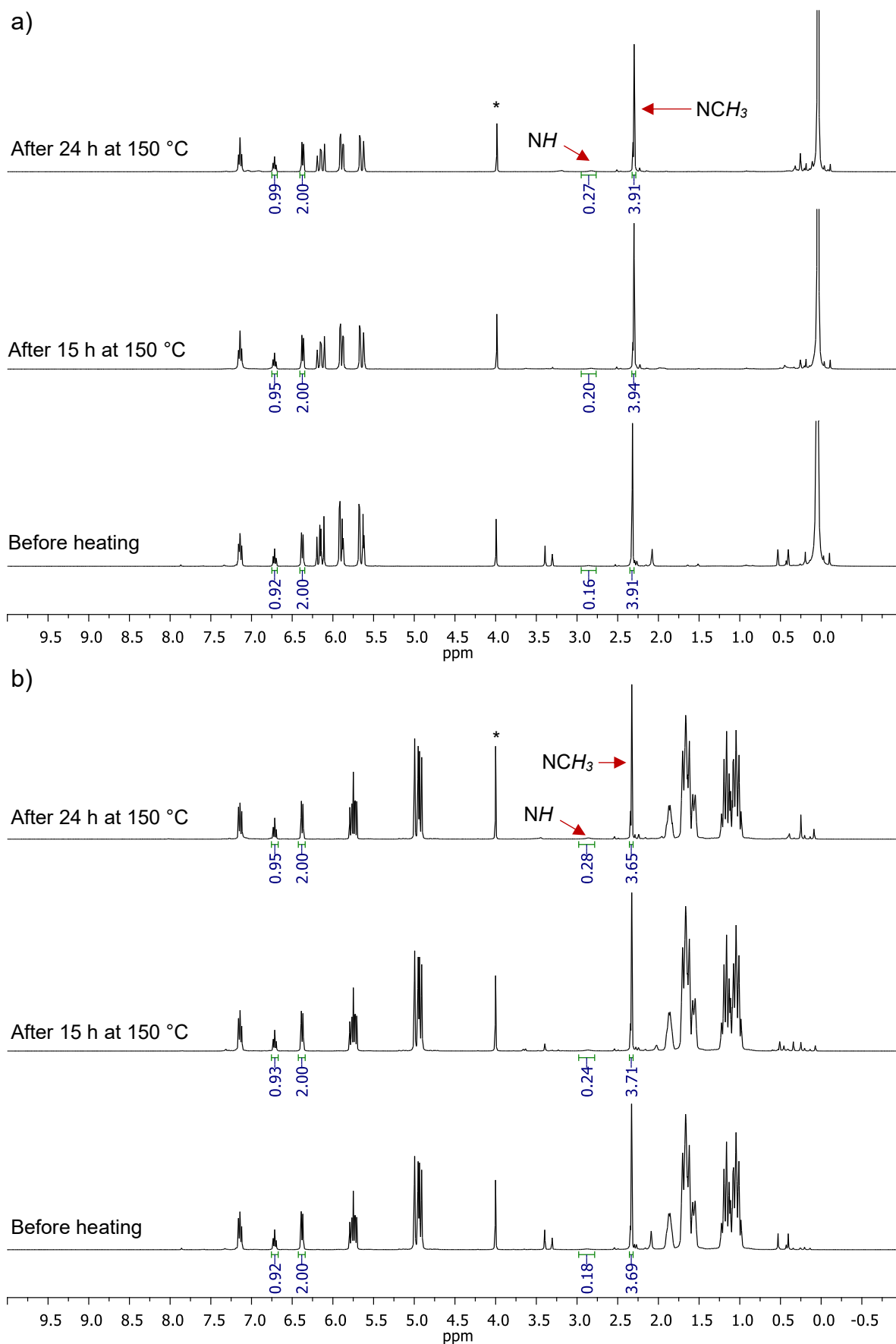
*Figure 27:* a) Reaction between 2 equiv trimethyl(vinyl)silane and *N-d-N*-methylaniline in the presence of 5 mol% **33c-Ta**. b) Reaction between 2 equiv vinylcyclohexane and *N-d-N*-methylaniline in the presence of 5 mol% **33c-Ta**. All NMR spectra were recorded in $C_6D_6$. Asterisk (*) indicates ferrocene.

## 3.6.  Reactivity of Complexes towards Alkenes

Since complexes **33-M** were rather unreactive towards *N*-methylaniline and all **33-Nb** complexes were able to isomerize terminal alkenes, it was of interest to investigate if the alkene would react or interact with niobium-based complex **33c-Nb**. Any hint for a new organometallic species bearing the alkene in $\eta^2$ fashion or even an C–H activated $\eta^3$ allylic intermediate would have been of great interest. The stoichiometric reaction of **33c-Nb** with 5.0 equiv of 4-phenyl-1-butene was therefore monitored *via* $^1$H NMR spectroscopy (Figure 28). No change in the $^1$H NMR spectra was observed at room temperature after heating to 60 °C for 18 h. A new signal next to the original peaks of the silyl groups was observed after heating the mixture to 90 °C for 2 h. This might suggest a new complex species or decomposition. However, up until this point
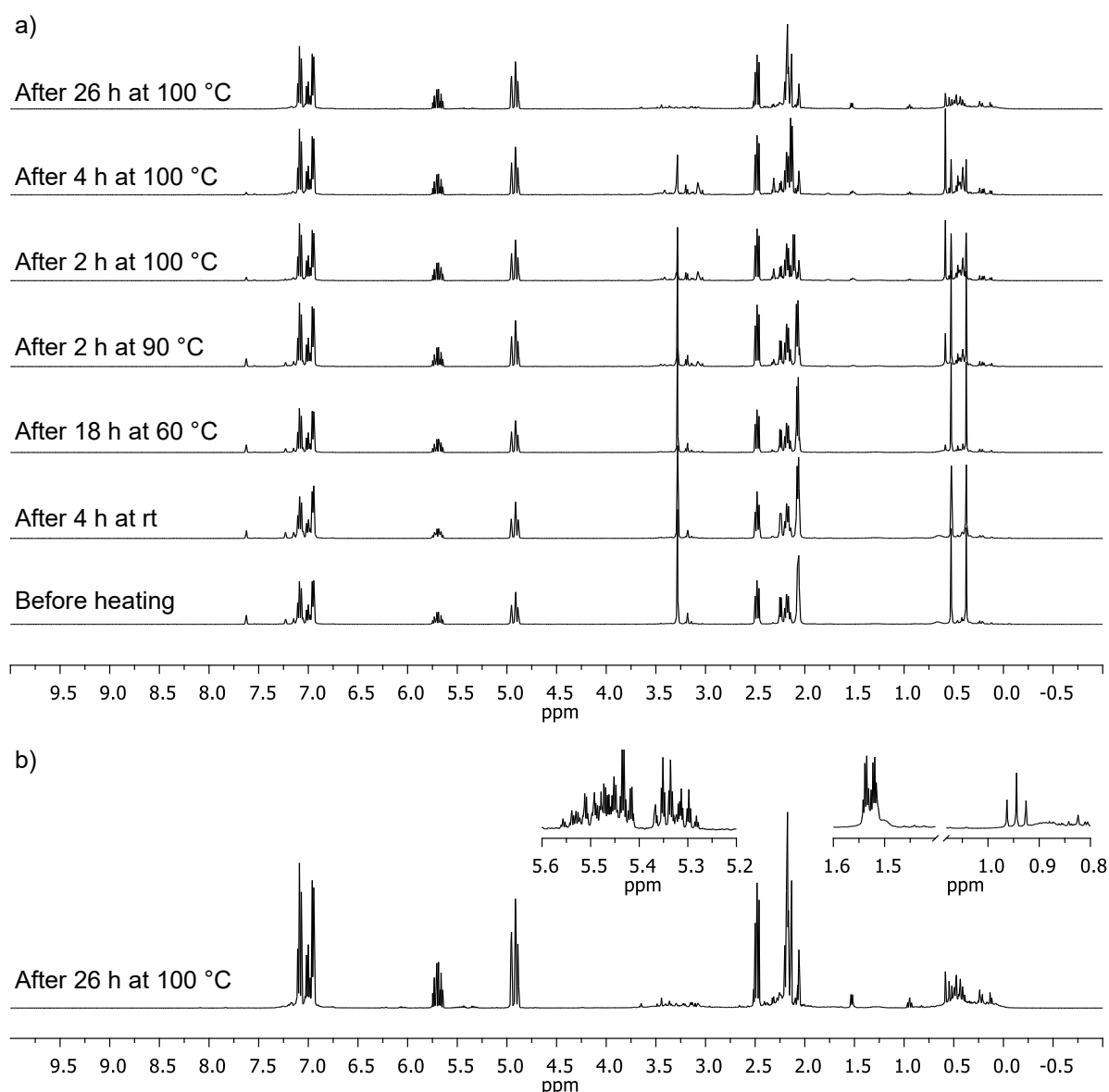


*Figure 28:* a) $^1$H NMR spectra of the reaction of complex **33c-Nb** with 5.0 equiv of 4-phenyl-1-butene at different temperatures for different reaction times. b) $^1$H NMR spectrum of the reaction mixture after 26 h at 100 °C. The NMR spectra were recorded in C$_6$D$_6$. Signals of isomerization products are highlighted.

in time, there is no indication for any coordination of the alkene. $^1$H NMR spectroscopy signals of isomerization products were observed after heating the mixture to 100 °C for 2 h and after heating the mixture for 26 h in total to 100 °C approximately 5 % of the alkene converted to the thermodynamically more stable internal alkenes. Unfortunately, no noticeable new $^1$H NMR spectroscopic signals indicating coordination or formation of an $\eta^3$ intermediate were observed and only complex decomposition was detected.

## 4. Conclusion and Outlook

In the realm of this master project three bisphenolate-type ligands and their niobium(V) and tantalum(V) complexes have been synthesized and characterized by $^1$H and $^{13}$C NMR spectroscopy, single crystal X-ray diffraction analysis and elemental analysis. Furthermore, complexes **33-M** have been investigated in regard to their catalytic activity in the intermolecular hydroaminoalkylation reaction of various alkenes and alkynes with *N*-methylaniline and other amines, intramolecular hydroamination of 2,2-diphenylaminopent-5-ene and intermolecular hydroamination of benzylamine and *N*-methylbenzylamine with 4-phenyl-1-butene.

The ligands were synthesized starting from 3-bromo-2-hydroxy-5-methylbenzaldehyde **31**, which was transformed into 3,3'-dibromo-2,2'-dihydroxy-5,5'-dimethyl-(*E*)-stilbene **32** in a McMurry coupling. Utilizing 3,3'-dibromo-(*E*)-stilbene **32** and the corresponding silyl chloride in a retro-Brook rearrangement led to the formation of the desired ligand **33** with yields ranging from 38 to 46 % upon purification. The complexes **33-M** were prepared from a stoichiometric reaction of ligand **33** with pentakis(dimethylamido)niobium(V) or pentakis(dimethyl-amido)tantalum(V) and after recrystallization 49 – 83 % of the pure product were obtained.

Unfortunately, the Group 5 metal complexes **33-M** were inactive in the hydroaminoalkylation reaction of secondary amines with terminal alkenes or internal alkynes. Instead, olefin isomerization was observed for the niobium(V) complexes **33-Nb**. Additionally, isotope-labelling experiments revealed that no metallaaziridine intermediate was formed. A combination of **33c-Nb** and TMS-Cl, in a 1:1.5 ratio, has shown to facilitate the hydroaminoalkylation reaction of *N*-methylaniline and 4-phenyl-1-butene. The conversion, however, was rather low compared to other active complexes, such as **7**.[74]

The stoichiometric reaction of **33b-Nb** and *N*-methylaniline with the objective of obtaining the *N*-methylanilino-bis(*N*-methylanilido)niobium(V) complex revealed to be rather challenging and surprisingly, rather harsh conditions and periodic removal of free dimethylamine *in vacuo* were necessary to introduce *N*-methylaniline into the coordination sphere of niobium(V).

Despite the poor catalytic reactivity in hydroamination and hydroaminoalkylation, niobium(V) and tantalum(V) complexes **33-M** could potentially be active in different catalytic reactions. The basic metalated ethylene bridge could enable synergistic actions of the metal centre and the ligand. This could give access to novel catalytic reactions. On the other hand, alternative approaches could potentially increase the catalytic activity of said complexes in hydroamination and hydroaminoalkylation. Modification of the ethylene bridge in ligands **33a–33c** by implementing substituents, such as methyl groups or fluorine, would result in an ethylene bridge

devoid of hydrogen atoms. This would prevent the C–H activation of the ethylene bridge. Alternatively, utilising sterically less hindered ligands, such as salicylic alcohol derivatives might deliver catalytically more active metal complexes.

# 5. Experimental Section

## 5.1. General

Unless otherwise stated, all glassware was oven-dried at 120 °C for at least 24 h before use and all reactions were performed under inert conditions, either using standard Schlenk techniques utilizing argon as inert gas or in an argon-filled MBraun® UNIlab pro glovebox. All solvents were distilled before use unless otherwise noted. Benzene, toluene and THF were distilled from sodium/benzophenone ketyl. Acetonitrile and amines were distilled from finely powdered $CaH_2$. Pentane, hexane, heptane, $Et_2O$ and DCM were directly used from the solvent purification system (SPS; MBRAUN SPS-800). All reagents were used as received from commercial suppliers unless otherwise noted. Ligands **33a-c** and complexes **33-M** were prepared according to the general procedure developed in the Hultzsch group by John Soltys. [136,137] The starting materials **30** and **31** for the synthesis of **33a-c** were synthesized during the Organisch-chemisches Fortgeschrittenenpraktikum – Modul OC-4. The reaction progress was monitored by thin layer chromatography (TLC) performed on aluminium plates coated with silica gel 60 with 0.2 mm thickness (Pre-coated TLC-sheets ALUGRAM® Xtra SIL G/UV254). Chromatograms were visualized by fluorescence quenching with UV light at 254 nm or 363 nm. Column chromatography was performed using silica gel 60 Å (230-400 Mesh particle size, Sigma-Aldrich) and Biotage® SP4 and Isolera Flash Systems.

Gas chromatography-mass spectrometry (GC-MS) was performed on an Agilent Technologies instrument with 5977B MSD High Efficiency Source and a 7820A GC-system equipped with a HP-5ms column (30 m, 250 μm, 0.25 μm) and a single quadrupole mass spectrometer.

Mass spectra were obtained using a Bruker maXis UHR-TOF spectrometer, using electrospray ionization (ESI). The main signals are reported in m/z units.

All $^1$H NMR and $^{13}$C NMR spectra were recorded using a Bruker BioSpin AV III 400, AV III 600 or AV III HD 700 spectrometer at 295 K. Chemical shifts are given in parts per million (ppm, δ), referenced to the solvent peak of $CDCl_3$, defined at δ = 7.26 ppm ($^1$H NMR) and δ = 77.16 ppm ($^{13}$C NMR), $C_6D_6$, defined at δ = 7.16 ppm ($^1$H NMR) and δ = 128.06 ppm ($^{13}$C NMR), acetone-$d_6$, defined at δ = 2.05 ppm ($^1$H NMR) and δ = 206.26 and 29.84 ppm ($^{13}$C NMR). Coupling constants are given in Hz ($J$).[177] $^1$H NMR splitting patterns are designated as singlet (s), doublet (d), triplet (t) or quartet (q) as they appeared in the spectrum. Splitting patterns that could not be interpreted or easily visualized are designated as multiplet (m) or broad (br). Signals assignments were based on the results of $^1$H,$^1$H COSY; $^1$H,$^1$H TOCSY; $^1$H,$^{13}$C HSQC; $^1$H,$^{13}$C HMBC and $^1$H,$^1$H NOESY experiments.

Elemental analysis measurements were performed on a Perkin Elmer 2400 CHN Elemental Analyzer at the Microanalytical Laboratory of the University of Vienna.

Single-crystal X-ray Diffraction measurements were performed at the Centre for X-ray Structure Analysis of the University of Vienna on a Bruker D8 dual source (Cu, Mo radiation) or STOE Stadivari dual source (CuKα (λ = 1.54178) and MoKα (λ = 0.71073) radiation) instrument, equipped with a Dectris EIGER2 R500 detector.The crystal structures were solved by direct methods and refined by full-matrix least-squares techniques. Non-hydrogen atoms were refined anisotropically. Hydrogen atoms were placed at calculated positions and refined as riding atoms with isotropic displacement parameters. The following software was used: *Bruker SAINT software package*[178] using a narrow-frame algorithm for frame integration, *SADABS*[179] for absorption correction, *OLEX2*[180] for structure solution, refinement, molecular diagrams and graphical user-interface, *SHELXLE*[181] for refinement and graphical user-interface, *SHELXS-2013*[182] for structure solution, *SHELXL-2013*[180] for refinement, *Platon* for symmetry check.

## 5.2. Ligand Synthesis

### 5.2.1. (*E*)-6,6'-(ethene-1,2-diyl)bis(2-bromo-4-methylphenol) – 32
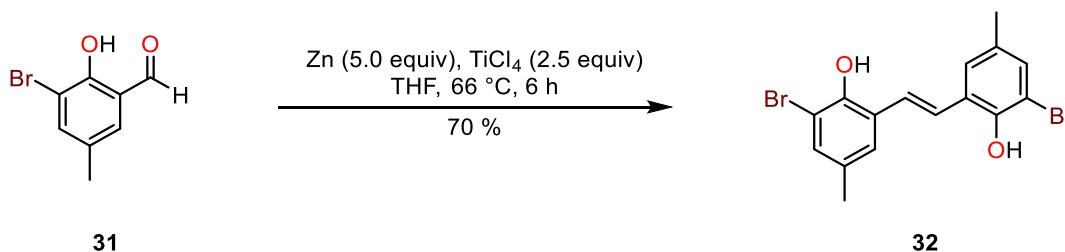


Following a procedure from John Soltys,[137] a Schlenk flask was charged with zinc dust (3.04 g, 46.5 mmol, 5.0 equiv) and stirred under vacuum. After 45 min, dry THF (60 mL) was added and the suspension was cooled to 0 °C. $TiCl_4$ (2.55 mL, d = 1.73 g/mL, 23.3 mmol, 2.5 equiv) was added dropwise and upon complete addition, the reaction mixture was heated to reflux for 2 h. After cooling to 0 °C, 3-bromo-5-methylsalicylaldehyde **31** (2.00 g, 9.3 mmol) was added to the reaction flask under a constant flow of argon. The black suspension was refluxed for 2 h before cooling down to room temperature. The reaction mixture was diluted with ethyl acetate (40 mL) and quenched with an ice-cold 10 % aqueous solution of potassium carbonate (30 mL). After stirring overnight, the suspension was filtered over Celite. The residual solids were washed thoroughly with ethyl acetate until the filtrate was colourless. The organic phase was washed with deionized water (3 × 20 mL), brine (30 mL), and dried over $MgSO_4$. The solvent was reduced to a volume of 15 – 20 mL *in vacuo*. The yellow-orange precipitate was filtered off and washed with a minimum amount of benzene to yield the desired product as a pale-yellow crystalline material (1.30 g, 3.3 mmol, 70 %).

**$^1$H NMR** (400 MHz, acetone-$d_6$): δ = 7.88 (s, 2H, O*H*), 7.49 (s, 2H, H-7), 7.44 (s, 2H, H-2), 7.28 (s, 2H, H-4), 2.29 (s, 6H, H-8) ppm.

**$^{13}$C {$^1$H} NMR** (101 MHz, acetone-$d_6$): δ = 149.7 (C-6), 132.8 (C-2), 131.8 (C-3), 127.6 (C-5), 127.2 (C-4), 125.3 (C-7), 111.9 (C-1), 20.3 ppm.



**HRMS** (ESI): Calc. for $C_{16}H_{14}Br_2O_2Na$ 418.9253, found 418.9250 [MNa]$^+$.
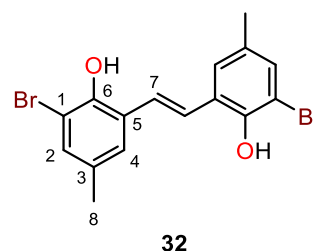
### 5.2.2. (*E*)-6,6'-(ethene-1,2-diyl)bis(4-methyl-2-(methyldiphenylsilyl)phenol) – 33a
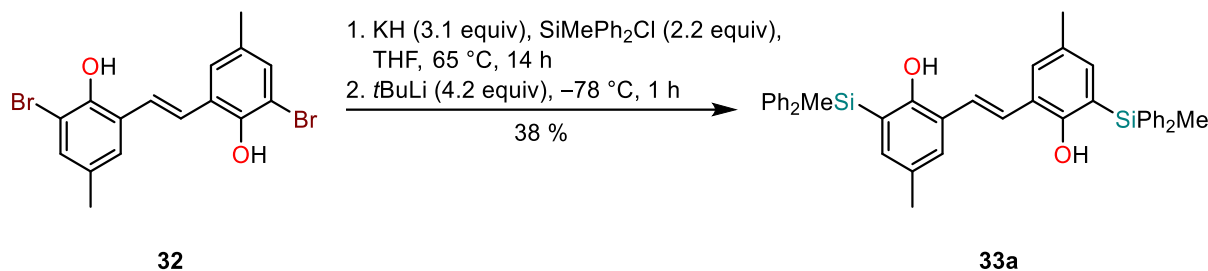


Following a procedure from John Soltys,[137] 3,3'-dibromo-2,2'-dihydroxy-5,5'-dimethyl-(*E*)-stilbene **32** (1000 mg, 2.5 mmol) was added to a 200 mL Schlenk tube and dissolved in dry THF (60 mL). KH (312 mg, 7.8 mmol, 3.1 equiv) was added and the resulting mixture was stirred for 1 h, followed by the addition of methyldiphenylchlorosilane (1.16 mL, d = 1.11 g/mL, 5.5 mmol, 2.2 equiv). The reaction mixture was stirred at 65 °C for 14 h. The solution was first allowed to cool down to room temperature, followed by cooling down to –78 °C. The mixture was slowly charged with *t*BuLi (1.7 M in hexanes, 6.2 mL, 10.5 mmol, 4.2 equiv) and stirred for 1 h. The resulting mixture was allowed to slowly warm up to room temperature over the course of 2 h. Then, the reaction was quenched with a saturated aqueous solution of ammonium chloride (20 mL) and the organic solvent was removed *in vacuo*. The remaining aqueous residue was extracted with Et$_2$O (2 × 30 mL), and the organic layers were combined, washed with deionized water (2 × 10 mL), brine (10 mL), and dried over MgSO$_4$. The solvent was removed *in vacuo* and a dark, yellow oil was obtained as a crude product. The product was separated from the impurities *via* flash column chromatography on silica gel (0–35 % EtOAc in heptanes) thus yielding a purified but still slightly impure product. A recrystallization from ethyl acetate (2.5 mL) yielded the pure product as a white crystalline material (601 mg, 0.95 mmol, 38 %).

**¹H NMR** (700 MHz, C$_6$D$_6$): δ = 7.66 – 7.60 (m, 8H, H-11), 7.33 (d, *J* = 1.9 Hz, 2H, H-4), 7.27 (s, 2H, H-7), 7.18 (d, *J* = 1.9 Hz, 2H, H-2), 7.18 – 7.15 (m, 12H, H-12 and H-13), 4.89 (s, 2H, O*H*), 2.07 (s, 6H, H-8), 0.85 (s, 6H, H-9) ppm.



**33a**

**¹³C {¹H} NMR** (176 MHz, C$_6$D$_6$): δ = 157.0 (C-6), 137.1 (C-2), 136.3 (C-10), 135.7 (C-11), 130.3 (C-4), 130.2 (C-3), 130.0 (C-13), 128.6 (C-12), 125.6 (C-1), 125.0 (C-7), 122.0 (C-5), 20.7 (C-8), –2.7 (C-9) ppm.

**HRMS** (ESI): Calc. for C$_{42}$H$_{40}$O$_2$Si$_2$Na 655.2459, found 655.2452 [MNa]⁺.
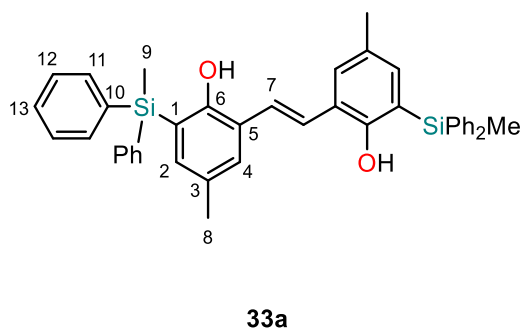
### 5.2.3.  (*E*)-6,6'-(ethene-1,2-diyl)bis(2-(dimethyl(phenyl)silyl)-4-methylphenol) – 33b
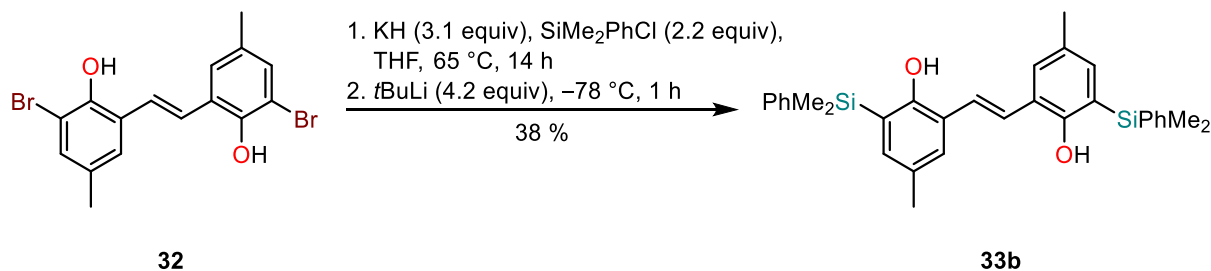


**32**                                                                  **33b**

Following a procedure from John Soltys,[137] 3,3'-dibromo-2,2'-dihydroxy-5,5'-dimethyl-(*E*)-stilbene **32** (1000 mg, 2.5 mmol) was added to a 200 mL Schlenk tube and dissolved in dry THF (60 mL). KH (312 mg, 7.8 mmol, 3.1 equiv) was added, and the resulting mixture was stirred for 1 h, followed by the addition of dimethylphenylchlorosilane (0.93 mL, d = 1.02 g/mL, 5.5 mmol, 2.2 equiv). The reaction mixture was stirred at 65 °C for 14 h. The solution was first allowed to cool down to room temperature followed by cooling down to –78 °C. The mixture was slowly charged with *t*BuLi (1.7 M in hexanes, 6.2 mL, 10.6 mmol, 4.2 equiv) and stirred for 1 h. The resulting mixture was allowed to slowly warm up to room temperature over the course of 2 h. Then, the reaction was quenched with a saturated aqueous solution of ammonium chloride (15 mL) and the organic solvent was removed under reduced pressure. The remaining aqueous residue was extracted with Et$_2$O (2 × 30 mL), and the organic layers were combined, washed with deionized water (2 × 10 mL), brine (10 mL), and dried over MgSO$_4$. The solvent was removed *in vacuo* and a dark yellow oil was obtained. The mixture was purified by flash column chromatography on silica gel (0–20 % EtOAc in heptanes) followed by a second flash column chromatography on silica gel (0–30 % DCM in heptanes) to yield the pure product as an off-white oil. Dissolving the product in ethyl acetate and subsequential removal of the solvent *in vacuo* led to the isolation of the desired product as an off-white solid (487.2 mg, 1.0 mmol, 38 %)

**¹H NMR (600 MHz, C$_6$D$_6$):** δ = 7.64 – 7.61 (m, 4H, H-11), 7.23 – 7.18 (m, 10H, H-2, H-4, H-12 and H-13), 7.00 (s, 2H, H-7), 4.63 (s, 2H, O*H*), 2.15 (s, 6H, H-8), 0.60 (s, 12H, H-9) ppm.



**33b**
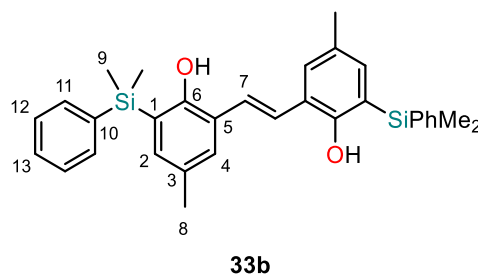
**¹³C {¹H} NMR (151 MHz, C$_6$D$_6$):** δ = 156.5 (C-6), 138.4 (C-10), 136.2 (C-2), 134.7 (C-11), 130.0 (C-3), 130.0 (C-4), 129.8 (C-13), 128.5 (C-12), 125.5 (C-7), 125.0 (C-5), 124.3 (C-1), 20.7 (C-8), –1.9 (C-9) ppm.

**HRMS (ESI):** Calc. for $C_{32}H_{36}O_2Si_2Na$ 531.2146, found 531.2141 [MNa]+.

### 5.2.4.  (*E*)-6,6'-(ethene-1,2-diyl)bis(4-methyl-2-(trimethylsilyl)phenol) – 33c
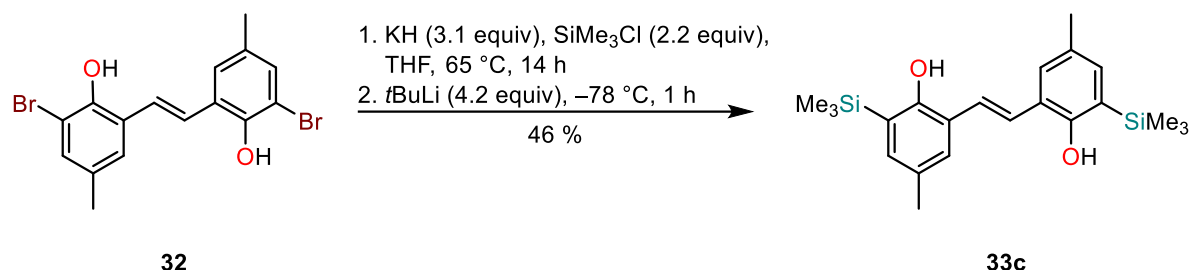


Following a general procedure from John Soltys,[137] 3,3'-dibromo-2,2'-dihydroxy-5,5'-dimethyl-(*E*)-stilbene **32** (1629 mg, 4.1 mmol) was added to a 200 mLSchlenk tube and dissolved in dry THF (90 mL). KH (509 mg, 9.8 mmol, 3.1 equiv) was added and the resulting mixture was stirred for 1 h, followed by the addition of trimethylchlorosilane (1.14 mL, d = 0.86 g/mL, 9.0 mmol, 2.2 equiv). The reaction mixture was stirred at 65 °C for 14 h. The solution was allowed to cool down to room temperature and was further cooled down to –78 °C. The mixture was slowly charged with *t*BuLi (1.7 M in hexanes, 10.1 mL, 17.2 mmol, 4.2 equiv) and stirred for 1.5 h. The resulting mixture was allowed to slowly warm up to room temperature over the course of 2 h. Then, the reaction was quenched with a saturated aqueous solution of ammonium chloride (20 mL) and the organic solvent was removed under reduced pressure. The remaining aqueous residue was extracted with Et$_2$O (2 × 30 mL), and the combined organic layers were washed with deionized water (2 × 10 mL), brine (10 mL), and dried over MgSO$_4$. The solvent was removed *in vacuo* and a dark, yellow crude oil was obtained. The viscous oil was loaded on a 100 g column cartridge and purified by flash column chromatography on silica gel (0–20 % EtOAc in heptanes) to give the pure product as a white solid. Additional impure fractions were recrystalized from a mixture of heptanes/ethyl acetate (90:10), filtered and washed with a minimum amount of heptane to yield the desired product as white crystalline needles (720 mg in total, 1.9 mmol, 46 %).

**1H NMR** (600 MHz, C$_6$D$_6$): δ = 7.24 (d, *J* = 1.8 Hz, 2H, H-2), 7.09 (d, *J* = 1.7 Hz, 2H, H-4), 6.74 (s, 2H, H-7), 4.50 (s, 2H, O*H*), 2.21 (s, 6H, H-8), 0.44 (s, 18H, H-9) ppm.



**13C {1H} NMR** (151 MHz, C$_6$D$_6$): δ = 156.1 (C-6), 135.9 (C-2), 129.9 (C-3), 129.7 (C-4), 126.5 (C-1), 126.1 (C-7), 124.1 (C-5), 20.7 (C-8), –0.6 (C-9) ppm.
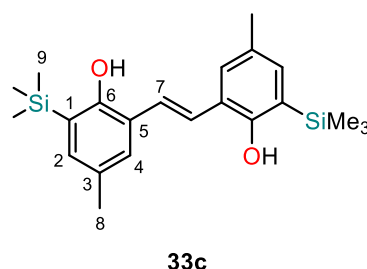
**HRMS** (ESI): Calc. for $C_{22}H_{32}O_2Si_2Na$ 407.1833, found 407.1832 $[MNa]^+$.

**Anal. Calcd.** for $C_{22}H_{32}O_2Si_2$: C, 68.69; H, 8.39; Found: C, 68.29; H, 8.36.

## 5.3. Metal Complex Synthesis

### 5.3.1. General Procedure for complexation



| 33 | Si |
|-----|----------|
| 33a | SiMePh₂ |
| 33b | SiMe₂Ph |
| 33c | SiMe₃ |

M = Nb, Ta

| cat. | Si |
|--------|----------|
| 33a-M | SiMePh₂ |
| 33b-M | SiMe₂Ph |
| 33c-M | SiMe₃ |
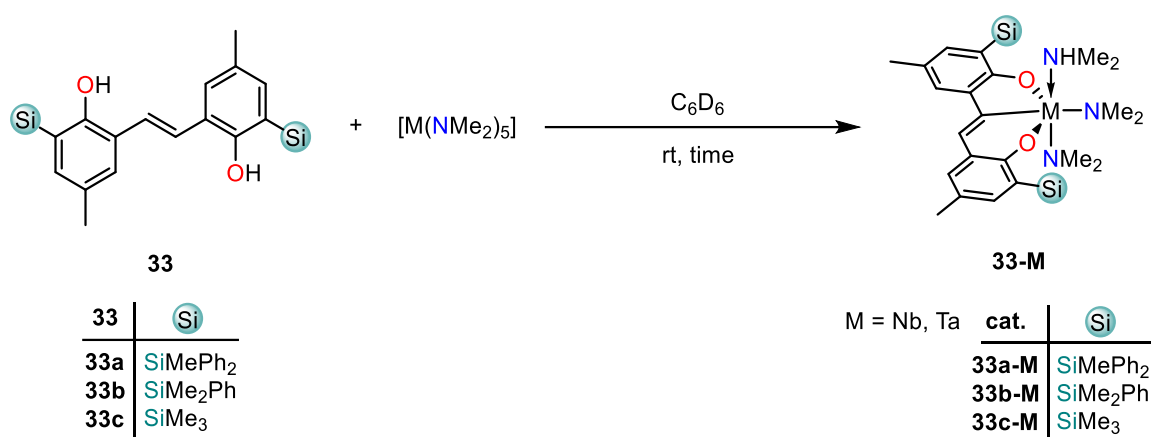
In the glovebox, two vials were charged with ligand **33** (0.025 mmol, 1.0 equiv) and $[M(NMe_2)_5]$ (M = Nb, Ta; 0.025 mmol, 1.0 equiv), respectively. Each compound was dissolved in $C_6D_6$ (0.25 mL). The solution containing ligand **33** was rapidly added to the solution containing the metal precursor $[M(NMe_2)_5]$ and the resulting mixture was then transferred back into the original vial of ligand **33**. The complexation was monitored by $^1H$ NMR spectroscopy and aliquots of the solution of the complex was used for catalytic experiments.

### 5.3.2. [(33a)Nb(NHMe₂)(NMe₂)₂] – 33a-Nb
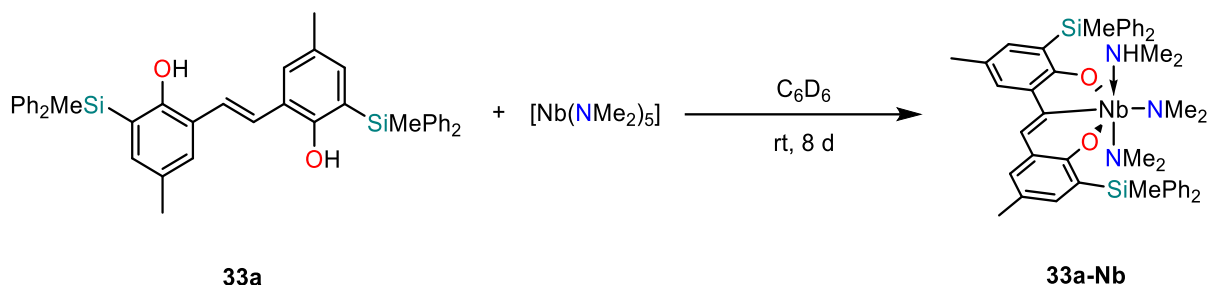


Complex **33a-Nb** was prepared according to the general procedure mentioned above. This solution was further used for catalysis.
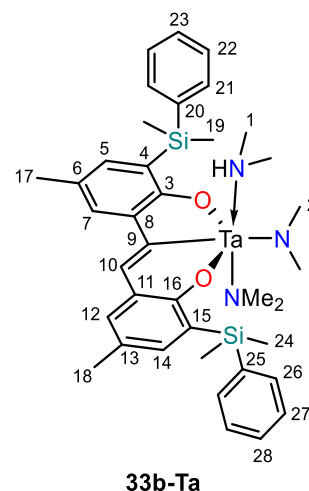
Crystals suitable for single-crystal X-ray diffraction analysis were obtained by the following procedure: In a glovebox, a vial was charged with ligand **33a** (15.8 mg, 0.025 mmol, 1.0 equiv)

and [Nb(NMe$_2$)$_5$] (7.8 mg, 0.025 mmol, 1.0 equiv). C$_6$D$_6$ (0.3 mL) was added, and the mixture was heated to 50 °C. After full dissolution of the starting material, the solution was heated for another 30 min. The solution was allowed to cool down to room temperature. Blood red crystals formed overnight (10.5 mg, 0.012 mmol, 49 %).

**¹H NMR** (700 MHz, C$_6$D$_6$): δ = 7.82 (s, 1H, H-10), 7.76 – 7.74 (m, 4H, Ar-H), 7.63 – 7.61 (m, 4H, Ar-H), 7.40 (d, $J$ = 1.6 Hz, 1H, Ar-H), 7.28 (d, $J$ = 2.2 Hz, 1H, Ar-H), 7.22 – 7.19 (m, 6H, Ar-H), 7.15 – 7.12 (m, 7H, Ar-H), 7.09 (d, $J$ = 1.5 Hz, 1H, Ar-H), 2.88 (s, 12H, H-2), 2.17 (s, 3H, Aryl-CH$_3$), 2.14 (s, 3H, Aryl-CH$_3$), 1.45 (d, $J$ = 5.7 Hz, 6H, H-1), 1.30 (br s, 1H, N$H$), 1.13 (s, 3H, SiCH$_3$), 0.95 (s, 3H, SiCH$_3$) ppm.



**33a-Nb**

**¹³C {¹H} NMR** (176 MHz, C$_6$D$_6$): δ = 198.5 (br, C-9), 175.1 (Ar-C$_q$), 161.1 (Ar-C$_q$), 138.6 (Ar-C$_q$), 137.6 (Ar-CH), 137.6 (Ar-C$_q$), 137.4 (Ar-CH), 137.2 (Ar-C$_q$), 137.2 (Ar-CH), 136.0 (Ar-CH), 135.7 (Ar-CH), 134.4 (Ar-C$_q$), 132.7 (Ar-C$_q$), 130.3 (Ar-CH), 129.3 (Ar-CH), 129.1 (Ar-CH), 128.6 (Ar-CH), 127.9 (Ar-C$_q$), 126.2 (C-10), 123.6 (Ar-CH), 122.3 (Ar-C$_q$), 119.2 (Ar-C$_q$), 45.1 (br, C-2), 39.0 (C-1), 21.0 (Aryl-CH$_3$), 20.7 (Aryl-CH$_3$), –2.5 (SiCH$_3$), –2.6 (SiCH$_3$) ppm.
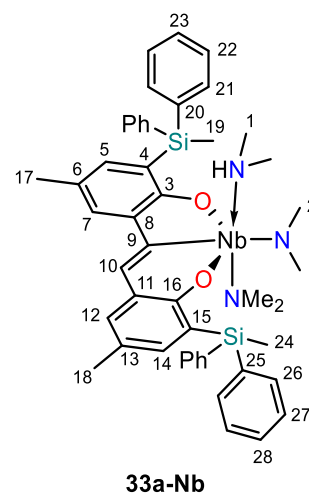
**Anal. Calcd.** for C$_{48}$H$_{56}$N$_3$NbO$_2$Si$_2$: C, 67.35; H, 6.59; N, 4.91; Found: C, 65.10; H, 6.04; N, 2.09.

### 5.3.3.   [(33a)Ta(NHMe$_2$)(NMe$_2$)$_2$] – 33a-Ta
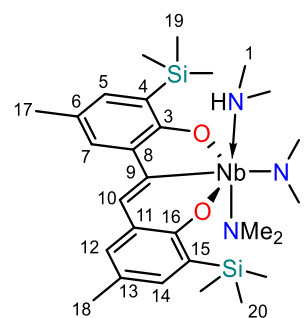


**33a**                    **33a-Ta**
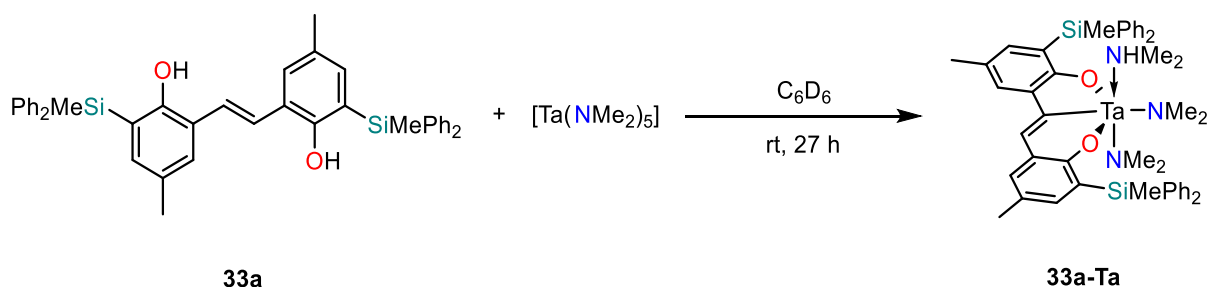
Complex **33a-Ta** was prepared according to the general procedure mentioned above. This solution was further used for catalysis.

Crystals suitable for single-crystal X-ray diffraction analysis were obtained by the following procedure: In a glovebox, a vial was charged with ligand **33a** (15.8 mg, 0.025 mmol, 1.0 equiv) and [Ta(NMe$_2$)$_5$] (10.0 mg, 0.025 mmol, 1.0 equiv). C$_6$D$_6$ (0.3 mL) was added, and the mixture was heated to 50 °C. After full dissolution of the starting material, the solution was heated for another 30 min. Finally, the solution was allowed to cool down to room temperature. Bright yellow crystals formed overnight (19.6 mg, 0.021 mmol, 83 %).

**¹H NMR** (700 MHz, C$_6$D$_6$): δ = 7.97 (s, 1H, H-10), 7.75 – 7.69 (m, 4H, Ar-H), 7.64 – 7.60 (m, 4H, Ar-H), 7.44 (d, *J* = 1.8 Hz, 1H, Ar-H), 7.26 (d, *J* = 1.9 Hz, 1H, Ar-H), 7.21 – 7.18 (m, 6H, Ar-H), 7.14 – 7.13 (m, 7H, Ar-H), 7.11 (d, *J* = 1.9 Hz, 1H, Ar-H), 3.09 (s, 12H, H-2), 2.17 (s, 3H, Aryl-CH$_3$), 2.13 (s, 3H, Aryl-CH$_3$), 1.45 (br s, 7H, N*H* and H-1), 1.16 (s, 3H, SiCH$_3$), 1.01 (s, 3H, SiCH$_3$) ppm.



**33a-Ta**

**¹³C {¹H} NMR** (176 MHz, C$_6$D$_6$): δ = 201.9 (C-9), 175.3 (Ar-C$_q$), 161.4 (Ar-C$_q$), 139.1 (Ar-C$_q$), 138.8 (Ar-C$_q$), 138.4 (Ar-CH), 138.1 (Ar-C$_q$), 137.7 (Ar-CH), 136.6 (Ar-CH), 136.4 (Ar-CH), 135.2 (Ar-CH), 134.5 (Ar-C$_q$), 131.3 (Ar-C$_q$), 130.0 (Ar-CH), 129.8 (Ar-CH), 129.2 (Ar-C$_q$), 129.2 (Ar-CH), 129.0 (C-10), 128.5 (Ar-CH), 124.9 (Ar-CH), 124.2 (Ar-C$_q$), 121.2 (Ar-C$_q$), 45.3 (C-2), 39.6 (C-1), 21.6 (Aryl-CH$_3$), 21.3 (Aryl-CH$_3$), –1.8 (SiCH$_3$), –2,0 (SiCH$_3$) ppm.

**Anal. Calcd.** for C$_{48}$H$_{56}$N$_3$TaO$_2$Si$_2$: C, 64.07; H, 5.98; N, 4.45; Found: C, 59.02; H, 5.85; N, 3.35.

### 5.3.4.   [(33b)Nb(NHMe$_2$)(NMe$_2$)$_2$] – 33b-Nb
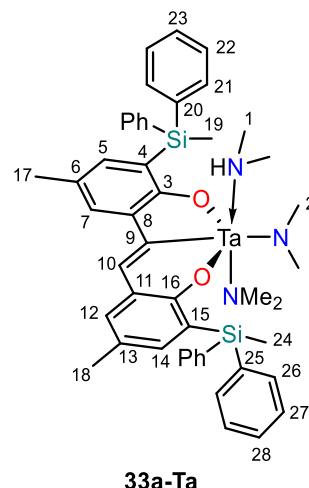


**33b**          +     [Nb(NMe$_2$)$_5$]     →  (C$_6$D$_6$, rt, 24 h)     **33b-Nb**
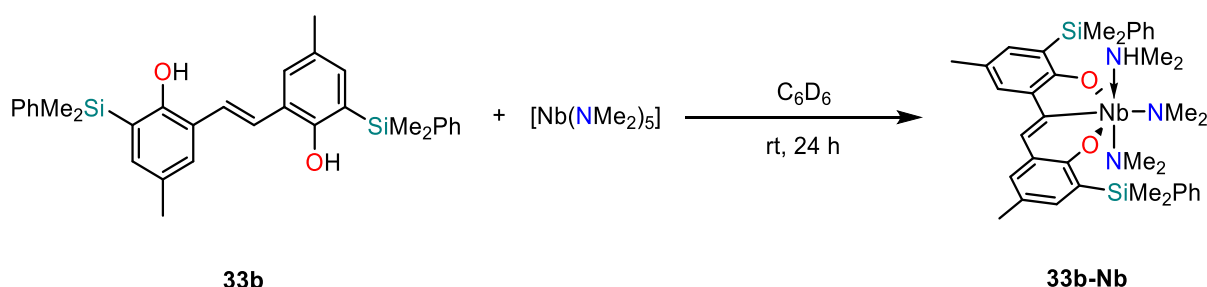
Complex **33b-Nb** was prepared according to the general procedure mentioned above. This solution was further used for catalysis.

Crystals were isolated by the following procedure: In a glovebox, one vial was charged with ligand **33b** (12.7 mg, 0.025 mmol, 1.0 equiv) and [Nb(NMe$_2$)$_5$] (7.8 mg, 0.025 mmol, 1.0 equiv). *n*-pentane (1.5 mL) was added, and the mixture was heated to 50 °C. After full dissolution of the

starting material, the solution was heated for another 30 min. Finally, the solution was allowed to slowly cool down to room temperature and placed in the freezer at – 30 °C. Blood red crystals formed overnight (12.4 mg, 0.017 mmol, 68 %).

**¹H NMR** (600 MHz, C$_6$D$_6$): δ = 7.76 (s, 1H, H-10), 7.72 – 7.70 (m, 2H, Ar-H), 7.57 – 7.54 (m, 2H, Ar-H), 7.38 (d, $J$ = 1.7 Hz, 1H, Ar-H), 7.27 (d, $J$ = 1.9 Hz, 1H, Ar-H), 7.25 (d, $J$ = 1.9 Hz, 1H, Ar-H), 7.22 – 7.19 (m, 4H, Ar-H), 7.13 – 7.10 (m, 3H, Ar-H), 3.05 (s, 12H, H-2), 2.28 (s, 3H, Aryl-CH$_3$), 2.26 (s, 3H, Aryl-CH$_3$), 1.64 (br s, 7H, N$H$ and H-1), 0.79 (s, 6H, SiCH$_3$), 0.63 (s, 6H, SiCH$_3$) ppm.



**33b-Nb**

**¹³C {¹H} NMR** (151 MHz, C$_6$D$_6$): δ = 199.1 (br, C-9), 175.2 (Ar-C$_q$), 160.4 (Ar-C$_q$), 141.0 (Ar-C$_q$), 139.8 (Ar-C$_q$), 137.1(Ar-C$_q$), 136.3 (Ar-CH), 135.5 (Ar-CH), 134.9 (Ar-CH), 134.6 (Ar-CH), 134.0 (Ar-CH), 133.2 (Ar-C$_q$), 130.5 (Ar-C$_q$), 129.0 (Ar-C$_q$), 128.7 (Ar-CH), 128.4 (Ar-CH), 127.9 (Ar-CH), 127.7(Ar-CH), 125.4 (C-10), 123.8 (Ar-C$_q$), 123.2 (Ar-CH), 120.7 (Ar-C$_q$), 45.9 (br, C-2), 38.9 (C-1), 21.1 (Aryl-CH$_3$), 20.8 (Aryl-CH$_3$), –1.24 (SiCH$_3$), –1.40 (SiCH$_3$) ppm.

**Anal. Calcd.** for C$_{38}$H$_{52}$N$_3$NbO$_2$Si$_2$: C, 62.36; H, 7.16; N, 5.74; Found: C, 60.29; H, 6.37; N, 2.03.
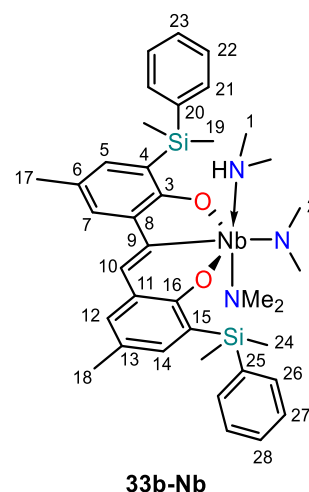
## 5.3.5.   [(33b)Ta(NHMe₂)(NMe₂)₂] – 33b-Ta



**33b**                                   **33b-Ta**
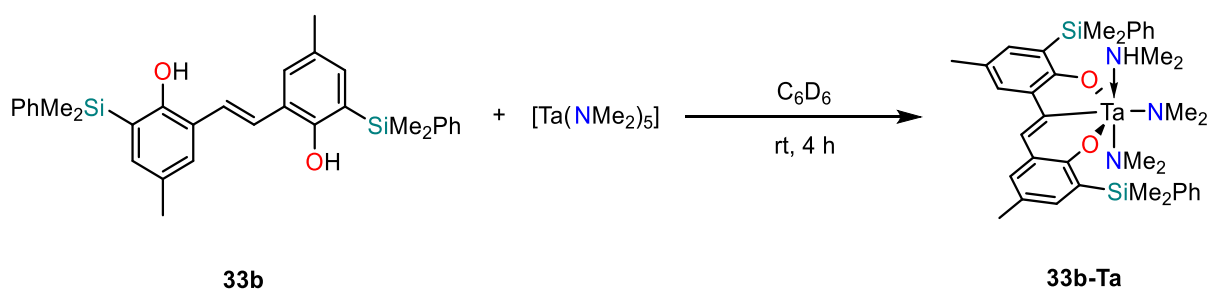
Complex **33b-Ta** was prepared according to the general procedure mentioned above. This solution was further used for catalysis.

Crystals suitable for single-crystal X-ray diffraction analysis were obtained by the following procedure: In a glovebox, a vial was charged with ligand **33b** (12.7 mg, 0.025 mmol, 1.0 equiv) and [Ta(NMe₂)₅] (10.0 mg, 0.025 mmol, 1.0 equiv). *n*-pentane (1.0 mL) was added, and the mixture was heated to 55 °C. After full dissolution of the starting material, the solution was heated for another 30 min. Finally, the solution was allowed to slowly cool down to room

temperature and placed in the freezer at – 30 °C. Bright yellow crystals formed overnight (11.4 mg, 0.014 mmol, 56 %).

**¹H NMR (600 MHz, C₆D₆):** δ = 7.94 (s, 1H, H-10), 7.72 – 7.66 (m, 2H, Ar-H), 7.60 – 7.55 (m, 2H, Ar-H), 7.43 (d, *J* = 1.6 Hz, 1H, Ar-H), 7.25 (s, 2H, Ar-H), 7.23 (d, *J* = 1.5 Hz, 1H, Ar-H), 7.21 – 7.17 (m, 3H, Ar-H), 7.14 – 7.12 (m, 3H, Ar-H), 3.19 (s, 12H, H-2), 2.28 (s, 3H, Aryl-CH₃), 2.26 (2, 3H, Aryl-CH₃), 1.56 (br s, 7H, N*H* and H-1), 0.78 (s, 6H, SiCH₃), 0.65 (s, 6H, SiCH₃) ppm.

**¹³C {¹H} NMR (151 MHz, C₆D₆):** δ = 200.9 (C-9), 174.1 (Ar-C$_q$), 160.1 (Ar-C$_q$), 140.8 (Ar-C$_q$), 139.7 (Ar-C$_q$), 138.2 (Ar-C$_q$), 136.4 (Ar-CH), 135.5 (Ar-CH), 134.8 (Ar-CH), 134.6 (Ar-CH), 134.1 (Ar-CH), 133.9 (Ar-C$_q$), 130.7 (Ar-C$_q$), 129.1 (Ar-CH), 128.8 (Ar-CH), 128.6 (C-10), 128.4 (Ar-CH), 128.0 (Ar-CH), 127.7 (Ar-C$_q$), 125.0 (Ar-C$_q$), 123.9 (Ar-CH), 122.1 (Ar-C$_q$), 44.9 (br, C-2), 38.9 (C-1), 21.1 (Aryl-CH₃), 20.7 (Aryl-CH₃), –1.3 (SiCH₃), –1.4 (SiCH₃) ppm.

**Anal. Calcd.** for C₃₈H₅₂N₃TaO₂Si₂: C, 55.66; H, 6.39; N, 5.12; Found: C, 53.58; H, 5.84; N, 1.81.

**33b-Ta**

### 5.3.6.  [(33c)Nb(NHMe₂)(NMe₂)₂] – 33c-Nb



**33c**          **33c-Nb**
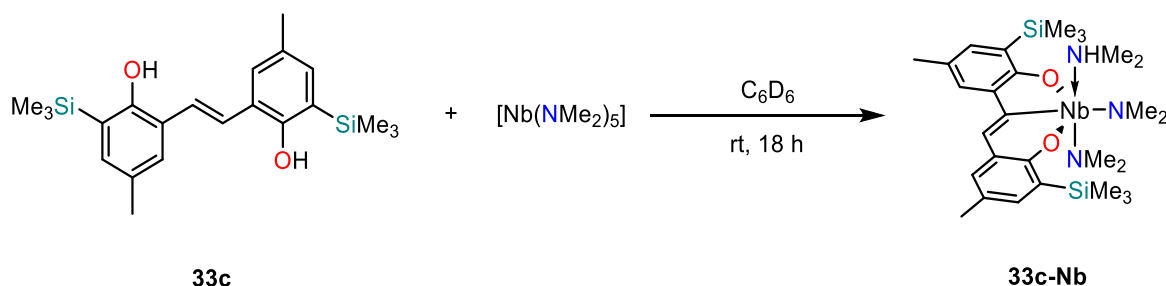
Complex **33c-Nb** was prepared according to the general procedure mentioned above. This solution was further used for catalysis.

Crystals suitable for single-crystal X-ray diffraction analysis were obtained by the following procedure: In a glovebox, a vial was charged with ligand **33c** (9.6 mg, 0.025 mmol, 1.0 equiv) and [Nb(NMe₂)₅] (7.8 mg, 0.025 mmol, 1.0 equiv). *n*-pentane (0.3 mL) was added, and the mixture was heated to 50 °C. After full dissolution of the starting material, the solution was heated for another 30 min. Finally, the solution was allowed to slowly cool down to room temperature and placed in the freezer at – 30 °C. Blood red crystals formed overnight (10.4 mg, 0.017 mmol, 68 %).

**¹H NMR** (600 MHz, C₆D₆): δ = 7.76 (s, 1H, H-10), 7.35 (d, $J$ = 1.6 Hz, 1H, H-7), 7.24 (d, $J$ = 2.2 Hz, 1H, H-12), 7.21 (d, $J$ = 2.2 Hz, 1H, H-14), 7.18 (d, $J$ = 1.6 Hz, 1H, H-5), 3.27 (s, 12H, H-2), 2.31 (s, 3H, Aryl-CH₃), 2.27 (s, 3H, Aryl-CH₃), 1.85 (br s, 6H, H-1), 1.74 (br s, 1H, N*H*), 0.59 (s, 9H, SiCH₃), 0.42 (s, 9H, SiCH₃) ppm.

**¹³C {¹H} NMR** (151 MHz, C₆D₆): δ = 199.0 (C-9), 174.7 (C-3), 160.1 (C-16), 137.1 (C-8), 135.3 (C-5), 134.5 (C-12), 133.5 (C-14), 133.0 (C-11), 130.7 (C-13), 128.4 (C-6), 125.7 (C-10), 125.7 (C-15), 123.1 (C-4), 122.8 (C-7), 45.9 (C-2), 39.3 (C-19), 21.1 (Aryl-CH₃), 20.8 (Aryl-CH₃), –0.1 (SiCH₃), –0.2 (SiCH₃) ppm.

**Anal. Calcd.** for C₂₈H₄₈N₃NbO₂Si₂: C, 55.33; H, 7.96; N, 6.91; Found: C, 53.47; H, 7.82; N, 5.25.



**33c-Nb**

### 5.3.7. [(33c)Ta(NHMe₂)(NMe₂)₂] – 33c-Ta



**33c**     +     [Ta(NMe₂)₅]   → (C₆D₆, rt, 1 h 30 min)     **33c-Ta**
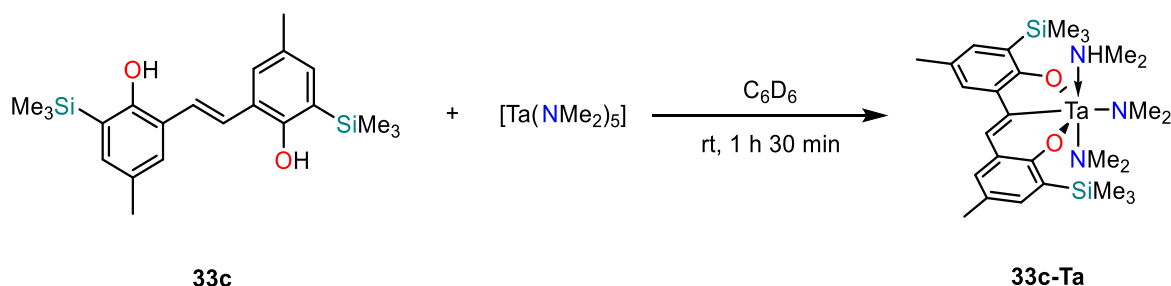
Complex **33c-Ta** was prepared according to the general procedure mentioned above. This solution was further used for catalysis.

Crystals suitable for single-crystal X-ray diffraction analysis were obtained by the following procedure: In a glovebox, a vial was charged with ligand **33c** (9.6 mg, 0.025 mmol, 1.0 equiv) and [Ta(NMe₂)₅] (10.0 mg, 0.025 mmol, 1.0 equiv). *n*-pentane (0.3 mL) was added, and the mixture was heated to 50 °C. After full dissolution of the starting material, the solution was heated for another 30 min. Finally, the solution was allowed to slowly cool down to room temperature and placed in the freezer at – 30 °C. Bright yellow crystals formed overnight (12.7 mg, 0.018 mmol, 73 %).



**33c-Ta**

**¹H NMR** (600 MHz, C₆D₆): δ = 7.94 (s, 1H, H-10), 7.41 (d, $J$ = 1.5 Hz, 1H, H-7), 7.23 (s, 1H, H-12), 7.22 (s, 2H, H-5 and H-14), 3.41 (s, 12H,
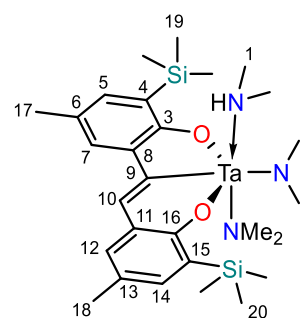
H-2), 2.32 (s, 3H, Aryl-CH$_3$), 2.28 (s, 3H, Aryl-CH$_3$), 1.87 (br s, 7H, H-1 and N*H*), 0.58 (s, 9H, SiCH$_3$), 0.43 (s, 9H, SiCH$_3$) ppm.

**$^{13}$C {$^1$H} NMR** (151 MHz, C$_6$D$_6$): δ = 200.9 (C-9), 173.7 (C-3), 159.8 (C-16), 138.1 (C-8), 135.4 (C-5), 134.4 (C-14), 133.8 (C-11), 133.7 (C-12), 130.9 (C-13), 128.7 (C-6), 128.4 (C-10), 126.8 (C-15), 124.3 (C-4), 123.5 (C-7), 45.1 (br, C-2), 39.3 (C-1), 21.1 (Aryl-CH$_3$), 20.8 (Aryl-CH$_3$), 0.0 (SiCH$_3$), –0.1 (SiCH$_3$) ppm.

**Anal. Calcd.** for C$_{28}$H$_{48}$N$_3$TaO$_2$Si$_2$: C, 48.33; H, 6.95; N, 6.04; Found: C, 45.95; H, 6.62; N, 3.29.

### 5.3.8.  [Ta(33c)$_2$] – (33c)$_2$-Ta
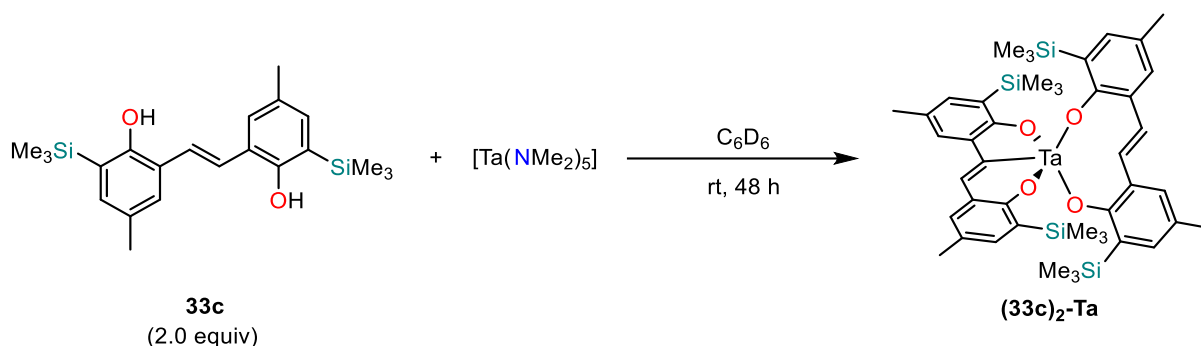


In the glovebox, two vials were charged with ligand **33c** (19.2 mg, 0.05 mmol, 2.0 equiv) and [Ta(NMe$_2$)$_5$] (10.0 mg, 0.025 mmol, 1.0 equiv), respectively. Each compound was dissolved in C$_6$D$_6$ (0.25 mL). Both solutions were combined by adding the solution containing ligand **33c** rapidly to the solution containing [Ta(NMe$_2$)$_5$]. The resulting mixture was finally transferred back into the original vial of ligand **33c**. Full complexation and quantitative conversion to the C–H activated complex was achieved after 48 h.

Crystals suitable for X-ray analysis were isolated by the following procedure: In a glovebox, one vial was charged with ligand **33c** (19.2 mg, 0.05 mmol, 2.0 equiv) and [Ta(NMe$_2$)$_5$] (10.0 mg, 0.025 mmol, 1.0 equiv). *n*-pentane (0.5 mL) was added, and the mixture was heated to 50 °C. After full dissolution of the starting material, the solution was heated for another 30 min. Finally, the solution was allowed to slowly cool down to room temperature and placed in the freezer at – 30 °C. Bright yellow crystals formed overnight. Attempts to purify the obtained complex by freeze drying or recrystallization failed and resulted in a higher concentration of the free ligand **33c**.

**1H NMR** (600 MHz, C6D6): δ = 8.20 (s, 1H, H-8), 7.26 (d, *J* = 1.4 Hz, 1H, Ar-H), 7.19 (d, *J* = 1.4 Hz, 2H, Ar-H), 7.16 (s, 2H, Ar-H), 7.14 (d, *J* = 1.7 Hz, 1H, Ar-H), 7.07 (d, *J* = 1.2 Hz, 1H, Ar-H), 7.04 (d, *J* = 2.0 Hz, 1H, Ar-H), 7.00 (s, 2H, Ar-H), 2.22 (s, 3H, Aryl-CH3), 2.16 (s, 9H, Aryl-CH3), 0.30 (s, 9H, SiCH3), 0.25 (s, 18H, SiCH3), 0.19 (s, 9H, SiCH3).



**(33c)₂-Ta**
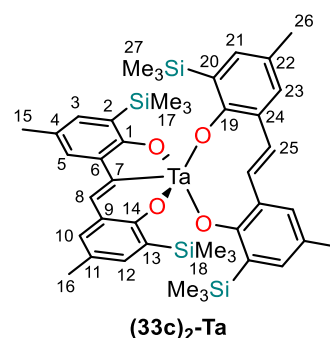
**13C {1H} NMR** (151 MHz, C6D6): δ = 193.8 (C-7), 168.2 (Ar-Cq), 162.2 (Ar-Cq), 140.5 (Ar-Cq), 137.1 (Ar-CH), 136.7 (Ar-CH), 136.6 (Ar-CH), 135.9 (Ar-CH), 133.6 (Ar-CH), 132.0 (Ar-Cq), 131.8 (Ar-Cq), 131.3 (Ar-Cq), 131.2 (Ar-Cq), 130.4 (Ar-Cq), 130.0 (br, Ar-CH), 129.2 (Ar-CH), 128.7 (Ar-Cq), 128.6 (Ar-Cq), 126.5 (Ar-Cq), 125.1 (Ar-CH), 124.6 (Ar-Cq), 21.8 (Aryl-CH3), 21.3 (Aryl-CH3), 0.1 (SiCH3), –0.1 (SiCH3), –0.5 (SiCH3).

## 5.4. Catalytic Studies

### 5.4.1. General Procedure for Catalysis

**General procedure for intermolecular hydroaminoalkylation on 0.2 mmol scale (GP2)**. In a glovebox, an oven-dried screw cap NMR tube was charged with an appropriate amine (0.2 mmol) and an alkene (0.4 mmol, 2.0 equiv). The prepared catalyst solution (0.2 mL, 0.01 mmol) was added alongside additional $C_6D_6$ (0.3 mL). The NMR tube was sealed, wrapped with Teflon tape, removed from the glovebox, and placed in a thermostated oil bath. The reaction progress was monitored periodically *via* $^1H$ NMR spectroscopy.

**General procedure for intermolecular hydroaminoalkylation on 0.05 mmol scale (GP3)**. In a glovebox, an oven-dried 1.5 mL vial was charged with amine (0.05 mmol), alkene (0.1 mmol, 2.0 equiv) and the previously prepared catalyst solution (50 µL, 0.0025 mmol). The additives [PhNHMe$_2$][B(C$_6$F$_5$)$_4$] and TMS-Cl were added to the catalyst solution, which was stirred for 15 min at room temperature before adding it to the substrate containing mixture. Additives, such as *t*BuCN, NaSCN, PhCN, KH or KO*t*Bu were added to the mixture containing the amine and alkene substrates prior to the addition of the catalyst solution. Additional $C_6H_6$, $C_7H_8$, THF, acetonitrile (75 µL) or $C_6H_5Br$ (500 µL) was added. The vial was sealed, wrapped with Teflon tape, removed from the glovebox, and placed on a preheated, thermostated heating block for 24 h. The reaction mixture was quenched after 24 h with an aqueous 10% KOH solution (1.0 mL), extracted with dichloromethane (3.0 mL) and filtered through a syringe filter. The resulting filtrate was analysed by GC-MS.

**General procedure for intramolecular hydroamination on 0.2 mmol scale (GP4)**. In a glovebox, an oven-dried screw cap NMR tube was charged with aminoalkene (0.2 mmol) and the prepared catalyst solution (0.2 mL, 0.01 mmol). Additional $C_6D_6$ (0.3 mL) was added. The NMR tube was sealed with a screw cap, wrapped with Teflon tape, removed from the glovebox, and placed in a thermostated oil bath. The conversion was monitored periodically *via* $^1H$ NMR spectroscopy.

**General procedure for intermolecular hydroamination on 0.05 mmol scale (GP5)**. In a glovebox, an oven-dried 1.5 mL vial was charged with amine (0.05 mmol), alkene (0.75 mmol, 15.0 equiv) and the previously prepared catalyst solution (50 µL, 0.0025 mmol,). The vial was sealed with a screw cap, wrapped with Teflon tape, removed from the glovebox, and placed on a preheated, thermostated heating block for 24 h. The reaction mixture was quenched with an

aqueous 10 % KOH solution (1.0 mL) after 24 h, extracted with dichloromethane (3.0 mL) and filtered through a syringe filter. The resulting filtrate was analysed by GC-MS.
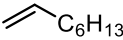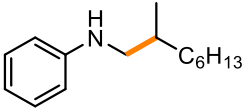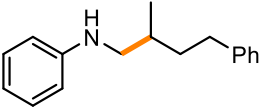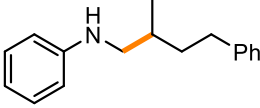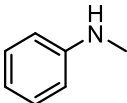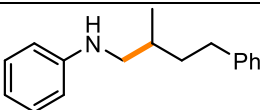
### 5.4.1.1.  Hydroaminoalkylation
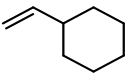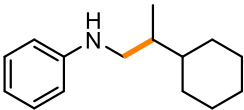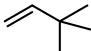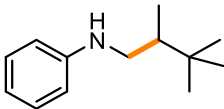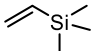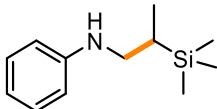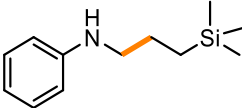
### 5.4.1.1.1.  Hydroaminoalkylation on 0.2 mmol NMR scale
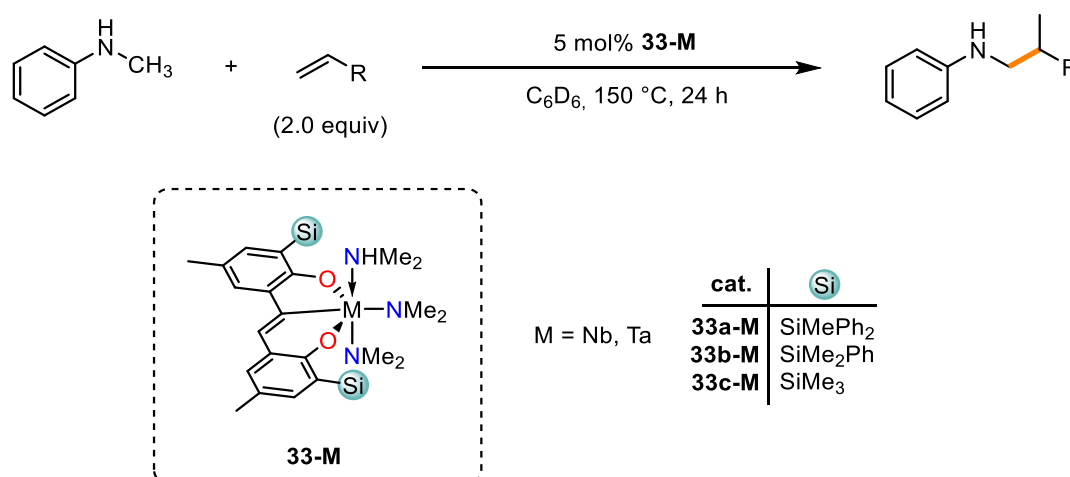


The hydroaminoalkylation reactions were conducted according to the general procedure for intermolecular hydroaminoalkylation on 0.2 mmol scale (GP2).

*Table 3:* Hydroaminoalkylation reactions on 0.2 mmol scale (GP2).

| Substrate: Alkene | Product | Catalyst | Conversion |
|---|---|---|---|
| $C_6H_{13}$ | $C_6H_{13}$ | 33a-Nb | 0 % |
| | | 33b-Nb | 0 % |
| | | 33c-Nb | 0 % |
| | | 33a-Ta | 0 % |
| | | 33b-Ta | 0 % |
| | | 33c-Ta | 0 % |
| Ph | Ph | 33a-Nb | 0 % |
| | | 33b-Nb | 0 % |
| | | 33c-Nb | 0 % |
| | | 33a-Ta | 0 % |
| | | 33b-Ta | 0 % |
| | | 33c-Ta | 0 % |

| Substrate: Alkene | Product | Catalyst | Conversion |
|---|---|---|---|
|  |  | **33a-Nb** | 0 % |
| | | **33b-Nb** | 0 % |
| | | **33c-Nb** | 0 % |
| | | **33a-Ta** | 0 % |
| | | **33b-Ta** | 0 % |
| | | **33c-Ta** | 0 % |
|  |  | **33a-Nb** | 0 % |
| | | **33b-Nb** | 0 % |
| | | **33c-Nb** | 0 % |
| | | **33a-Ta** | 0 % |
| | | **33b-Ta** | 0 % |
| | | **33c-Ta** | 0 % |
|  |   or/and   | **33a-Nb** | 0 % |
| | | **33b-Nb** | 0 % |
| | | **33c-Nb** | 0 % |
| | | **33a-Ta** | 0 % |
| | | **33b-Ta** | 0 % |
| | | **33c-Ta** | 0 % |
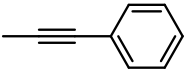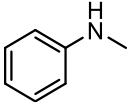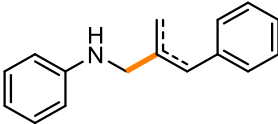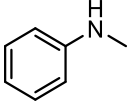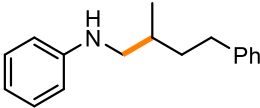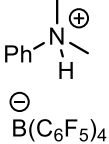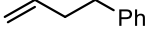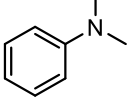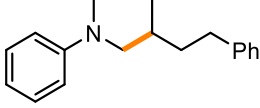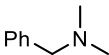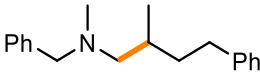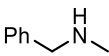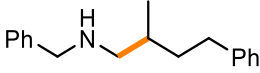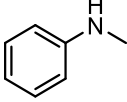
## 5.4.1.1.2.     Hydroaminoalkylation on 0.05 mmol scale
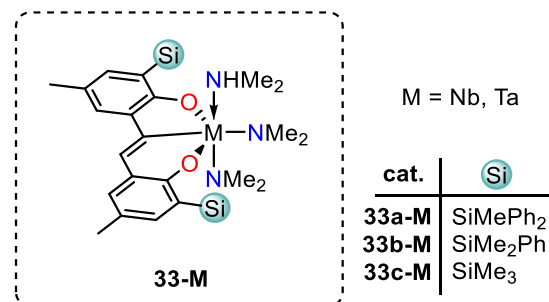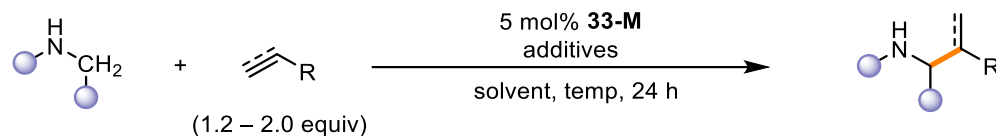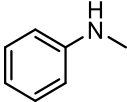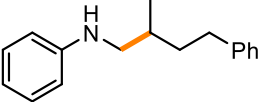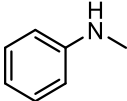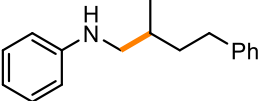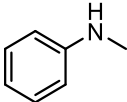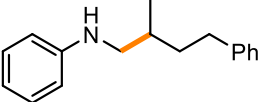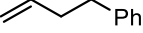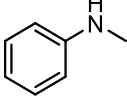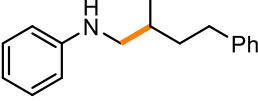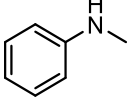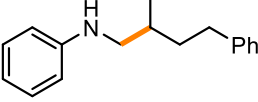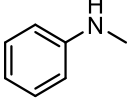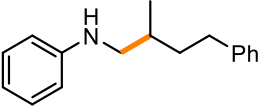


The hydroaminoalkylation reactions were conducted according to the procedure for intermolecular hydroaminoalkylation on 0.05 mmol scale (GP3).

*Table 4:* Reactions performed on 0.05 mmol scale (GP3). [a]Isomerization of alkene observed. [b]Reduction of alkyne to alkene observed by GC-MS. [c]Reduction of alkene to alkane in trace amounts observed by GC-MS. [d]15.0 equiv of alkene were used. [e]10.5 mol% [PhNHMe2][B(C6F5)4] was used. [f]5 mol% *t*BuNC was used. [g]5 mol% of NaSCN was used. [h]100 mol% PhCN was used. [i]7.5 mol% TMS-Cl was used. [j]15.0 mol% TMS-Cl was used. [k]50 mol% KH was used. [l]50 mol% KO*t*Bu was used.
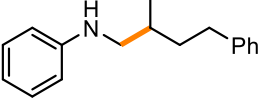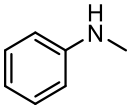
| Substrate | | Product | Additive | Temp-erature | Solvent | 33-M | Conversion |
|---|---|---|---|---|---|---|---|
| Alkene/Alkyne | Amine | | | | | | |
| Ph | pyrrolidine (H-N) | product | | 150 °C | C7H8 | 33b-Nb | 0 %[a] |
| | | | | | | 33b-Ta | 0 % |
| | | | | | | 33c-Nb | 0 %[a] |
| | | | | | | 33c-Ta | 0 % |
| Ph | tetrahydroquinoline | product | | 150 °C | C7H8 | 33b-Nb | 0 %[a] |
| | | | | | | 33b-Ta | 0 % |
| | | | | | | 33c-Nb | 0 %[a] |

| Substrate | | Product | Additive | Temperature | Solvent | 33-M | Conversion |
|---|---|---|---|---|---|---|---|
| Alkene/Alkyne | Amine | | | | | | |
| | | | | | | 33c-Ta | 0 % |
| (1-phenyl-1-propyne) | N-methylaniline | allyl amine product | | 150 °C | $C_7H_8$ | 33b-Nb | 0 %[b] |
| | | | | | | 33b-Ta | 0 % |
| (4-phenyl-1-butene) | N-methylaniline | amine product | $Ph-\overset{+}{N}H(CH_3)H \cdot B(C_6F_5)_4^{-}$ | 150 °C | $C_6H_5Br$ | 33c-Nb | 0 %[a,e] |
| | | | | | | 33c-Ta | 0 %[e] |
| (4-phenyl-1-butene) | N,N-dimethylaniline | amine product | | 150 °C | | 33c-Nb | 0 %[a,c,d] |
| | | | | | | 33c-Ta | 0 %[d] |
| (4-phenyl-1-butene) | $Ph\text{-}CH_2\text{-}N(CH_3)_2$ | amine product | | 150 °C | | 33c-Nb | 0 %[d] |
| | | | | | | 33c-Ta | 0 %[d] |
| (4-phenyl-1-butene) | $Ph\text{-}CH_2\text{-}NH(CH_3)$ | amine product | | 150 °C | | 33c-Nb | 0 %[a,d] |
| | | | | | | 33c-Ta | 0 %[d] |
| (4-phenyl-1-butene) | N-methylaniline | amine product | $t$BuNC | 150 °C | $C_7H_8$ | 33c-Nb | 0 %[a,f] |
| | | | | | | 33c-Ta | 0 %[f] |
| (4-phenyl-1-butene) | N-methylaniline | amine product | NaSCN | 150 °C | $C_7H_8$ | 33c-Nb | 0 %[a,g] |
| | | | | | | 33c-Ta | 0 %[g] |

| Alkene | Amine | Product | Additive | Temp | Solvent | Catalyst | Yield |
|---|---|---|---|---|---|---|---|
| (homoallylbenzene) | (N-methylaniline) | (product) | PhCN | 150 °C | $C_7H_8$ | **33c-Nb** | 0 %[a,h] |
| | | | | | | **33c-Ta** | 0 %[h] |
| (homoallylbenzene) | (N-methylaniline) | (product) | | 120 °C | $C_7H_8$ | **33c-Nb** | 0 %[a] |
| | | | | | | **33c-Ta** | 0 % |
| | | | | 170 °C | $C_7H_8$ | **33c-Nb** | 0 %[a] |
| | | | | | | **33c-Ta** | 0 % |
| (homoallylbenzene) | (N-methylaniline) | (product) | | 150 °C | THF | **33c-Nb** | 0 %[a] |
| | | | | | | **33c-Ta** | 0 % |
| (homoallylbenzene) | (N-methylaniline) | (product) | | 150 °C | $CH_3CN$ | **33c-Nb** | 0 %[a] |
| | | | | | | **33c-Ta** | 0 % |
| (homoallylbenzene) | (N-methylaniline) | (product) | TMS-Cl | 150 °C | $C_7H_8$ | **33c-Nb** | 0 %[a,i] |
| | | | | | | **33c-Ta** | 9 %[i] |
| | | | | | | **33c-Nb** | 0 %[a,j] |
| | | | | | | **33c-Ta** | 31 %[j] |
| (homoallylbenzene) | (N-methylaniline) | (product) | KH | 150 °C | $C_7H_8$ | **33c-Nb** | traces[k] |
| | | | | | | **33c-Ta** | 0 %[k] |

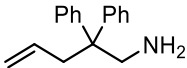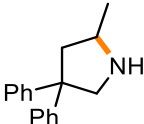| | | | | | | 33c-Nb | 0 %[l] |
|---|---|---|---|---|---|---|---|
| | | | KOtBu | 150 °C | C₇H₈ | 33c-Ta | 0 %[l] |

## 5.4.1.2. Hydroamination

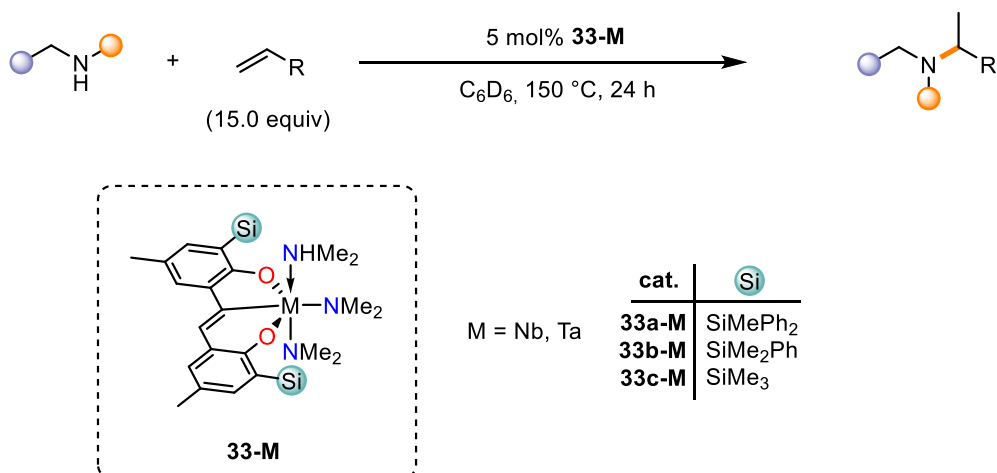### 5.4.1.2.1. Intramolecular Hydroamination on 0.2 mmol scale
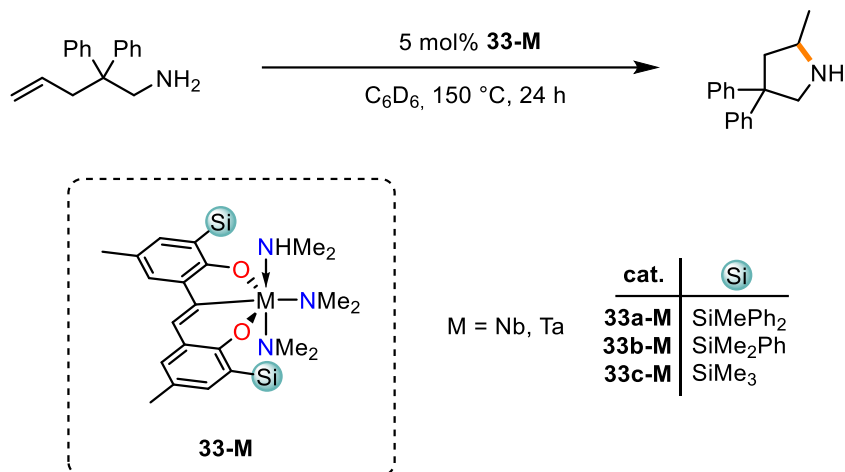


The hydroamination reactions were conducted according to the general procedure for intramolecular hydroamination on 0.2 mmol scale (GP4).

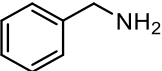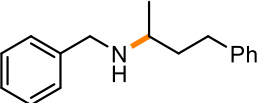*Table 5:* Intramolecular hydroamination reactions performed on 0.2 mmol scale (GP4).
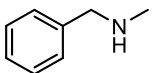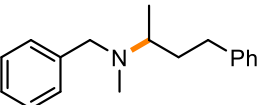
| Substrate: Aminoalkene | Product | Catalyst | Conversion |
|---|---|---|---|
| | | **33a-Nb** | 13 % |
| | | **33b-Nb** | 40 % |
| | | **33c-Nb** | 17 % |
| | | **33a-Ta** | 25 % |
| | | **33b-Ta** | 27 % |
| | | **33c-Ta** | 28 % |

### 5.4.1.2.2. Hydroamination on 0.05 mmol scale

The hydroamination reactions were conducted according to the general procedure for intermolecular hydroamination on 0.05 mmol scale (GP5).

*Table 6:* Reactions performed on 0.05 mmol scale (GP5). [a]Condensation of benzylamine to dibenzylamine and *N*-benzylbenzaldimine observed. [b]Isomerization of alkene observed. [c]10.0 equiv of alkene was used. [d]30.0 equiv of alkene was used. [e]Reduction of alkene to alkane in trace amounts observed.
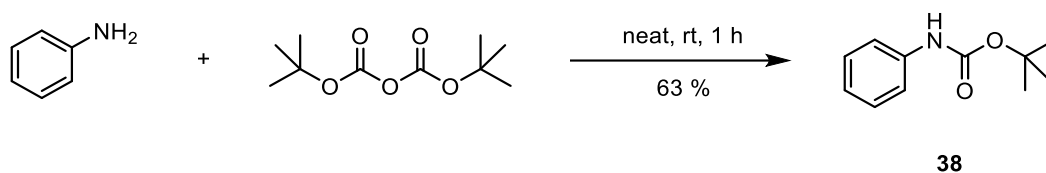
| Substrate | | Product | Temperature | additives | 33-M | Conversion |
|---|---|---|---|---|---|---|
| Alkene | Amine | | | | | |
|  (alkene, Ph) |  (benzylamine, NH₂) |  (product) | 150 °C | | 33c-Nb | 0 %[a,b] |
| | | | | | | 0 %[b,c] |
| | | | | | | 0 %[b,d] |
| | | | | TMS-Cl | | 0 %[a,b,e] |
| | | | | | 33c-Ta | 0 % |
| | | | | | | 0 %[c] |
| | | | | | | 0 %[d] |
| | | | | TMS-Cl | | 0 %[a,b] |
| | | | 120 °C | | 33c-Nb | 0 % |
| | | | | | 33c-Ta | 0 % |
| | | | 170 °C | | 33c-Nb | 0 %[b] |
| | | | | | 33c-Ta | 0 % |
|  (alkene, Ph) |  (N-methylbenzylamine) |  (product) | 150 °C | | 33c-Nb | 0 %[b] |
| | | | | | 33c-Ta | 0 % |

105

## 5.5. Deuterium – Labeling Studies

### 5.5.1. Synthesis of *tert*-butyl phenylcarbamate 38



The procedure was adapted from literature.[44] A round bottom flask was charged with aniline (2.94 mL, 32 mmol) and di-*tert*-butyldicarbonat (7.02 g, 32 mmol, 1.0 equiv) and stirred until it solidified. The mixture was then manually stirred with a glass rod for a total of 1 h. The crude product was recrystallized from isopropanol (15 mL) to yield the desired product as a white crystalline material (3.92 g, 20 mmol, 63 %).

**¹H NMR** (400 MHz, CDCl₃): δ = 7.36 (d, $J$ = 7.9 Hz, 2H, H-3), 7.29 (t, $J$ = 7.9 Hz, 2H, H-2), 7.03 (t, $J$ = 7.3 Hz, 1H, H-1), 6.45 (br s, 1H, N*H*), 1.52 (s, 9H, H-7) ppm.
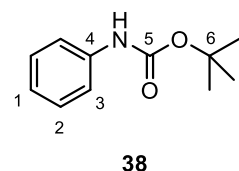
**¹³C {¹H} NMR** (101 MHz, CDCl₃): δ = 152.9 (C-5), 138.5 (C-4), 129.1 (C-2), 123.2 (C-3), 118.7 (C-1), 80.7 (C-6), 28.5 (C-7) ppm.
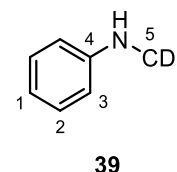
### 5.5.2. Synthesis of *N*-(methyl-*d₃*)aniline 39
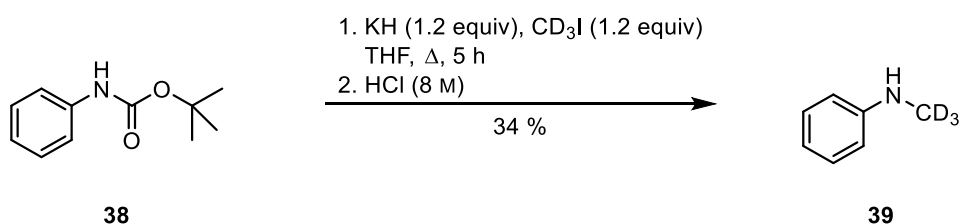


The procedure was adapted from literature.[183] A 100-mL round-bottom Schlenk flask was introduced into the glovebox and charged with potassium hydride (374 mg, 9.3 mmol, 1.2 equiv). The Schlenk flask was removed from the glovebox and dry THF (20 mL), as well as *N*-Boc-aniline (1.50 g, 7.8 mmol), were added. The mixture was stirred for 10 min before iodomethane-*d₃* (0.58 mL, 9.3 mmol, 1.2 equiv) was added dropwise over the period of 2 min. The reaction mixture was refluxed for 5 h, allowed to cool down to room temperature and finally quenched with distilled water (4 mL). Hydrochloric acid (6 M, 36 mL) was added to the reaction mixture and the resulting pale-yellow solution was refluxed for 10 h. An aqueous solution of sodium hydroxide was added until the reaction mixture showed a pH-value above 10. The

mixture was extracted with Et$_2$O (15 mL). The organic phase was washed with distilled water (3 × 10 mL), brine (10 mL) and dried over MgSO$_4$. The solution was filtered through cotton and the solvent was removed *in vacuo* to yield a dark brown oil. Flash column chromatography on silica gel (0–20 % EtOAc in heptanes) resulted in a yellow oil, which was distilled under vacuum (2.5×10$^{-2}$ mbar, 35 °C) to give a pale-yellow oil. The product was dried over CaH$_2$ for 18 h and distilled under vacuum (2.5×10$^{-2}$ mbar, 35 °C) to yield the dry product as a colourless liquid (446 mg, 4.0 mmol, 34 %).

**¹H NMR** (700 MHz, CDCl$_3$): δ = 7.20 (dd, *J* = 8.5, 7.4 Hz, 2H, H-2), 6.72 (tt, *J* = 7.3, 0.9 Hz, 1H, H-1), 6.63 (dd, *J* = 8.6, 1.0 Hz, 2H, H-3), 3.67 (s, 1H, N*H*) ppm.

**¹³C {¹H} NMR** (176 MHz, CDCl$_3$): δ = 149.5 (C-4), 129.3 (C-2), 117.4 (C-1), 112.5 (C-3), 30.0 (p, *J* = 22.2 Hz, C-5) ppm.

### 5.5.3. Synthesis of *N-d-N*-methylaniline 40
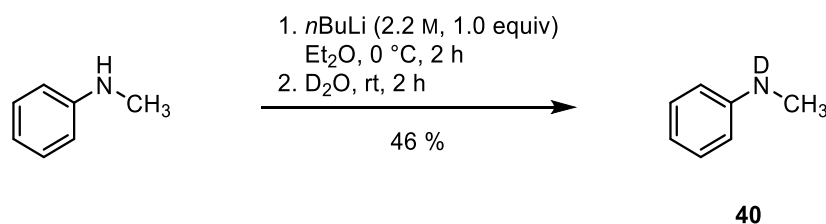


The procedure was adapted from literature.[172] A 25 mL Schlenk flask containing a stirring bar was introduced into the glovebox and charged with dry *N*-methylaniline (0.5 mL, 4.6 mmol) and Et$_2$O (3 mL). The Schlenk flask was connected to the Schlenk line and cooled down to 0 °C. *n*BuLi (2.1 mL, 2.2 M in hexanes, 4.6 mmol, 1.0 equiv) was added dropwise to the solution while stirring. The reaction mixture was allowed to slowly warm up to room temperature and stirred for 2 h. D$_2$O was purged with argon gas for 1.5 h. The degassed D$_2$O (80 µL, 4.5 mmol, 0.97 equiv) was added dropwise to the reaction mixture and stirred for 2 h. The product was recondensed into a 25 mL Schlenk-tube (30 °C, 8.0×10$^{-2}$ mbar). The obtained, slightly yellow oil (227 mg, 2.1 mmol, 46 %) was stored at –30 °C over molecular sieves. ¹H NMR spectroscopy revealed a deuterium content of >98 % in the product.

**¹H NMR** (400 MHz, C$_6$D$_6$): δ = 7.18 (d, *J* = 7.6 Hz, 2H, H-2), 6.76 (t, *J* = 7.3 Hz, 1H, H-1), 6.40 (d, *J* = 8.1 Hz, 2H, H-3), 2.30 (s, 3H, H-5) ppm.
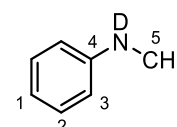
**¹³C {¹H} NMR** (101 MHz, C$_6$D$_6$): δ = 149.8 (C-4), 129.4 (C-2), 117.4 (C-1), 112.6 (C-3), 30.2 (C-5) ppm.

## 6. References

[1]    P. J. Harrington, L. S. Hegedus, K. F. McDaniel, *J. Am. Chem. Soc.* **1987**, *109*, 4335–4338.

[2]    S. Arseniyadis, J. Sartoretti, *Tetrahedron Lett.* **1985**, *26*, 729–732.

[3]    G. Enierga, M. Espiritu, P. Perlmutter, N. Pham, M. Rose, S. Sjöberg, N. Thienthong, K. Wong, *Tetrahedron Asymmetry* **2001**, *12*, 597–604.

[4]    R. N. Salvatore, C. H. Yoon, K. W. Jung, *Tetrahedron* **2001**, *57*, 7785–7811.

[5]    S. Hong, T. J. Marks, *Acc. Chem. Res.* **2004**, *37*, 673–686.

[6]    D. Reich, A. Trowbridge, M. J. Gaunt, *Angew. Chem. Int. Ed.* **2020**, *132*, 2276–2281.

[7]    P. J. Waller, S. J. Lyle, T. M. Osborn Popp, C. S. Diercks, J. A. Reimer, O. M. Yaghi, *J. Am. Chem. Soc.* **2016**, *138*, 15519–15522.

[8]    A. M. Fracaroli, H. Furukawa, M. Suzuki, M. Dodd, S. Okajima, F. Gándara, J. A. Reimer, O. M. Yaghi, *J. Am. Chem. Soc.* **2014**, *136*, 8863–8866.

[9]    T. M. McDonald, D. M. D'Alessandro, R. Krishna, J. R. Long, *Chem. Sci.* **2011**, *2*, 2022–2028.

[10]   D. Chen, S. J. Su, Y. Cao, *J. Mater. Chem. C* **2014**, *2*, 9565–9578.

[11]   D. J. Gilmour, T. Tomkovic, N. Kuanr, M. R. Perry, H. Gildenast, S. G. Hatzikiriakos, L. L. Schafer, *ACS Appl. Polym. Mater.* **2021**, *3*, 2330–2335.

[12]   S. S. Scott, S. C. Roşca, D. J. Gilmour, P. Brant, L. L. Schafer, *ACS Macro Lett.* **2021**, *10*, 1266–1272.

[13]   L. J. Gooßen, L. Huang, M. Arndt, K. Gooßen, H. Heydt, *Chem. Rev.* **2015**, *115*, 2596–2697.

[14]   O. I. Afanasyev, E. Kuchuk, D. L. Usanov, D. Chusov, *Chem. Rev.* **2019**, *119*, 11857–11911.

[15]   M. S. Gibson, R. W. Bradshaw, *Angew. Chem. Int. Ed.* **1968**, *7*, 919–930.

[16]   R. Dorel, C. P. Grugel, A. M. Haydl, *Angew. Chem. Int. Ed.* **2019**, *58*, 17118–17129.

[17]   M. Arend, B. Westermann, N. Risch, *Angew. Chem. Int. Ed.* **1998**, *37*, 1044–1070.

[18]   L. H. Amundsen, L. S. Nelson, *J. Am. Chem. Soc.* **1951**, *73*, 242–244.

[19]   D. B. Bagal, B. M. Bhanage, *Adv. Synth. Catal.* **2015**, *357*, 883–900.

[20]   F. Rolla, *J. Org. Chem.* **1982**, *47*, 4327–4329.

[21]   H. Boyer, *J. Am. Chem. Soc.* **1951**, *73*, 5865–5866.

[22]   O. Mitsunobu, *Synth.* **1981**, 1–28.

[23]   O. Mitsunobu, M. Yamada, *Bull. Chem. Soc. Jpn.* **1967**, *40*, 2380–2382.

[24] B. M. Trost, *Acc. Chem. Res.* **2002**, *35*, 695–705.

[25] E. A. Werner, *J. Chem. Soc. Trans.* **1918**, *113*, 899–902.

[26] T. E. Müller, K. C. Hultzsch, M. Yus, F. Foubelo, M. Tada, *Chem. Rev.* **2008**, *108*, 3795–3892.

[27] P. M. Edwards, L. L. Schafer, *Chem. Commun.* **2018**, *54*, 12543–12560.

[28] R. C. Dipucchio, S. C. Rosca, L. L. Schafer, *J. Am. Chem. Soc.* **2022**, *144*, 11459–11481.

[29] J. Hannedouche, E. Schulz, *Organometallics* **2018**, *37*, 4313–4326.

[30] U. Dingerdissen, A. Henne, J. Herrmann, J. Pfeffinger, P. Stops, *Process for the Preparation of Tert. Butylamine*, **1996**, DE19500839A1.

[31] Z. Xu, W. Hu, Q. Liu, L. Zhang, Y. Jia, *J. Org. Chem.* **2010**, *75*, 7626–7635.

[32] V. M. Arredondo, S. Tian, F. E. McDonald, T. J. Marks, *J. Am. Chem. Soc.* **1999**, *121*, 3633–3639.

[33] T. Jiang, T. Livinghouse, *Org. Lett.* **2010**, *12*, 4271–4273.

[34] K. A. Parker, D. Fokas, *J. Org. Chem.* **2006**, *71*, 449–455.

[35] H. Hao, K. A. Thompson, Z. M. Hudson, L. L. Schafer, *Chem. - Eur. J.* **2018**, *24*, 5562–5568.

[36] M. Weers, L. H. Lühning, V. Lührs, C. Brahms, S. Doye, *Chem. - Eur. J.* **2017**, *23*, 1237–1240.

[37] J. Zheng, B. Breit, *Angew. Chem. Int. Ed.* **2019**, *58*, 3392–3397.

[38] S. B. Herzon, J. F. Hartwig, *J. Am. Chem. Soc.* **2007**, *129*, 6690–6691.

[39] S. B. Herzon, J. F. Hartwig, *J. Am. Chem. Soc.* **2008**, *130*, 14940–14941.

[40] A. L. Reznichenko, T. J. Emge, S. Audörsch, E. G. Klauber, K. C. Hultzsch, B. Schmidt, *Organometallics* **2011**, *30*, 921–924.

[41] P. Garcia, Y. Y. Lau, M. R. Perry, L. L. Schafer, *Angew. Chem. Int. Ed.* **2013**, *52*, 9144–9148.

[42] Z. Zhang, J. D. Hamel, L. L. Schafer, *Chem. - Eur. J.* **2013**, *19*, 8751–8754.

[43] L. H. Lühning, C. Brahms, J. P. Nimoth, M. Schmidtmann, S. Doye, *Z. Anorg. Allg. Chem.* **2015**, *641*, 2071–2082.

[44] M. Warsitz, S. Doye, *Chem. - Eur. J.* **2020**, *26*, 15121–15125.

[45] E. Chong, P. Garcia, L. L. Schafer, *Synth.* **2014**, *46*, 2884–2896.

[46] S. Oda, J. Franke, M. J. Krische, *Chem. Sci.* **2016**, *7*, 136–141.

[47] P. Verma, J. M. Richter, N. Chekshin, J. X. Qiao, J. Q. Yu, *J. Am. Chem. Soc.* **2020**, *142*, 5117–5125.

[48] D. Yamauchi, T. Nishimura, H. Yorimitsu, *Angew. Chem. Int. Ed.* **2017**, *56*, 7200–7204.

[49] G. Lahm, T. Opatz, *Org. Lett.* **2014**, *16*, 4201–4203.

[50] D. C. Schmitt, J. Lee, A. M. R. Dechert-Schmitt, E. Yamaguchi, M. J. Krische, *Chem. Commun.* **2013**, *49*, 6096–6098.

[51] V. Smout, A. Peschiulli, S. Verbeeck, E. A. Mitchell, W. Herrebout, P. Bultinck, C. M. L. Vande Velde, D. Berthelot, L. Meerpoel, B. U. W. Maes, *J. Org. Chem.* **2013**, *78*, 9803–9814.

[52] S. Pan, Y. Matsuo, K. Endo, T. Shibata, *Tetrahedron* **2012**, *68*, 9009–9015.

[53] C. H. Jun, D. C. Hwang, S. J. Na, *Chem. Commun.* **1998**, 1405–1406.

[54] N. Chatani, T. Asaumi, S. Yorimitsu, T. Ikeda, F. Kakiuchi, S. Murai, *J. Am. Chem. Soc.* **2001**, *123*, 10935–10941.

[55] A. Seayad, M. Ahmed, H. Klein, R. Jackstell, T. Gross, M. Beller, *Science* **2002**, *297*, 1676–1678.

[56] D. Crozet, M. Urrutigoity, P. Kalck, *ChemCatChem* **2011**, *3*, 1102–1118.

[57] M. Ahmed, A. M. Seayad, R. Jackstell, M. Beller, *J. Am. Chem. Soc.* **2003**, *125*, 10311–10318.

[58] J. Dörfler, T. Preuß, A. Schischko, M. Schmidtmann, S. Doye, *Angew. Chem. Int. Ed.* **2014**, *53*, 7918–7922.

[59] T. Preuß, W. Saak, S. Doye, *Chem. - Eur. J.* **2013**, *19*, 3833–3837.

[60] J. Dörfler, T. Preuß, C. Brahms, D. Scheuer, S. Doye, *Dalton Trans.* **2015**, *44*, 12149–12168.

[61] J. Dörfler, S. Doye, *Angew. Chem. Int. Ed.* **2013**, *52*, 1806–1809.

[62] J. Dörfler, S. Doye, *Eur. J. Org. Chem.* **2014**, *2014*, 2790–2797.

[63] T. Kaper, M. Fischer, M. Warsitz, R. Zimmering, R. Beckhaus, S. Doye, *Chem. - Eur. J.* **2020**, *26*, 14300–14304.

[64] T. Kaper, M. Fischer, H. Thye, D. Geik, M. Schmidtmann, R. Beckhaus, S. Doye, *Chem. - Eur. J.* **2021**, *27*, 6899–6903.

[65] E. N. Bahena, S. E. Griffin, L. L. Schafer, *J. Am. Chem. Soc.* **2020**, *142*, 20566–20571.

[66] M. G. Clerici, F. Maspero, *Synth.* **1980**, *4*, 305–306.

[67] W. A. Nugent, D. W. Ovenall, S. J. Holmes, *Organometallics* **1983**, *2*, 161–162.

[68] N. Coles, M. C. J. Harris, R. J. Whitby, J. Blagg, *Organometallics* **1994**, 190–199.

[69] E. Sebe, I. A. Guzei, M. J. Heeg, L. M. Liable-Sands, A. L. Rheingold, C. H. Winter, *Eur. J. Inorg. Chem.* **2005**, 3955–3961.

[70] P. R. Woodman, C. J. Sanders, N. W. Alcock, P. B. Hitchcock, P. Scott, *New J. Chem.* **1999**, *23*, 815–817.

[71] J. M. Lauzon, P. Eisenberger, S. C. Roşca, L. L. Schafer, *ACS Catal.* **2017**, *7*, 5921–5931.

[72] S. Bi, Z. Lin, R. F. Jordan, *Organometallics* **2004**, *23*, 4882–4890.

[73]  T. Preuß, W. Saak, S. Doye, *Chem. - Eur. J.* **2013**, *19*, 3833–3837.

[74]  P. Eisenberger, R. O. Ayinla, J. M. P. Lauzon, L. L. Schafer, *Angew. Chem. Int. Ed.* **2009**, *48*, 8361–8365.

[75]  G. Zi, F. Zhang, H. Song, *Chem. Commun.* **2010**, *46*, 6296–6298.

[76]  F. Zhang, H. Song, G. Zi, *Dalton Trans.* **2011**, *40*, 1547–1566.

[77]  A. L. Reznichenko, K. C. Hultzsch, *J. Am. Chem. Soc.* **2012**, *134*, 3300–3311.

[78]  A. J. Musacchio, B. C. Lainhart, X. Zhang, S. G. Naguib, T. C. Sherwood, R. R. Knowles, *Science* **2017**, *355*, 727–730.

[79]  D. C. Miller, J. M. Ganley, A. J. Musacchio, T. C. Sherwood, W. R. Ewing, R. R. Knowles, *J. Am. Chem. Soc.* **2019**, *141*, 16590–16594.

[80]  J. Haggin, *Chem. Eng. News* **1993**, *71*, 22, 23–27.

[81]  D. R. Coulson, *Tetrahedron Lett.* **1971**, *12*, 429–430.

[82]  S. Tobisch, *J. Am. Chem. Soc.* **2005**, *127*, 11979–11988.

[83]  S. Hong, A. M. Kawaoka, T. J. Marks, *J. Am. Chem. Soc.* **2003**, *125*, 15878–15892.

[84]  J. Pawlas, Y. Nakao, M. Kawatsura, J. F. Hartwig, *J. Am. Chem. Soc.* **2002**, *124*, 3669–3679.

[85]  L. T. Kaspar, B. Fingerhut, L. Ackermann, *Angew. Chem. Int. Ed.* **2005**, *44*, 5972–5974.

[86]  J. S. Ryu, G. Y. Li, T. J. Marks, *J. Am. Chem. Soc.* **2003**, *125*, 12584–12605.

[87]  P. J. Walsh, A. M. Baranger, R. G. Bergman, *J. Am. Chem. Soc.* **1992**, *114*, 1708–1719.

[88]  J. S. Johnson, R. G. Bergman, *J. Am. Chem. Soc.* **2001**, *123*, 2923–2924.

[89]  Y. Li, T. J. Marks, *Organometallics* **1996**, *15*, 3770–3772.

[90]  Z. Zhang, S. Du Lee, R. A. Widenhoefer, *J. Am. Chem. Soc.* **2009**, *131*, 5372–5373.

[91]  A. L. Reznichenko, H. N. Nguyen, K. C. Hultzsch, *Angew. Chem. Int. Ed.* **2010**, *49*, 8984–8987.

[92]  C. S. Sevov, J. Zhou, J. F. Hartwig, *J. Am. Chem. Soc.* **2012**, *134*, 11960–11963.

[93]  B. M. Trost, W. Tang, *J. Am. Chem. Soc.* **2002**, *124*, 14542–14543.

[94]  G. P. Pez, J. E. Galle, *Pure Appl. Chem.* **1985**, *57*, 1917–1926.

[95]  D. Tzalis, C. Koradin, P. Knochel, *Tetrahedron Lett.* **1999**, *40*, 6193–6195.

[96]  B. W. Howk, E. L. Little, S. L. Scott, G. M. Whitman, *J. Am. Chem. Soc.* **1954**, *76*, 1899–1902.

[97]  L. Davin, A. Hernán-Gómez, C. McLaughlin, A. R. Kennedy, R. McLellan, E. Hevia, *Dalton Trans.* **2019**, *48*, 8122–8130.

[98]  H. Lehmkuhl, D. Reinehr, *J. Organomet. Chem.* **1973**, *55*, 215–220.

[99]  I. Bytschkov, S. Doye, *Eur. J. Org. Chem.* **2003**, 935–946.

[100]  A. Tillack, I. Garcia Castro, C. G. Hartung, M. Beller, *Angew. Chem. Int. Ed.* **2002**, *41*, 2541–2543.

[101]  L. Ackermann, R. G. Bergman, R. N. Loy, *J. Am. Chem. Soc.* **2003**, *125*, 11956–11963.

[102]  M. C. Wood, D. C. Leitch, C. S. Yeung, J. A. Kozak, L. L. Schafer, *Angew. Chem. Int. Ed.* **2007**, *46*, 354–358.

[103]  J. Takaya, J. F. Hartwig, *J. Am. Chem. Soc.* **2005**, *127*, 5756–5757.

[104]  H. Deng, S. Grunder, K. E. Cordova, C. Valente, H. Furukawa, M. Hmadeh, F. Gándara, A. C. Whalley, Z. Liu, S. Asahina, H. Kazumori, M. O'Keeffe, O. Terasaki, J. F. Stoddart, O. M. Yaghi, *Science* **2012**, *336*, 1018–1023.

[105]  A. C. Wiseman, *Clin. J. Am. Soc. Nephrol.* **2016**, *11*, 332–343.

[106]  S. Kaplan, *Org. Magn. Reson.* **1981**, *15*, 197–199.

[107]  T. Ramdahl, K. Urdal, *Anal. Chem.* **1982**, *54*, 2256–2260.

[108]  Z. Lu, J. Liu, X. Zhang, Y. Liao, R. Wang, K. Zhang, J. Lyu, O. K. Farha, J. T. Hupp, *J. Am. Chem. Soc.* **2020**, *142*, 21110–21121.

[109]  T. Panda, T. Kundu, R. Banerjee, *Chem. Commun.* **2012**, *48*, 5464–5466.

[110]  A. Haskel, T. Straub, M. S. Eisen, *Organometallics* **1996**, *15*, 3773–3775.

[111]  P. N. O'Shaughnessy, C. M. Paul D. Knight, K. M. Gillespie, P. Scott, *Chem. Commun* **2003**, 1770–1771.

[112]  Y. Li, T. J. Marks, *J. Am. Chem. Soc.* **1998**, *120*, 1757–1771.

[113]  S. Tian, V. M. Arredondo, C. L. Stern, T. J. Marks, *Organometallics* **1999**, *18*, 2568–2570.

[114]  H. N. Nguyen, H. Lee, S. Audörsch, A. L. Reznichenko, A. J. Nawara-Hultzsch, B. Schmidt, K. C. Hultzsch, *Organometallics* **2018**, *37*, 4358–4379.

[115]  D. V Gribkov, K. C. Hultzsch, F. Hampel, *J. Am. Chem. Soc.* **2006**, *128*, 3748–3759.

[116]  P. L. McGrane, M. Jensen, T. Livinghouse, *J. Am. Chem. Soc.* **1992**, *114*, 5459–5460.

[117]  A. M. Baranger, P. J. Walsh, R. G. Bergman, *J. Am. Chem. Soc.* **1993**, *115*, 2753–2763.

[118]  M. A. Aljuhani, Z. Zhang, S. Barman, M. El Eter, L. Failvene, S. Ould-Chikh, E. Guan, E. Abou-Hamad, A. H. Emwas, J. D. A. Pelletier, B. C. Gates, L. Cavallo, J. M. Basset, *ACS Catal.* **2019**, *9*, 8719–8725.

[119]  M. E. Jung, G. Piizzi, *Chem. Rev.* **2005**, *105*, 1735–1766.

[120]  Y. K. Joon, T. Livinghouse, *Org. Lett.* **2005**, *7*, 1737–1739.

[121]  Y. K. Kim, T. Livinghouse, *Angew. Chem. Int. Ed.* **2002**, *41*, 3645–3647.

[122]  F. Lauterwasser, P. G. Hayes, S. Bräse, W. E. Piers, L. L. Schafer,

*Organometallics* **2004**, *23*, 2234–2237.

[123] L. L. Schafer, M. Manßen, P. M. Edwards, E. K. J. Lui, S. E. Griffin, C. R. Dunbar, in *Advances in Organometallic Chemistry*, **2020**, pp. 405–468.

[124] J. C. H. Yim, J. A. Bexrud, R. O. Ayinla, D. C. Leitch, L. L. Schafer, *J. Org. Chem.* **2014**, *79*, 2015–2028.

[125] M. C. Hansen, C. A. Heusser, T. C. Narayan, K. E. Fong, N. Hara, A. W. Kohn, A. R. Venning, A. L. Rheingold, A. R. Johnson, *Organometallics* **2011**, *30*, 4616–4623.

[126] C. Lorber, R. Choukroun, L. Vendier, *Organometallics* **2004**, *23*, 1845–1850.

[127] L. L. Anderson, J. Arnold, R. G. Bergman, *Org. Lett.* **2004**, *6*, 2519–2522.

[128] L. L. Anderson, J. Arnold, R. G. Bergman, *Org. Lett.* **2006**, *8*, 2245.

[129] M. R. Gagné, T. J. Marks, *J. Am. Chem. Soc.* **1989**, *111*, 4108–4109.

[130] S. Datta, P. W. Roesky, S. Blechern, *Organometallics* **2007**, *26*, 4392–4394.

[131] B. Liu, T. Roisnel, J. F. Carpentier, Y. Sarazin, *Chem. - Eur. J.* **2013**, *19*, 13445–13462.

[132] W. J. Van Zeist, F. M. Bickelhaupt, *Dalton Trans.* **2011**, *40*, 3028–3038.

[133] P. W. N. M. Van Leeuwen, P. C. J. Kamer, J. N. H. Reek, P. Dierkes, *Chem. Rev.* **2000**, *100*, 2741–2769.

[134] M. Kranenburg, Y. E. M. van der Burgt, P. C. J. Kamer, P. W. N. M. van Leeuwen, K. Goubitz, J. Fraanje, *Organometallics* **1995**, *14*, 3081–3089.

[135] B. C. Hamann, J. F. Hartwig, *J. Am. Chem. Soc.* **1998**, *120*, 3694–3703.

[136] J. Soltys, *Report*, **15 June 2013**.

[137] J. Soltys, *Report*, **6 March 2014**.

[138] J. Soltys, M. J. Wolff, A. J. Nawara-Hultzsch, A. Prado-Roller, K. C. Hultzsch, *Unpublished Results*.

[139] J. Soltys, Q. M. Riedl, M. Wolff, T. Grüne, K. C. Hultzsch, *Unpublished Results*.

[140] B. Jones, *J. Am. Chem. Soc.* **1941**, *63*, 358–364.

[141] J. F. Larrow, E. N. Jacobsen, Y. Gao, Y. Hong, X. Nie, C. M. Zepp, *J. Org. Chem.* **1994**, *59*, 1939–1942.

[142] S. Bhatt, K. Roy, S. K. Nayak, *Synth. Commun.* **2010**, *40*, 2736–2746.

[143] K. Maruoka, T. Itoh, Y. Araki, T. Shirasaka, H. Yamamoto, *Bull. Chem. Soc. Jpn.* **1988**, *61*, 2975–2976.

[144] A. B. Smith, M. Xian, W. S. Kim, D. S. Kim, *J. Am. Chem. Soc.* **2006**, *128*, 12368–12369.

[145] W. H. Moser, *Tetrahedron* **2001**, *57*, 2065–2084.

[146] J. M. Hoerter, K. M. Otte, S. H. Gellman, Q. Cui, S. S. Stahl, *J. Am. Chem. Soc.* **2008**, *130*, 647–654.

[147] M. J. Humphries, M. L. H. Green, R. E. Douthwaite, L. H. Rees, *J. Chem. Soc. Dalt. Trans.* **2000**, 4555–4562.

[148] A. Castro, M. V. Galakhov, M. Gómez, F. Sánchez, *J. Organomet. Chem.* **1999**, *580*, 161–168.

[149] U. Jayarathne, J. T. Mague, J. P. Donahue, *Polyhedron* **2013**, *58*, 13–17.

[150] W. Scherer, D. J. Wolstenholme, V. Herz, G. Eickerling, A. Brück, P. Benndorf, P. W. Roesky, *Angew. Chem. Int. Ed.* **2010**, *49*, 2242–2246.

[151] P. Daneshmand, S. C. Roşca, R. Dalhoff, K. Yin, R. C. Dipucchio, R. A. Ivanovich, D. E. Polat, A. M. Beauchemin, L. L. Schafer, *J. Am. Chem. Soc.* **2020**, *142*, 15740–15750.

[152] P. R. Payne, P. Garcia, P. Eisenberger, J. C. H. Yim, L. L. Schafer, *Org. Lett.* **2013**, *15*, 2182–2185.

[153] J. W. Brandt, E. Chong, L. L. Schafer, *ACS Catal.* **2017**, *7*, 6323–6330.

[154] J. M. P. Lauzon, L. L. Schafer, *Dalton Trans.* **2012**, *41*, 11539–11550.

[155] T. Agapie, M. W. Day, J. E. Bercaw, *Organometallics* **2008**, *27*, 6123–6142.

[156] T. R. Helgert, T. K. Hollis, E. J. Valente, *Organometallics* **2012**, *31*, 3002–3009.

[157] Y. Nakayama, M. Tanimoto, T. Shiono, *Macromol. Rapid Commun.* **2007**, *28*, 646–650.

[158] M. Sietzen, H. Wadepohl, J. Ballmann, *Inorg. Chem.* **2015**, *54*, 4094–4103.

[159] I. A. Tonks, L. M. Henling, M. W. Day, J. E. Bercaw, *Inorg. Chem.* **2009**, *48*, 5096–5105.

[160] M. R. Crimmin, I. J. Casely, M. S. Hill, *J. Am. Chem. Soc.* **2005**, *127*, 2042–2043.

[161] X. Zhang, T. J. Emge, K. C. Hultzsch, *Angew. Chem. Int. Ed.* **2012**, *51*, 394–398.

[162] P. H. Martínez, K. C. Hultzsch, F. Hampel, *Chem. Commun.* **2006**, 2221–2223.

[163] A. Ates, C. Quinet, *Eur. J. Org. Chem.* **2003**, 1623–1626.

[164] K. Manna, A. Ellern, A. D. Sadow, *Chem. Commun.* **2010**, *46*, 339–341.

[165] S. Majumder, A. L. Odom, *Organometallics* **2008**, *27*, 1174–1177.

[166] M. R. Gagné, C. L. Stern, T. J. Marks, *J. Am. Chem. Soc.* **1992**, *114*, 275–294.

[167] D. Riegert, J. Collin, A. Meddour, E. Schulz, A. Trifonov, *J. Org. Chem.* **2006**, *71*, 2514–2517.

[168] Y. Takahaschi, N. Onoyama, Y. Ishikawa, S. Motojima, K. Sugiyama, *Chem. Lett.* **1978**, *7*, 525–528.

[169] M. V Galakhov, M. Gómez, G. Jiménez, P. Royo, *Organometallics* **1995**, *14*, 1901–1910.

[170] P. Roquette, A. Maronna, M. Reinmuth, E. Kaifer, M. Enders, H. J. Himmel, *Inorg. Chem.* **2011**, *50*, 1942–1955.

[171] O. E. Palomero, R. A. Jones, *Organometallics* **2020**, *39*, 3689–3694.

[172] J. W. Brandt, E. Chong, L. L. Schafer, *ACS Catal.* **2017**, *7*, 6323–6330.

[173] I. V. Alabugin, in *Stereoelectronic Effects*, John Wiley & Sons, Ltd., **2016**, pp. 257–274.

[174] R. Koppang, *J. Fluor. Chem.* **1975**, *5*, 323–333.

[175] W. S. Matthews, J. E. Bares, J. E. Bartmess, F. J. Cornforth, G. E. Drucker, R. J. McCallum, G. J. McCollum, N. R. Vanier, F. G. Bordwell, Z. Margolin, *J. Am. Chem. Soc.* **1975**, *97*, 7006–7014.

[176] M. J. P. Mandigma, M. Domański, J. P. Barham, *Org. Biomol. Chem.* **2020**, *18*, 7697–7723.

[177] G. R. Fulmer, A. J. M. Miller, N. H. Sherden, H. E. Gottlieb, A. Nudelman, B. M. Stoltz, J. E. Bercaw, K. I. Goldberg, *Organometallics* **2010**, *29*, 2176–2179.

[178] *Bruker SAINT V7.68A, V8.32B Copyright © 2005-2018 Bruker AXS, Madison, Wisconsin, USA*, **2012**.

[179] *G. M. Sheldrick, SHELX-97 (SHELXS 97 and SHELXL 97), Programs for Crystal Structure Analyses, University of Göttingen: Göttingen (Germany)*, **1998**.

[180] O. V. Dolomanov, L. J. Bourhis, R. J. Gildea, J. A. K. Howard, H. Puschmann, *J. Appl. Crystallogr.* **2009**, *42*, 339–341.

[181] C. B. Hübschle, G. M. Sheldrick, B. Dittrich, *J. Appl. Crystallogr.* **2011**, *44*, 1281–1284.

[182] G. M. Sheldrick, *Acta Crystallogr. Sect. A Found. Crystallogr.* **2008**, *64*, 112–122.

[183] J. P. Dinnocenzo, S. B. Karki, J. P. Jones, *J. Am. Chem. Soc.* **1993**, *115*, 7111–7116.

# 7. Supplementary Information

## 7.1. NMR Spectra

### 7.1.1. (*E*)-6,6'-(ethene-1,2-diyl)bis(2-bromo-4-methylphenol) − 32
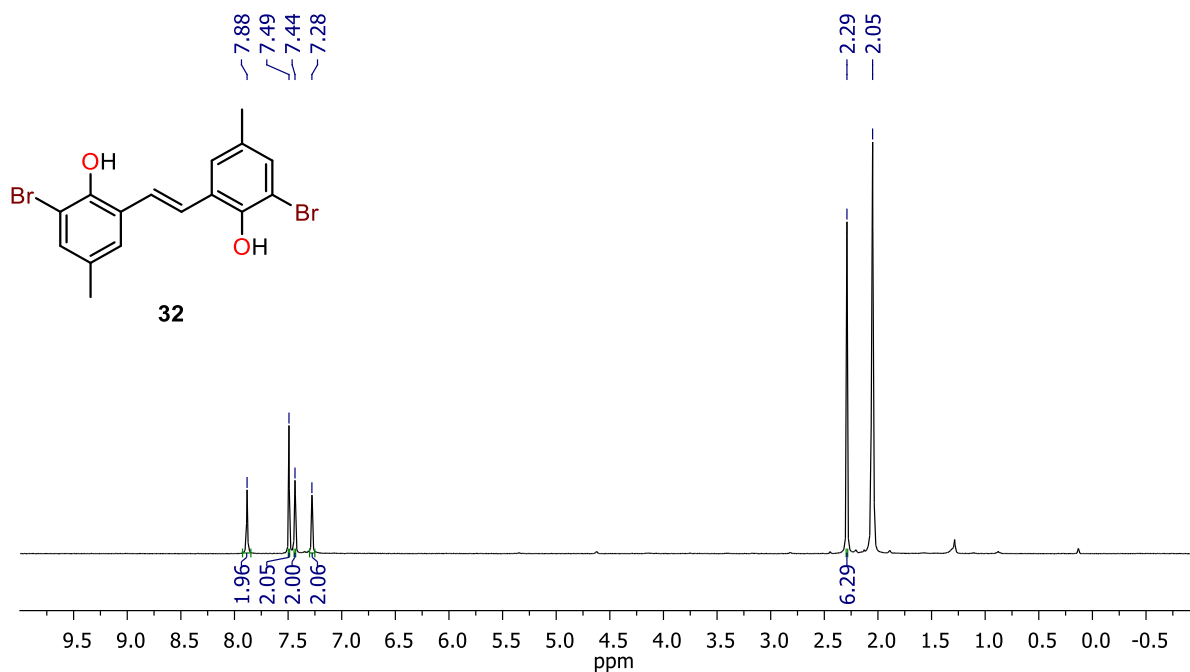


*Figure 30:* $^1$H NMR spectrum (400 MHz) of compound **32** at 295 K in acetone-$d_6$. Asterisk (*) indicates solvent peak.
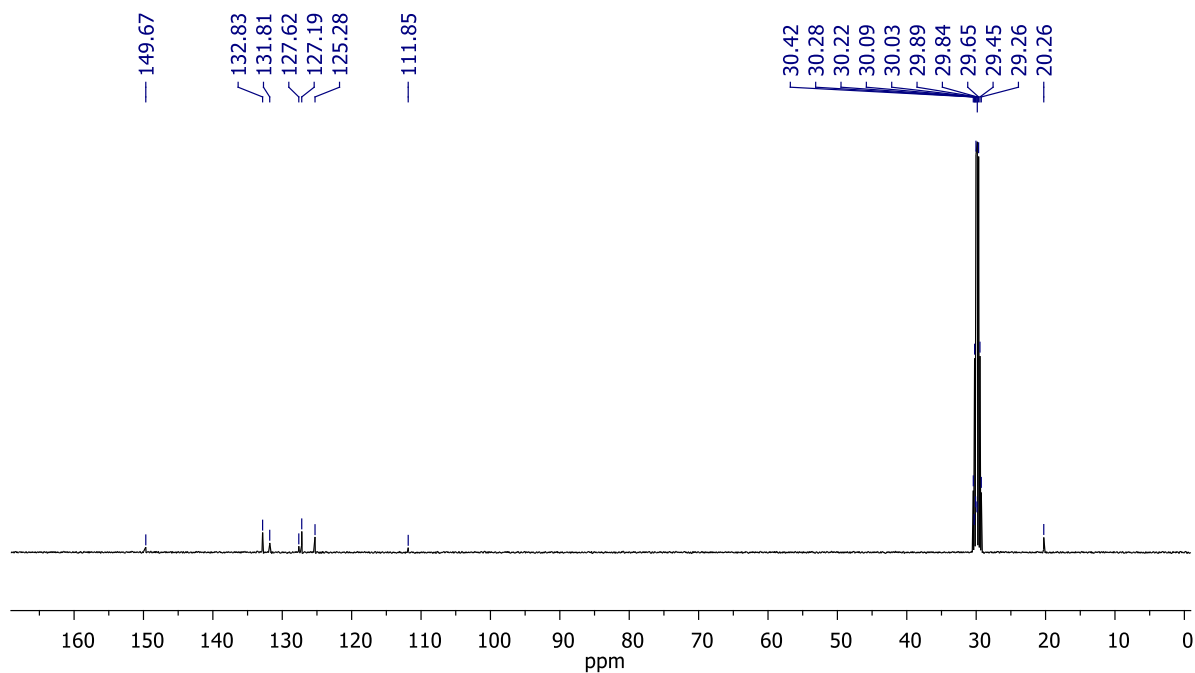


*Figure 29:* $^{13}$C {$^1$H} NMR spectrum (101 MHz) of compound **32** at 295 K in acetone-$d_6$. Asterisk (*) indicates solvent peak.

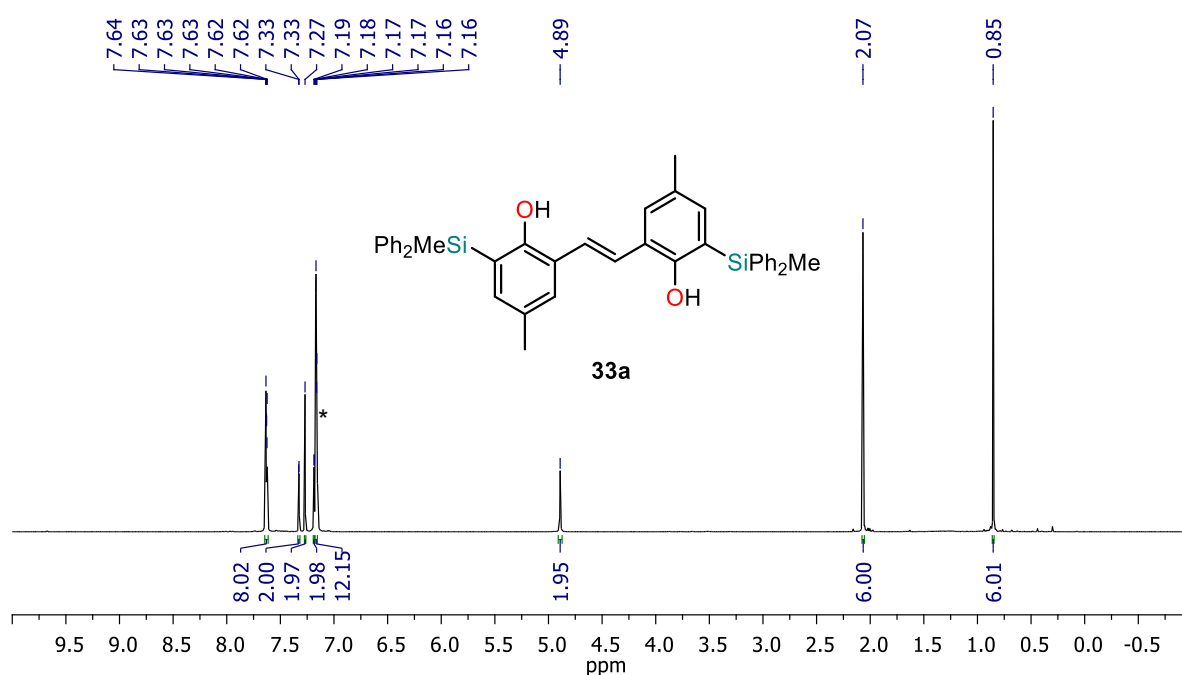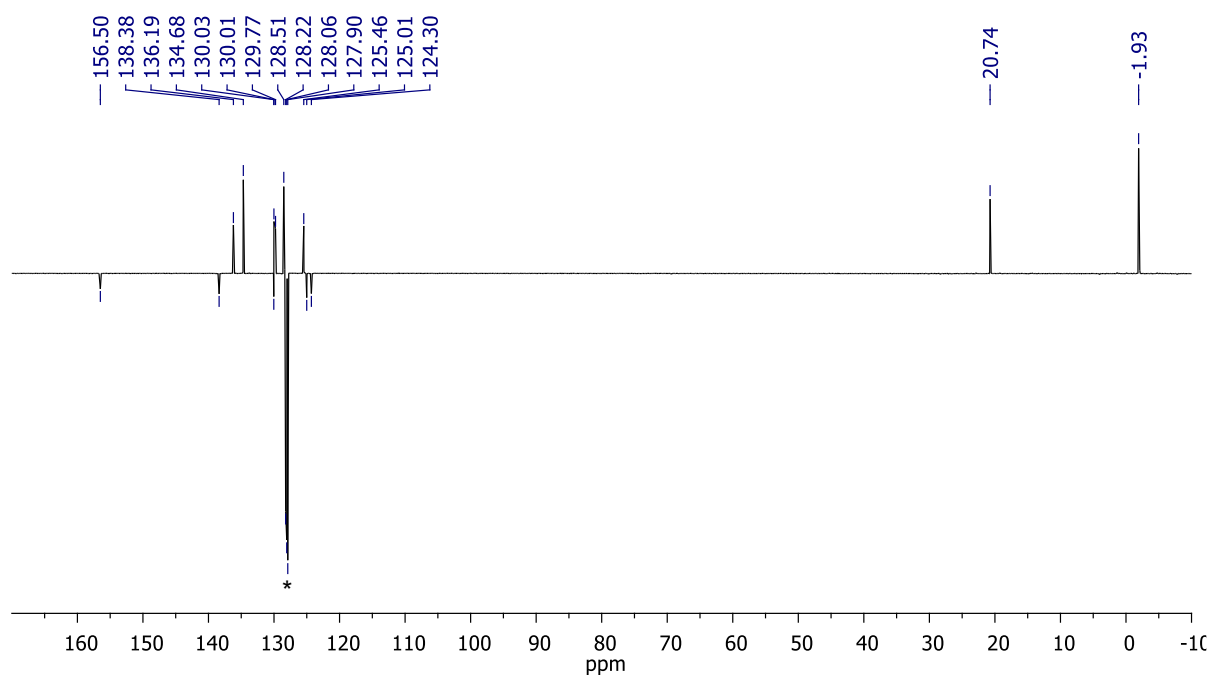## 7.1.2. (*E*)-6,6'-(ethene-1,2-diyl)bis(4-methyl-2-(methyldiphenylsilyl)phenol) – 33a
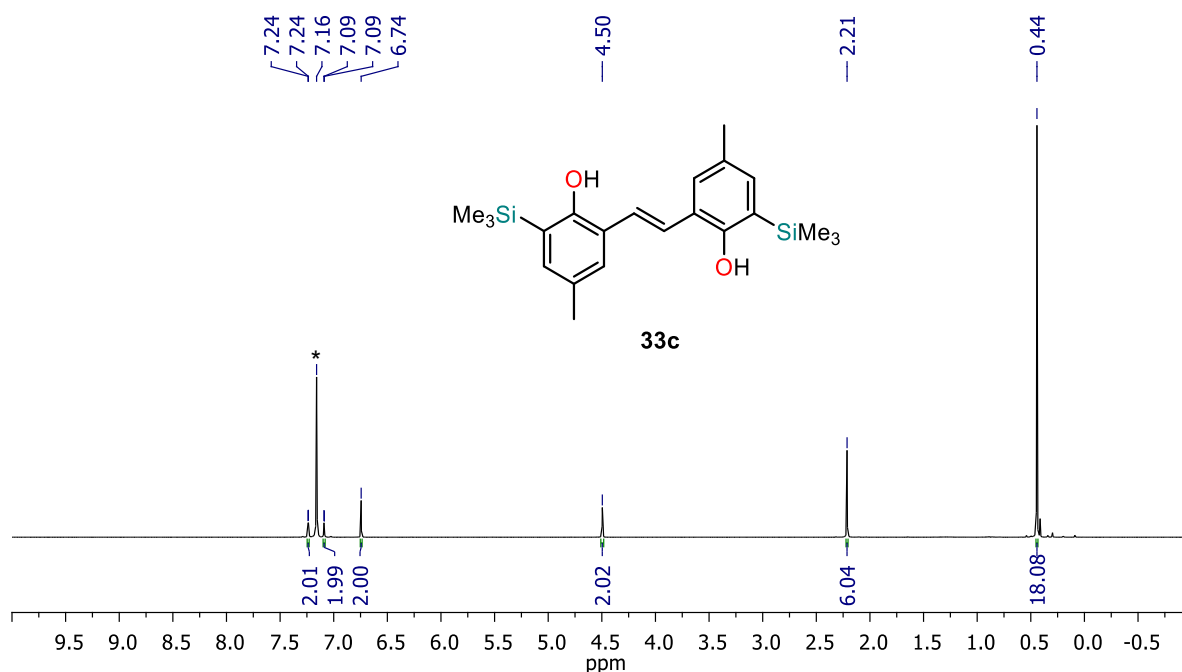


*Figure 31:* $^1$H NMR spectrum (700 MHz) of compound **33a** at 295 K in benzene-$d_6$. Asterisk (*) indicates solvent peak.
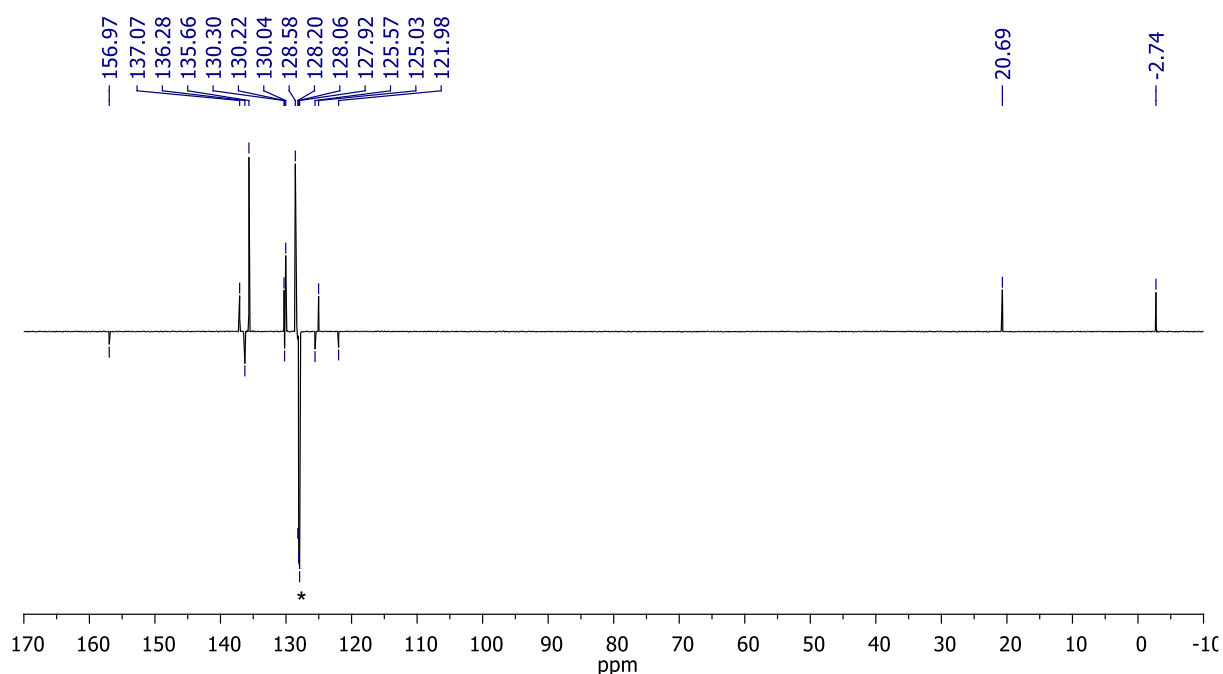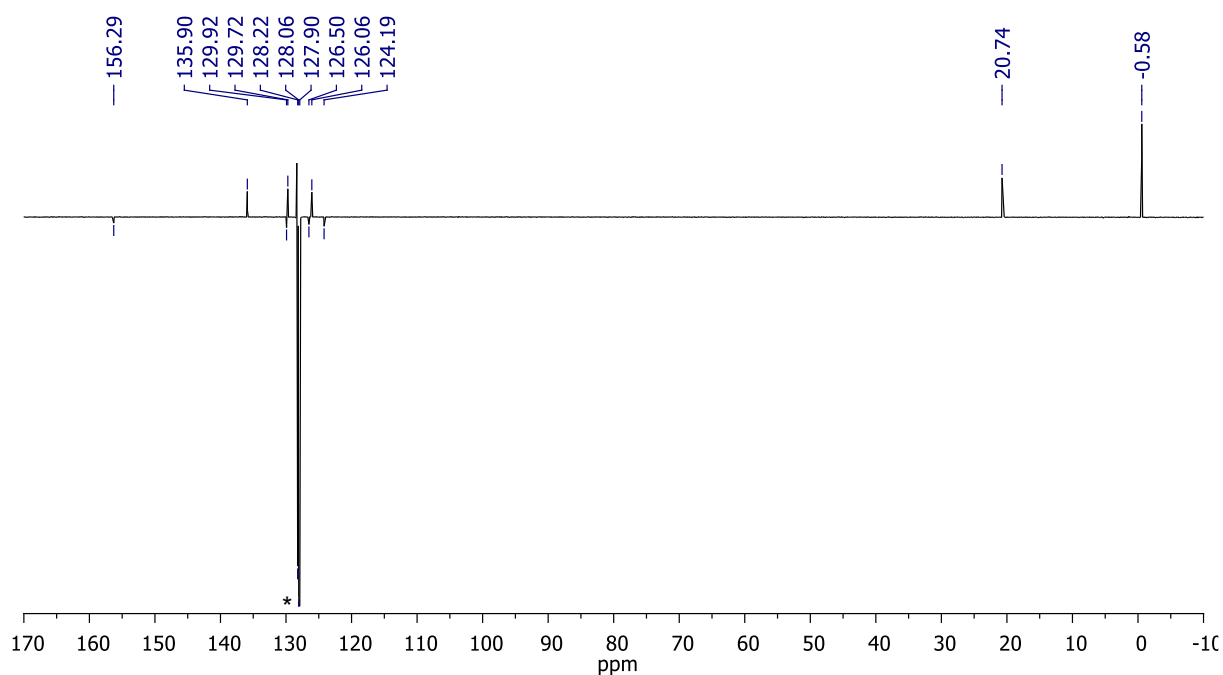


*Figure 32:* $^{13}$C(APT) NMR spectrum (176 MHz) of compound **33a** at 295 K in benzene-$d_6$. Asterisk (*) indicates solvent peak.

### 7.1.3.  (*E*)-6,6'-(ethene-1,2-diyl)bis(2-(dimethyl(phenyl)silyl)-4-methylphenol) – 33b
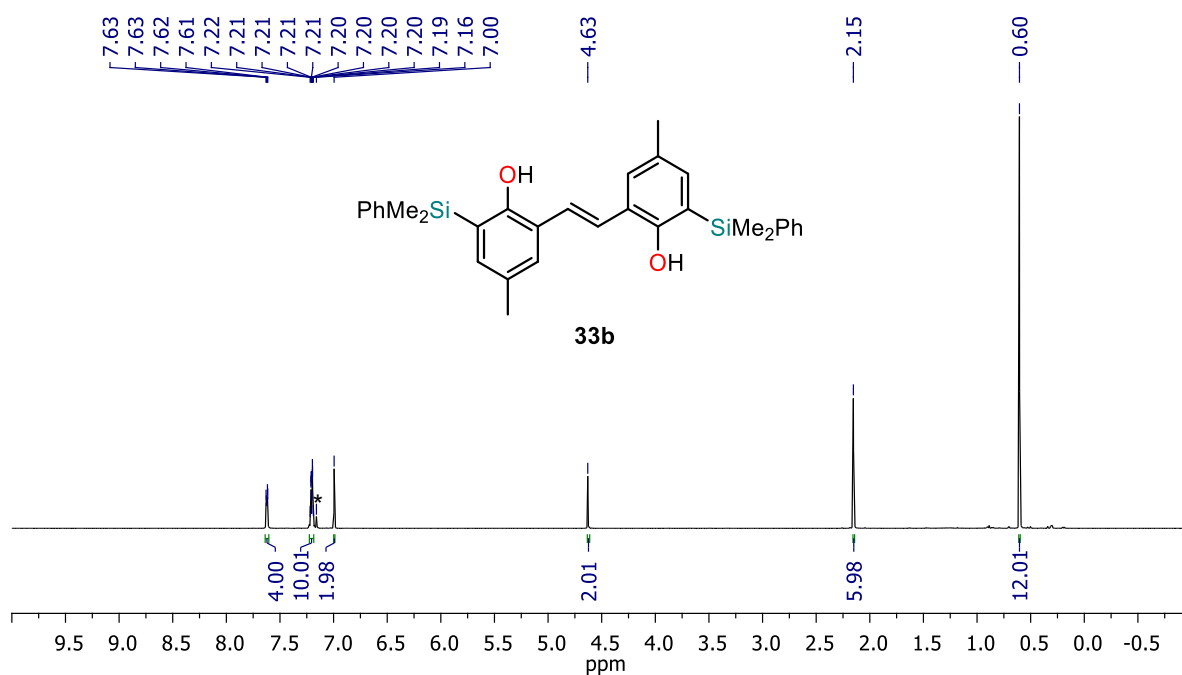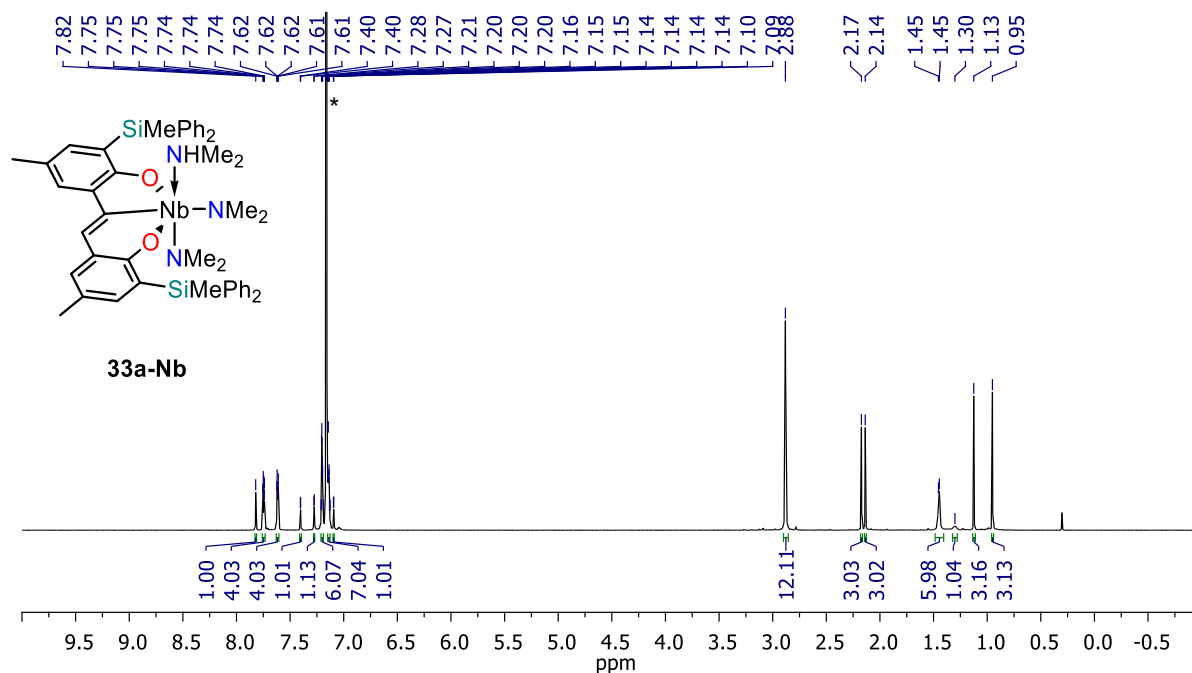


*Figure 33:* ¹H NMR spectrum (600 MHz) of compound **33b** at 295 K in benzene-*d₆*. Asterisk (*) indicates solvent peak.



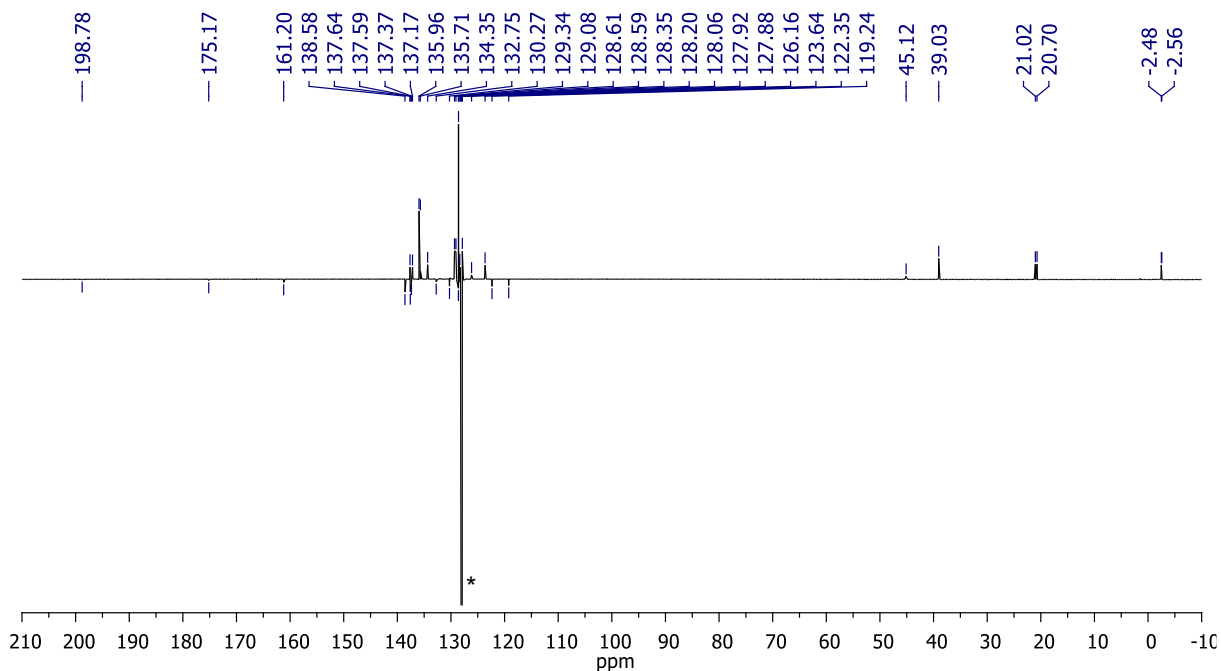*Figure 34:* ¹³C(APT) NMR spectrum (151 MHz) of compound **33b** at 295 K in benzene-*d₆*. Asterisk (*) indicates solvent peak.

### 7.1.4. (*E*)-6,6'-(ethene-1,2-diyl)bis(4-methyl-2-(trimethylsilyl)phenol) – 33c



*Figure 35:* $^1$H NMR spectrum (600 MHz) of compound **33c** at 295 K in benzene-$d_6$. Asterisk (*) indicates solvent peak.



*Figure 36:* $^{13}$C(APT) NMR spectrum (151 MHz) of compound **33c** at 295 K in benzene-$d_6$. Asterisk (*) indicates solvent peak.

## 7.1.5.  [(33a)Nb(NHMe₂)(NMe₂)₂] – 33a-Nb



*Figure 37:* ¹H NMR spectrum (700 MHz) of compound **33a-Nb** at 295 K in benzene-*d₆*. Asterisk (*) indicates solvent peak.



*Figure 38:* ¹³C(APT) NMR spectrum (176 MHz) of compound **33a-Nb** at 295 K in benzene-*d₆*. Asterisk (*) indicates solvent peak.
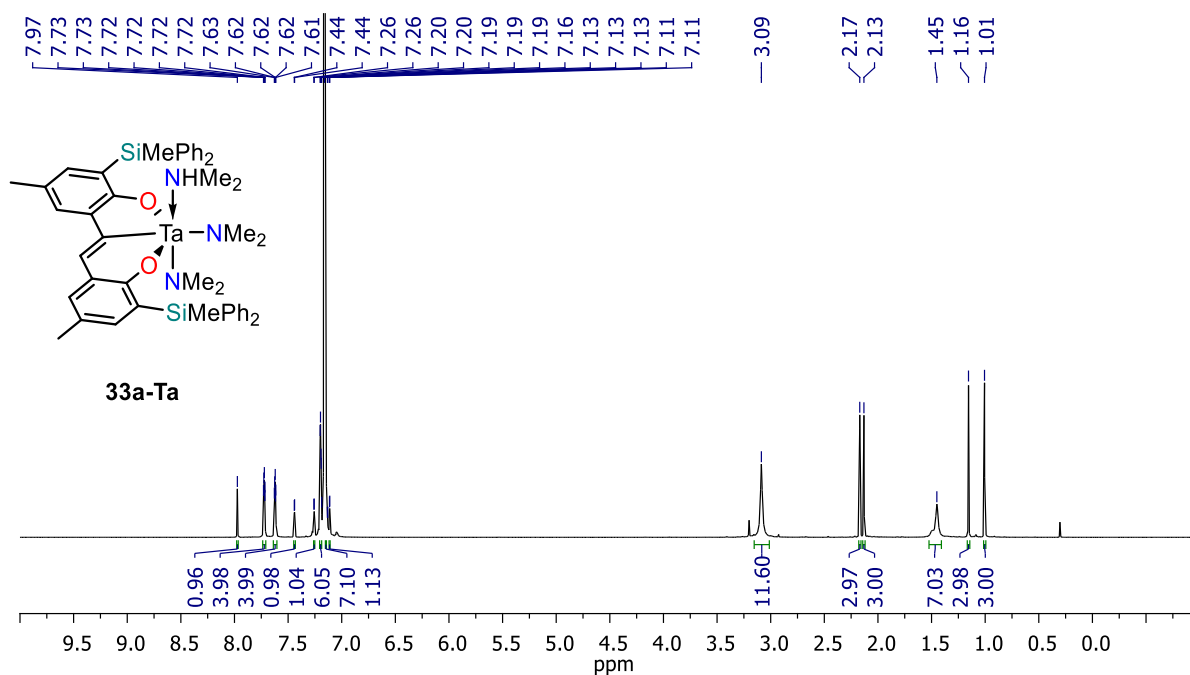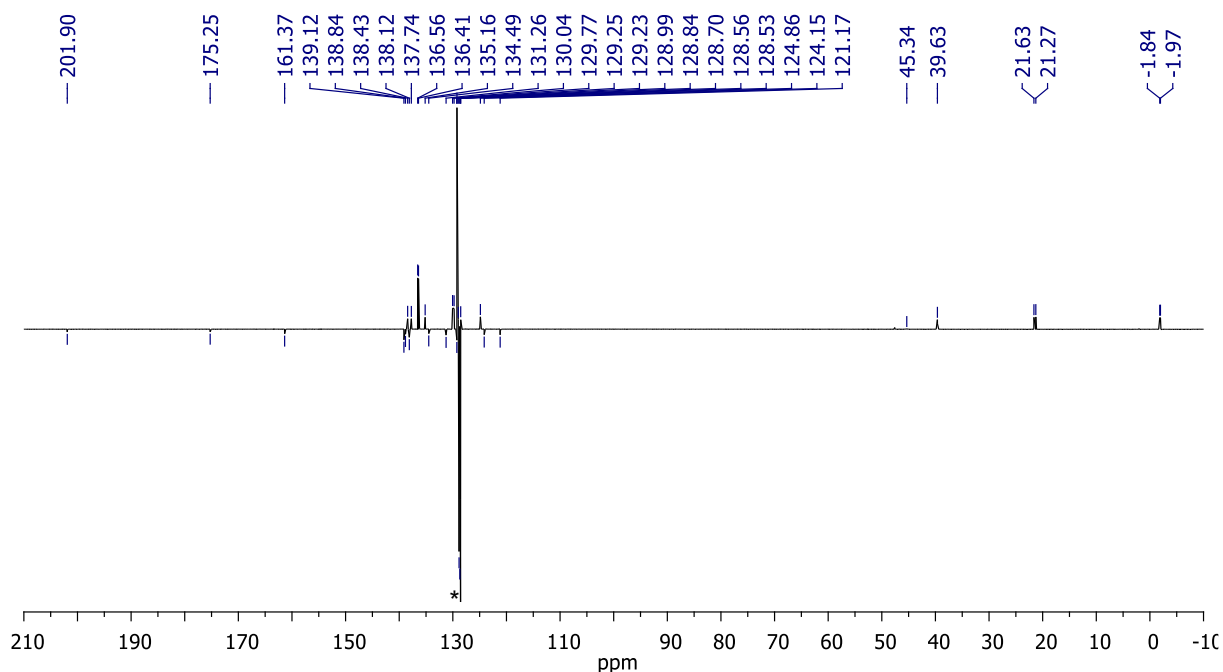
## 7.1.6. [(33a)Ta(NHMe₂)(NMe₂)₂] – 33a-Ta



*Figure 39:* ¹H NMR spectrum (700 MHz) of compound **33a-Ta** at 295 K in benzene-*d₆*. Asterisk (*) indicates solvent peak.



*Figure 40:* ¹³C(APT) NMR spectrum (176 MHz) of compound **33a-Ta** at 295 K in benzene-*d₆*. Asterisk (*) indicates solvent peak.

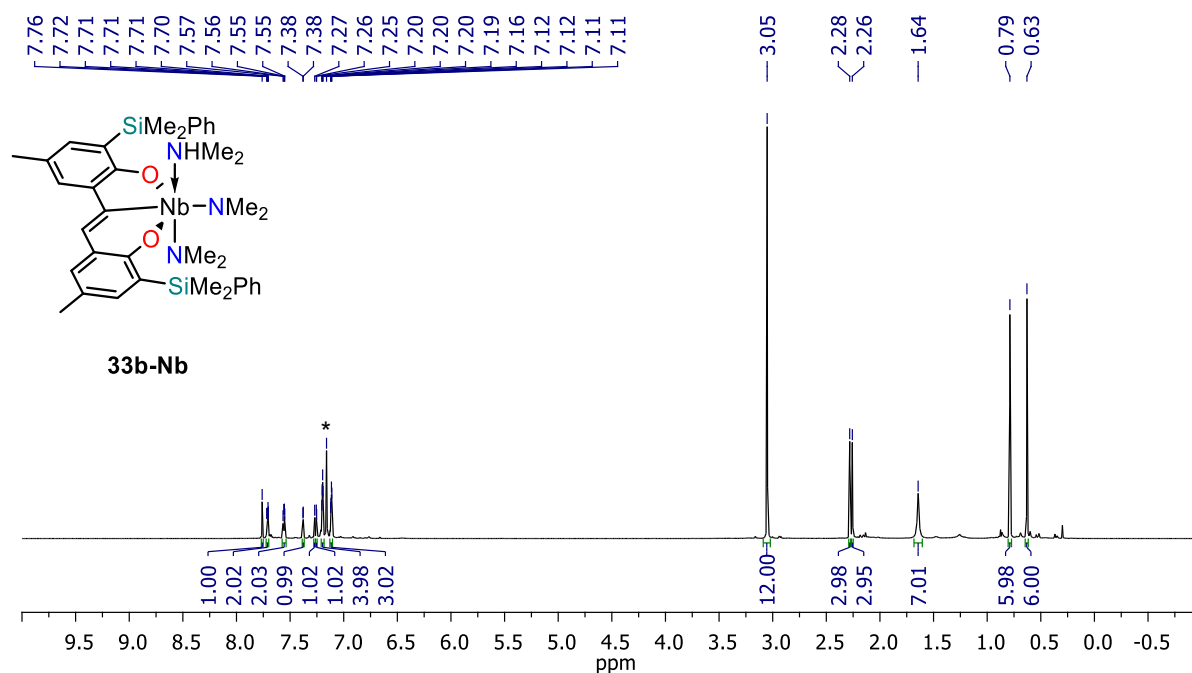## 7.1.7.  [(33b)Nb(NHMe₂)(NMe₂)₂] – 33b-Nb



*Figure 41:* ¹H NMR spectrum (600 MHz) of compound **33b-Nb** at 295 K in benzene-*d₆*. Asterisk (*) indicates solvent peak.
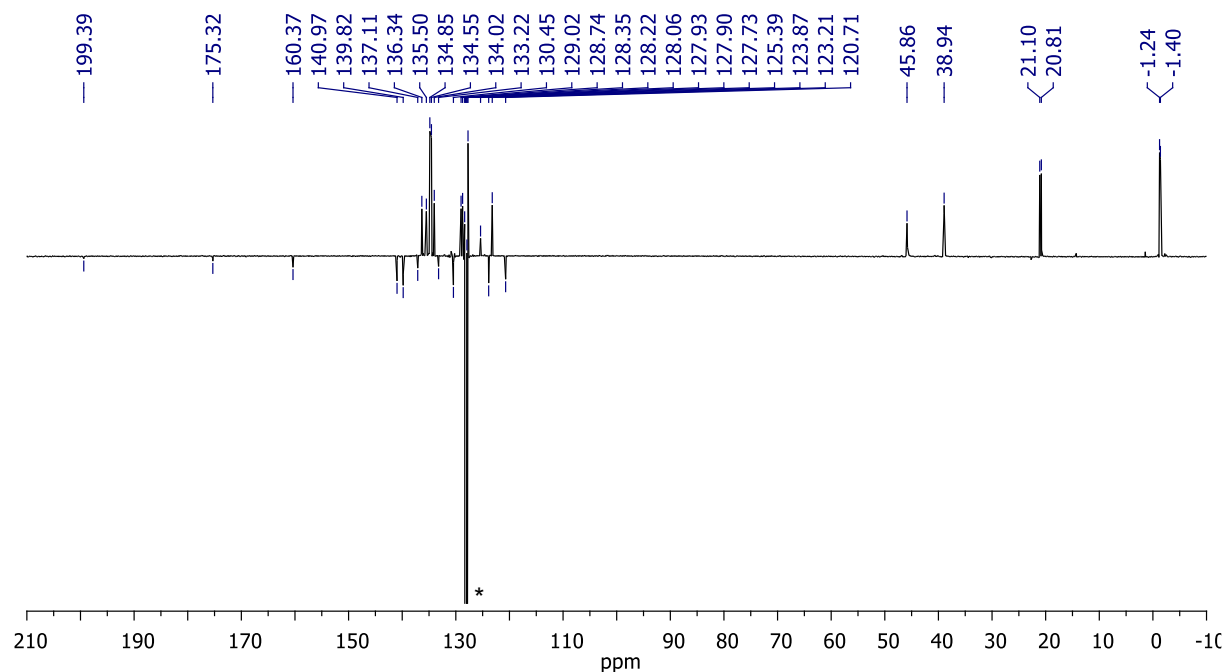


*Figure 42:* ¹³C(APT) NMR spectrum (151 MHz) of compound **33b-Nb** at 295 K in benzene-*d₆*. Asterisk (*) indicates solvent peak.
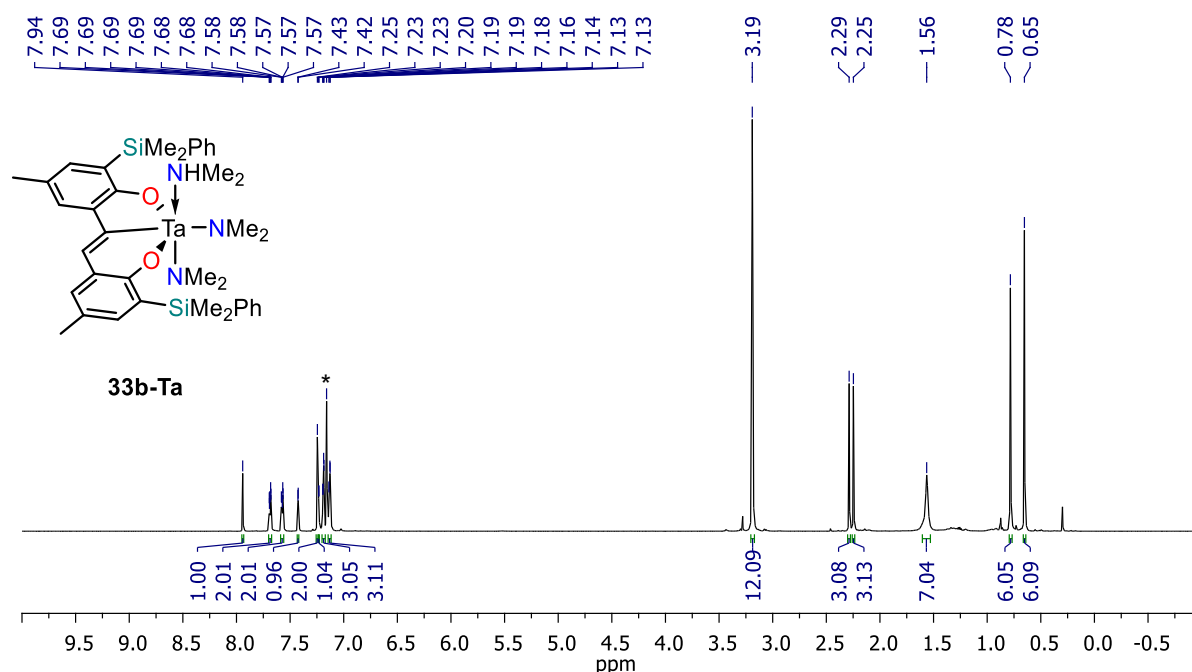
## 7.1.8. [(33b)Ta(NHMe₂)(NMe₂)₂] – 33b-Ta



*Figure 43:* ¹H NMR spectrum (600 MHz) of compound **33b-Ta** at 295 K in benzene-$d_6$. Asterisk (*) indicates solvent peak.
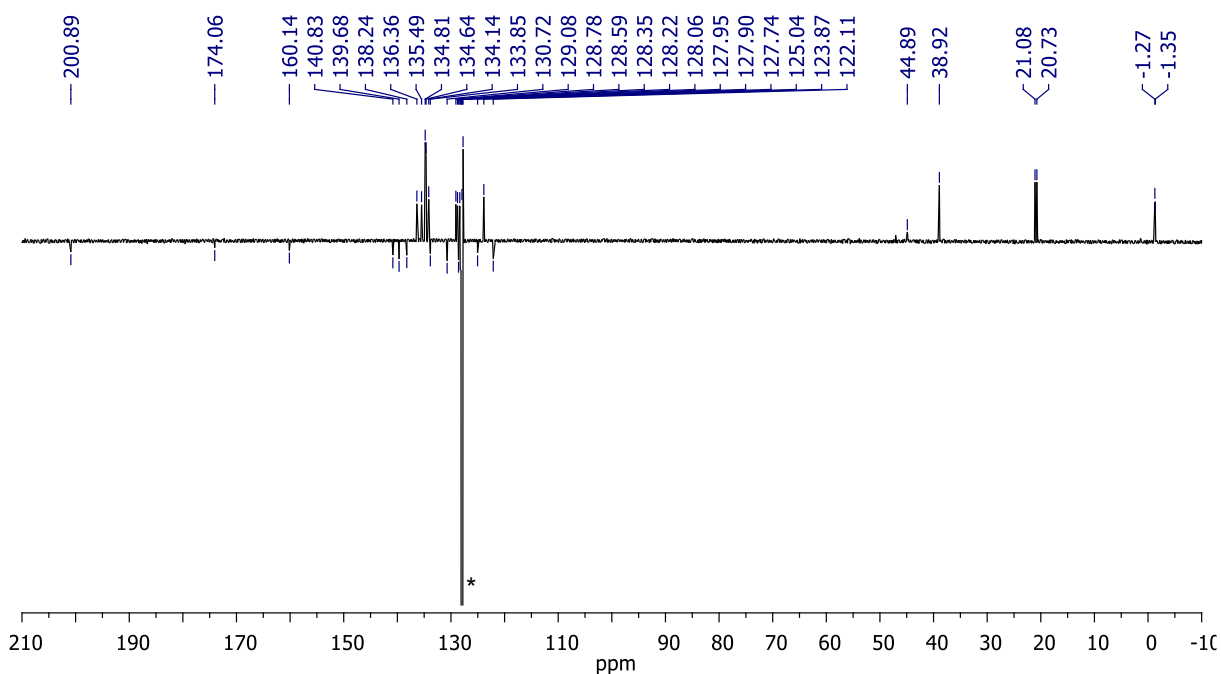


*Figure 44:* ¹³C(APT) NMR spectrum (151 MHz) of compound **33b-Ta** at 295 K in benzene-$d_6$. Asterisk (*) indicates solvent peak.
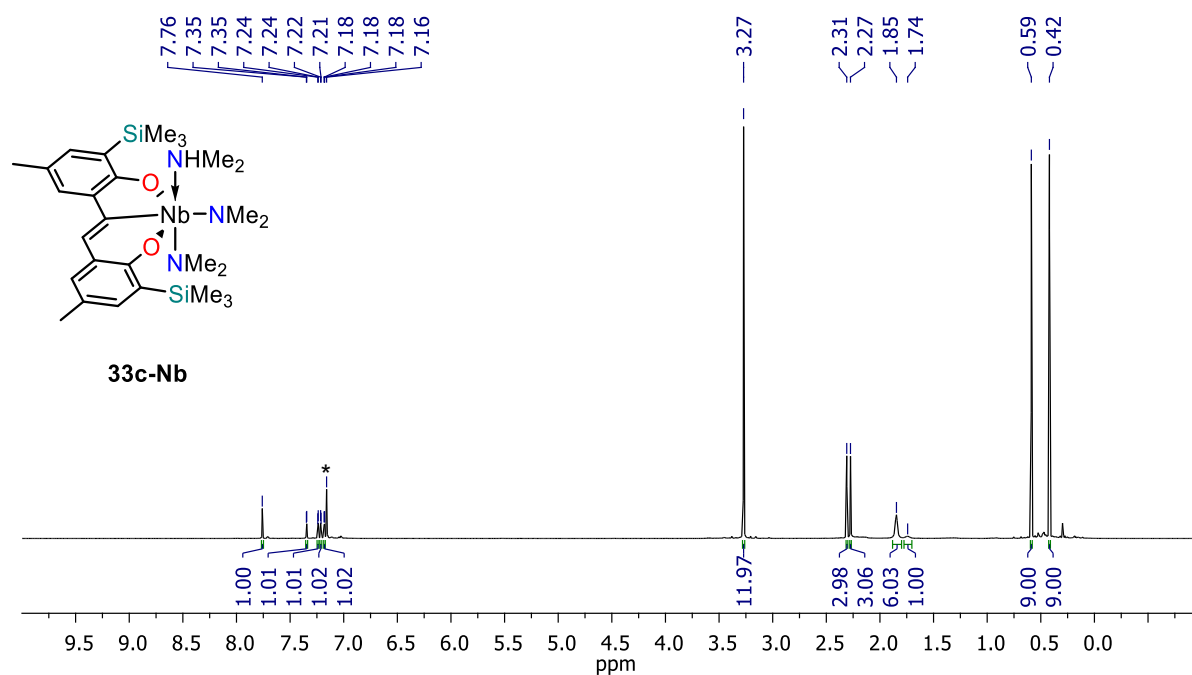
## 7.1.9.   [(33c)Nb(NHMe₂)(NMe₂)₂] – 33c-Nb



*Figure 45:* ¹H NMR spectrum (600 MHz) of compound **33c-Nb** at 295 K in benzene-$d_6$. Asterisk (*) indicates solvent peak.



*Figure 46:* ¹³C(APT) NMR spectrum (151 MHz) of compound **33c-Nb** at 295 K in benzene-$d_6$. Asterisk (*) indicates solvent peak.

## 7.1.10. [(33c)Ta(NHMe₂)(NMe₂)₂] – 33c-Ta



*Figure 47:* ¹H NMR spectrum (600 MHz) of compound **33c-Ta** at 295 K in benzene-*d₆*. Asterisk (*) indicates solvent peak.
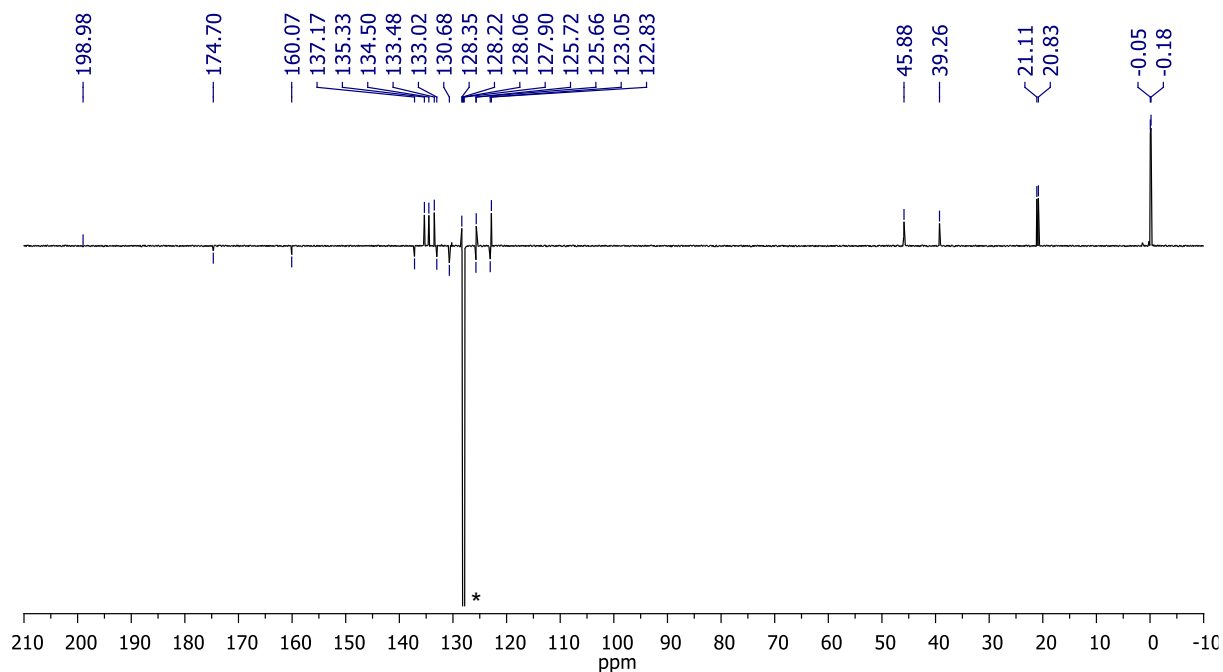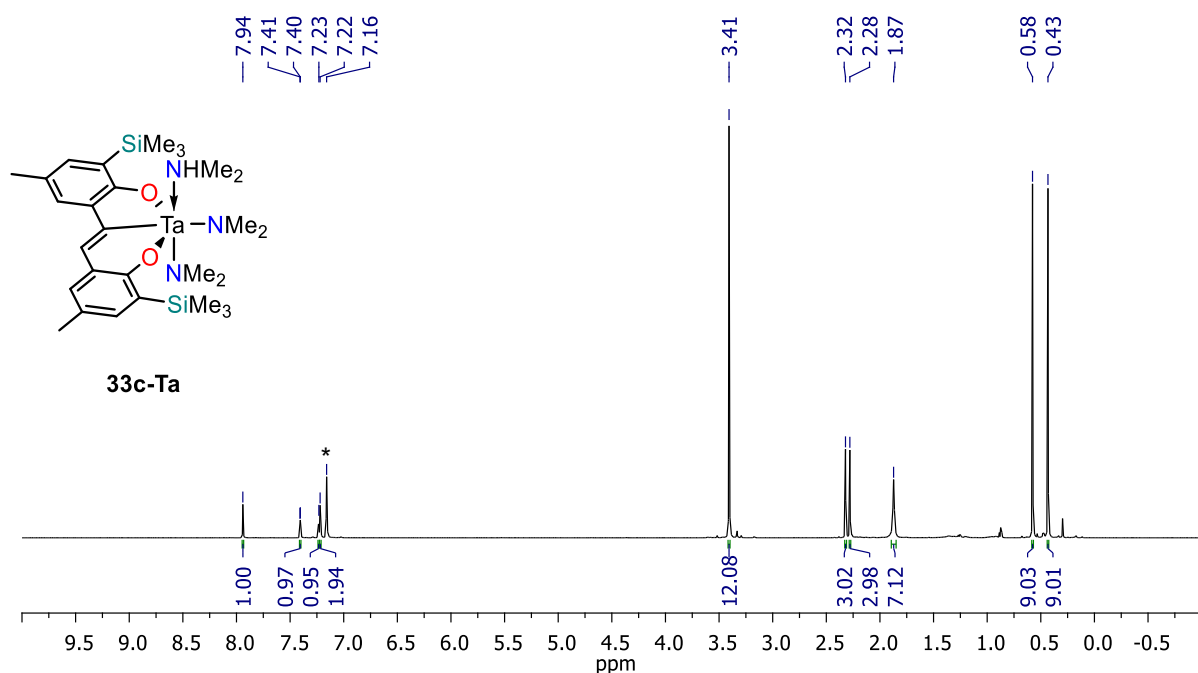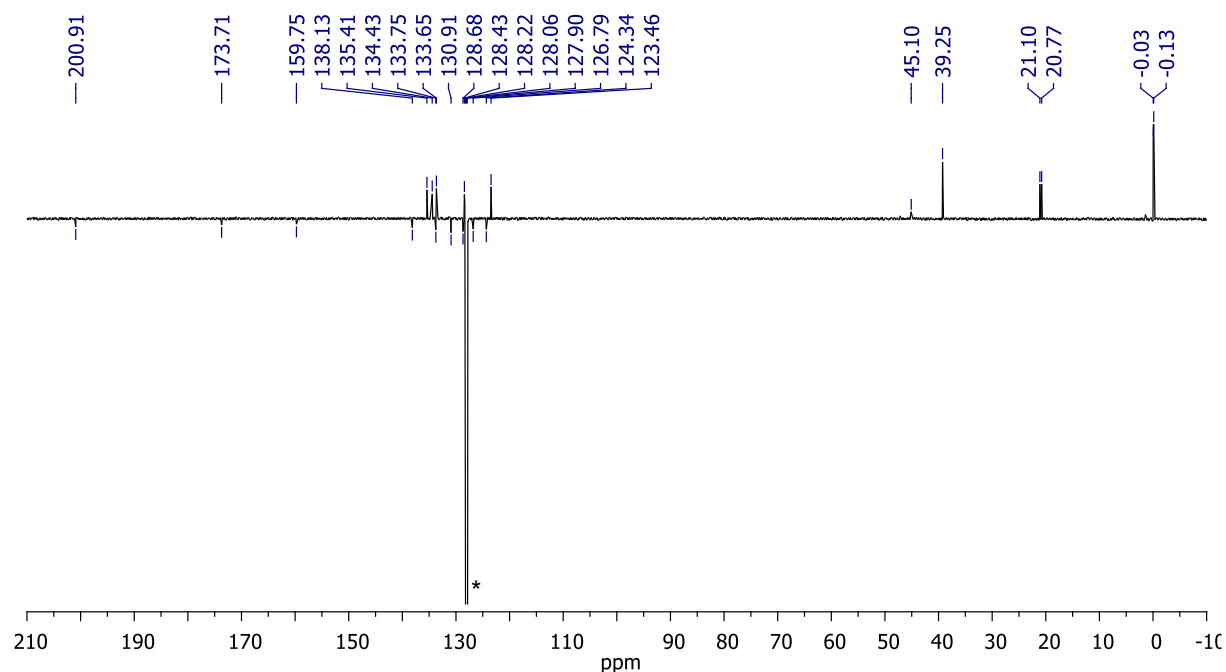


*Figure 48:* ¹³C(APT) NMR spectrum (151 MHz) of compound **33c-Ta** at 295 K in benzene-*d₆*. Asterisk (*) indicates solvent peak.

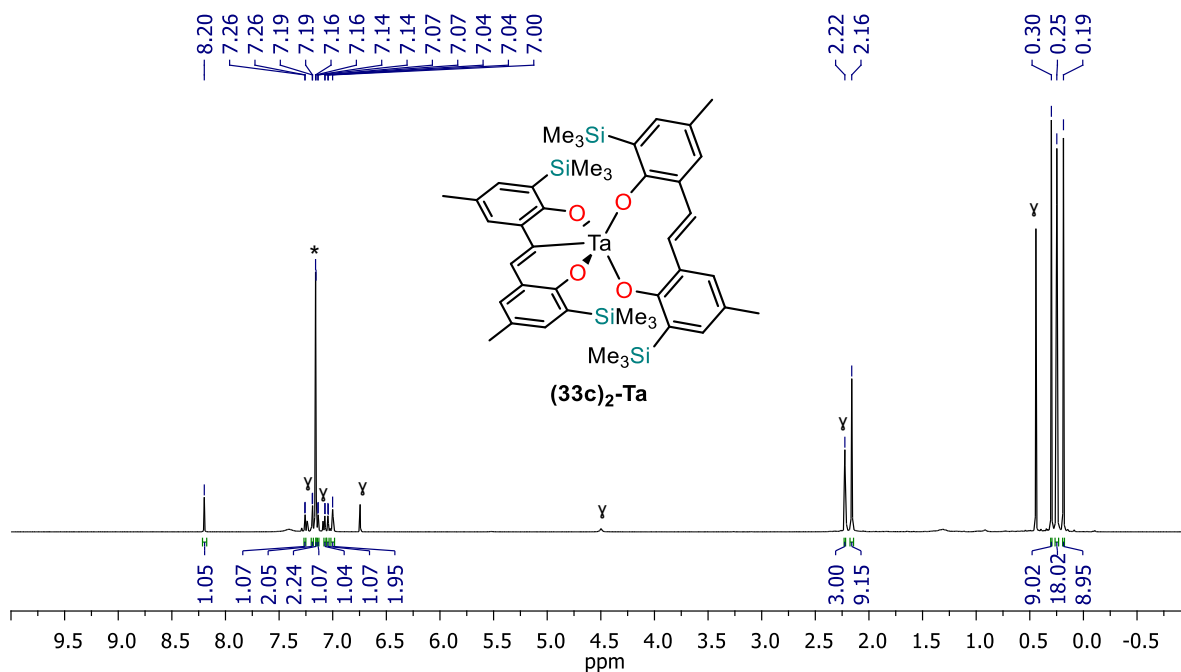## 7.1.11. [Ta(33c)₂] – (33c)₂-Ta



*Figure 49:* ¹H NMR spectrum (600 MHz) of compound **(33c)₂-Ta** at 295 K in benzene-*d₆*. Asterisk (*) indicates solvent peak. Small gamma (ɣ) indicates peaks of ligand **33c**.
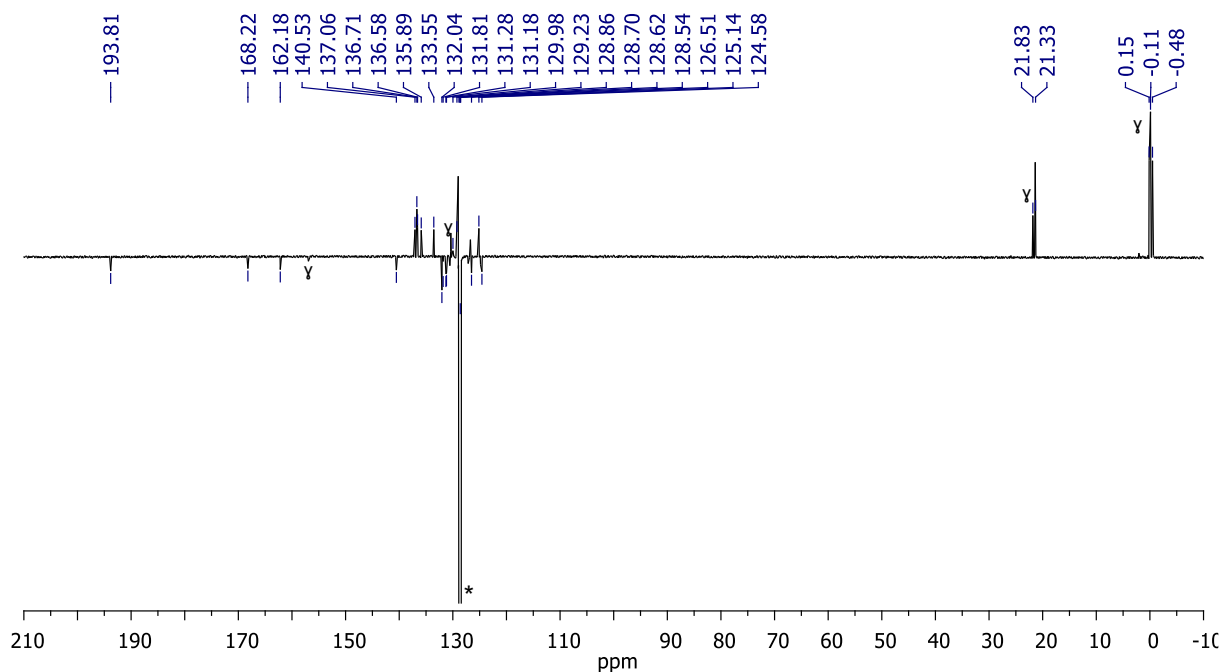


*Figure 50:* ¹³C(APT) NMR spectrum (151 MHz) of compound **(33c)₂-Ta** at 295 K in benzene-*d₆*. Asterisk (*) indicates solvent peak. Small gamma (ɣ) indicates peaks of ligand **33c**.

## 7.1.12. *tert*-butyl phenylcarbamate 38



*Figure 51:* $^1$H NMR spectrum (400 MHz) of compound **38** at 295 K in CDCl$_3$. Asterisk (*) indicates solvent peak.
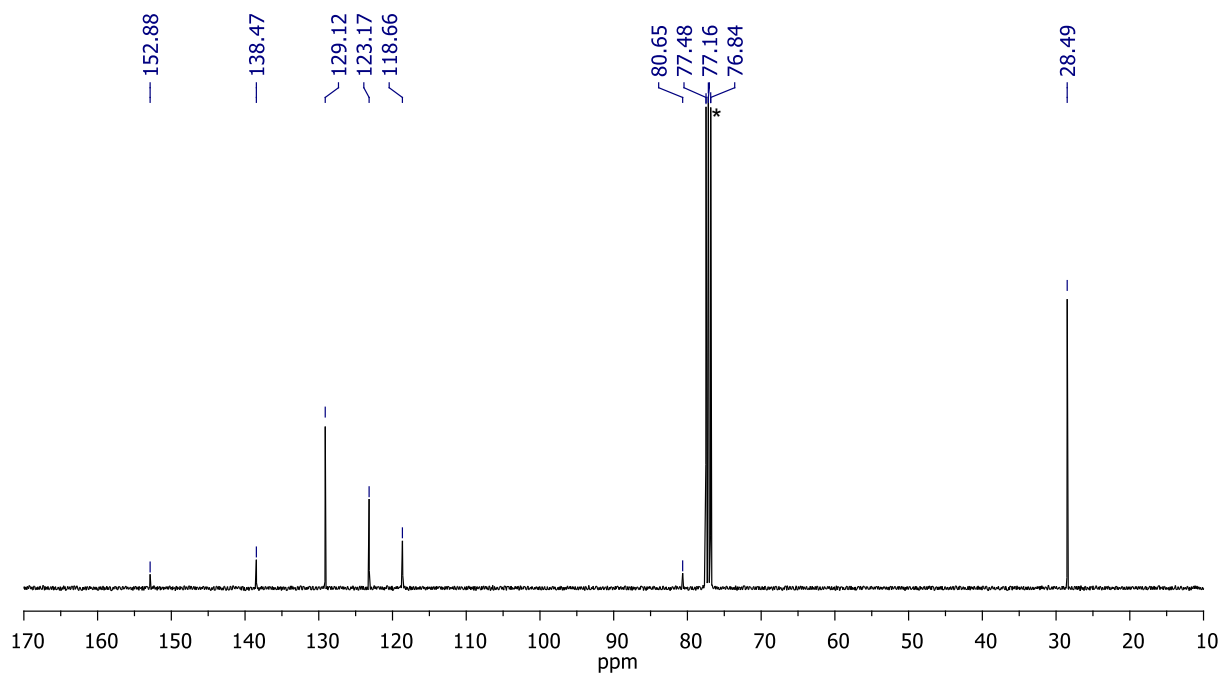


*Figure 52:* $^{13}$C {$^1$H} NMR spectrum (101 MHz) of compound **38** at 295 K in CDCl$_3$. Asterisk (*) indicates solvent peak.

## 7.1.13. *N*-(methyl-*d₃*)aniline 39



*Figure 54:* ¹H NMR spectrum (400 MHz) of compound **39** at 295 K in CDCl₃. Asterisk (*) indicates solvent peak.



*Figure 53:* ¹³C(APT) NMR spectrum (101 MHz) of compound **39** at 295 K in CDCl₃. Asterisk (*) indicates solvent peak.

## 7.1.14. *N-d-N*-methylaniline 40



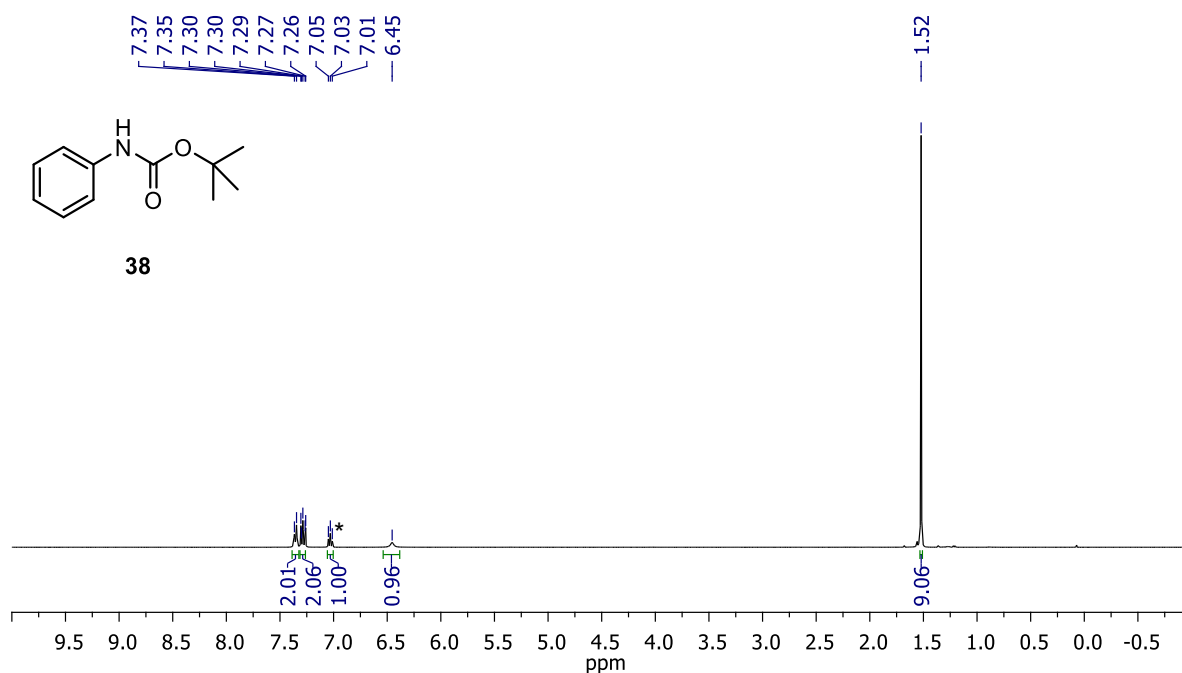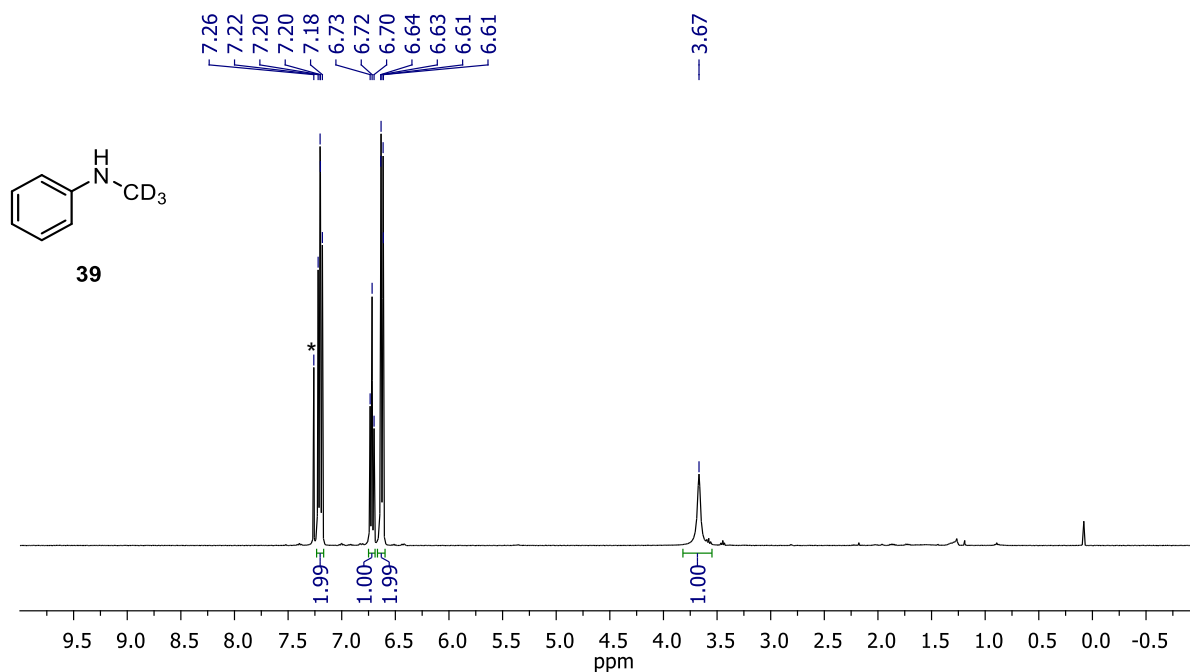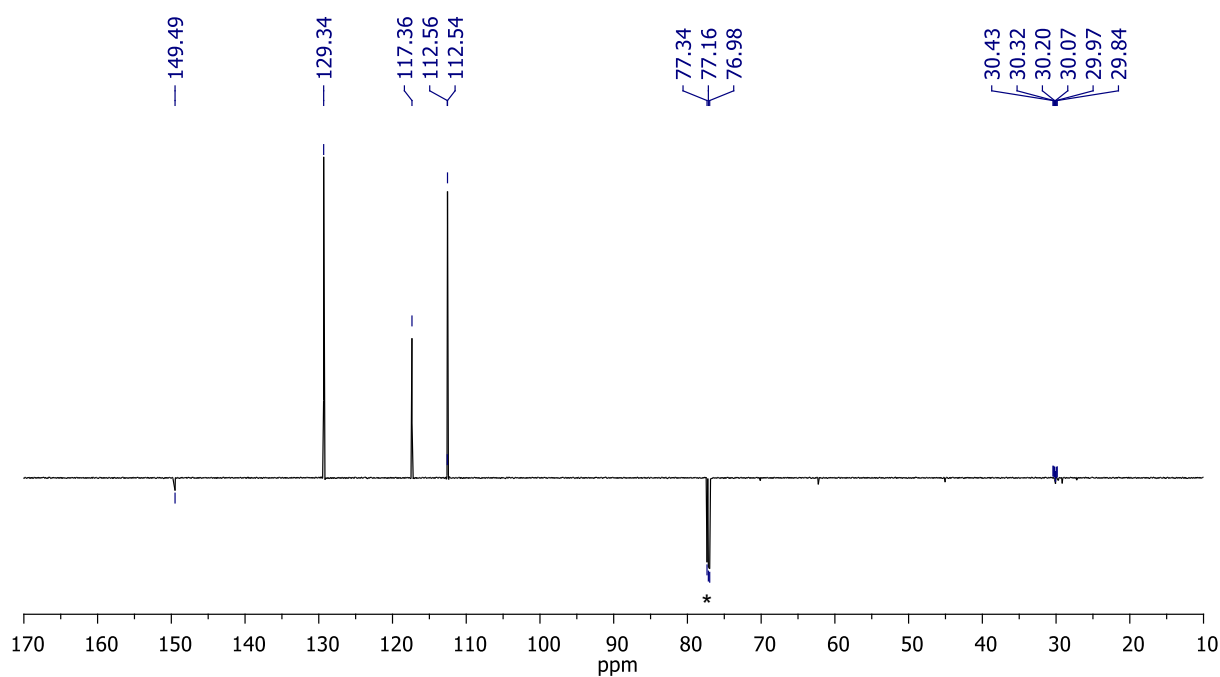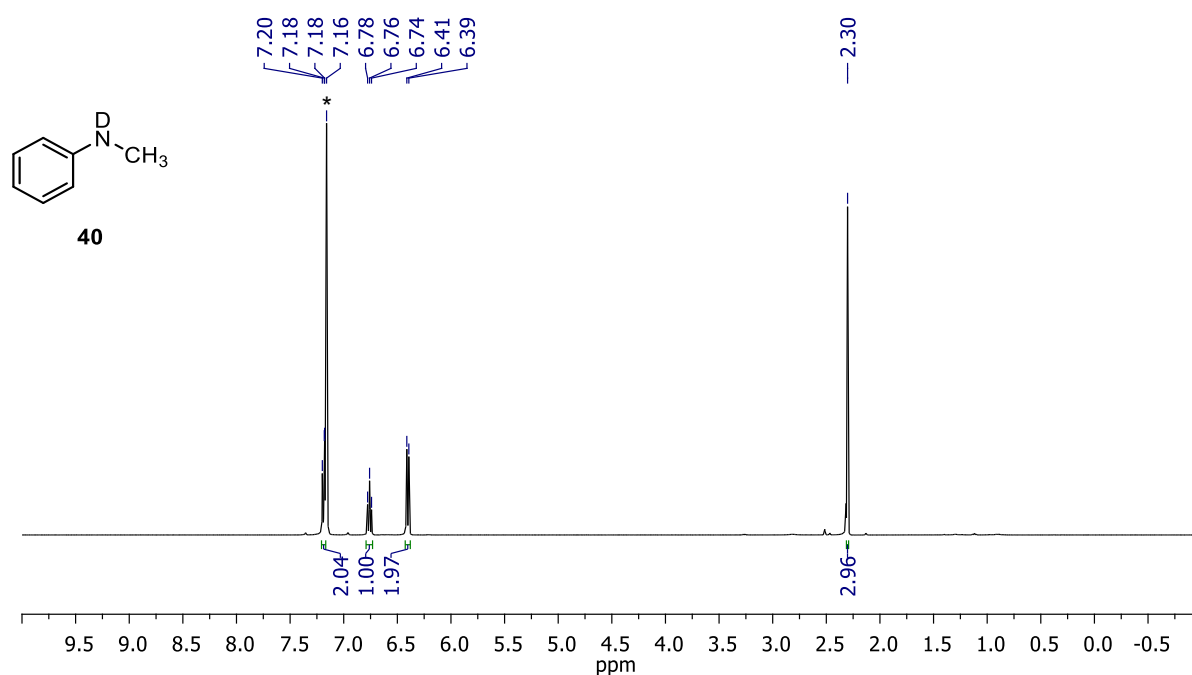*Figure 55:* $^1$H NMR spectrum (400 MHz) of compound **40** at 295 K in benzene-$d_6$. Asterisk (*) indicates solvent peak.
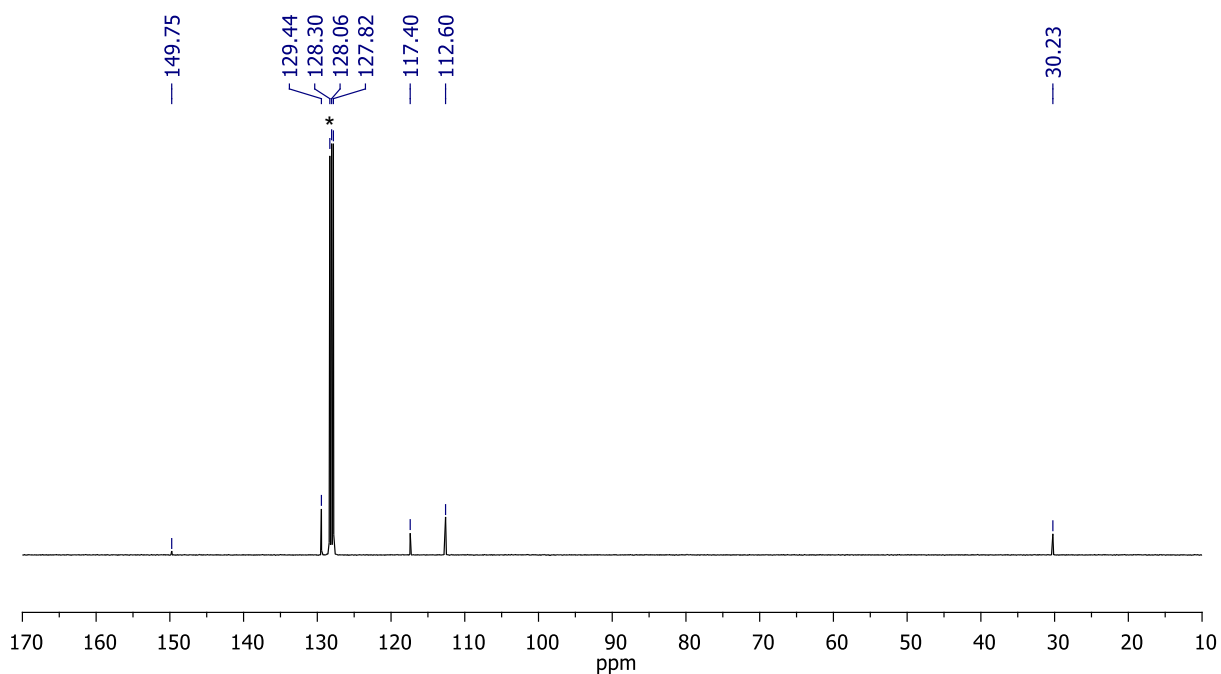


*Figure 56:* $^{13}$C {$^1$H} NMR spectrum (101 MHz) of compound **40** at 295 K in benzene-$d_6$. Asterisk (*) indicates solvent peak.

## 7.2. X-Ray Diffraction Analysis

*Table 7:* Crystal data refinement for **33a-Nb**, **33c-Nb**, **33a-Ta**, **33b-Ta** and **33c-Ta**.

| Parameter | 33a-Nb | 33c-Nb | 33a-Ta | 33b-Ta | 33c-Ta |
|---|---|---|---|---|---|
| Empirical formular | $C_{48}H_{56}N_3O_2Si_2Nb$ | $C_{28}H_{48}N_3O_2Si_2Nb$ | $C_{48}H_{56}N_3O_2Si_2Ta$ | $C_{38}H_{52}N_3O_2Si_2Ta$ | $C_{28}H_{48}N_3O_2Si_2Ta$ |
| Formula weight | 856,07 g/mol | 607.78 g/mol | 944,11 g/mol | 819.95 g/mol | 695,83 g/mol |
| Temperature | 100(2) K | 100(2) K | 100(2) K | 100(2) K | 100 K |
| Crystal system | monoclinic | monoclinic | monoclinic | orthorhombic | monoclinic |
| Space group | $P\,2_1$ | $P\,2_1/n$ | $P\,2_1/m$ | $P\,2_1\,2_1\,2_1$ | $P\,2_1/n$ |
| Unit cell dimensions | $a$ = 9.4079(5) Å, $\alpha$ = 90° $b$ = 24.0298(15) Å, $\beta$ = 105.893(3)° $c$ = 10.2160(4) Å, $\gamma$ = 90° | $a$ = 11.0822(4) Å, $\alpha$ = 90° $b$ = 18.2090(7) Å, $\beta$ = 103.072(3)° $c$ = 16.1059(6)Å, $\gamma$ = 90° | $a$ = 9.3955(7) Å, $\alpha$ = 90° $b$ = 24.1549(18) Å, $\beta$ = 105.639(5)° $c$ = 10.1959(8) Å, $\gamma$ = 90° | $a$ = 14.296(3) Å, $\alpha$ = 90° $b$ = 15.844(4) Å, $\beta$ = 90.05(3)° $c$ = 16.963(4) Å, $\gamma$ = 90° | $a$ = 11.0850(4) Å, $\alpha$ = 90° $b$ = 18.1892(4) Å, $\beta$ = 103.279(3)° $c$ = 16.1059(6) Å, $\gamma$ = 90° |
| Volume | 2221.25 Å$^3$ | 3165.88 Å$^3$ | 2228.27 Å$^3$ | 3842.22 Å$^3$ | 3160.56 Å$^3$ |
| Z | 2 | 4 | 2 | 4 | 4 |
| Density (calculated) | 1.280 | 1.275 | 1.407 | 1.417 | 1.460 |
| Absorption coefficient µ | 3.036 | 0.483 | 5.378 | 6.144 | 7.355 |
| F(000) | 900 | 1288 | 964 | 1672 | 1412 |
| Crystal size | Not given | 0.310×0.267×0.243 mm$^3$ | Not given | 0.055×0.048×0.040 mm$^3$ | 0.160×0.130×0.090 mm$^3$ |

| Radiation | CuKα (λ = 1.54178) | MoKα (λ = 0.71073) | CuKα (λ = 1.54178) | CuKα (λ = 1.54186) | CuKα (λ = 1.54186) |
|---|---|---|---|---|---|
| 2θ range for data collection | 3.679 to 59.396° | 1.713 to 31.187° | 3.660 to 50.428° | 6.97 to 57.65° | 3.722 to 72.138° |
| Index ranges | $-10 \leq h \leq 10$, $-26 \leq k \leq 26$, $-11 \leq l \leq 11$ | $-9 \leq h \leq 16$, $-22 \leq k \leq 26$, $-23 \leq l \leq 18$ | $-9 \leq h \leq 7$, $-24 \leq k \leq 24$, $-10 \leq l \leq 10$ | $-17 \leq h \leq 17$, $-12 \leq k \leq 19$, $-15 \leq 20$ | $-13 \leq h \leq 12$, $-17 k \leq 22$, $-10 \leq l \leq 19$ |
| Reflections collected | 23502 | 122805 | 24913 | 24226 | 51570 |
| Independent reflections | 6265 [$R_{int}$ = 0.1631, $R_{sigma}$ = 0.1690] | 10118 [$R_{int}$ = 0.0375, $R_{sigma}$ = 0.0607] | 2404 [$R_{int}$ = 0.1425, $R_{sigma}$ = 0.0760] | 6697 [$R_{int}$ = 0.2248, $R_{sigma}$ = 0.1559] | 6167 [$R_{int}$ = 0.0159, $R_{sigma}$ = 0.0071] |
| Data / restraints / parameter | 6265/472/506 | 10118/0/339 | 2404/336/295 | 6697/379/427 | 6167/0/339 |
| Goodness-of-fit on $F^2$ | 1.106 | 0.922 | 1.033 | 1.209 | 1.101 |
| Final R indices [I>2σ (I)] | $R_1$ = 0.0827, $wR_2$ = 0.1940 | $R_1$ = 0.0238, $wR_2$ = 0.0523 | $R_1$ = 0.0413, $wR_2$ = 0.0842 | $R_1$ = 0.1255, $wR_2$ = 0.3269 | $R_1$ = 0.0195, $wR_2$ = 0.0450 |
| Final R indices [all data] | $R_1$ = 0.1193, $wR_2$ = 0.2105 | $R_1$ = 0.0372, $wR_2$ = 0.0530 | $R_1$ = 0.0693, $wR_2$ = 0.0920 | $R_1$ = 0.1649, $wR_2$ = 0.3540 | $R_1$ = 0.0200, $wR_2$ = 0.0453 |
| Largest diff. peak and hole | 1.193/-1.054 eÅ$^{-3}$ | 1.401/-0.858 eÅ$^{-3}$ | 0.596/-0.513 eÅ$^{-3}$ | 4.807/-1.667 eÅ$^{-3}$ | 1.438/-1.160 eÅ$^{-3}$ |

$R_{int} = \Sigma|F_o^2 - F_o^2(mean)| / \Sigma[F_o^2]$

$R_1 = \Sigma||F_o| - |F_c|| / \Sigma|F_o|$

$GOOF = S = \{\Sigma[w(F_o^2 - F_c^2)^2] / (n - p)\}^{1/2}$

$wR_2 = \{\Sigma[w(F_o^2 - F_c^2)^2] / \Sigma[w(F_o^2)^2]\}^{1/2}$

$w = 1 / [\sigma(F_o^2) + (aP)^2 + bP]$ where P is $[2F_c^2 + Max(F_o^2. 0)] / 3$

*Table 8:* Crystal data refinement for **33a·2EtOAc**, **33b** and **(33c)₂-Ta**.

| Parameter | 33a·2EtOAc | 33b | (33c)2-Ta |
|---|---|---|---|
| Empirical formular | $C_{42}H_{40}O_2Si_2$, $2(C_4H_8O_2)$ | $C_{32}H_{36}O_2Si_2$ | $C_{44}H_{59}O_4Si_4Ta$ |
| Formula weight | 632,95 g/mol + 2(88,11 g/mol) | 508,81 g/mol | 945,24 g/mol |
| Temperature | 100.0 K | 100(2) K | 100(2) K |
| Crystal system | triclinic | monoclinic | monoclinic |
| Space group | P 1 | P 2₁/c | P 2₁/n |
| Unit cell dimensions | **a** = 7.2037(3) Å, **α** = 90.9241(19)° **b** = 12.2790(5) Å, **β** = 98.7947(15)° **c** = 13.5023(5) Å, **γ** = 106.7683(15)° | **a** = 14.8995(4) Å, **α** = 90° **b** = 7.4660(2) Å, **β** = 90.9855(14)° **c** = 12.8691(4) Å, **γ** = 90° | **a** = 15.221(3) Å, **α** = 90° **b** = 17.819(2) Å, **β** = 90.59(3)° **c** = 18.976(3) Å, **γ** = 90° |
| Volume | 1127.81 | 1431.34 | 5146.45 |
| Z | 1 | 2 | 2 |
| Density (calculated) | 1.191 | 1.181 | 1.307 |
| Absorption coefficient μ | 0.126 | 0.150 | 5.140 |
| F(000) | 432 | 544 | 2100 |
| Crystal size | $0.15 \times 0.3 \times 0.3$ mm³ | $0.1 \times 0.25 \times 0.36$ mm³ | $0 \times 070 \times 0.037 \times 0.020$ mm³ |
| Radiation | MoKα (λ = 0.71073) | MoKα (λ = 0.71073) | CuKα (λ = 1.54186) |
| 2θ range for data collection | 2.239 to 30.120° | 2.735 to 30.823° | 3.402 to 71.509° |

| Index ranges | -10 ≤ h ≤ 10, -14 ≤ k ≤ 17, -19 ≤ l ≤ 19 | -20 ≤ h ≤ 21, -10 ≤ k ≤ 10, -18 ≤ l ≤ 15 | -14 ≤ h ≤ 12, -9 ≤ k ≤ 21, -17 ≤ l ≤16 |
|---|---|---|---|
| Reflections collected | 41518 | 19280 | 9089 |
| Independent reflections | 6613 [$R_{int}$ = 0.0622, $R_{sigma}$ = 0.0520] | 4396 [$R_{int}$ = 0.0662, $R_{sigma}$ = 0.0653] | 4599 [$R_{int}$ = 0.0574, $R_{sigma}$ = 0.1160] |
| Data / restraints / parameter | 6613/0/267 | 4396/0/167 | 4599/937/603 |
| Goodness-of-fit on $F^2$ | 1.01892 | 1.019 | 1.033 |
| Final R indices [I>2σ (I)] | $R_1$ = 0.0492, w$R_2$ = 0.1022 | $R_1$ = 0.0484, w$R_2$ = 0.0978 | $R_1$ = 0.0624, w$R_2$ = 0.1160 |
| Final R indices [all data] | $R_1$ = 0.0859, w$R_2$ = 0.1159 | $R_1$ = 0.0957, w$R_2$ = 0.1155 | $R_1$ = 0.1303, w$R_2$ = 0.1408 |
| Largest diff. peak and hole | 0.339/ -0.369 e$Å^{-3}$ | 0.317/-0.294 e$Å^{-3}$ | 1.307/-0.627 e$Å^{-3}$ |

$R_{int} = \Sigma|F_o^2 - F_o^2(mean)| / \Sigma[F_o^2]$

$R_1 = \Sigma||F_o| - |F_c|| / \Sigma|F_o|$

$GOOF = S = \{\Sigma[w(F_o^2 - F_c^2)^2] / (n - p)\}^{1/2}$

$wR_2 = \{\Sigma[w(F_o^2 - F_c^2)^2] / \Sigma[w(F_o^2)^2]\}^{1/2}$

$w = 1 / [\sigma(F_o^2) + (aP)^2 + bP]$ where P is $[2F_c^2 + Max(F_o^2. 0)] / 3$